جامعة القاهرة كلية الهندسة
قسم هندسة القوى الميكانيكية
معمل التحكم الأوتوماتيكى

ACC Virtual Labs
Automatic Control Circuits &Virtual Labs for Mechanical Power Systems
معمل التحكم الأتوماتيكى و المعامل الإفتراضية لأنظمة القوى الميكانيكية

Diploma of Automatic Control Applications

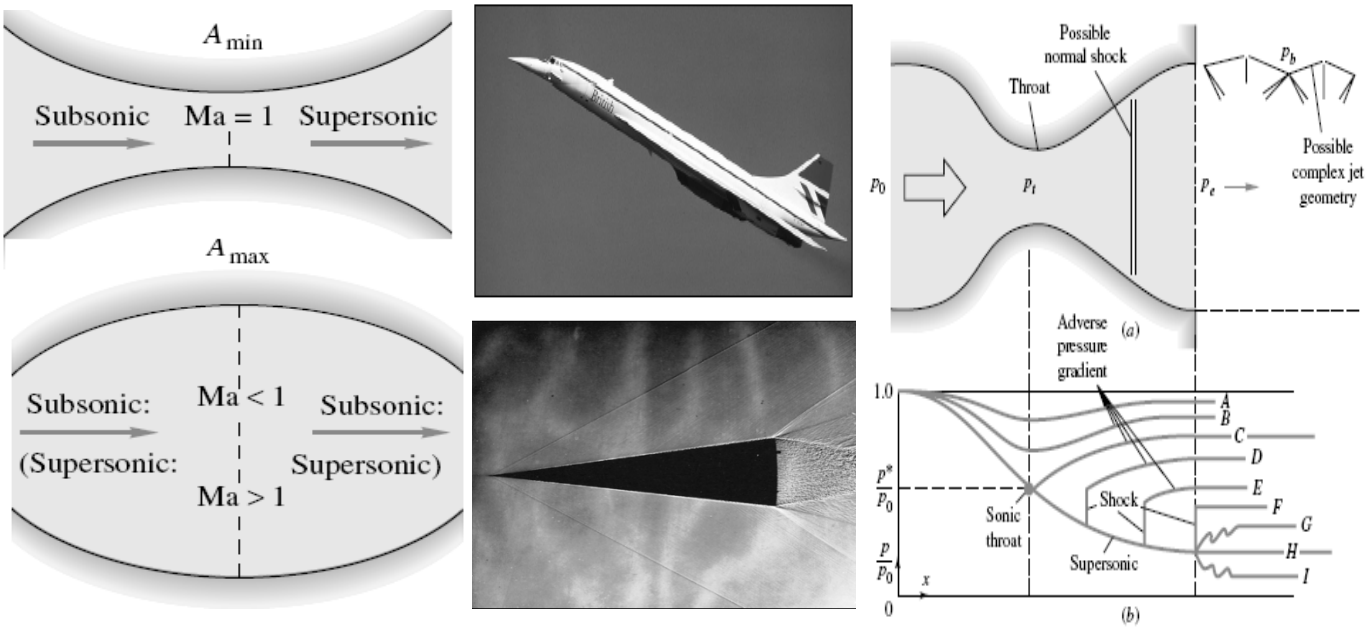

Notes on the course: MEP 580

Selected Topics in Pipe Lines

Compressible Flow (Gas Dynamics)

Compiled and Edited by

Dr. Mohsen Soliman

June 2018

Part (6)*

Introduction to Compressible Flow (Gas Dynamics)

6.1 Introduction:

Motivation. All of our previous chapters have been concerned with "low-speed" or "incompressible" flow, i.e., where the fluid velocity is much less than its speed of sound. In fact, we did not even develop an expression for the speed of sound of a fluid. That is done in this chapter.

When a fluid moves at speeds comparable to its speed of sound, density changes become significant and the flow is termed *compressible*. Such flows are difficult to obtain in liquids, since high pressures of order 1000 atm are needed to generate sonic velocities. In gases, however, a pressure ratio of only 2:1 will likely cause sonic flow. Thus compressible gas flow is quite common, and this subject is often called *gas dynamics*.

Probably the two most important and distinctive effects of compressibility on flow are (1) *choking*, wherein the duct flow rate is sharply limited by the sonic condition, and (2) *shock waves*, which are nearly discontinuous property changes in a supersonic flow. The purpose of this chapter is to explain such striking phenomena and to familiarize the reader with engineering calculations of compressible flow.

We took a brief look in part (1) [Eqs.a,b,c,d &f below] to see when we might safely neglect the compressibility inherent in every real fluid. We found that the proper criterion for a nearly incompressible flow was a small Mach number $\mathrm{Ma} = V/a \ll 1$ where V is the flow velocity and a is the speed of sound of the fluid. Under small-Mach-number conditions, changes in fluid density are everywhere small in the flow field. The energy equation becomes uncoupled, and temperature effects can be either ignored or put aside for later study. The equation of state degenerates into the simple statement that density is nearly constant. This means that an incompressible flow requires only a momentum and continuity analysis, as we showed with many examples in parts 1, 2, 3 &4.

When is a given flow approximately incompressible? We can derive a nice criterion by playing a little fast and loose with density approximations. In essence, we wish to slip density out of the divergence in continuity eq. and approximate a typical term as, e.g.,

$$\frac{\partial}{\partial x}(\rho u) \approx \rho \frac{\partial u}{\partial x} \qquad \text{(a)}$$

This is equivalent to the strong inequality

$$\left| u \frac{\partial \rho}{\partial x} \right| \ll \left| \rho \frac{\partial u}{\partial x} \right|$$

or

$$\left| \frac{\delta \rho}{\rho} \right| \ll \left| \frac{\delta V}{V} \right| \qquad \text{(b)}$$

As we shall see in this part , the pressure change is approximately proportional to the density change and the square of the speed of sound a of the fluid

$$\delta p \approx a^2 \, \delta \rho \qquad \text{(c)}$$

Meanwhile, if elevation changes are negligible, the pressure is related to the velocity change by Bernoulli's equation

---

*** Ref.:(1) Bruce R. Munson, Donald F. Young, Theodore H. Okiishi "Fundamental of Fluid Mechanics" 4th ed., John Wiley & Sons, Inc., 2002.**

$$\delta p \approx -\rho V\, \delta V \qquad \text{(d)}$$

Combining Eqs.(b) to(d), we obtain an explicit criterion for incompressible flow:

$$\frac{V^2}{a^2} = \mathrm{Ma}^2 \ll 1 \qquad \text{(f)}$$

where Ma = *V*/*a* is the dimensionless *Mach number* of the flow. How small is small? The commonly accepted limit is $\mathrm{Ma} \leq 0.3$

For air at standard conditions, a flow can thus be considered incompressible if the velocity is less than about 100 m/s (330 ft/s). This encompasses a wide variety of airflows: automobile and train motions, light aircraft, landing and takeoff of high-speed aircraft, most pipe flows, and turbomachinery at moderate rotational speeds. Further, it is clear that almost all liquid flows are incompressible, since flow velocities are small and the speed of sound is very large.[3]

[3]An exception occurs in geophysical flows, where a density change is imposed thermally or mechanically rather than by the flow conditions themselves. An example is fresh water layered upon saltwater or warm air layered upon cold air in the atmosphere. We say that the fluid is *stratified*, and we must account for vertical density changes even if the velocities are small.

This chapter treats compressible flows, which have Mach numbers greater than about 0.3 and thus exhibit nonnegligible density changes. If the density change is significant, it follows from the equation of state that the temperature and pressure changes are also substantial. Large temperature changes imply that the energy equation can no longer be neglected. Therefore the work is doubled from two basic equations to four

1. Continuity equation
2. Momentum equation
3. Energy equation
4. Equation of state

to be solved simultaneously for four unknowns: pressure, density, temperature, and flow velocity (p, ρ, T, V). Thus the general theory of compressible flow is quite complicated, and we try here to make further simplifications, especially by assuming a reversible adiabatic or *isentropic* flow.

6.1.1 The Mach Number:

The Mach number is the dominant parameter in compressible-flow analysis, with different effects depending upon its magnitude. Aerodynamicists especially make a distinction between the various ranges of Mach number, and the following rough classifications are commonly used:

$\mathrm{Ma} < 0.3$:	*incompressible flow*, where density effects are negligible.
$0.3 < \mathrm{Ma} < 0.8$:	*subsonic flow*, where density effects are important but no shock waves appear.
$0.8 < \mathrm{Ma} < 1.2$:	*transonic flow*, where shock waves first appear, dividing subsonic and supersonic regions of the flow. Powered flight in the transonic region is difficult because of the mixed character of the flow field.
$1.2 < \mathrm{Ma} < 3.0$:	*supersonic flow*, where shock waves are present but there are no subsonic regions.
$3.0 < \mathrm{Ma}$:	*hypersonic flow* [13], where shock waves and other flow changes are especially strong.

The numerical values listed above are only rough guides. These five categories of flow are appropriate to external high-speed aerodynamics. For internal (duct) flows, the most important question is simply whether the flow is subsonic (Ma $<$ 1) or supersonic (Ma $>$ 1), because the effect of area changes reverses, as we show in Sec. 9.4. Since supersonic-flow effects may go against intuition, you should study these differences carefully.

6.1.2 The Specific-Heat Ratio:

In addition to geometry and Mach number, compressible-flow calculations also depend upon a second dimensionless parameter, the *specific-heat ratio* of the gas:

$$k = \frac{c_p}{c_v} \tag{6.1}$$

Earlier, in parts 1 and 4, we used the same symbol k to denote the thermal conductivity of a fluid. We apologize for the duplication; thermal conductivity does not appear in these later chapters of the text.

Recall from Fig. (a) that k for the common gases decreases slowly with temperature and lies between 1.0 and 1.7. Variations in k have only a slight effect upon compressible-flow computations, and air, $k \approx 1.40$, is the dominant fluid of interest. Therefore, although we assign some problems involving, e.g., steam and CO_2 and helium, the compressible-flow tables in App. B are based solely upon the single value $k = 1.40$ for air.

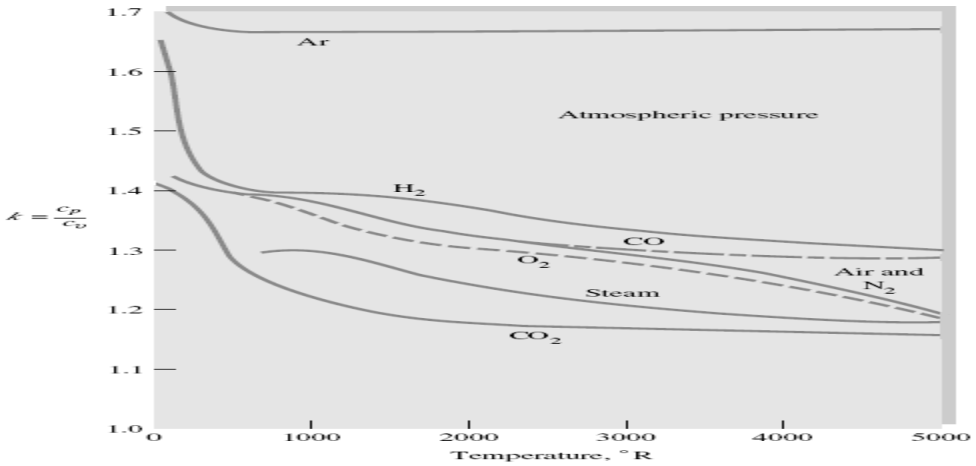

Fig. (a) Specific-heat ratio of eight common gases as a function of temperature. *(Data from Ref. 12.)*

This text contains only a single chapter on compressible flow, but, as usual, whole books have been written on the subject. References 1 to 6, 26, 29, and 33 are introductory, fairly elementary treatments, while Refs. 7 to 14, 27 to 28, 31 to 32, and 35 are advanced. From time to time we shall defer some specialized topic to these texts.

We note in passing that there are at least two flow patterns which depend strongly upon very small density differences, acoustics, and natural convection. Acoustics [9, 14] is the study of sound-wave propagation, which is accompanied by extremely small changes in density, pressure, and temperature. Natural convection is the gentle circulating pattern set up by buoyancy forces in a fluid stratified by uneven heating or uneven concentration of dissolved materials. Here we are concerned only with steady compressible flow where the fluid velocity is of magnitude comparable to that of the speed of sound.

6.1.3 The Perfect Gas Relations:

In principle, compressible-flow calculations can be made for any fluid equation of state, and we shall assign problems involving the steam tables [15], the gas tables [16], and liquids [Eq.(g)].

{The density of a liquid usually decreases slightly with temperature and increases moderately with pressure. If we neglect the temperature effect, an empirical pressure-density relation for a liquid is

$$\frac{p}{p_a} \approx (B + 1)\left(\frac{\rho}{\rho_a}\right)^n - B \tag{g}$$

where B and n are dimensionless parameters which vary slightly with temperature and p_a and ρ_a are standard atmospheric values. Water can be fitted approximately to the values $B \approx 3000$ and $n \approx 7$.

Seawater is a variable mixture of water and salt and thus requires three thermodynamic properties to define its state. These are normally taken as pressure, temperature, and the *salinity* $\hat{S}$, defined as the weight of the dissolved salt divided by the weight of the mixture. The average salinity of seawater is 0.035, usually written as 35 parts per 1000, or 35 ‰. The average density of seawater is 2.00 slugs/ft^3. Strictly speaking, seawater has three specific heats, all approximately equal to the value for pure water of 25,200 ft^2/(s^2 · °R) = 4210 m^2/(s^2 · K).}

But in fact most elementary treatments are confined to the perfect gas with constant specific heats

$$p = \rho RT \qquad R = c_p - c_v = \text{const} \qquad k = \frac{c_p}{c_v} = \text{const} \tag{6.2}$$

For all real gases, c_p, c_v, and k vary with temperature but only moderately; for example, c_p of air increases 30 percent as temperature increases from 0 to 5000°F. Since we rarely deal with such large temperature changes, it is quite reasonable to assume constant specific heats.

Recall from Sec. 1.6 that the gas constant is related to a universal constant Λ divided by the gas molecular weight

$$R_{\text{gas}} = \frac{\Lambda}{M_{\text{gas}}} \tag{6.3}$$

where $\Lambda = 49{,}720 \text{ ft}^2/(\text{s}^2 \cdot {}^\circ\text{R}) = 8314 \text{ m}^2/(\text{s}^2 \cdot \text{K})$

For air, $M = 28.97$, and we shall adopt the following property values for air throughout this chapter: $R = 1717 \text{ ft}^2/(\text{s}^2 \cdot {}^\circ\text{R}) = 287 \text{ m}^2/(\text{s}^2 \cdot \text{K})$ $\qquad k = 1.400$

$$c_v = \frac{R}{k-1} = 4293 \text{ ft}^2/(\text{s}^2 \cdot {}^\circ\text{R}) = 718 \text{ m}^2/(\text{s}^2 \cdot \text{K}) \tag{6.4}$$

$$c_p = \frac{kR}{k-1} = 6010 \text{ ft}^2/(\text{s}^2 \cdot {}^\circ\text{R}) = 1005 \text{ m}^2/(\text{s}^2 \cdot \text{K})$$

Experimental values of k for eight common gases were shown in Fig.(a) . From this figure and the molecular weight, the other properties can be computed, as in Eqs. (6.4).

The changes in the internal energy $\hat{u}$ and enthalpy h of a perfect gas are computed for constant specific heats as

$$\hat{u}_2 - \hat{u}_1 = c_v(T_2 - T_1) \qquad h_2 - h_1 = c_p(T_2 - T_1) \tag{6.5}$$

For variable specific heats one must integrate $\hat{u} = \int c_v \, dT$ and $h = \int c_p \, dT$ or use the gas tables [16]. Most modern thermodynamics texts now contain software for evaluating properties of nonideal gases [17].

6.1.4 The Isentropic Process:

The isentropic approximation is common in compressible-flow theory. We compute the entropy change from the first and second laws of thermodynamics for a pure substance [17 or 18]

$$T\,ds = dh - \frac{dp}{\rho} \tag{6.6}$$

Introducing $dh = c_p \, dT$ for a perfect gas and solving for ds, we substitute $\rho T = p/R$ from the perfect-gas law and obtain

$$\int_1^2 ds = \int_1^2 c_p \frac{dT}{T} - R \int_1^2 \frac{dp}{p} \tag{6.7}$$

If c_p is variable, the gas tables will be needed, but for constant c_p we obtain the analytic results

$$s_2 - s_1 = c_p \ln \frac{T_2}{T_1} - R \ln \frac{p_2}{p_1} = c_v \ln \frac{T_2}{T_1} - R \ln \frac{\rho_2}{\rho_1} \tag{6.8}$$

Equations (6.8) are used to compute the entropy change across a shock wave (Sec. 6.5), which is an irreversible process.

For isentropic flow, we set $s_2 = s_1$ and obtain the interesting power-law relations for an isentropic perfect gas

$$\frac{p_2}{p_1} = \left(\frac{T_2}{T_1}\right)^{k/(k-1)} = \left(\frac{\rho_2}{\rho_1}\right)^k \tag{6.9}$$

These relations are used in Sec. 6.3.

Example 6.1:

Argon flows through a tube such that its initial condition is $p_1 = 1.7$ MPa and $\rho_1 = 18 \text{ kg/m}^3$ and its final condition is $p_2 = 248$ kPa and $T_2 = 400$ K. Estimate (*a*) the initial temperature, (*b*) the final density, (*c*) the change in enthalpy, and (*d*) the change in entropy of the gas.

Solution

From Table A.4 for argon, $R = 208 \text{ m}^2/(\text{s}^2 \cdot \text{K})$ and $k = 1.67$. Therefore estimate its specific heat at constant pressure from Eq. (6.4)

$$c_p = \frac{kR}{k-1} = \frac{1.67(208)}{1.67-1} \approx 519 \text{ m}^2/(\text{s}^2 \cdot \text{K})$$

The initial temperature and final density are estimated from the ideal gas law, Eq. (6.2)

$$T_1 = \frac{p_1}{\rho_1 R} = \frac{1.7 \text{ E6 N/m}^2}{(18 \text{ kg/m}^3)[208 \text{ m}^2/(\text{s}^2 \cdot \text{K})]} = 454 \text{ K} \qquad \textit{Ans. (a)}$$

$$\rho_2 = \frac{p_2}{T_2 R} = \frac{248 \text{ E3 N/m}^2}{(400 \text{ K})[208 \text{ m}^2/(\text{s}^2 \cdot \text{K})]} = 2.98 \text{ kg/m}^3 \qquad \textit{Ans. (b)}$$

From Eq. (6.5) the enthalpy change is

$$h_2 - h_1 = c_p(T_2 - T_1) = 519(400 - 454) \approx -28{,}000 \text{ J/kg (or m}^2/\text{s}^2) \qquad \textit{Ans. (c)}$$

The argon temperature and enthalpy decrease as we move down the tube. Actually, there may not be any external cooling; i.e., the fluid enthalpy may be converted by friction to increased kinetic energy (Sec. 6.7).

Finally, the entropy change is computed from Eq. (6.8): $s_2 - s_1 = c_p \ln \frac{T_2}{T_1} - R \ln \frac{p_2}{p_1}$

$$= 519 \ln \frac{400}{454} - 208 \ln \frac{0.248 \text{ E6}}{1.7 \text{ E6}}$$

$$= -66 + 400 \approx 334 \text{ m}^2/(\text{s}^2 \cdot \text{K}) \qquad \textit{Ans. (d)}$$

The fluid entropy has increased. If there is no heat transfer, this indicates an irreversible process. Note that entropy has the same units as the gas constant and specific heat.

This problem is not just arbitrary numbers. It correctly simulates the behavior of argon moving subsonically through a tube with large frictional effects (Sec. 6.7).

Example 6.2:

Air flows steadily between two sections in a long straight portion of 4-in.-diameter pipe as is indicated in Fig. E6.2 . The uniformly distributed temperature and pressure at each section are $T_1 = 540\ ^\circ\text{R}$, $p_1 = 100$ psia, and $T_2 = 453\ ^\circ\text{R}$, $p_2 = 18.4$ psia. Calculate the (a) change in internal energy between sections (1) and (2), (b) change in enthalpy between sections (1) and (2), and (c) change in density between sections (1) and (2).

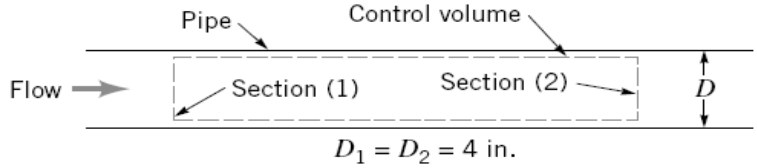

■ FIGURE E 6.2

Solution:

(a) Assuming air behaves as an ideal gas, we can evaluate the change in internal energy between sections (1) and (2). Thus

$$\breve{u}_2 - \breve{u}_1 = c_v(T_2 - T_1) \qquad \textbf{(1)}$$

we have

$$c_v = \frac{R}{k-1} \qquad \textbf{(2)}$$

and from Table 1.7, $R = 1716\ (\text{ft} \cdot \text{lb})/(\text{slug} \cdot {}^\circ\text{R})$ and $k = 1.4$. Throughout this book, we use the nominal values of k for common gases listed in Tables 1.7 and 1.8 and consider these values as being representative. From Eq. 2 we obtain

$$c_v = \frac{1716}{(1.4-1)}\ (\text{ft} \cdot \text{lb})/(\text{slug} \cdot {}^\circ\text{R}) = 4290\ (\text{ft} \cdot \text{lb})/(\text{slug} \cdot {}^\circ\text{R}) \qquad \textbf{(3)}$$

Combining Eqs. 1 and 3 yields

$$\breve{u}_2 - \breve{u}_1 = c_v(T_2 - T_1) = 4290\ (\text{ft} \cdot \text{lb})/(\text{slug} \cdot {}^\circ\text{R})$$
$$\times (453\ ^\circ\text{R} - 540\ ^\circ\text{R}) = -3.73 \times 10^5 \text{ ft} \cdot \text{lb/slug} \qquad \textbf{(Ans)}$$

(b) For enthalpy change we use $\breve{h}_2 - \breve{h}_1 = c_p(T_2 - T_1)$ **(4)**

Table A.4 Properties of Common Gases at 1 atm and 20°C (68°F)

Gas	Molecular weight	R, $m^2/(s^2 \cdot K)$	ρg, N/m^3	μ, $N \cdot s/m^2$	Specific-heat ratio	Power-law exponent $n^\dagger$
H_2	2.016	4124	0.822	9.05 E-6	1.41	0.68
He	4.003	2077	1.63	1.97 E-5	1.66	0.67
H_2O	18.02	461	7.35	1.02 E-5	1.33	1.15
Ar	39.944	208	16.3	2.24 E-5	1.67	0.72
Dry air	28.96	287	11.8	1.80 E-5	1.40	0.67
CO_2	44.01	189	17.9	1.48 E-5	1.30	0.79
CO	28.01	297	11.4	1.82 E-5	1.40	0.71
N_2	28.02	297	11.4	1.76 E-5	1.40	0.67
O_2	32.00	260	13.1	2.00 E-5	1.40	0.69
NO	30.01	277	12.1	1.90 E-5	1.40	0.78
N_2O	44.02	189	17.9	1.45 E-5	1.31	0.89
Cl_2	70.91	117	28.9	1.03 E-5	1.34	1.00
CH_4	16.04	518	6.54	1.34 E-5	1.32	0.87

†The power-law curve fit, Eq. (1.27), $\mu/\mu_{293K} \approx (T/293)^n$, fits these gases to within ±4 percent in the range $250 \le T \le 1000$ K. The temperature must be in kelvins.

TABLE 1.7

Approximate Physical Properties of Some Common Gases at Standard Atmospheric Pressure (BG Units)

Gas	Temperature (°F)	Density, ρ (slugs/ft^3)	Specific Weight, γ (lb/ft^3)	Dynamic Viscosity, μ (lb · s/ft^2)	Kinematic Viscosity, ν (ft^2/s)	Gas Constant,[a] R (ft · lb/slug · °R)	Specific Heat Ratio,[b] k
Air (standard)	59	2.38 E − 3	7.65 E − 2	3.74 E − 7	1.57 E − 4	1.716 E + 3	1.40
Carbon dioxide	68	3.55 E − 3	1.14 E − 1	3.07 E − 7	8.65 E − 5	1.130 E + 3	1.30
Helium	68	3.23 E − 4	1.04 E − 2	4.09 E − 7	1.27 E − 3	1.242 E + 4	1.66
Hydrogen	68	1.63 E − 4	5.25 E − 3	1.85 E − 7	1.13 E − 3	2.466 E + 4	1.41
Methane (natural gas)	68	1.29 E − 3	4.15 E − 2	2.29 E − 7	1.78 E − 4	3.099 E + 3	1.31
Nitrogen	68	2.26 E − 3	7.28 E − 2	3.68 E − 7	1.63 E − 4	1.775 E + 3	1.40
Oxygen	68	2.58 E − 3	8.31 E − 2	4.25 E − 7	1.65 E − 4	1.554 E + 3	1.40

[a]Values of the gas constant are independent of temperature.

[b]Values of the specific heat ratio depend only slightly on temperature.

TABLE 1.8

Approximate Physical Properties of Some Common Gases at Standard Atmospheric Pressure (SI Units)

Gas	Temperature (°C)	Density, ρ (kg/m^3)	Specific Weight, γ (N/m^3)	Dynamic Viscosity, μ (N · s/m^2)	Kinematic Viscosity, ν (m^2/s)	Gas Constant,[a] R (J/kg · K)	Specific Heat Ratio,[b] k
Air (standard)	15	1.23 E + 0	1.20 E + 1	1.79 E − 5	1.46 E − 5	2.869 E + 2	1.40
Carbon dioxide	20	1.83 E + 0	1.80 E + 1	1.47 E − 5	8.03 E − 6	1.889 E + 2	1.30
Helium	20	1.66 E − 1	1.63 E + 0	1.94 E − 5	1.15 E − 4	2.077 E + 3	1.66
Hydrogen	20	8.38 E − 2	8.22 E − 1	8.84 E − 6	1.05 E − 4	4.124 E + 3	1.41
Methane (natural gas)	20	6.67 E − 1	6.54 E + 0	1.10 E − 5	1.65 E − 5	5.183 E + 2	1.31
Nitrogen	20	1.16 E + 0	1.14 E + 1	1.76 E − 5	1.52 E − 5	2.968 E + 2	1.40
Oxygen	20	1.33 E + 0	1.30 E + 1	2.04 E − 5	1.53 E − 5	2.598 E + 2	1.40

[a]Values of the gas constant are independent of temperature.

[b]Values of the specific heat ratio depend only slightly on temperature.

where since $k = c_p/c_v$ we obtain

$$c_p = kc_v = (1.4)[4290\ (\text{ft}\cdot\text{lb})/(\text{slug}\cdot{}^\circ\text{R})] = 6006\ (\text{ft}\cdot\text{lb})/(\text{slug}\cdot{}^\circ\text{R}) \quad (5)$$

From Eqs. 4 and 5 we obtain

$$\breve{h}_2 - \breve{h}_1 = c_p(T_2 - T_1) = 6006\ (\text{ft}\cdot\text{lb})/(\text{slug}\cdot{}^\circ\text{R}) \times (453\ {}^\circ\text{R} - 540\ {}^\circ\text{R}) = -5.22 \times 10^5\ \text{ft}\cdot\text{lb/slug} \quad \text{(Ans)}$$

(c) For density change we use the ideal gas equation of state to get

$$\rho_2 - \rho_1 = \frac{p_2}{RT_2} - \frac{p_1}{RT_1} = \frac{1}{R}\left(\frac{p_2}{T_2} - \frac{p_1}{T_1}\right) \quad (6)$$

Using the pressures and temperatures given in the problem statement we calculate from Eq. 6

$$\rho_2 - \rho_1 = \frac{1}{1716\ (\text{ft}\cdot\text{lb})/(\text{slug}\cdot{}^\circ\text{R})} \times \left[\frac{(18.4\ \text{psia})(144\ \text{in.}^2/\text{ft}^2)}{453\ {}^\circ\text{R}} - \frac{(100\ \text{psia})(144\ \text{in.}^2/\text{ft}^2)}{540\ {}^\circ\text{R}}\right]$$

or

$$\rho_2 - \rho_1 = -0.0121\ \text{slug/ft}^3 \quad \text{(Ans)}$$

This is a significant change in density when compared with the upstream density

$$\rho_1 = \frac{p_1}{RT_1} = \frac{(100\ \text{psia})(144\ \text{in.}^2/\text{ft}^2)}{[1716\ (\text{ft}\cdot\text{lb})/(\text{slug}\cdot{}^\circ\text{R})](540\ {}^\circ\text{R})} = 0.0155\ \text{slug/ft}^3$$

Compressibility effects are important for this flow.

For compressible flows, changes in the thermodynamic property *entropy*, s, are important. For any pure substance including ideal gases, the "first $T\,ds$ equation" is

$$T\,ds = d\breve{u} + p\,d\left(\frac{1}{\rho}\right) \quad (6.10)$$

The fluid property enthalpy, $\breve{h}$, is defined as: $\breve{h} = \breve{u} + \dfrac{p}{\rho}$

where T is absolute temperature, s is entropy, $\breve{u}$ is internal energy, p is absolute pressure, and ρ is density. Differentiating the above equation leads to

$$d\breve{h} = d\breve{u} + p\,d\left(\frac{1}{\rho}\right) + \left(\frac{1}{\rho}\right)dp \quad (6.11)$$

By combining Eqs. 6.10 and 6.11, we obtain

$$T\,ds = d\breve{h} - \left(\frac{1}{\rho}\right)dp \quad (6.12)$$

Equation 6.12 is often referred to as the "second $T\,ds$ equation." For an ideal gas,

$$ds = c_v\frac{dT}{T} + \frac{R}{1/\rho}\,d\left(\frac{1}{\rho}\right) \quad (6.13)$$

and

$$ds = c_p\frac{dT}{T} - R\frac{dp}{p} \quad (6.14)$$

If c_p and c_v are assumed to be constant for a given gas, Eqs. 6.13 and 6.14 can be integrated to get

$$\boxed{s_2 - s_1 = c_v \ln\frac{T_2}{T_1} + R\ln\frac{\rho_1}{\rho_2}} \quad (6.15)$$

and

$$\boxed{s_2 - s_1 = c_p \ln\frac{T_2}{T_1} - R\ln\frac{p_2}{p_1}} \quad (6.16)$$

Equations 6.15 and 6.16 allow us to calculate the change of entropy of an ideal gas flowing from one section to another with constant specific heat values (c_p and c_v).

Example 6.3:

For the air flow of **Example** 6.2 , calculate the change in entropy, $s_2 - s_1$, between sections (1) and (2).

Solution:

Assuming that the flowing air in Fig. E 6.2 behaves as an ideal gas, we can calculate the entropy change between sections by using either Eq. 6.15 or Eq. 6.16 . We use both to demonstrate that the same result is obtained either way.

From Eq. 6.15 ,
$$s_2 - s_1 = c_v \ln \frac{T_2}{T_1} + R \ln \frac{\rho_1}{\rho_2} \tag{1}$$

To evaluate $s_2 - s_1$ from Eq. 1 we need the density ratio, ρ_1/ρ_2, which can be obtained from the ideal gas equation of state as
$$\frac{\rho_1}{\rho_2} = \left(\frac{p_1}{T_1}\right)\left(\frac{T_2}{p_2}\right) \tag{2}$$

and thus from Eqs. 1 and 2,
$$s_2 - s_1 = c_v \ln \frac{T_2}{T_1} + R \ln \left[\left(\frac{p_1}{T_1}\right)\left(\frac{T_2}{p_2}\right)\right] \tag{3}$$

By substituting values already identified in the Example 6.2 problem statement and solution into Eq. 3 we get
$$s_2 - s_1 = [4290\ (\text{ft} \cdot \text{lb})/(\text{slug} \cdot {}^\circ\text{R})] \ln\left(\frac{453\ {}^\circ\text{R}}{540\ {}^\circ\text{R}}\right) + [1716\ (\text{ft} \cdot \text{lb})/(\text{slug} \cdot {}^\circ\text{R})] \ln\left[\left(\frac{100\ \text{psia}}{540\ {}^\circ\text{R}}\right)\left(\frac{453\ {}^\circ\text{R}}{18.4\ \text{psia}}\right)\right]$$

or $s_2 - s_1 = 1850\ (\text{ft} \cdot \text{lb})/(\text{slug} \cdot {}^\circ\text{R})$ **(Ans)**

From Eq. 6.16 ,
$$s_2 - s_1 = c_p \ln \frac{T_2}{T_1} - R \ln \frac{p_2}{p_1} \tag{4}$$

By substituting known values into Eq. 4 we obtain
$$s_2 - s_1 = [6006\ (\text{ft} \cdot \text{lb})/(\text{slug} \cdot {}^\circ\text{R})] \ln\left(\frac{453\ {}^\circ\text{R}}{540\ {}^\circ\text{R}}\right) - [1716\ (\text{ft} \cdot \text{lb})/(\text{slug} \cdot {}^\circ\text{R})] \ln\left(\frac{18.4\ \text{psia}}{100\ \text{psia}}\right)$$

or $s_2 - s_1 = 1850\ (\text{ft} \cdot \text{lb})/(\text{slug} \cdot {}^\circ\text{R})$ **(Ans)**

As anticipated, both Eqs. 6.15 and 6.16 yield the same result for the entropy change, $s_2 - s_1$.

Note that since the ideal gas equation of state was used in the derivation of the entropy difference equations, both the pressures and temperatures used must be absolute.

++++++++++++++++++++++++++++++

The second law of thermodynamics requires that the adiabatic and frictionless flow of any fluid results in $ds = 0$ or $s_2 - s_1 = 0$. Constant entropy flow is called *isentropic* flow. For isentropic flow of an ideal gas with constant c_p and c_v, we get from Eqs.6.15 and 6.16:
$$c_v \ln \frac{T_2}{T_1} + R \ln \frac{\rho_1}{\rho_2} = c_p \ln \frac{T_2}{T_1} - R \ln \frac{p_2}{p_1} = 0 \tag{6.17}$$

By combining Eq. 6.17 with Eqs. 6.2 and 6.4 we obtain
$$\left(\frac{T_2}{T_1}\right)^{k/(k-1)} = \left(\frac{\rho_2}{\rho_1}\right)^k = \left(\frac{p_2}{p_1}\right) \tag{6.18}$$

which is a useful relationship between temperature, density, and pressure for the isentropic flow of an ideal gas. From Eq. 6.18 we can conclude that $\frac{p}{\rho^k} = \text{constant}$

6.2 .1 The Mach Number and Speed of Sound:

The Mach number, Ma, was introduced in part (1) and sec.6.1 as a dimensionless measure of compressibility in a fluid flow. In this and subsequent sections, we develop some useful relationships involving the Mach number. The Mach number is defined as the ratio of the value of the local flow velocity, V, to the local speed of sound, c (some times we use a not c).

In other words, $\text{Ma} = \text{V/c}$ (or $\text{Ma} = \text{V/a}$)

What we perceive as sound generally consists of weak pressure pulses that move through air. When our ear drums respond to a succession of moving pressure pulses, we hear sounds.

To better understand the notion of speed of sound, we analyze the one-dimensional fluid mechanics of an infinitesimally thin, weak pressure pulse moving at the speed of sound through a fluid at rest (see Fig. 6.1 a). Ahead of the pressure pulse, the fluid velocity is zero and the fluid pressure and density are p and ρ. Behind the pressure pulse, the fluid velocity has changed by an amount δV, and the pressure and density of the fluid have also changed by amounts δp and $\delta\rho$. We select an infinitesimally thin control volume that moves with the pressure pulse as is sketched in Fig. 6.1 a . The speed of the weak pressure pulse is considered constant and in one direction only; thus, our control volume is inertial.

For an observer moving with this control volume (Fig. 6.1 b), it appears as if fluid is entering the control volume through surface area A with speed c at pressure p and density ρ and leaving the control volume through surface area A with speed $c - \delta V$, pressure $p + \delta p$, and density $\rho + \delta\rho$. When the continuity equation is applied to the flow through this control volume, the result is

$$\rho Ac = (\rho + \delta\rho)A(c - \delta V) \qquad (6.19)$$

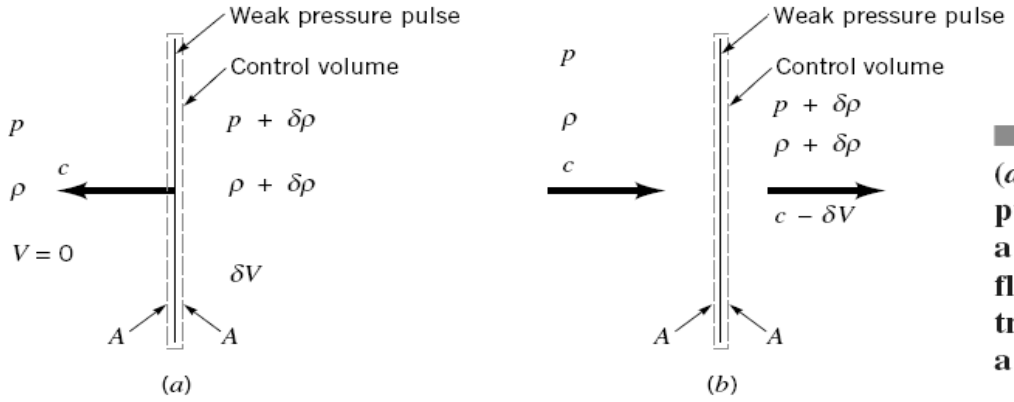

■ **FIGURE 6.1**
(*a*) Weak pressure pulse moving through a fluid at rest. (*b*) The flow relative to a control volume containing a weak pressure pulse.

or $$\rho c = \rho c - \rho\,\delta V + c\,\delta\rho - (\delta\rho)(\delta V) \qquad (6.20)$$

Since $(\delta\rho)(\delta V)$ is much smaller than the other terms in Eq. 6.20 , we drop it from furuner consideration and keep

$$\rho\,\delta V = c\,\delta\rho \qquad (6.21)$$

The linear momentum equation can also be applied to the flow through the control volume of Fig. 6.1 b . The result ıs

$$-c\rho cA + (c - \delta V)(\rho + \delta\rho)(c - \delta V)A = pA - (p + \delta p)A \qquad (6.22)$$

Note that any frictional forces are considered as being negligibly small. We again neglect higher order terms [such as $(\delta V)^2$ compared to $c\,\delta V$, for example] and combine Eqs. 6.19 and 6.22 to get

$$-c\rho cA + (c - \delta V)\rho Ac = -\delta pA$$

or $$\rho\delta V = \frac{\delta p}{c} \qquad (6.23)$$

From Eqs. 6.21 (continuity) and 6.23 (linear momentum) we obtain $c^2 = \dfrac{\delta p}{\delta\rho}$

or $$c = \sqrt{\frac{\delta p}{\delta\rho}} \qquad (6.24)$$

This expression for the speed of sound results from application of the conservation of mass and conservation of linear momentum principles to the flow through the control volume of Fig. 6.1 b.

The conservation of energy principle can also be applied to the flow through the control volume of Fig. 6.1 b . If the energy equation is used for the flow through this control volume, the result is

$$\frac{\delta p}{\rho} + \delta\left(\frac{V^2}{2}\right) + g\,\delta z = \delta(\text{loss}) \qquad (6.25)$$

For gas flow we can consider $g\,\delta z$ as being negligibly small in comparison to the other terms in the equation. Also, if we assume that the flow is frictionless, then $\delta(\text{loss}) = 0$ and Eq. 6.25 becomes

$$\frac{\delta p}{\rho} + \frac{(c - \delta V)^2}{2} - \frac{c^2}{2} = 0$$

or, neglecting $(\delta V)^2$ compared to $c\,\delta V$, we obtain $\rho\,\delta V = \dfrac{\delta p}{c}$ (6.26)

By combining Eqs. 6.21 (continuity) and 6.26 (energy) we again find that $c = \sqrt{\dfrac{\delta p}{\delta \rho}}$

which is identical to Eq. 6.24 . Thus, the conservation of linear momentum and the conservation of energy principles lead to the same result. If we further assume that the frictionless flow through the control volume of Fig. 6.1 b is adiabatic (no heat transfer), then the flow is isentropic. In the limit, as δp becomes vanishingly small ($\delta p \to \partial p \to 0$)

$$c = \sqrt{\left(\frac{\partial p}{\partial \rho}\right)_s} \qquad (6.27)$$

where the subscript s is used to designate that the partial differentiation occurs at constant entropy.

Equation 6.27 suggests to us that we can calculate the speed of sound by determining the partial derivative of pressure with respect to density at constant entropy. For the isentropic flow of an ideal gas (with constant c_p and c_v), we learned earlier (Eq. 6.18) that

$$p = (\text{constant})(\rho^k)$$

and thus

$$\left(\frac{\partial p}{\partial \rho}\right)_s = (\text{constant})\,k\rho^{k-1} = \frac{p}{\rho^k}\,k\rho^{k-1} = \frac{p}{\rho}\,k = RTk \qquad (6.28)$$

Thus, for an ideal gas

$$c = \sqrt{RTk} \qquad (6.29)$$

More generally, the bulk modulus of elasticity, E_v, of any fluid including liquids is defined as

$$E_v = \frac{dp}{d\rho/\rho} = \rho\left(\frac{\partial p}{\partial \rho}\right)_s \qquad (6.30)$$

Thus, in general, from Eqs. 6.27 and 6.30,

$$c = \sqrt{\frac{E_v}{\rho}} \qquad (6.31)$$

Values of the speed of sound are tabulated in **Tables B.1** and **B.2** for water and in **Tables B.3** and **B.4** for air. From experience we know that air is more easily compressed than water. Note from the values of c in Tables B.1 through B.4 that the speed of sound in air is much less than it is in water. From Eq. 6.30 , we can conclude that if a fluid is truly incompressible, its bulk modulus would be infinitely large, as would be the speed of sound in that fluid. Thus, an incompressible flow must be considered an idealized approximation of reality.

The speed of sound increases as the square root of the absolute temperature. For air, with $k = 1.4$ and $R = 1717$ (ft^2/s^2·°R), an easily memorized dimensional formula is

$$a\ (\text{ft/s}) \approx 49[T\ (^\circ\text{R})]^{1/2}$$

$$a\ (\text{m/s}) \approx 20[T\ (\text{K})]^{1/2}$$

At sea-level standard temperature, 60°F = 520°R, $a = 1117$ ft/s. This decreases in the upper atmosphere, which is cooler; at 50,000-ft standard altitude, $T = -69.7^\circ\text{F} = 389.9^\circ\text{R}$ and $a = 49(389.9)^{1/2} = 968$ ft/s, or 13 percent less.

Some representative values of sound speed in various materials are given in Table 6.1. For liquids and solids it is common to define the *bulk modulus* K of the material (or E_v)

$$K = -\mathcal{V}\left.\frac{\partial p}{\partial \mathcal{V}}\right|_s = \rho\left.\frac{\partial p}{\partial \rho}\right|_s$$

For example, at standard conditions, the bulk modulus of carbon tetrachloride is 163,000 lbf/in^2 absolute, and its density is 3.09 slugs/ft^3. Its speed of sound is therefore $[163{,}000(144)/3.09]^{1/2} = 2756$ ft/s, or 840 m/s. Steel has a bulk modulus of about 29×10^6 lbf/in^2 absolute and water about 320×10^3 lbf/in^2 absolute, or 90 times less.

For solids, it is sometimes assumed that the bulk modulus is approximately equivalent to Young's modulus of elasticity E, but in fact their ratio depends upon Poisson's ratio σ

$$\frac{E}{K} = 3(1 - 2\sigma)$$

The two are equal for $\sigma = \frac{1}{3}$, which is approximately the case for many common metals such as steel and aluminum.

TABLE B.1

Physical Properties of Water (BG Units)[a]

Temperature (°F)	Density, ρ (slugs/ft^3)	Specific Weight[b], γ (lb/ft^3)	Dynamic Viscosity, μ (lb·s/ft^2)	Kinematic Viscosity, ν (ft^2/s)	Surface Tension[c], σ (lb/ft)	Vapor Pressure, p_v [lb/in^2(abs)]	Speed of Sound[d], c (ft/s)
32	1.940	62.42	3.732 E − 5	1.924 E − 5	5.18 E − 3	8.854 E − 2	4603
40	1.940	62.43	3.228 E − 5	1.664 E − 5	5.13 E − 3	1.217 E − 1	4672
50	1.940	62.41	2.730 E − 5	1.407 E − 5	5.09 E − 3	1.781 E − 1	4748
60	1.938	62.37	2.344 E − 5	1.210 E − 5	5.03 E − 3	2.563 E − 1	4814
70	1.936	62.30	2.037 E − 5	1.052 E − 5	4.97 E − 3	3.631 E − 1	4871
80	1.934	62.22	1.791 E − 5	9.262 E − 6	4.91 E − 3	5.069 E − 1	4819
90	1.931	62.11	1.500 E − 5	8.233 E − 6	4.86 E − 3	6.979 E − 1	4960
100	1.927	62.00	1.423 E − 5	7.383 E − 6	4.79 E − 3	9.493 E − 1	4995
120	1.918	61.71	1.164 E − 5	6.067 E − 6	4.67 E − 3	1.692 E + 0	5049
140	1.908	61.38	9.743 E − 6	5.106 E − 6	4.53 E − 3	2.888 E + 0	5091
160	1.896	61.00	8.315 E − 6	4.385 E − 6	4.40 E − 3	4.736 E + 0	5101
180	1.883	60.58	7.207 E − 6	3.827 E − 6	4.26 E − 3	7.507 E + 0	5195
200	1.869	60.12	6.342 E − 6	3.393 E − 6	4.12 E − 3	1.152 E + 1	5089
212	1.860	59.83	5.886 E − 6	3.165 E − 6	4.04 E − 3	1.469 E + 1	5062

[a]Based on data from *Handbook of Chemistry and Physics*, 69th Ed., CRC Press, 1988. Where necessary, values obtained by interpolation.

[b]Density and specific weight are related through the equation $\gamma = \rho g$. For this table, $g = 32.174$ ft/s^2.

[c]In contact with air.

[d]From R. D. Blevins, *Applied Fluid Dynamics Handbook*, Van Nostrand Reinhold Co., Inc., New York, 1984.

TABLE B.2

Physical Properties of Water (SI Units)[a]

Temperature (°C)	Density, ρ (kg/m^3)	Specific Weight[b], γ (kN/m^3)	Dynamic Viscosity, μ (N·s/m^2)	Kinematic Viscosity, ν (m^2/s)	Surface Tension[c], σ (N/m)	Vapor Pressure, p_v [N/m^2(abs)]	Speed of Sound[d], c (m/s)
0	999.9	9.806	1.787 E − 3	1.787 E − 6	7.56 E − 2	6.105 E + 2	1403
5	1000.0	9.807	1.519 E − 3	1.519 E − 6	7.49 E − 2	8.722 E + 2	1427
10	999.7	9.804	1.307 E − 3	1.307 E − 6	7.42 E − 2	1.228 E + 3	1447
20	998.2	9.789	1.002 E − 3	1.004 E − 6	7.28 E − 2	2.338 E + 3	1481
30	995.7	9.765	7.975 E − 4	8.009 E − 7	7.12 E − 2	4.243 E + 3	1507
40	992.2	9.731	6.529 E − 4	6.580 E − 7	6.96 E − 2	7.376 E + 3	1526
50	988.1	9.690	5.468 E − 4	5.534 E − 7	6.79 E − 2	1.233 E + 4	1541
60	983.2	9.642	4.665 E − 4	4.745 E − 7	6.62 E − 2	1.992 E + 4	1552
70	977.8	9.589	4.042 E − 4	4.134 E − 7	6.44 E − 2	3.116 E + 4	1555
80	971.8	9.530	3.547 E − 4	3.650 E − 7	6.26 E − 2	4.734 E + 4	1555
90	965.3	9.467	3.147 E − 4	3.260 E − 7	6.08 E − 2	7.010 E + 4	1550
100	958.4	9.399	2.818 E − 4	2.940 E − 7	5.89 E − 2	1.013 E + 5	1543

[a]Based on data from *Handbook of Chemistry and Physics*, 69th Ed., CRC Press, 1988.

[b]Density and specific weight are related through the equation $\gamma = \rho g$. For this table, $g = 9.807$ m/s^2.

[c]In contact with air.

[d]From R. D. Blevins, *Applied Fluid Dynamics Handbook*, Van Nostrand Reinhold Co., Inc., New York, 1984.

TABLE B.3

Physical Properties of Air at Standard Atmospheric Pressure (BG Units)[a]

Temperature (°F)	Density, ρ (slugs/ft^3)	Specific Weight[b], γ (lb/ft^3)	Dynamic Viscosity, μ (lb·s/ft^2)	Kinematic Viscosity, ν (ft^2/s)	Specific Heat Ratio, k (—)	Speed of Sound, c (ft/s)
−40	2.939 E − 3	9.456 E − 2	3.29 E − 7	1.12 E − 4	1.401	1004
−20	2.805 E − 3	9.026 E − 2	3.34 E − 7	1.19 E − 4	1.401	1028
0	2.683 E − 3	8.633 E − 2	3.38 E − 7	1.26 E − 4	1.401	1051
10	2.626 E − 3	8.449 E − 2	3.44 E − 7	1.31 E − 4	1.401	1062
20	2.571 E − 3	8.273 E − 2	3.50 E − 7	1.36 E − 4	1.401	1074
30	2.519 E − 3	8.104 E − 2	3.58 E − 7	1.42 E − 4	1.401	1085
40	2.469 E − 3	7.942 E − 2	3.60 E − 7	1.46 E − 4	1.401	1096
50	2.420 E − 3	7.786 E − 2	3.68 E − 7	1.52 E − 4	1.401	1106
60	2.373 E − 3	7.636 E − 2	3.75 E − 7	1.58 E − 4	1.401	1117
70	2.329 E − 3	7.492 E − 2	3.82 E − 7	1.64 E − 4	1.401	1128
80	2.286 E − 3	7.353 E − 2	3.86 E − 7	1.69 E − 4	1.400	1138
90	2.244 E − 3	7.219 E − 2	3.90 E − 7	1.74 E − 4	1.400	1149
100	2.204 E − 3	7.090 E − 2	3.94 E − 7	1.79 E − 4	1.400	1159
120	2.128 E − 3	6.846 E − 2	4.02 E − 7	1.89 E − 4	1.400	1180
140	2.057 E − 3	6.617 E − 2	4.13 E − 7	2.01 E − 4	1.399	1200
160	1.990 E − 3	6.404 E − 2	4.22 E − 7	2.12 E − 4	1.399	1220
180	1.928 E − 3	6.204 E − 2	4.34 E − 7	2.25 E − 4	1.399	1239
200	1.870 E − 3	6.016 E − 2	4.49 E − 7	2.40 E − 4	1.398	1258
300	1.624 E − 3	5.224 E − 2	4.97 E − 7	3.06 E − 4	1.394	1348
400	1.435 E − 3	4.616 E − 2	5.24 E − 7	3.65 E − 4	1.389	1431
500	1.285 E − 3	4.135 E − 2	5.80 E − 7	4.51 E − 4	1.383	1509
750	1.020 E − 3	3.280 E − 2	6.81 E − 7	6.68 E − 4	1.367	1685
1000	8.445 E − 4	2.717 E − 2	7.85 E − 7	9.30 E − 4	1.351	1839
1500	6.291 E − 4	2.024 E − 2	9.50 E − 7	1.51 E − 3	1.329	2114

[a]Based on data from R. D. Blevins, *Applied Fluid Dynamics Handbook*, Van Nostrand Reinhold Co., Inc., New York, 1984.
[b]Density and specific weight are related through the equation $\gamma = \rho g$. For this table $g = 32.174$ ft/s^2.

TABLE B.4

Physical Properties of Air at Standard Atmospheric Pressure (SI Units)[a]

Temperature (°C)	Density, ρ (kg/m^3)	Specific Weight[b], γ (N/m^3)	Dynamic Viscosity, μ (N·s/m^2)	Kinematic Viscosity, ν (m^2/s)	Specific Heat Ratio, k (—)	Speed of Sound, c (m/s)
−40	1.514	14.85	1.57 E − 5	1.04 E − 5	1.401	306.2
−20	1.395	13.68	1.63 E − 5	1.17 E − 5	1.401	319.1
0	1.292	12.67	1.71 E − 5	1.32 E − 5	1.401	331.4
5	1.269	12.45	1.73 E − 5	1.36 E − 5	1.401	334.4
10	1.247	12.23	1.76 E − 5	1.41 E − 5	1.401	337.4
15	1.225	12.01	1.80 E − 5	1.47 E − 5	1.401	340.4
20	1.204	11.81	1.82 E − 5	1.51 E − 5	1.401	343.3
25	1.184	11.61	1.85 E − 5	1.56 E − 5	1.401	346.3
30	1.165	11.43	1.86 E − 5	1.60 E − 5	1.400	349.1
40	1.127	11.05	1.87 E − 5	1.66 E − 5	1.400	354.7
50	1.109	10.88	1.95 E − 5	1.76 E − 5	1.400	360.3
60	1.060	10.40	1.97 E − 5	1.86 E − 5	1.399	365.7
70	1.029	10.09	2.03 E − 5	1.97 E − 5	1.399	371.2
80	0.9996	9.803	2.07 E − 5	2.07 E − 5	1.399	376.6
90	0.9721	9.533	2.14 E − 5	2.20 E − 5	1.398	381.7
100	0.9461	9.278	2.17 E − 5	2.29 E − 5	1.397	386.9
200	0.7461	7.317	2.53 E − 5	3.39 E − 5	1.390	434.5
300	0.6159	6.040	2.98 E − 5	4.84 E − 5	1.379	476.3
400	0.5243	5.142	3.32 E − 5	6.34 E − 5	1.368	514.1
500	0.4565	4.477	3.64 E − 5	7.97 E − 5	1.357	548.8
1000	0.2772	2.719	5.04 E − 5	1.82 E − 4	1.321	694.8

[a]Based on data from R. D. Blevins, *Applied Fluid Dynamics Handbook*, Van Nostrand Reinhold Co., Inc., New York, 1984.
[b]Density and specific weight are related through the equation $\gamma = \rho g$. For this table $g = 9.807$ m/s^2.

Table 6.1 Sound Speed of Various Materials at 60°F (15.5°C) and 1 atm

Material	a, ft/s	a, m/s
Gases:		
H_2	4,246	1,294
He	3,281	1,000
Air	1,117	340
Ar	1,040	317
CO_2	873	266
CH_4	607	185
$^{238}UF_6$	297	91
Liquids:		
Glycerin	6,100	1,860
Water	4,890	1,490
Mercury	4,760	1,450
Ethyl alcohol	3,940	1,200
Solids:*		
Aluminum	16,900	5,150
Steel	16,600	5,060
Hickory	13,200	4,020
Ice	10,500	3,200

*Plane waves. Solids also have a *shear-wave speed*.

Example 6.4:

Estimate the speed of sound of carbon monoxide at 200-kPa pressure and 300°C in m/s.

Solution

From Table A.4, for CO, the molecular weight is 28.01 and $k \approx 1.40$. Thus from Eq. (9.3) $R_{CO} = 8314/28.01 = 297\ m^2/(s^2 \cdot K)$, and the given temperature is 300°C + 273 = 573 K. Thus we estimate

$$a_{CO} = (kRT)^{1/2} = [1.40(297)(573)]^{1/2} = 488\ m/s \qquad Ans.$$

Example 6.5:

Verify the speed of sound for air at 0 °C listed in Table B.4.

Solution:

In Table B.4, we find the speed of sound of air at 0 °C given as 331.4 m/s. Assuming that air behaves as an ideal gas, we can calculate the speed of sound as

$$c = \sqrt{RTk} \qquad (1)$$

The value of the gas constant is obtained from Table 1.8 as $R = 286.9\ J/(kg \cdot K)$ and the specific heat ratio is listed in Table B.4 as $k = 1.401$

By substituting values of R, k, and T into Eq. 1 we obtain

$$c = \sqrt{[(286.9)\ J/(kg \cdot K)](273.15K)(1.401)[1(kg \cdot m)/(N \cdot s^2)][1(N \cdot m)/J]} \quad (Ans)$$

$$= 331.4\ m/s$$

The value of the speed of sound calculated with Eq. 6.29 agrees very well with the value of c listed in Table B.4.

****

6.2.2 Example on Compressibility Effects:

One of the main assumptions is that the fluid is incompressible. Although this is reasonable for most liquid flows, it can, in certain instances, introduce considerable errors for gases.

In the previous section, we saw that the stagnation pressure is greater than the static pressure by an amount $\rho V^2/2$, provided that the density remains constant. If this dynamic pressure is not too large compared with the static pressure, the density change between two points is not very large and the flow can be considered incompressible. However, since the dynamic pressure varies as V^2, the error associated with the assumption that a fluid is incompressible increases with the square of the velocity of the fluid. To account for compressibility effects we must return to Eq. 3.6 and properly integrate the term $\int dp/\rho$ when ρ is not constant.

A simple, although specialized, case of compressible flow occurs when the temperature of a perfect gas remains constant along the streamline—isothermal flow. Thus, we consider $p = \rho RT$, where T is constant. (In general, p, ρ, and T will vary.) For steady, inviscid, isothermal flow, the Bernoulli's equation becomes

$$RT \int \frac{dp}{p} + \frac{1}{2}V^2 + gz = \text{constant}$$

where we have used $\rho = p/RT$. The pressure term is easily integrated and the constant of integration evaluated if z_1, p_1, and V_1 are known at some location on the streamline. The result is

$$\frac{V_1^2}{2g} + z_1 + \frac{RT}{g}\ln\left(\frac{p_1}{p_2}\right) = \frac{V_2^2}{2g} + z_2 \tag{6.32}$$

Equation 6.32 is the inviscid, isothermal analog of the incompressible Bernoulli equation. In the limit of small pressure difference, $p_1/p_2 = 1 + (p_1 - p_2)/p_2 = 1 + \varepsilon$, with $\varepsilon \ll 1$ and Eq. 6.32 reduces to the standard incompressible Bernoulli equation. This can be shown by use of the approximation $\ln(1 + \varepsilon) \approx \varepsilon$ for small ε. The use of Eq. 6.32 in practical applications is restricted by the inviscid flow assumption, since (as is discussed in Section 6.1) most isothermal flows are accompanied by viscous effects.

A much more common compressible flow condition is that of isentropic (constant entropy) flow of a perfect gas. Such flows are reversible adiabatic processes—"no friction or heat transfer"—and are closely approximated in many physical situations. As discussed fully in section 6.1 , for isentropic flow of a perfect gas the density and pressure are related by $p/\rho^k = C$, where k is the specific heat ratio and C is a constant. Hence, the $\int dp/\rho$ integral of Eq. 3.6 can be evaluated as follows. The density can be written in terms of the pressure as $\rho = p^{1/k}C^{-1/k}$ so that Bernoulli's eqn. becomes

$$C^{1/k} \int p^{-1/k}\, dp + \frac{1}{2}V^2 + gz = \text{constant}$$

The pressure term can be integrated between points (1) and (2) on the streamline and the constant C evaluated at either point ($C^{1/k} = p_1^{1/k}/\rho_1$ or $C^{1/k} = p_2^{1/k}/\rho_2$) to give the following:

$$C^{1/k}\int_{p1}^{p2} p^{-1/k}\, dp = C^{1/k}\left(\frac{k}{k-1}\right)\left[p_2^{(k-1)/k} - p_1^{(k-1)/k}\right]$$
$$= \left(\frac{k}{k-1}\right)\left(\frac{p_2}{\rho_2} - \frac{p_1}{\rho_1}\right)$$

Thus, the final form of Bernoulli's eqn. for compressible, isentropic, steady flow of a perfect gas is

$$\left(\frac{k}{k-1}\right)\frac{p_1}{\rho_1} + \frac{V_1^2}{2} + gz_1 = \left(\frac{k}{k-1}\right)\frac{p_2}{\rho_2} + \frac{V_2^2}{2} + gz_2 \tag{6.33}$$

The similarities between the results for compressible isentropic flow (Eq. 6.33) and incompressible isentropic flow (the Bernoulli equation, Eq.6.32) are apparent. The only differences are the factors of $[k/(k-1)]$ that multiply the pressure terms and the fact that the densities are different ($\rho_1 \neq \rho_2$). In the limit of "low-speed flow" the two results are exactly the same as is seen by the following.

We consider the stagnation point flow of figure 6.2 to illustrate the difference between the incompressible and compressible results. As is shown in section 6.1 , Eq. 6.33 can be written in dimensionless form as

$$\frac{p_2 - p_1}{p_1} = \left[\left(1 + \frac{k-1}{2}\text{Ma}_1^2\right)^{k/k-1} - 1\right] \text{(compressible)} \tag{6.34}$$

where (1) denotes the upstream conditions and (2) the stagnation conditions. We have assumed $z_1 = z_2$, $V_2 = 0$, and have denoted $\text{Ma}_1 = V_1/c_1$ as the upstream *Mach number*—the ratio of the fluid velocity to the speed of sound, $c_1 = \sqrt{kRT_1}$.

A comparison between this compressible result and the incompressible result is perhaps most easily seen if we write the incompressible flow result in terms of the pressure ratio and the Mach number. Thus, we divide each term in the Bernoulli equation, $\rho V_1^2/2 + p_1 = p_2$, by p_1 and use the perfect gas law, $p_1 = \rho RT_1$, to obtain

$$\frac{p_2}{p_1} = \frac{V_1^2}{2RT_1}$$

Since $\text{Ma}_1 = V_1/\sqrt{kRT_1}$ this can be written as

$$\frac{p_2 - p_1}{p_1} = \frac{k\text{Ma}_1^2}{2} \text{ (incompressible)} \tag{6.35}$$

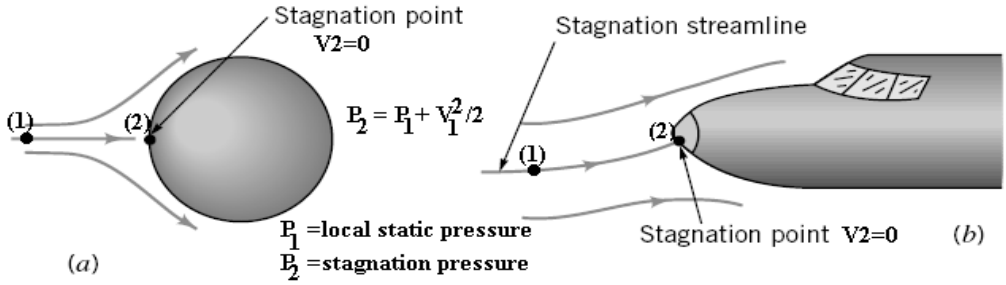

■ FIGURE 6.2 **Stagnation points on bodies in flowing fluids.**

Equations 6.33 and 6.34 are plotted in Fig. 6.3 . In the low-speed limit of $Ma_1 \to 0$, both of the results are the same. This can be seen by denoting $(k-1)Ma_1^2/2 = \tilde{\varepsilon}$ and using the binomial expansion, $(1+\tilde{\varepsilon})^n = 1 + n\tilde{\varepsilon} + n(n-1)\tilde{\varepsilon}^2/2 + \cdots$, where $n = k/(k-1)$, to write Eq. 6.34 as

$$\frac{p_2 - p_1}{p_1} = \frac{kMa_1^2}{2}\left(1 + \frac{1}{4}Ma_1^2 + \frac{2-k}{24}Ma_1^4 + \cdots\right) \text{(compressible)}$$

For $Ma_1 \ll 1$ this compressible flow result agrees with Eq. 6.35 . The incompressible and compressible equations agree to within about 2% up to a Mach number of approximately $Ma_1 = 0.3$. For larger Mach numbers the disagreement between the two results increases.

Thus, a "rule of thumb" is that the flow of a perfect gas may be considered as incompressible provided the Mach number is less than about 0.3. In standard air ($T_1 = 59°F$, $c_1 = \sqrt{kRT_1} = 1117$ ft/s) this corresponds to a speed of $V_1 = c_1 Ma_1 = 0.3(1117 \text{ ft/s}) = 335 \text{ ft/s} = 228$ mi/hr. At higher speeds, compressibility may become important.

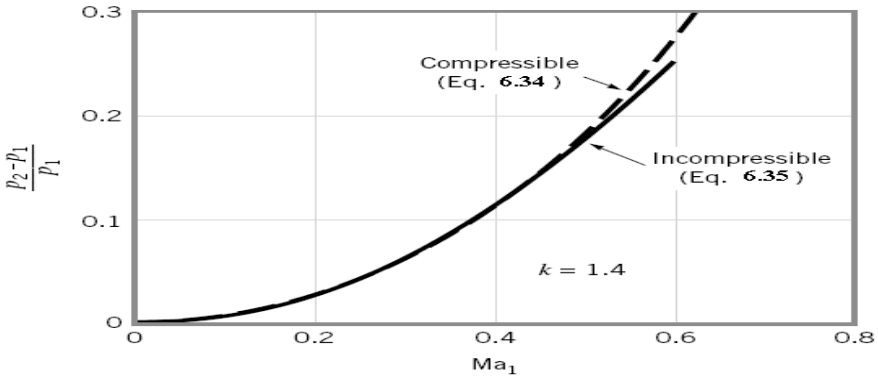

■ FIGURE 6.3 **Pressure ratio as a function of Mach number for incompressible and compressible (isentropic) flow.**

Example 6.6:

A Boeing 777 flies at Mach 0.82 at an altitude of 10 km in a standard atmosphere. Determine the stagnation pressure on the leading edge of its wing if the flow is incompressible; and if the flow is compressible isentropic.

Solution:

From Tables 1.8 and C.2 we find that $p_1 = 26.5$ kPa (abs), $T_1 = -49.9$ °C, $\rho = 0.414$ kg/m^3, and $k = 1.4$. Thus, if we assume incompressible flow, Eq. 6.35 gives

$$\frac{p_2 - p_1}{p_1} = \frac{kMa_1^2}{2} = 1.4\frac{(0.82)^2}{2} = 0.471$$

or

$$p_2 - p_1 = 0.471\,(26.5 \text{ kPa}) = 12.5 \text{ kPa} \quad \text{(Ans)}$$

On the other hand, if we assume isentropic flow, Eq. 6.34 gives

$$\frac{p_2 - p_1}{p_1} = \left\{\left[1 + \frac{(1.4-1)}{2}(0.82)^2\right]^{1.4/(1.4-1)} - 1\right\} = 0.555$$

or

$$p_2 - p_1 = 0.555\,(26.5 \text{ kPa}) = 14.7 \text{ kPa} \quad \text{(Ans)}$$

We see that at Mach 0.82 compressibility effects are of importance. The pressure (and, to a first approximation, the lift and drag on the airplane; see Part (5)) is approximately 14.7/12.5 = 1.18 times greater according to the compressible flow calculations. This may be very significant. As discussed in section 6.1 , for Mach numbers greater than 1 (supersonic flow) the differences between incompressible and compressible results are often not only quantitative but also qualitative.

Note that if the airplane were flying at Mach 0.30 (rather than 0.82) the corresponding values would be $p_2 - p_1 = 1.670$ kPa for incompressible flow and $p_2 - p_1 = 1.707$ kPa for compressible flow. The difference between these two results is about 2 percent.

TABLE C.2
Properties of the U.S. Standard Atmosphere (SI Units)[a]

Altitude (m)	Temperature (°C)	Acceleration of Gravity, g (m/s^2)	Pressure, p [N/m^2(abs)]	Density, ρ (kg/m^3)	Dynamic Viscosity, μ (N·s/m^2)
−1,000	21.50	9.810	1.139 E + 5	1.347 E + 0	1.821 E − 5
0	15.00	9.807	1.013 E + 5	1.225 E + 0	1.789 E − 5
1,000	8.50	9.804	8.988 E + 4	1.112 E + 0	1.758 E − 5
2,000	2.00	9.801	7.950 E + 4	1.007 E + 0	1.726 E − 5
3,000	−4.49	9.797	7.012 E + 4	9.093 E − 1	1.694 E − 5
4,000	−10.98	9.794	6.166 E + 4	8.194 E − 1	1.661 E − 5
5,000	−17.47	9.791	5.405 E + 4	7.364 E − 1	1.628 E − 5
6,000	−23.96	9.788	4.722 E + 4	6.601 E − 1	1.595 E − 5
7,000	−30.45	9.785	4.111 E + 4	5.900 E − 1	1.561 E − 5
8,000	−36.94	9.782	3.565 E + 4	5.258 E − 1	1.527 E − 5
9,000	−43.42	9.779	3.080 E + 4	4.671 E − 1	1.493 E − 5
10,000	−49.90	9.776	2.650 E + 4	4.135 E − 1	1.458 E − 5
15,000	−56.50	9.761	1.211 E + 4	1.948 E − 1	1.422 E − 5
20,000	−56.50	9.745	5.529 E + 3	8.891 E − 2	1.422 E − 5
25,000	−51.60	9.730	2.549 E + 3	4.008 E − 2	1.448 E − 5
30,000	−46.64	9.715	1.197 E + 3	1.841 E − 2	1.475 E − 5
40,000	−22.80	9.684	2.871 E + 2	3.996 E − 3	1.601 E − 5
50,000	−2.50	9.654	7.978 E + 1	1.027 E − 3	1.704 E − 5
60,000	−26.13	9.624	2.196 E + 1	3.097 E − 4	1.584 E − 5
70,000	−53.57	9.594	5.221 E + 0	8.283 E − 5	1.438 E − 5
80,000	−74.51	9.564	1.052 E + 0	1.846 E − 5	1.321 E − 5

[a]Data abridged from *U.S. Standard Atmosphere*, 1976, U.S. Government Printing Office, Washington, D.C.

6.2.3 The Mach Cone and The Categories of Compressible Flow:

In Section 6.2.2, we learned that the effects of compressibility become more significant as the Mach number increases. For example, the error associated with using $\rho V^2/2$ in calculating the stagnation pressure of an ideal gas increases at larger Mach numbers. From Fig. 6.3 we can conclude that incompressible flows can only occur at low Mach numbers.

Experience has also demonstrated that compressibility can have a large influence on other important flow variables. For example, in Fig. 6.4 the variation of drag coefficient with Reynolds number and Mach number is shown for air flow over a sphere. Compressibility effects can be of considerable importance.

To further illustrate some curious features of compressible flow, a simplified example is considered. Imagine the emission of weak pressure pulses from a point source. These pressure waves are spherical and expand radially outward from the point source at the speed of sound, c. If a pressure wave is emitted at different times, t_{wave}, we can determine where

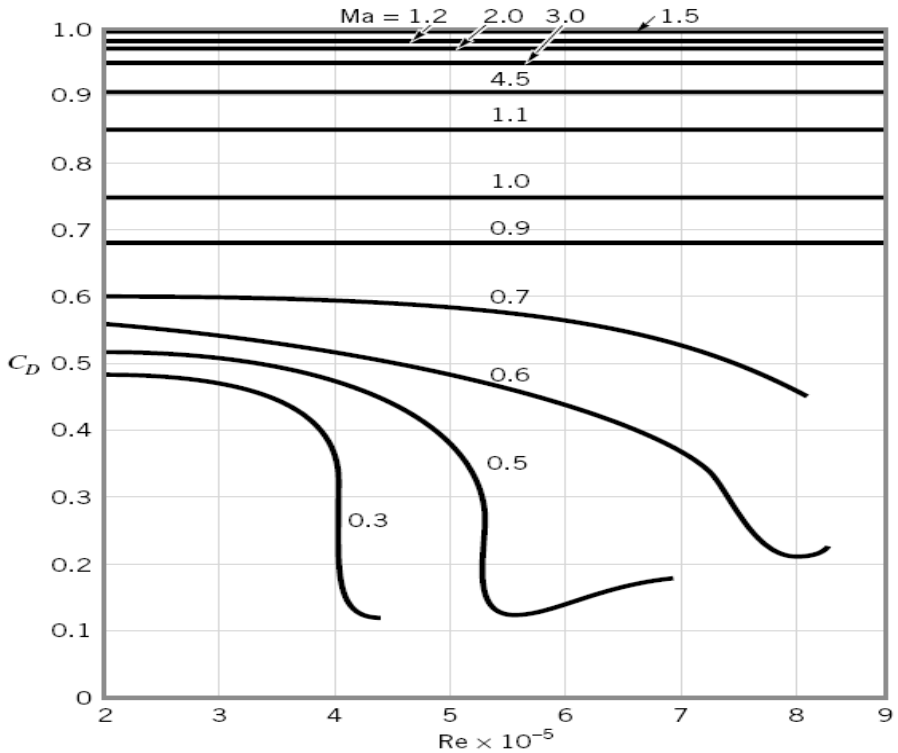

FIGURE 6.4
The variation of the drag coefficient of a sphere with Reynolds number and Mach number.

several waves will be at a common instant of time, t, by using the relationship

$$r = (t - t_{wave})c$$

where r is the radius of the sphere-shaped wave emitted at time $= t_{wave}$. For a stationary point source, the symmetrical wave pattern shown in Fig. 6.5 a is involved.

When the point source moves to the left with a constant velocity, V, the wave pattern is no longer symmetrical. In Figs. 6.5 b , 6.5 c , and 6.5 d are illustrated the wave patterns at $t = 3$ s for different values of V. Also shown with a "+" are the positions of the moving point source at values of time, t, equal to 0 s, 1 s, 2 s, and 3 s. Knowing where the point source has been at different instances is important because it indicates to us where the different waves originated.

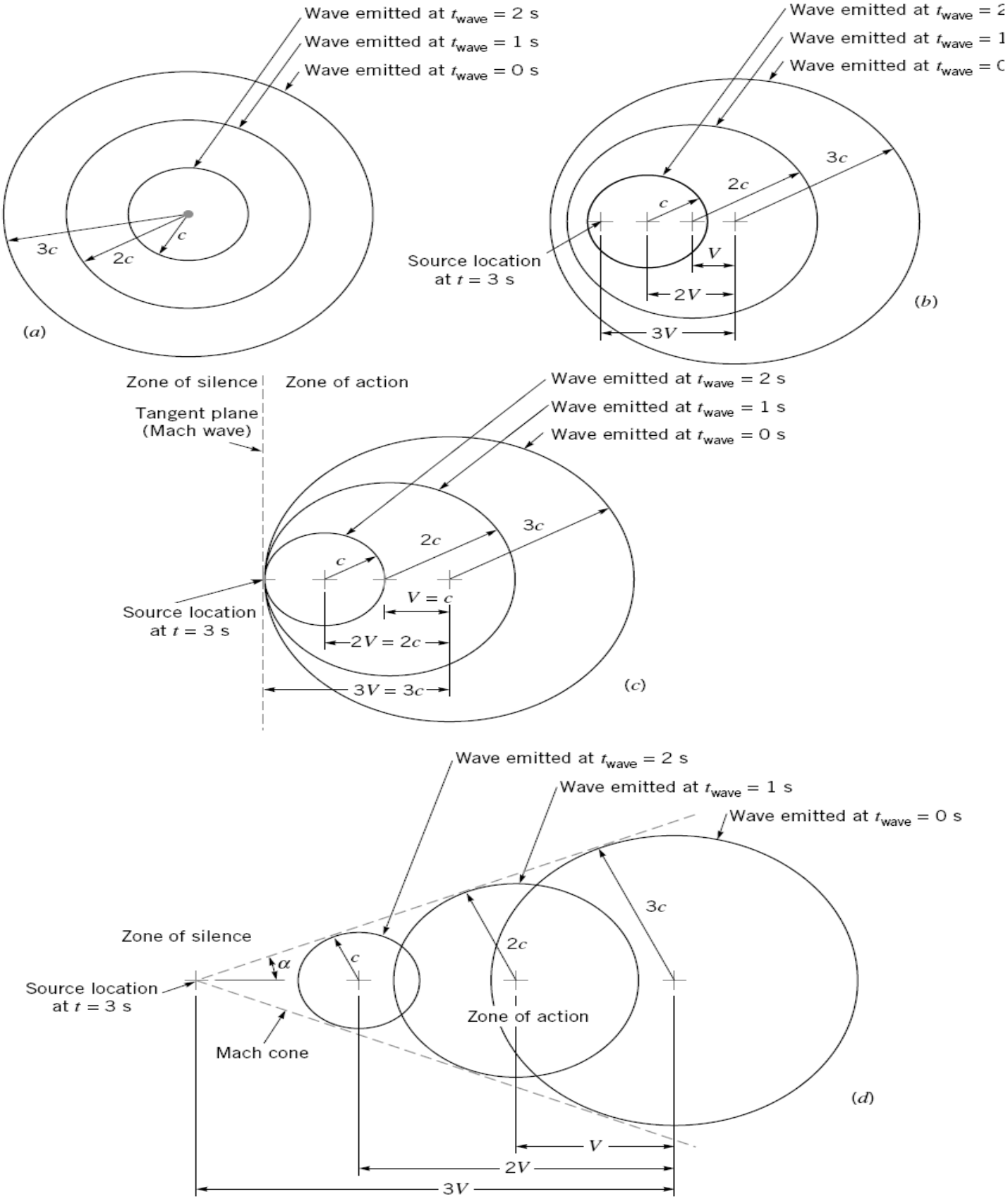

■ **FIGURE 6.5** **(*a*) Pressure waves at $t = 3$ s, $V = 0$; (*b*) Pressure waves at $t = 3$ s, $V < c$; (*c*) Pressure waves at $t = 3$ s, $V = c$; (*d*) Pressure waves at $t = 3$ s, $V > c$.**

From the pressure wave patterns of Fig. 6.5 , we can draw some useful conclusions. Before doing this we should recognize that if instead of moving the point source to the left, we held the point source stationary and moved the fluid to the right with velocity V, the resulting pressure wave patterns would be identical to those indicated in Fig. 6.5 .

When the point source and the fluid are stationary, the pressure wave pattern is symmetrical (Fig. 6.5 a) and an observer anywhere in the pressure field would hear the same sound frequency from the point source. When the velocity of the point source (or the fluid) is very small in comparison with the speed of sound, the pressure wave pattern will still be nearly symmetrical. The speed of sound in an incompressible fluid is infinitely large. Thus, the stationary point source and stationary fluid situation are representative of incompressible flows. For truly incompressible flows, the communication of pressure information throughout the flow field is unrestricted and instantaneous ($c = \infty$).

When the point source moves in fluid at rest (or when fluid moves past a stationary point source), the pressure wave patterns vary in asymmetry, with the extent of asymmetry depending on the ratio of the point source (or fluid) velocity and the speed of sound. When $V/c < 1$, the wave pattern is similar to the one shown in Fig. 6.5 b . This flow is considered *subsonic* and compressible. A stationary observer will hear a different sound frequency coming from the point source depending on where the observer is relative to the source because the wave pattern is asymmetrical. We call this phenomenon the Doppler effect. Pressure information can still travel unrestricted throughout the flow field, but not symmetrically or instantaneously.

When $V/c = 1$, pressure waves are not present ahead of the moving point source. The flow is *sonic*. If you were positioned to the left of the moving point source, you would not hear the point source until it was coincident with your location. For flow moving past a stationary point source at the speed of sound ($V/c = 1$), the pressure waves are all tangent to a plane that is perpendicular to the flow and that passes through the point source. The concentration of pressure waves in this tangent plane suggests the formation of a significant pressure variation across the plane. This plane is often called a Mach wave. Note that communication of pressure information is restricted to the region of flow downstream of the Mach wave. The region of flow upstream of the Mach wave is called the *zone of silence* and the region of flow downstream of the tangent plane is called the *zone of action*.

When $V > c$, the flow is *supersonic* and the pressure wave pattern resembles the one depicted in Fig. 6.5 d . A cone (*Mach cone*) that is tangent to the pressure waves can be constructed to represent the Mach wave that separates the zone of silence from the zone of action in this case. The communication of pressure information is restricted to the zone of action. From the sketch of Fig. 6.5 d , we can see that the angle of this cone, α, is given by

$$\sin \alpha = \frac{c}{V} = \frac{1}{\text{Ma}} \qquad (6.36)$$

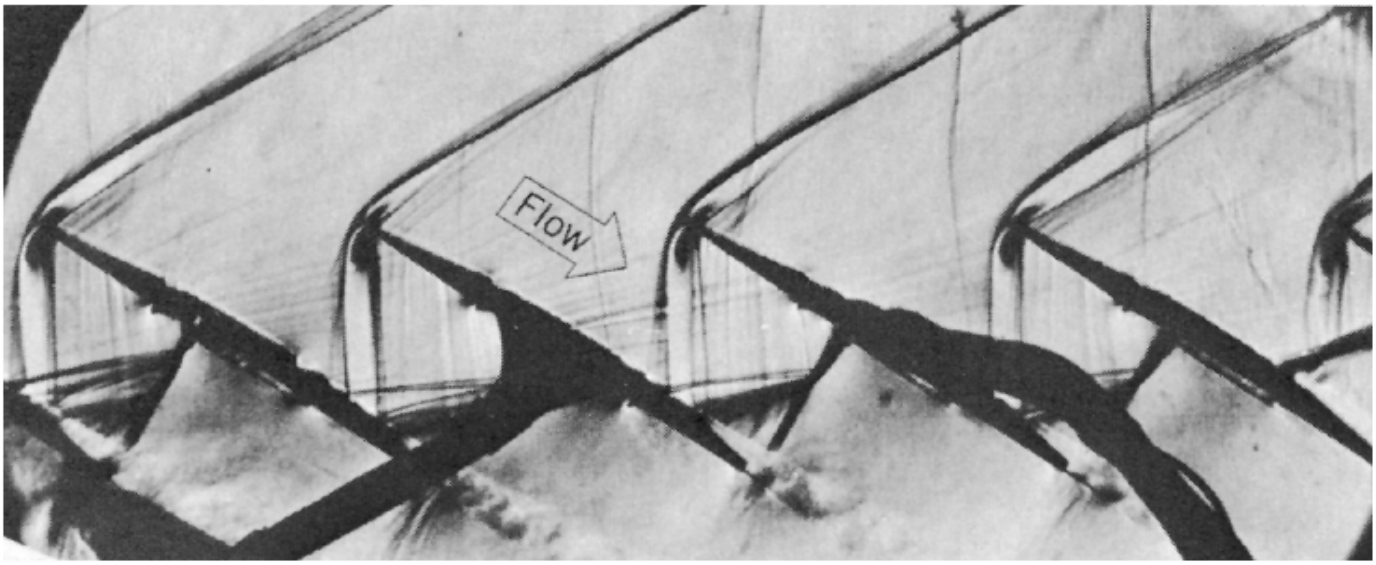

■ FIGURE 6.6 **The schlieren visualization of flow (supersonic to subsonic) through a row of compressor airfoils. (Photograph provided by Dr. Hans Starken of the DLR Köln-Porz, Germany.)**

Equation 6.36 is often used to relate the Mach cone angle, α, and the flow Mach number, Ma, when studying flows involving $V/c > 1$. The concentration of pressure waves at the surface of the Mach cone suggests a significant pressure, and thus density, variation across the cone surface. (See the **photograph** at the beginning of this chapter.) An abrupt density change can be visualized in a flow field by using special optics. Examples of flow visualization methods include the schlieren, shadowgraph, and interferometer techniques (see Ref. 5). A schlieren photo of a flow for which $V > c$ is shown in Fig. 6.6 . The air flow through the row of compressor blade airfoils is as shown with the arrow. The flow enters supersonically ($Ma_1 = 1.14$) and leaves subsonically ($Ma_2 = 0.86$). The center two airfoils have pressure tap hoses connected to them. Regions of significant changes in fluid density appear in the supersonic portion of the flow. Also, the region of separated flow on each airfoil is visible.

This discussion about pressure wave patterns suggests the following categories of fluid flow:

1. Incompressible flow: Ma $\leq$ 0.3. Unrestricted, nearly symmetrical and instantaneous pressure communication.
2. Compressible subsonic flow: 0.3 $<$ Ma $<$ 1.0. Unrestricted but noticeably asymmetrical pressure communication.
3. Compressible supersonic flow: Ma $\geq$ 1.0. Formation of Mach wave; pressure communication restricted to zone of action.

In addition to the above-mentioned categories of flows, two other regimes are commonly referred to: namely, transonic flows ($0.9 \leq Ma \leq 1.2$) and hypersonic flows (Ma $>$ 5). Modern aircraft are mainly powered by gas turbine engines that involve transonic flows. When a space shuttle reenters the earth's atmosphere, the flow is hypersonic. Future aircraft may be expected to operate from subsonic to hypersonic flow conditions.

Example 6.7:

An aircraft cruising at 1000-m elevation, z, above you moves past in a flyby. How many seconds after the plane passes overhead do you expect to wait before you hear the aircraft if it is moving with a Mach number equal to 1.5 and the ambient temperature is 20 °C?

Solution:

Since the aircraft is moving supersonically (Ma $>$ 1), we can imagine a Mach cone originating from the forward tip of the craft as is illustrated in Fig. E6.7 . When the surface of

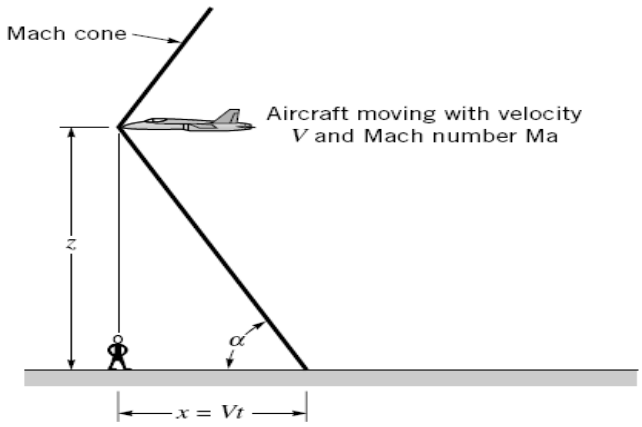

■ FIGURE E 6.7

the cone reaches the observer, the "sound" of the aircraft is perceived. The angle α in Fig. E 6.7 is related to the elevation of the plane, z, and the ground distance, x, by

$$\alpha = \tan^{-1}\frac{z}{x} = \tan^{-1}\frac{1000}{Vt} \qquad (1)$$

Also, assuming negligible change of Mach number with elevation, we can use Eq. 6.36 to relate Mach number to the angle α. Thus, $\text{Ma} = 1 / \sin\alpha$ (2)

Combining Eqs. 1 and 2 we obtain

$$\text{Ma} = \frac{1}{\sin\left[\tan^{-1}(1000/Vt)\right]} \qquad (3)$$

The speed of the aircraft can be related to the Mach number with

$$V = (\text{Ma})c \qquad (4)$$

where c is the speed of sound. From **Table B.4**, $c = 343.3$ m/s. Using Ma = 1.5, we get from Eqs. 3 and 4

$$1.5 = \frac{1}{\sin\left\{\tan^{-1}\left[\dfrac{1000\text{ m}}{(1.5)(343.3\text{ m/s})t}\right]\right\}}$$

or

$$t = 2.17\text{ s} \qquad \text{(Ans)}$$

6.3 Adiabatic and Isentropic Steady Flow (Stagnation-Reference Properties):

As mentioned in Sec. 6.1, the isentropic approximation greatly simplifies a compressible-flow calculation. So does the assumption of adiabatic flow, even if nonisentropic.

Consider high-speed flow of a gas past an insulated wall, as in Fig. 6.7. There is no shaft work delivered to any part of the fluid. Therefore every streamtube in the flow satisfies steady-flow energy equation (1st law of thermodynamics, see part 1) in the form of

$$h_1 + \tfrac{1}{2}V_1^2 + gz_1 = h_2 + \tfrac{1}{2}V_2^2 + gz_2 - q + w_v \qquad (6.37)$$

where point 1 is upstream of point 2. We saw that potential-energy changes of a gas are extremely small compared with kinetic-energy and enthalpy terms. We shall neglect the terms gz_1 and gz_2 in all gas-dynamic analyses.

Inside the thermal and velocity boundary layers in Fig. 6.7 the heat-transfer and viscous-work terms q and w_v are not zero. But outside the boundary layer q and w_v are zero by definition, so that the outer flow satisfies the simple relation

$$h_1 + \tfrac{1}{2}V_1^2 = h_2 + \tfrac{1}{2}V_2^2 = \text{const} \qquad (6.38)$$

The constant in Eq. (6.38) is equal to the maximum enthalpy which the fluid would achieve if brought to rest adiabatically. We call this value h_0, the *stagnation enthalpy* of the flow. Thus we rewrite Eq. (6.38) in the form

$$h + \tfrac{1}{2}V^2 = h_0 = \text{const} \qquad (6.39)$$

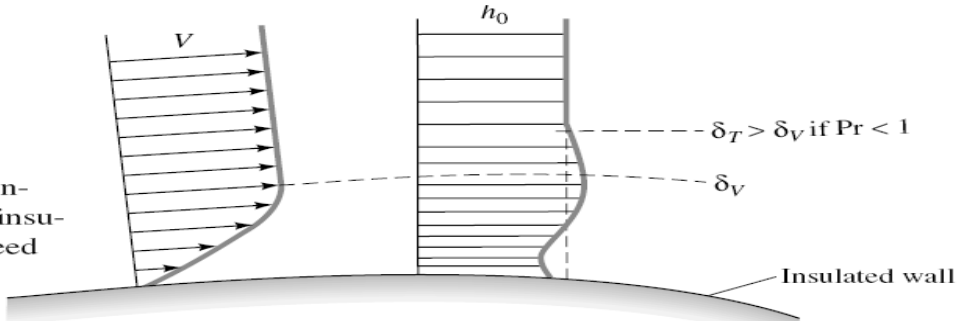

Fig. 6.7 Velocity and stagnation-enthalpy distributions near an insulated wall in a typical high-speed gas flow.

This should hold for steady adiabatic flow of any compressible fluid outside the boundary layer. The wall in Fig. 6.7 could be either the surface of an immersed body or the wall of a duct. We have shown the details of Fig. 6.7; typically the thermal-layer thickness δ_T is greater than the velocity-layer thickness δ_V because most gases have a dimensionless Prandtl number Pr less than unity (see, e.g., Ref. 19, & part (4)). Note that the stagnation enthalpy varies inside the thermal boundary layer, but its average value is the same as that at the outer layer due to the insulated wall.

For nonperfect gases we may have to use the steam tables [15] or the gas tables [16] to implement Eq. (6.39). But for a perfect gas $h = c_pT$, and Eq. (6.39) becomes

$$c_pT + \tfrac{1}{2}V^2 = c_pT_0 \qquad (6.40)$$

This establishes the stagnation temperature T_0 of an adiabatic perfect-gas flow, i.e., the temperature it achieves when decelerated to rest adiabatically.

An alternate interpretation of Eq. (6.39) occurs when the enthalpy and temperature drop to (absolute) zero, so that the velocity achieves a maximum value

$$V_{\max} = (2h_0)^{1/2} = (2c_pT_0)^{1/2} \qquad (6.41)$$

No higher flow velocity can occur unless additional energy is added to the fluid through shaft work or heat transfer (Sec. 6.8).

6.3.1 The Mach Number-Stagnation Relations:

The dimensionless form of Eq. (6.40) brings in the Mach number Ma as a parameter, by using the speed of sound of a perfect gas. Divide through by c_pT to obtain

$$1 + \frac{V^2}{2c_pT} = \frac{T_0}{T} \qquad (6.42)$$

But, from the perfect-gas law, $c_pT = [kR/(k-1)]T = a^2/(k-1)$, so that Eq. (6.42) becomes

$$1 + \frac{(k-1)V^2}{2a^2} = \frac{T_0}{T}$$

or

$$\frac{T_0}{T} = 1 + \frac{k-1}{2}\text{Ma}^2 \qquad \text{Ma} = \frac{V}{a} \qquad (6.43)$$

This relation is plotted in Fig. 6.8 versus the Mach number for $k = 1.4$. At Ma = 5 the temperature has dropped to $\frac{1}{6}T_0$.

Since $a \propto T^{1/2}$, the ratio a_0/a is the square root of (6.43)

$$\frac{a_0}{a} = \left(\frac{T_0}{T}\right)^{1/2} = \left[1 + \frac{1}{2}(k-1)\text{Ma}^2\right]^{1/2} \tag{6.44}$$

Equation (6.44) is also plotted in Fig. 6.8 . At Ma = 5 the speed of sound has dropped to 41 percent of the stagnation value.

Note that Eqs. (6.43) and (6.44) require only adiabatic flow and hold even in the presence of irreversibilities such as friction losses or shock waves.

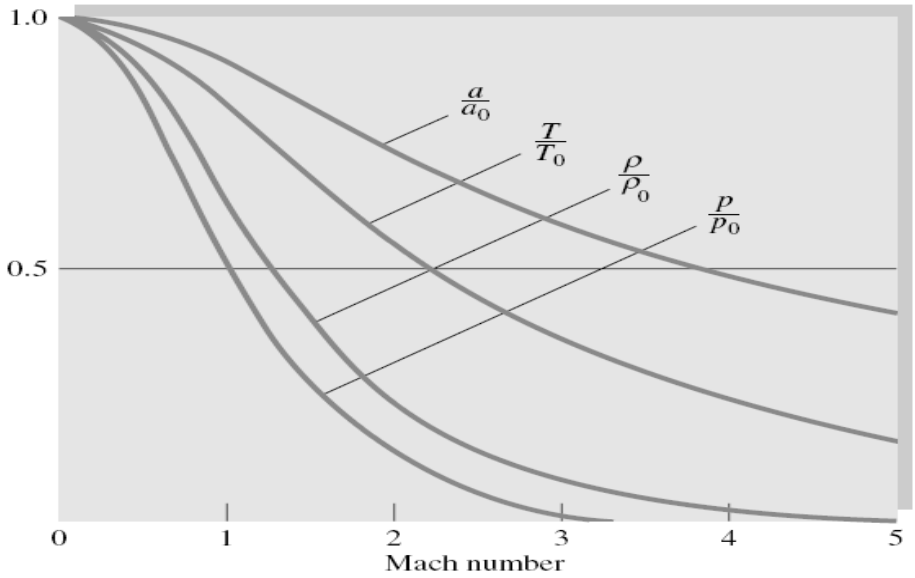

Fig. 6.8 Adiabatic (T/T_0 and a/a_0) and isentropic (p/p_0 and ρ/ρ_0) properties versus Mach number for $k = 1.4$.

If the flow is also *isentropic*, then for a perfect gas the pressure and density ratios can be computed from Eq. (6.9) as a power of the temperature ratio

$$\frac{p_0}{p} = \left(\frac{T_0}{T}\right)^{k/(k-1)} = \left[1 + \frac{1}{2}(k-1)\,\text{Ma}^2\right]^{k/(k-1)} \tag{6.45a}$$

$$\frac{\rho_0}{\rho} = \left(\frac{T_0}{T}\right)^{1/(k-1)} = \left[1 + \frac{1}{2}(k-1)\,\text{Ma}^2\right]^{1/(k-1)} \tag{6.45b}$$

These relations are also plotted in Fig. 6.8 ; at Ma = 5 the density is 1.13 percent of its stagnation value, and the pressure is only 0.19 percent of stagnation pressure.

The quantities p_0 and ρ_0 are the isentropic stagnation pressure and density, respectively, i.e., the pressure and density which the flow would achieve if brought isentropically to rest. In an adiabatic nonisentropic flow p_0 and ρ_0 retain their local meaning, but they vary throughout the flow as the entropy changes due to friction or shock waves. The quantities h_0, T_0, and a_0 are constant in an adiabatic nonisentropic flow (see Sec. 6.7 for further details).

6.3.2 The Relationship to Bernoulli's Equation:

The isentropic assumptions (6.45) are effective, but are they realistic? Yes. To see why, differentiate Eq. (6.39)

Adiabatic: $$dh + V\,dV = 0 \tag{6.46}$$

Meanwhile, from Eq. (6.6), if $ds = 0$ (isentropic process),

$$dh = \frac{dp}{\rho} \tag{6.47}$$

Combining (6.46) and (6.47), we find that an isentropic streamtube flow must be

$$\frac{dp}{\rho} + V\,dV = 0 \tag{6.48}$$

But this is exactly the Bernoulli relation, see part (4), for steady frictionless flow with negligible gravity terms. Thus we see that the isentropic-flow assumption is equivalent to use of the Bernoulli or streamline form of the frictionless momentum equation.

6.3.3 The Critical Reference Properties at Sonic Velocity:

The stagnation values (a_0, T_0, p_0, ρ_0) are useful reference conditions in a compressible flow, but of comparable usefulness are the conditions where the flow is sonic, Ma = 1.0. These sonic, or *critical*, properties are denoted by asterisks: p^*, ρ^*, a^*, and T^*. They are certain ratios of the stagnation properties as given by Eqs. (6.43) to (6.45) when Ma = 1.0; for $k = 1.4$

$$\frac{p^*}{p_0} = \left(\frac{2}{k+1}\right)^{k/(k-1)} = 0.5283 \qquad \frac{\rho^*}{\rho_0} = \left(\frac{2}{k+1}\right)^{1/(k-1)} = 0.6339$$
$$\frac{T^*}{T_0} = \frac{2}{k+1} = 0.8333 \qquad \frac{a^*}{a_0} = \left(\frac{2}{k+1}\right)^{1/2} = 0.9129 \tag{6.49}$$

In all isentropic flow, all critical properties are constant; in adiabatic nonisentropic flow, a^* and T^* are constant, but p^* and ρ^* may vary.

The critical velocity V^* equals the sonic sound speed a^* by definition and is often used as a reference velocity in isentropic or adiabatic flow

$$V^* = a^* = (kRT^*)^{1/2} = \left(\frac{2k}{k+1}RT_0\right)^{1/2} \tag{6.50}$$

The usefulness of these critical values will become clearer as we study compressible duct flow with friction or heat transfer later in this chapter.

6.3.4 Some Useful Numbers for Air:

Since the great bulk of our practical calculations are for air, $k = 1.4$, the stagnation-property ratios p/p_0, etc., from Eqs. (6.43) to (6.45), are tabulated for this value in Table B.1. The increments in Mach number are rather coarse in this table because the values are only meant as a guide; these equations are now a trivial matter to manipulate on a hand calculator. Thirty years ago every text had extensive compressible-flow tables with Mach-number spacings of about 0.01, so that accurate values could be interpolated.

For $k = 1.4$, the following numerical versions of the isentropic and adiabatic flow formulas are obtained:

$$\frac{T_0}{T} = 1 + 0.2\,\mathrm{Ma}^2 \qquad \frac{\rho_0}{\rho} = (1 + 0.2\,\mathrm{Ma}^2)^{2.5}$$
$$\frac{p_0}{p} = (1 + 0.2\,\mathrm{Ma}^2)^{3.5} \tag{6.51}$$

Or, if we are given the properties, it is equally easy to solve for the Mach number (again with $k = 1.4$)

$$\mathrm{Ma}^2 = 5\left(\frac{T_0}{T} - 1\right) = 5\left[\left(\frac{\rho_0}{\rho}\right)^{2/5} - 1\right] = 5\left[\left(\frac{p_0}{p}\right)^{2/7} - 1\right] \tag{6.52}$$

Note that these isentropic-flow formulas serve as the equivalent of the frictionless adiabatic momentum and energy equations. They relate velocity to physical properties for a perfect gas, but they are *not* the "solution" to a gas-dynamics problem. The complete solution is not obtained until the continuity equation has also been satisfied, for either one-dimensional (Sec.6.4) or multidimensional (Sec. 6.9) flow.

One final note: These isentropic-ratio–versus–Mach-number formulas are seductive, tempting one to solve all problems by jumping right into the tables. Actually, many problems involving (dimensional) velocity and temperature can be solved more easily from the original raw dimensional energy equation (6.40) plus the perfect-gas law (6.2), as the next example will illustrate.

Example 6.8:

Air flows adiabatically through a duct. At point 1 the velocity is 240 m/s, with $T_1 = 320$ K and $p_1 = 170$ kPa. Compute (*a*) T_0, (*b*) p_{01}, (*c*) ρ_0, (*d*) Ma, (*e*) V_{max}, and (*f*) V^*. At point 2 further downstream $V_2 = 290$ m/s and $p_2 = 135$ kPa. (*g*) What is the stagnation pressure p_{02}?

Solution

For air take $k = 1.4$, $c_p = 1005$ m^2/(s^2 · K), and $R = 287$ m^2/(s^2 · K). With V_1 and T_1 known, we can compute T_{01} from Eq. (6.40) without using the Mach number:

$$T_{01} = T_1 + \frac{V_1^2}{2c_p} = 320 + \frac{(240\text{ m/s})^2}{2[1005\text{ m}^2/(\text{s}^2\cdot\text{K})]} = 320 + 29 = 349\text{ K} \qquad \textit{Ans. (a)}$$

Then compute Ma_1 from the known temperature ratio, using Eq. (6.52):

$$Ma_1^2 = 5\left(\frac{349}{320} - 1\right) = 0.453 \qquad Ma_1 = 0.67 \qquad \textit{Ans. (d)}$$

Alternately compute $a_1 = \sqrt{kRT_1} = 359$ m/s, whence $Ma_1 = V_1/a_1 = 240/359 = 0.67$. The stagnation pressure at section 1 follows from Eq. (6.51):

$$p_{01} = p_1(1 + 0.2\ Ma_1^2)^{3.5} = (170\ \text{kPa})[1 + 0.2(0.67)^2]^{3.5} = 230\ \text{kPa} \qquad \textit{Ans. (b)}$$

We need the density from the perfect-gas law before we can compute the stagnation density:

$$\rho_1 = \frac{p_1}{RT_1} = \frac{170{,}000}{(287)(320)} = 1.85\ \text{kg/m}^3$$

whence $$\rho_{01} = \rho_1(1 + 0.2\ Ma_1^2)^{2.5} = (1.85)[1 + 0.2(0.67)^2]^{2.5} = 2.29\ \text{kg/m}^3 \qquad \textit{Ans. (c)}$$

Alternately, we could have gone directly to $\rho_0 = p_0/(RT_0) = (230\ \text{E3})/[(287)(349)] = 2.29\ \text{kg/m}^3$. Meanwhile, the maximum velocity follows from Eq. (6.41)

$$V_{max} = (2c_pT_0)^{1/2} = [2(1005)(349)]^{1/2} = 838\ \text{m/s} \qquad \textit{Ans. (e)}$$

and the sonic velocity from Eq. (6.50) is

$$V^* = \left(\frac{2k}{k+1}RT_0\right)^{1/2} = \left[\frac{2(1.4)}{1.4+1}(287)(349)\right]^{1/2} = 342\ \text{m/s} \qquad \textit{Ans. (f)}$$

At point 2, the temperature is not given, but since we know the flow is adiabatic, the stagnation temperature is constant: $T_{02} = T_{01} = 349$ K. Thus, from Eq. (6.40),

$$T_2 = T_{02} - \frac{V_2^2}{2c_p} = 349 - \frac{(290)^2}{2(1005)} = 307\ \text{K}$$

Then, although the flow itself is not isentropic, the local stagnation pressure is computed by the *local* isentropic condition

$$p_{02} = p_2\left(\frac{T_{02}}{T_2}\right)^{k/(k-1)} = (135)\left(\frac{349}{307}\right)^{3.5} = 211\ \text{kPa} \qquad \textit{Ans. (g)}$$

This is 8 percent less than the upstream stagnation pressure p_{01}. Notice that, in this last part, we took advantage of the given information (T_{02}, p_2, V_2) to obtain p_{02} in an efficient manner. You may verify by comparison that approaching this part through the (unknown) Mach number Ma_2 is more laborious.

6.4 One-Dimensional Isentropic Flow With Area Changes:

By combining the isentropic- and/or adiabatic-flow relations with the equation of continuity we can study practical compressible-flow problems. This section treats the one-dimensional flow approximation.

Figure 6.9 illustrates the one-dimensional flow assumption. A real flow, Fig. 6.9 a, has no slip at the walls and a velocity profile $V(x, y)$ which varies across the duct section. If, however, the area change is small and the wall radius of curvature large

$$\frac{dh}{dx} \ll 1 \qquad h(x) \ll R(x) \tag{6.53}$$

then the flow is approximately one-dimensional, as in Fig. 6.9 b, with $V \approx V(x)$ reacting to area change $A(x)$. Compressible-flow nozzles and diffusers do not always satisfy conditions (6.53), but we use the one-dimensional theory anyway because of its simplicity.

For steady one-dimensional flow the equation of continuity is

$$\rho(x)V(x)A(x) = \dot{m} = \text{const} \tag{6.54}$$

Before applying this to duct theory, we can learn a lot from the differential form of Eq. (6.54)

$$\frac{d\rho}{\rho} + \frac{dV}{V} + \frac{dA}{A} = 0 \tag{6.55}$$

The differential forms of the frictionless momentum equation (6.48) and the sound-speed relation (6.27) are recalled here for convenience:

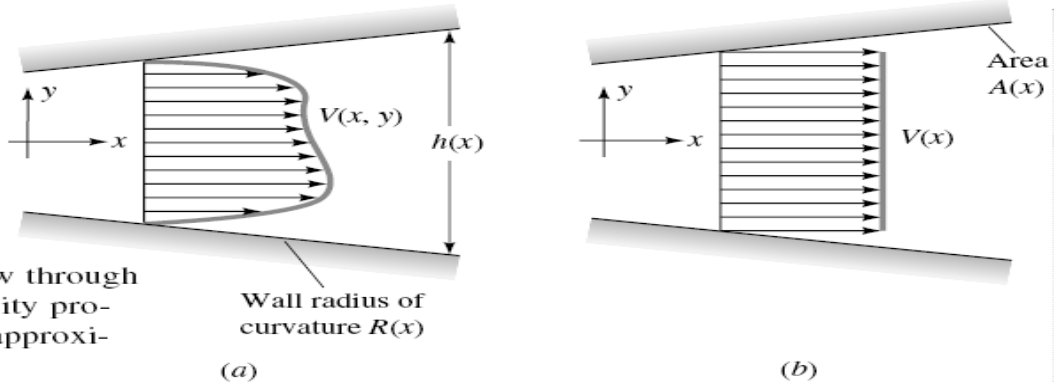

Fig. 6.9 Compressible flow through a duct: (*a*) real-fluid velocity profile; (*b*) one-dimensional approximation.

Momentum $$\frac{dp}{\rho} + V\,dV = 0$$

Sound speed: $$dp = a^2\,d\rho \qquad (6.56)$$

Now eliminate dp and $d\rho$ between Eqs. (6.55) and (6.56) to obtain the following relation between velocity change and area change in isentropic duct flow:

$$\frac{dV}{V} = \frac{dA}{A}\frac{1}{\mathrm{Ma}^2 - 1} = -\frac{dp}{\rho V^2} \qquad (6.57)$$

Inspection of this equation, without actually solving it, reveals a fascinating aspect of compressible flow: Property changes are of opposite sign for subsonic and supersonic flow because of the term $\mathrm{Ma}^2 - 1$. There are four combinations of area change and Mach number, summarized in Fig. 6.10

From earlier chapters we are used to subsonic behavior (Ma < 1): When area increases, velocity decreases and pressure increases, which is denoted a subsonic diffuser. But in supersonic flow (Ma > 1), the velocity actually increases when the area increases, a supersonic nozzle. The same opposing behavior occurs for an area decrease, which speeds up a subsonic flow and slows down a supersonic flow.

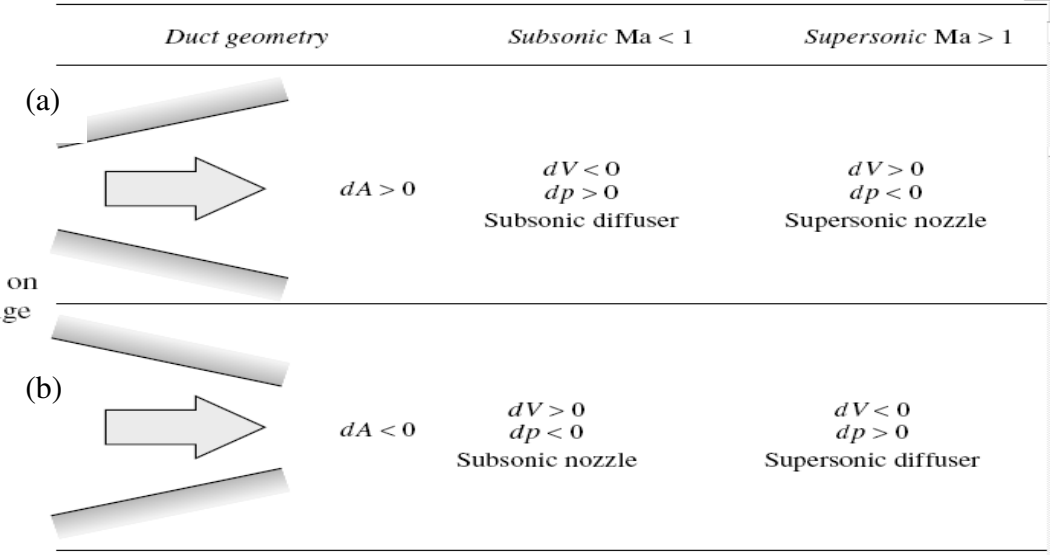

Fig. 6.10 Effect of Mach number on property changes with area change in duct flow.

What about the sonic point Ma = 1? Since infinite acceleration is physically impossible, Eq. (6.57) indicates that dV can be finite only when $dA = 0$, that is, a minimum area (throat) or a maximum area (bulge). In Fig. 6.11 we patch together a throat section and a bulge section, using the rules from Fig. 6.10. The throat or converging-diverging section can smoothly accelerate a subsonic flow through sonic to supersonic flow, as in Fig. 6.11a. This is the only way a supersonic flow can be created by expanding the gas from a stagnant reservoir. The bulge section fails; the bulge Mach number moves away from a sonic condition rather than toward it.

Although supersonic flow downstream of a nozzle requires a sonic throat, the opposite is not true: A compressible gas can pass through a throat section without becoming sonic.

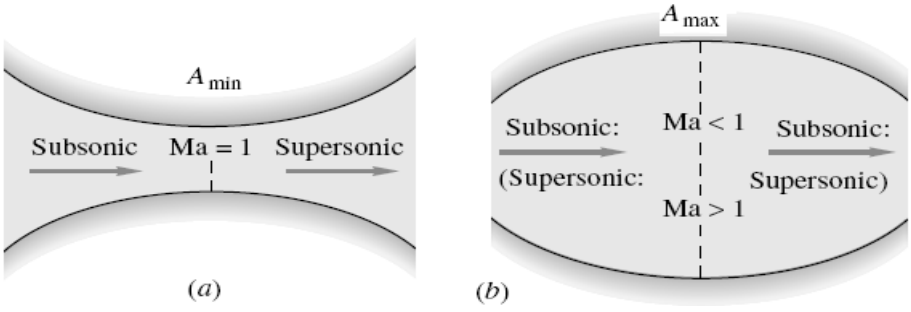

Fig. 6.11 From Eq. (9.40), in flow through a throat (*a*) the fluid can accelerate smoothly through sonic and supersonic flow. In flow through the bulge (*b*) the flow at the bulge cannot be sonic on physical grounds.

6.4.1 Example on Detailed Prove of Equations (6.57):

When fluid flows steadily through a conduit that has a flow cross-section area that varies with axial distance, the conservation of mass (continuity) equation

$$\dot{m} = \rho A V = \text{constant} \qquad (E.1)$$

can be used to relate the flow rates at different sections. For incompressible flow, the fluid density remains constant and the flow velocity from section to section varies inversely with cross-section area. However, when the flow is compressible, density, cross-section area, and flow velocity can all vary from section to section. We proceed to determine how fluid density and flow velocity change with axial location in a variable area duct when the fluid is an ideal gas and the flow through the duct is steady and isentropic.

In Part (4) , Newton's second law was applied to the inviscid (frictionless) and steady flow of a fluid particle. For the streamwise direction, the result Bernoulli's equation for either compressible or incompressible flows is

$$dp + \tfrac{1}{2}\rho\, d(V^2) + \gamma\, dz = 0 \qquad (E.2)$$

The frictionless flow from section to section through a finite control volume is also governed by Eq. E.2 , if the flow is one-dimensional, because every particle of fluid involved will have the same experience. For ideal gas flow, the potential energy difference term, $\gamma\, dz$, can be dropped because of its small size in comparison to the other terms, namely, dp and $d(V^2)$. Thus, an appropriate equation of motion in the streamwise direction for the steady, one-dimensional, and isentropic (adiabatic and frictionless) flow of an ideal gas is obtained from Eq. E.2 as

$$\frac{dp}{\rho V^2} = -\frac{dV}{V} \qquad (E.3)$$

If we form the logarithm of both sides of the continuity equation (Eq. E.1), the result is

$$\ln \rho + \ln A + \ln V = \text{constant} \qquad (E.4)$$

Differentiating Eq. E.4 we get

$$\frac{d\rho}{\rho} + \frac{dA}{A} + \frac{dV}{V} = 0$$

or

$$-\frac{dV}{V} = \frac{d\rho}{\rho} + \frac{dA}{A} \qquad (E.5)$$

Now we combine Eqs. E.3 and E.5 to obtain

$$\frac{dp}{\rho V^2}\left(1 - \frac{V^2}{dp/d\rho}\right) = \frac{dA}{A} \qquad (E.6)$$

Since the flow being considered is isentropic, the speed of sound is related to variations of pressure with density by Eq. 6.27 , repeated here for convenience as

$$c = \sqrt{\left(\frac{\partial p}{\partial \rho}\right)_s}$$

Equation 6.27 , combined with the definition of Mach number

$$\text{Ma} = \frac{V}{c} \qquad (E.7)$$

and Eq. E.6 yields

$$\frac{dp}{\rho V^2}(1 - \text{Ma}^2) = \frac{dA}{A} \qquad (E.8)$$

Equations E.3 and E.8 merge to form

$$\frac{dV}{V} = -\frac{dA}{A}\frac{1}{(1 - \text{Ma}^2)} \qquad (E.9)$$

We can use Eq. E.9 to conclude that when the flow is subsonic (Ma $<$ 1), velocity and section area changes are in opposite directions. In other words, the area increase associated with subsonic flow through a diverging duct like the one shown in Fig. 6.10 a is accompanied by a velocity decrease. Subsonic flow through a converging duct (see Fig. 6.10b) involves an increase of velocity. These trends are consistent with incompressible flow behavior, which we described earlier in this book, for instance, in parts 2 and 4 .

Equation E.9 also serves to show us that when the flow is supersonic (Ma $>$ 1), velocity and area changes are in the same direction. A diverging duct (Fig. 6.10a) will accelerate a supersonic flow. A converging duct (Fig. 6.10b) will decelerate a supersonic flow. These trends are the opposite of what happens for incompressible and subsonic compressible flows.

To better understand why subsonic and supersonic duct flows are so different, we combine Eqs. E.5 and E.9 to form

$$\frac{d\rho}{\rho} = \frac{dA}{A}\frac{\text{Ma}^2}{(1 - \text{Ma}^2)} \qquad (E.10)$$

Using Eq. E.10 , we can conclude that for subsonic flows (Ma $<$ 1), density and area changes are in the same direction, whereas for supersonic flows (Ma $>$ 1), density and area changes are in opposite directions. Since $\rho A V$ must remain constant (Eq. E.1), when the duct diverges and the flow is subsonic, density and area both increase and thus flow velocity must decrease. However, for supersonic flow through a diverging duct, when the area increases, the density decreases enough so that the flow velocity has to increase to keep $\rho A V$ constant.

By rearranging Eq. 11.48, we can obtain

$$\frac{dA}{dV} = -\frac{A}{V}(1 - \text{Ma}^2) \qquad (E.11)$$

Equation E.11 gives us some insight into what happens when Ma = 1. For Ma = 1, Eq. E.11 requires that $dA/dV = 0$. This result suggests that the area associated with Ma = 1 is either a minimum or a maximum amount.

6.4.2 Analysis of Flow in a Converging-Diverging Duct:

A converging-diverging duct (Fig. 6.11a) involves a minimum area. If the flow entering such a duct were subsonic, Eq. E.9 discloses that the fluid velocity would increase in the converging portion of the duct, and achievement of a sonic condition (Ma = 1) at the minimum area location appears possible. If the flow entering the converging-diverging duct is supersonic, Eq. E.9 states that the fluid velocity would decrease in the converging portion of the duct and the sonic condition at the minimum area is possible.

A diverging-converging duct (Fig. 6.11b), on the other hand, would involve a maximum area. If the flow entering this duct were subsonic, the fluid velocity would decrease in the diverging portion of the duct and the sonic condition could not be attained at the maximum area location. For supersonic flow in the diverging portion of the duct, the fluid velocity would increase and thus Ma = 1 at the maximum area is again impossible.

For the steady isentropic flow of an ideal gas, we conclude that the sonic condition (Ma = 1) can be attained in a converging-diverging duct at the minimum area location. This minimum area location is often called the *throat* of the converging-diverging duct. Furthermore, to achieve supersonic flow from a subsonic state in a duct, a converging-diverging area variation is necessary. For this reason, we often refer to such a duct as a *converging-diverging nozzle*. Note that a converging-diverging duct can also decelerate a supersonic flow to subsonic conditions. Thus, a converging-diverging duct can be a nozzle or a diffuser depending on whether the flow in the converging portion of the duct is subsonic or supersonic. A supersonic wind tunnel test section is generally preceded by a converging-diverging nozzle and followed by a converging-diverging diffuser (see Ref. 1). Further details about steady, isentropic, ideal gas flow through a converging-diverging duct are discussed in the next section.

It is convenient to use the stagnation state of the fluid as a reference state for compressible flow calculations. The stagnation state is associated with zero flow velocity and an entropy value that corresponds to the entropy of the flowing fluid. The subscript 0 is used to designate the stagnation state. Thus, stagnation temperature and pressure are T_0 and p_0. For example, if the fluid flowing through the converging-diverging duct of Fig. 6.11a were drawn isentropically from the atmosphere, the atmospheric pressure and temperature would represent the stagnation state of the flowing fluid. The stagnation state can also be achieved by isentropically decelerating a flow to zero velocity. This can be accomplished with a diverging duct for subsonic flows or a converging-diverging duct for supersonic flows. Also, as discussed earlier in sec.6.2.2 , an approximately isentropic deceleration can be accomplished with a Pitot-static tube (see Fig. 6.2). It is thus possible to measure, with only a small amount of uncertainty, values of stagnation pressure, p_0, and stagnation temperature, T_0, of a flowing fluid.

In Section 6.2 , we demonstrated that for the isentropic flow of an ideal gas (see Eq.6.18)

$$\frac{p}{\rho^k} = \text{constant} = \frac{p_0}{\rho_0^k}$$

The streamwise equation of motion for steady and frictionless flow (Eq. E.2) can be expressed for an ideal gas as

$$\frac{dp}{\rho} + d\left(\frac{V^2}{2}\right) = 0 \qquad \text{(E.12)}$$

since the potential energy term, $\gamma\, dz$ can be considered as being negligibly small in comparison with the other terms involved.

By incorporating Eq. 6.18 into Eq. E.12 we obtain

$$\frac{p_0^{1/k}}{\rho_0}\frac{dp}{(p)^{1/k}} + d\left(\frac{V^2}{2}\right) = 0 \qquad \text{(E.13)}$$

Consider the steady, one-dimensional, isentropic flow of an ideal gas with constant c_p and c_v through the converging-diverging nozzle of Fig.6.11a . Equation E.13 is valid for this flow and can be integrated between the common stagnation state of the flowing fluid to the state of the gas at any location in the converging-diverging duct to give

$$\frac{k}{k-1}\left(\frac{p_0}{\rho_0} - \frac{p}{\rho}\right) - \frac{V^2}{2} = 0 \qquad \text{(E.14)}$$

By using the ideal gas equation of state with Eq. E.14 we obtain

$$\frac{kR}{k-1}(T_0 - T) - \frac{V^2}{2} = 0 \qquad \text{(E.15)}$$

It is of interest to note that combining Eq E.15 and $c_p = \dfrac{Rk}{k-1}$ leads to

$$c_p (T_0 - T) - \frac{V^2}{2} = 0$$

which results in

$$\check{h}_0 - \left(\check{h} + \frac{V^2}{2}\right) = 0 \qquad \text{(E.16)}$$

where $\check{h}_0$ is the stagnation enthalpy. If the steady flow energy equation (see Part1) is applied to the flow situation we are presently considering, the resulting equation will be identical to

Eq. E.16 . Further, we conclude that the stagnation enthalpy is constant. The conservation of momentum and energy principles lead to the same equation (Eq. E.16) for steady isentropic flows.The definition of Mach number (Eq. E.7) and the speed of sound relationship for ideal gases (Eq. 6.29) can be combined with Eq. E.15 to yield

$$\frac{T}{T_0} = \frac{1}{1 + [(k-1)/2]\mathrm{Ma}^2} \qquad (E.17)$$

With Eq. E.17 we can calculate the temperature of an ideal gas anywhere in the converging-diverging duct of Fig. 6.11a if the flow is steady, one-dimensional, and isentropic, provided we know the value of the local Mach number and the stagnation temperature.

We can also develop an equation for pressure variation. Since $p/\rho = RT$, then

$$\left(\frac{p}{p_0}\right)\left(\frac{\rho_0}{\rho}\right) = \frac{T}{T_0} \qquad (E.18)$$

From Eqs. E.18 and 6.18 we obtain

$$\left(\frac{p}{p_0}\right) = \left(\frac{T}{T_0}\right)^{k/(k-1)} \qquad (E.19)$$

Combining Eqs. E.19 and E.17 leads to

$$\frac{p}{p_0} = \left\{\frac{1}{1 + [(k-1)/2]\mathrm{Ma}^2}\right\}^{k/(k-1)} \qquad (E.20)$$

For density variation we consolidate Eqs. E.17 , E.18 , and E.20 to get

$$\frac{\rho}{\rho_0} = \left\{\frac{1}{1 + [(k-1)/2]\mathrm{Ma}^2}\right\}^{1/(k-1)} \qquad (E.21)$$

6.4.3 The T-S Diagram:

A very useful means of keeping track of the states of an isentropic flow of an ideal gas involves a temperature-entropy ($T - s$) diagram, as is shown in Fig.6.11c. Experience has shown (see, for example, Refs. 2 and 3) that lines of constant pressure are generally as are sketched in Fig.6.11c. An isentropic flow is confined to a vertical line on a $T - s$ diagram. The vertical line in Fig.6.11c is representative of flow between the stagnation state and any state within the converging-diverging nozzle. Equation E.17 shows that fluid temperature

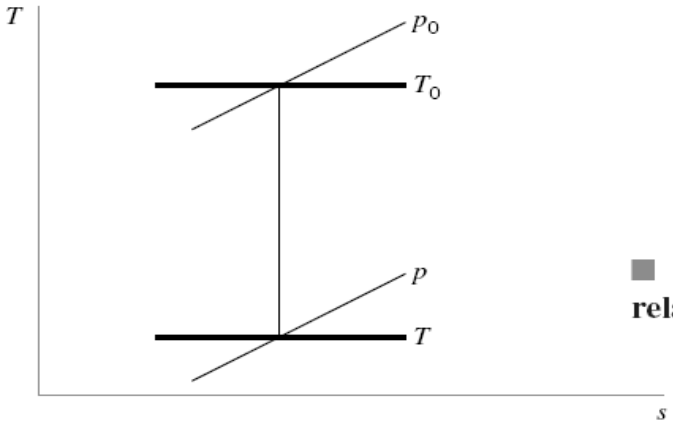

■ FIGURE 6.11 C **The $T-s$ diagram relating stagnation and static states.**

decreases with an increase in Mach number. Thus, the lower temperature levels on a $T - s$ diagram correspond to higher Mach numbers. Equation E.20 suggests that fluid pressure also decreases with an increase in Mach number. Thus, lower fluid temperatures and pressures are associated with higher Mach numbers in our isentropic converging-diverging duct example.

One way to produce flow through a converging-diverging duct like the one in Fig. 6.11a is to connect the downstream end of the duct to a vacuum pump. When the pressure at the downstream end of the duct (the back pressure) is decreased slightly, air will flow from the atmosphere through the duct and vacuum pump. Neglecting friction and heat transfer and considering the air to act as an ideal gas, Eqs. E.17 , E.20 , and E.21 and a $T - s$ diagram can be used to describe steady flow through the converging-diverging duct.

If the pressure in the duct is only slightly less than atmospheric pressure, we predict with Eq. E.20 that the Mach number levels in the duct will be low. Thus, with Eq. E.21 we conclude that the variation of fluid density in the duct is also small. The continuity equation (Eq. E.1) leads us to state that there is a small amount of fluid flow acceleration in the converging portion of the duct followed by flow deceleration in the diverging portion of the duct. We considered this type of flow when we discussed the Venturi meter in ideal flow. The $T - s$ diagram for this flow is sketched in Fig.6.11d

We next consider what happens when the back pressure is lowered further. Since the flow starts from rest upstream of the converging portion of the duct of Fig.6.11a , Eqs. E.9 and E.11 reveal to us that flow up to the nozzle throat can be accelerated to a maximum allowable Mach number of 1 at the throat. Thus, when the duct back pressure is lowered sufficiently, the Mach number at the throat of the duct will be 1. Any further decrease of the back pressure will not affect the flow in the converging portion of the duct because, as is discussed in Section 6.5 , information about pressure cannot move upstream when Ma = 1. When Ma = 1 at the throat of the converging-diverging duct, we have a condition called *choked flow*.

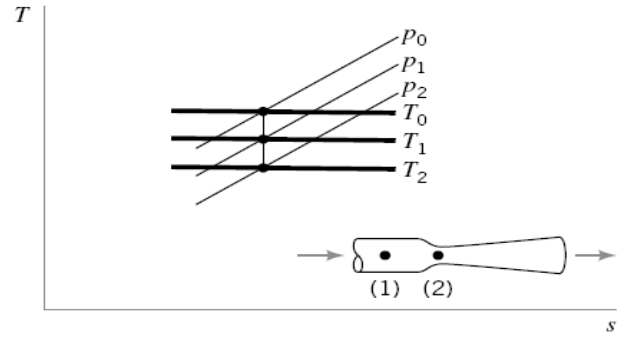

■ FIGURE 6.11 d **The $T-s$ diagram for Venturi meter flow.**

The stagnation and critical pressures and temperatures are shown on the $T - s$ diagram of Fig.6.11e.

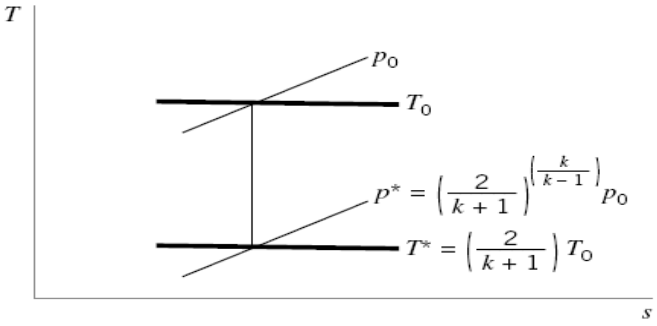

■ FIGURE 6.11e **The relationship between the stagnation and critical states.**

6.4.4 Further Analysis of The Perfect-Gas Isentropic- Relations:

We can use the perfect-gas and isentropic-flow relations to convert the continuity relation (6.54) into an algebraic expression involving only area and Mach number, as follows. Equate the mass flow at any section to the mass flow under sonic conditions (which may not actually occur in the duct)

$$\rho V A = \rho^* V^* A^*$$

or

$$\frac{A}{A^*} = \frac{\rho^*}{\rho}\frac{V^*}{V} \tag{6.58}$$

Both the terms on the right are functions only of Mach number for isentropic flow. From Eqs. (6.45) and (6.49)

$$\frac{\rho^*}{\rho} = \frac{\rho^*}{\rho_0}\frac{\rho_0}{\rho} = \left\{\frac{2}{k+1}\left[1 + \frac{1}{2}(k-1)\,\mathrm{Ma}^2\right]\right\}^{1/(k-1)} \tag{6.59}$$

From Eqs. (6.43) and (6.49) we obtain

$$\frac{V^*}{V} = \frac{(kRT^*)^{1/2}}{V} = \frac{(kRT)^{1/2}}{V}\left(\frac{T^*}{T_0}\right)^{1/2}\left(\frac{T_0}{T}\right)^{1/2}$$

$$= \frac{1}{\mathrm{Ma}}\left\{\frac{2}{k+1}\left[1 + \frac{1}{2}(k-1)\,\mathrm{Ma}^2\right]\right\}^{1/2} \tag{6.60}$$

Combining Eqs. (6.58) to (6.60), we get the desired result

$$\frac{A}{A^*} = \frac{1}{\mathrm{Ma}}\left[\frac{1 + \frac{1}{2}(k-1)\,\mathrm{Ma}^2}{\frac{1}{2}(k+1)}\right]^{(1/2)(k+1)/(k-1)} \tag{6.61}$$

For $k = 1.4$, Eq. (6.61) takes the numerical form

$$\frac{A}{A^*} = \frac{1}{\mathrm{Ma}}\frac{(1 + 0.2\,\mathrm{Ma}^2)^3}{1.728} \tag{6.62}$$

which is plotted in Fig.6.12. Equations (6.62) and (6.51) enable us to solve any one-dimensional isentropic-airflow problem given, say, the shape of the duct $A(x)$ and the stagnation conditions and assuming that there are no shock waves in the duct.

Figure 6.12 shows that the minimum area which can occur in a given isentropic duct flow is the sonic, or critical, throat area. All other duct sections must have A greater than A^*. In many flows a critical sonic throat is not actually present, and the flow in the duct is either entirely subsonic or, more rarely, entirely supersonic.

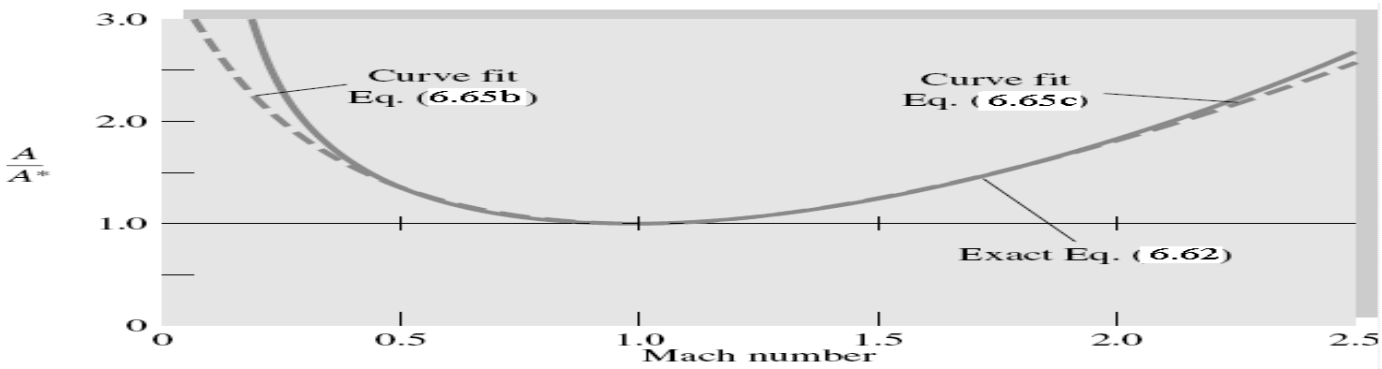

Fig. 6.12 Area ratio versus Mach number for isentropic flow of a perfect gas with $k = 1.4$.

6.4.5 The Choking:

From Eq. (6.58) the inverse ratio A^*/A equals $\rho V/(\rho^* V^*)$, the mass flow per unit area at any section compared with the critical mass flow per unit area. From Fig. 6.12 this inverse ratio rises from zero at Ma = 0 to unity at Ma = 1 and back down to zero at large Ma. Thus, for given stagnation conditions, the maximum possible mass flow passes through a duct when its throat is at the critical or sonic condition. The duct is then said to be *choked* and can carry no additional mass flow unless the throat is widened. If the throat is constricted further, the mass flow through the duct must decrease. From Eqs. (6.49) and (6.50) the maximum mass flow is

$$\dot{m}_{\max} = \rho^* A^* V^* = \rho_0 \left(\frac{2}{k+1}\right)^{1/(k-1)} A^* \left(\frac{2k}{k+1} RT_0\right)^{1/2}$$

$$= k^{1/2} \left(\frac{2}{k+1}\right)^{(1/2)(k+1)/(k-1)} A^* \rho_0 (RT_0)^{1/2} \qquad (6.63a)$$

For $k = 1.4$ this reduces to

$$\dot{m}_{\max} = 0.6847 A^* \rho_0 (RT_0)^{1/2} = \frac{0.6847 p_0 A^*}{(RT_0)^{1/2}} \qquad (6.63b)$$

For isentropic flow through a duct, the maximum mass flow possible is proportional to the throat area and stagnation pressure and inversely proportional to the square root of the stagnation temperature. These are somewhat abstract facts, so let us illustrate with some examples.

6.4.6 The Local Mass Flow Function:

Equation (6.63) gives the *maximum* mass flow, which occurs at the choking condition (sonic exit). It can be modified to predict the actual (nonmaximum) mass flow at any section where local area A and pressure p are known.[1] The algebra is convoluted, so here we give only the final result, expressed in dimensionless form:

$$\text{Mass-flow function} = \frac{\dot{m}}{A} \frac{\sqrt{RT_0}}{p_0} = \sqrt{\frac{2k}{k-1} \left(\frac{p}{p_0}\right)^{2/k} \left[1 - \left(\frac{p}{p_0}\right)^{(k-1)/k}\right]} \qquad (6.64)$$

We stress that p and A in this relation are the *local* values at position x. As p/p_0 falls, this function rises rapidly and then levels out at the maximum of Eq. (6.63). A few values may be tabulated here for $k = 1.4$:

p/p_0	1.0	0.98	0.95	0.9	0.8	0.7	0.6	≤0.5283
Function	0.0	0.1978	0.3076	0.4226	0.5607	0.6383	0.6769	**0.6847**

Equation (6.64) is handy if stagnation conditions are known and the flow is not choked.

The only cumbersome algebra in these problems is the inversion of Eq. (6.62) to compute the Mach number when A/A^* is known. If available, EES is ideal for this situation and will yield Ma in a flash. In the absence of EES, the following curve-fitted formulas are suggested; given A/A^*, they estimate the Mach number within ±2 percent for $k = 1.4$ if you stay within the ranges listed for each formula:

$$\text{Ma} \approx \begin{cases} \dfrac{1 + 0.27(A/A^*)^{-2}}{1.728 A/A^*} & 1.34 < \dfrac{A}{A^*} < \infty \quad (6.65a) \\ 1 - 0.88\left(\ln \dfrac{A}{A^*}\right)^{0.45} & 1.0 < \dfrac{A}{A^*} < 1.34 \quad (6.65b) \end{cases} \text{ subsonic flow}$$

$$\text{Ma} \approx \begin{cases} 1 + 1.2\left(\dfrac{A}{A^*} - 1\right)^{1/2} & 1.0 < \dfrac{A}{A^*} < 2.9 \quad (6.65c) \\ \left[216 \dfrac{A}{A^*} - 254\left(\dfrac{A}{A^*}\right)^{2/3}\right]^{1/5} & 2.9 < \dfrac{A}{A^*} < \infty \quad (6.65d) \end{cases} \text{ supersonic flow}$$

Formulas (6.65a) and (6.65d) are asymptotically correct as $A/A^* \to \infty$, while (6.65b) and (6.65c) are just curve fits. However, formulas (6.65b) and (6.65c) are seen in Fig. 6.12 to be accurate within their recommended ranges.

Note that two solutions are possible for a given A/A^*, one subsonic and one supersonic. The proper solution cannot be selected without further information, e.g., known pressure or temperature at the given duct section.

Example 6.9:

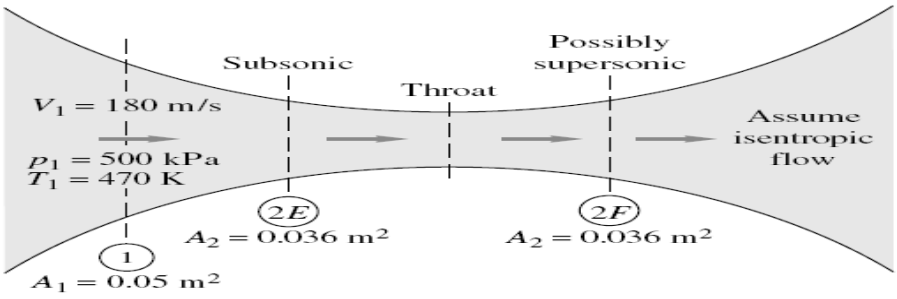

E6.9

Air flows isentropically through a duct. At section 1 the area is 0.05 m^2 and $V_1 = 180$ m/s, $p_1 = 500$ kPa, and $T_1 = 470$ K. Compute (*a*) T_0, (*b*) Ma_1, (*c*) p_0, and (*d*) both A^* and $\dot{m}$. If at section 2 the area is 0.036 m^2, compute Ma_2 and p_2 if the flow is (*e*) subsonic or (*f*) supersonic. Assume $k = 1.4$.

Solution

Part (a)

A general sketch of the problem is shown in Fig.E6.9 . With V_1 and T_1 known, the energy equation (6.40) gives

$$T_0 = T_1 + \frac{V_1^2}{2c_p} = 470 + \frac{(180)^2}{2(1005)} = 486 \text{ K} \qquad \textit{Ans. (a)}$$

Part (b)

The local sound speed $a_1 = \sqrt{kRT_1} = [(1.4)(287)(470)]^{1/2} = 435$ m/s. Hence

$$\text{Ma}_1 = \frac{V_1}{a_1} = \frac{180}{435} = 0.414 \qquad \textit{Ans. (b)}$$

Part (c)

With Ma_1 known, the stagnation pressure follows from Eq. (6.51):

$$p_0 = p_1(1 + 0.2\ \text{Ma}_1^2)^{3.5} = (500 \text{ kPa})[1 + 0.2(0.414)^2]^{3.5} = 563 \text{ kPa} \qquad \textit{Ans. (c)}$$

Part (d)

Similarly, from Eq. (6.62), the critical sonic-throat area is

$$\frac{A_1}{A^*} = \frac{(1 + 0.2\ \text{Ma}_1^2)^3}{1.728\ \text{Ma}_1} = \frac{[1 + 0.2(0.414)^2]^3}{1.728(0.414)} = 1.547$$

or

$$A^* = \frac{A_1}{1.547} = \frac{0.05 \text{ m}^2}{1.547} = 0.0323 \text{ m}^2 \qquad \textit{Ans. (d)}$$

This throat must *actually be present* in the duct if the flow is to become supersonic.

We now know A^*. So to compute the mass flow we can use Eq. (6.63), which remains valid, based on the numerical value of A^*, whether or not a throat actually exists:

$$\dot{m} = 0.6847 \frac{p_0 A^*}{\sqrt{RT_0}} = 0.6847 \frac{(563{,}000)(0.0323)}{\sqrt{(287)(486)}} = 33.4 \text{ kg/s} \qquad \textit{Ans. (d)}$$

Or we could fare equally well with our new "local mass flow" formula, Eq. (6.64), using, say, the pressure and area at section 1. Given $p_1/p_0 = 500/563 = 0.889$, Eq. (6.64) yields

$$\dot{m}\frac{\sqrt{287(486)}}{563{,}000(0.05)} = \sqrt{\frac{2(1.4)}{0.4}(0.889)^{2/1.4}[1 - (0.889)^{0.4/1.4}]} = 0.447 \qquad \dot{m} = 33.4 \frac{\text{kg}}{\text{s}} \quad \textit{Ans. (d)}$$

Part (e)

Assume *subsonic* flow corresponds to section 2*E* in Fig.E6.9 . The duct contracts to an area ratio $A_2/A^* = 0.036/0.0323 = 1.115$, which we find on the left side of Fig.6.12 or the subsonic part of Table B.1. Neither the figure nor the table is that accurate. There are two accurate options. First, Eq. (6.65b) gives the estimate $\text{Ma}_2 \approx 1 - 0.88 \ln (1.115)^{0.45} \approx 0.676$ (error less than 0.5 percent). Second, EES (App. E) will give an arbitrarily accurate solution with only three statements (in SI units):

```
A2 = 0.036
Astar = 0.0323
A2/Astar = (1+0.2*Ma2^2)^3/1.2^3/Ma2
```

Specify that you want a *subsonic* solution (e.g., limit $\text{Ma}_2 < 1$), and EES reports

$$\text{Ma}_2 = \mathbf{0.6758} \qquad \textit{Ans. (e)}$$

[Ask for a supersonic solution and you receive `Ma2 = 1.4001`, which is the answer to part (*f*).]

The pressure is given by the isentropic relation

$$p_2 = \frac{p_0}{[1 + 0.2(0.676)^2]^{3.5}} = \frac{563 \text{ kPa}}{1.358} \approx 415 \text{ kPa} \qquad \textit{Ans. (e)}$$

Part (*e*) does *not* require a throat, sonic or otherwise; the flow could simply be contracting subsonically from A_1 to A_2.

Part (f)

This time assume *supersonic* flow, corresponding to section 2*F* in Fig. E6.9. Again the area ratio is $A_2/A^* = 0.036/0.0323 = 1.115$, and we look on the *right* side of Fig. 6.12 or the supersonic part of Table B.1—the latter can be read quite accurately as $\mathrm{Ma}_2 \approx 1.40$. Again there are two other accurate options. First, Eq. (6.65c) gives the curve-fit estimate $\mathrm{Ma}_2 \approx 1 + 1.2(1.115 - 1)1^{1/2} \approx 1.407$, only 0.5 percent high. Second, EES will give a very accurate solution with the same three statements from part (*e*). Specify that you want a *supersonic* solution (e.g., limit $\mathrm{Ma}_2 > 1$), and EES reports $\mathrm{Ma}_2 = \mathbf{1.4001}$ *Ans. (f)*

Again the pressure is given by the isentropic relation at the new Mach number:

$$p_2 = \frac{p_0}{[1 + 0.2(1.4001)^2]^{3.5}} = \frac{563 \text{ kPa}}{3.183} = 177 \text{ kPa} \qquad \textit{Ans. (f)}$$

Note that the supersonic-flow pressure level is much less than p_2 in part (*e*), and a sonic throat *must* have occurred between sections 1 and 2F.

Example 6.10:

It is desired to expand air from $p_0 = 200$ kPa and $T_0 = 500$ K through a throat to an exit Mach number of 2.5. If the desired mass flow is 3 kg/s, compute (*a*) the throat area and the exit (*b*) pressure, (*c*) temperature, (*d*) velocity, and (*e*) area, assuming isentropic flow, with $k = 1.4$.

Solution

The throat area follows from Eq. (6.64), because the throat flow must be sonic to produce a supersonic exit:

$$A^* = \frac{\dot{m}(RT_0)^{1/2}}{0.6847 p_0} = \frac{3.0[287(500)]^{1/2}}{0.6847(200{,}000)} = 0.00830 \text{ m}^2 = \frac{1}{4}\pi D^{*2}$$

or

$$D_{\text{throat}} = 10.3 \text{ cm} \qquad \textit{Ans. (a)}$$

With the exit Mach number known, the isentropic-flow relations give the pressure and temperature:

$$p_e = \frac{p_0}{[1 + 0.2(2.5)^2]^{3.5}} = \frac{200{,}000}{17.08} = 11{,}700 \text{ Pa} \qquad \textit{Ans. (b)}$$

$$T_e = \frac{T_0}{1 + 0.2(2.5)^2} = \frac{500}{2.25} = 222 \text{ K} \qquad \textit{Ans. (c)}$$

The exit velocity follows from the known Mach number and temperature

$$V_e = \mathrm{Ma}_e (kRT_e)^{1/2} = 2.5[1.4(287)(222)]^{1/2} = 2.5(299 \text{ m/s}) = 747 \text{ m/s} \qquad \textit{Ans. (d)}$$

The exit area follows from the known throat area and exit Mach number and Eq. (6.62):

$$\frac{A_e}{A^*} = \frac{[1 + 0.2(2.5)^2]^3}{1.728(2.5)} = 2.64$$

or

$$A_e = 2.64A^* = 2.64(0.0083 \text{ m}^2) = 0.0219 \text{ m}^2 = \tfrac{1}{4}\pi D_e^2$$

or

$$D_e = 16.7 \text{ cm} \qquad \textit{Ans. (e)}$$

One point might be noted: The computation of the throat area A^* did not depend in any way on the numerical value of the exit Mach number. The exit was supersonic; therefore the throat is sonic and choked, and no further information is needed.

Example 6.11:

A converging duct passes air steadily from standard atmospheric conditions to a receiver pipe as illustrated in Fig. E6.11a . The throat (minimum) flow cross-section area of the converging

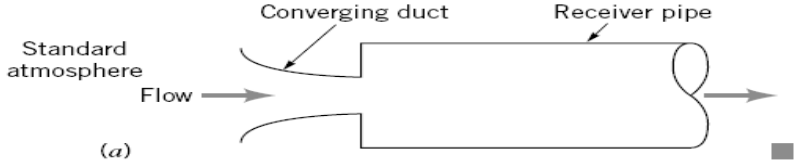

■ FIGURE E6.11

duct is 1×10^{-4} m^2. Determine the mass flowrate through the duct if the receiver pressure is (a) 80 kPa (abs), (b) 40 kPa (abs). Sketch temperature-entropy diagrams for situations (a) and (b).

Solution:----------

To determine the mass flowrate through the converging duct we use Eq. E.1. Thus,

$$\dot{m} = \rho A V = \text{constant}$$

or in terms of the given throat area, A_{th},

$$\dot{m} = \rho_{\text{th}} A_{\text{th}} V_{\text{th}} \qquad \textbf{(1)}$$

We assume that the flow through the converging duct is isentropic and that the air behaves as an ideal gas with constant c_p and c_v. Then, from Eq. E.21

$$\frac{\rho_{\text{th}}}{\rho_0} = \left\{ \frac{1}{1 + [(k-1)/2]\mathrm{Ma}_{\text{th}}^2} \right\}^{1/(k-1)} \qquad \textbf{(2)}$$

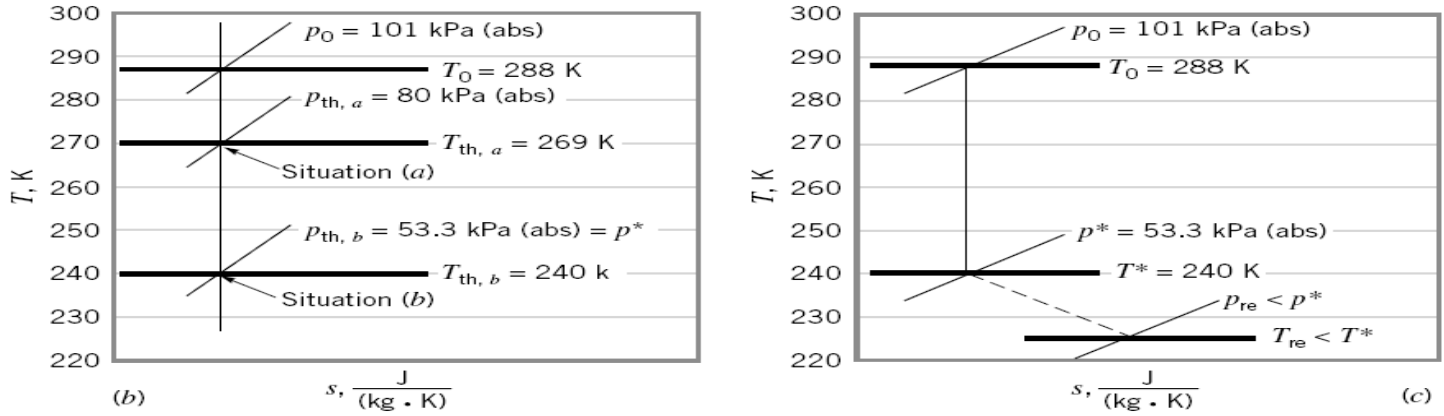

■ FIGURE E6.11 (*Continued*)

The stagnation density, ρ_0, for standard atmosphere is 1.23 kg/m^3 and the specific heat ratio is 1.4. To determine the throat Mach number, Ma_{th}, we can use Eq. E.20 ,

$$\frac{p_{th}}{p_0} = \left\{\frac{1}{1 + [(k-1)/2]Ma_{th}^2}\right\}^{k/(k-1)} \tag{3}$$

The critical pressure, p^*, is obtained from Eq. 6.49 as

$$p^* = 0.528p_0 = 0.528p_{atm} = (0.528)[101\text{ kPa(abs)}] = 53.3\text{ kPa(abs)}$$

If the receiver pressure, p_{re}, is greater than or equal to p^*, then $p_{th} = p_{re}$. If $p_{re} < p^*$, then $p_{th} = p^*$ and the flow is choked. With p_{th}, p_0, and k known, Ma_{th} can be obtained from Eq. 3, and ρ_{th} can be determined from Eq. 2.

The flow velocity at the throat can be obtained from Eqs. 6.29 and E.7 as

$$V_{th} = Ma_{th}c_{th} = Ma_{th}\sqrt{RT_{th}k} \tag{4}$$

The value of temperature at the throat, T_{th}, can be calculated from Eq. E.17,

$$\frac{T_{th}}{T_0} = \frac{1}{1 + [(k-1)/2]Ma_{th}^2} \tag{5}$$

Since the flow through the converging duct is assumed to be isentropic, the stagnation temperature is considered constant at the standard atmosphere value of T_0 = 15 K + 273 K = 288 K. Note that absolute pressures and temperatures are used.

(a) For p_{re} = 80 kPa(abs) > 53.3 kPa(abs) = p^*, we have p_{th} = 80 kPa(abs). Then from Eq. 3

$$\frac{80\text{ kPa(abs)}}{101\text{ kPa(abs)}} = \left\{\frac{1}{1 + [(1.4-1)/2]Ma_{th}^2}\right\}^{1.4/(1.4-1)}$$

or $$Ma_{th} = 0.587$$

From Eq. 2

$$\frac{\rho_{th}}{1.23\text{ kg/m}^3} = \left\{\frac{1}{1 + [(1.4-1)/2](0.587)^2}\right\}^{1/(1.4-1)}$$

or $$\rho_{th} = 1.04\text{ kg/m}^3$$

From Eq. 5

$$\frac{T_{th}}{288\text{ K}} = \frac{1}{1 + [(1.4-1)/2](0.587)^2}$$

or $$T_{th} = 269\text{ K}$$

Substituting Ma_{th} = 0.587 and T_{th} = 269 K into Eq. 4 we obtain

$$V_{th} = 0.587\sqrt{[286.9\text{ J/(kg}\cdot\text{K)}](269\text{ K})(1.4)[1(\text{kg}\cdot\text{m})/(\text{N}\cdot\text{s}^2)][1(\text{N}\cdot\text{m})/\text{J}]}$$

or $$V_{th} = 193\text{ m/s}$$

Finally from Eq. 1 we have

$$\dot{m} = (1.04\text{ kg/m}^3)(1 \times 10^{-4}\text{ m}^2)(193\text{ m/s}) = 0.0201\text{ kg/s} \quad \textbf{(Ans)}$$

(b) For p_{re} = 40 kPa(abs) < 53.3 kPa(abs) = p^*, we have $p_{th} = p^*$ = 53.3 kPa(abs) and Ma_{th} = 1. The converging duct is choked. From Eq. 2

$$\frac{\rho_{th}}{1.23\text{ kg/m}^3} = \left\{\frac{1}{1 + [(1.4-1)/2](1)^2}\right\}^{1/(1.4-1)}$$

or $$\rho_{th} = 0.780\text{ kg/m}^3$$

From Eq. 5

$$\frac{T_{th}}{288\text{ K}} = \frac{1}{1 + [(1.4-1)/2](1)^2}$$

or $$T_{th} = 240\text{ K}$$

From Eq. 4,

$$V_{th} = (1)\sqrt{[286.9\text{ J/(kg}\cdot\text{K)}](240\text{ K})(1.4)[1(\text{kg}\cdot\text{m})/(\text{N}\cdot\text{s}^2)][1(\text{N}\cdot\text{m})/\text{J}]} = 310\text{ m/s}$$

Finally from Eq. 1

$$\dot{m} = (0.780 \text{ kg/m}^3)(1 \times 10^{-4} \text{ m}^2)(310 \text{ m/s}) = 0.0242 \text{ kg/s} \quad \textbf{(Ans)}$$

From the values of throat temperature and throat pressure calculated above for flow situations (a) and (b), we can construct the temperature–entropy diagram shown in Fig. E6.11b .

Note that the flow from standard atmosphere to the receiver for receiver pressure, p_{re}, greater than or equal to the critical pressure, p^*, is isentropic. When the receiver pressure is less than the critical pressure as in situation (b) above, what is the flow like downstream from the exit of the converging duct? Experience suggests that this flow, when $p_{re} < p^*$, is three-dimensional and nonisentropic and involves a drop in pressure from p_{th} to p_{re}, a drop in temperature, and an increase of entropy as are indicated in Fig. E6.11c .

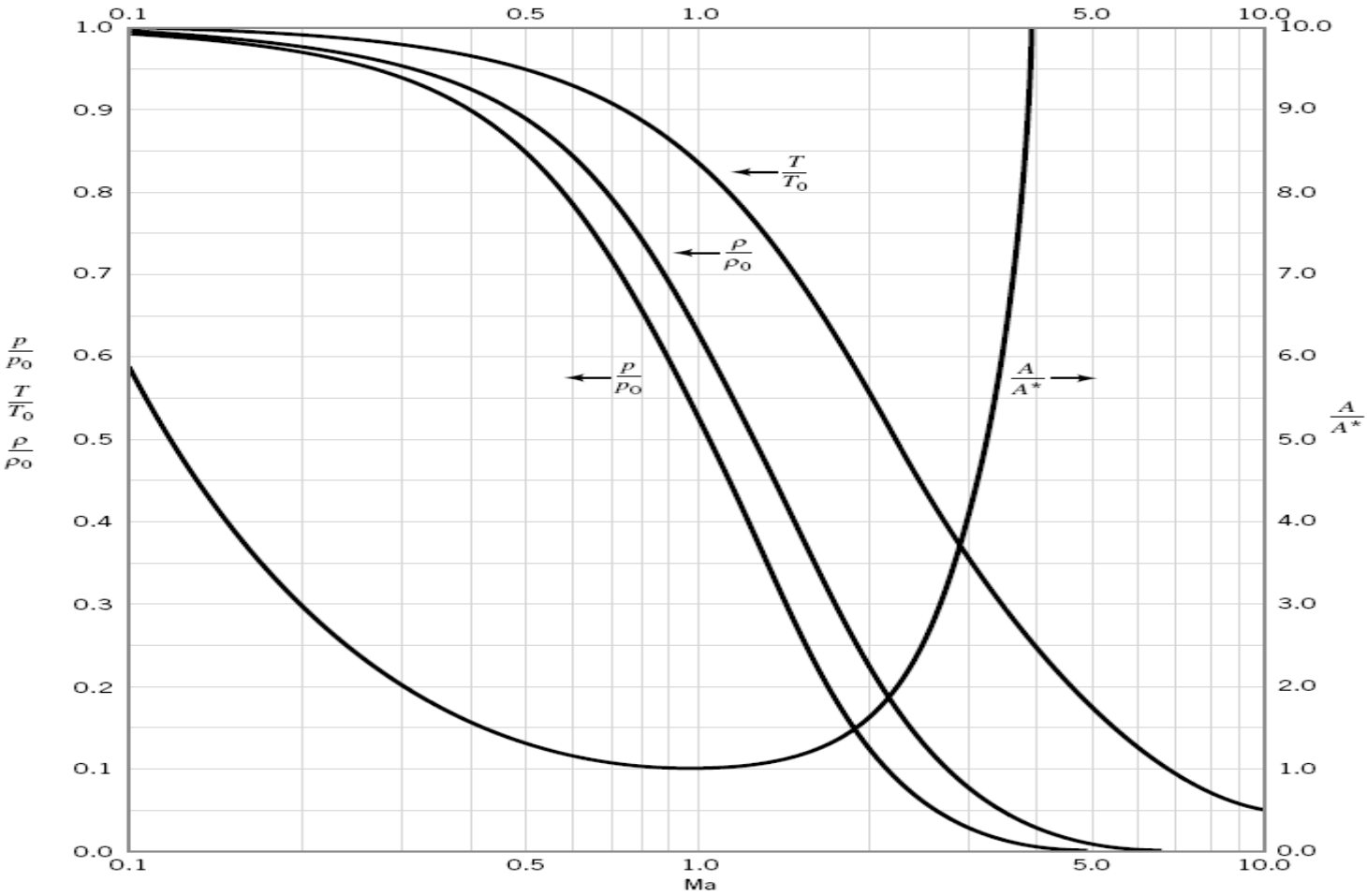

FIGURE D.1 Isentropic flow of an ideal gas with $k = 1.4$. (Graph provided by Professor Bruce A. Reichert of Kansas State University.)

Isentropic flow Eqs. E.17 , E.20 , and E.21 have been used to construct Fig. D.1 in Appendix D for air ($k = 1.4$). Examples 6.12 and 6.13 illustrate how these graphs of T/T_0, p/p_0, and ρ/ρ_0 as a function of Mach number, Ma, can be used to solve compressible flow problems.

Example 6.12:

Solve Example 6.11 using Fig. D.1 of Appendix D.

Solution:

We still need the density and velocity of the air at the converging duct throat to solve for mass flowrate from

$$\dot{m} = \rho_{th} A_{th} V_{th} \quad \textbf{(1)}$$

(a) Since the receiver pressure, $p_{re} = 80$ kPa(abs), is greater than the critical pressure, $p^* = 53.3$ kPa(abs), the throat pressure, p_{th}, is equal to the receiver pressure. Thus

$$\frac{p_{th}}{p_0} = \frac{80 \text{ kPa(abs)}}{101 \text{ kPa(abs)}} = 0.792$$

From Fig. D.1, for $p/p_0 = 0.79$, we get from the graph

$$\text{Ma}_{th} = 0.59$$

$$\frac{T_{th}}{T_0} = 0.94 \quad \textbf{(2)}$$

$$\frac{\rho_{th}}{\rho_0} = 0.85 \quad \textbf{(3)}$$

Thus, from Eqs. 2 and 3

and

$$T_{th} = (0.94)(288 \text{ K}) = 271 \text{ K}$$

$$\rho_{th} = (0.85)(1.23 \text{ kg/m}^3) = 1.04 \text{ kg/m}^3$$

Furthermore, using Eqs. 6.29 and E.7 we get

$$V_{th} = Ma_{th}\sqrt{RT_{th}k}$$
$$= (0.59)\sqrt{[286.9\ J/(kg\cdot K)](269\ K)(1.4)[1(kg\cdot m)/(N\cdot s^2)][1(N\cdot m)/J]}$$
$$= 194\ m/s$$

Finally, from Eq. 1

$$\dot{m} = (1.04\ kg/m^3)(1\times 10^{-4}\ m^2)(194\ m/s) = 0.0202\ kg/s \quad \text{(Ans)}$$

(b) For $p_{re} = 40$ kPa(abs) < 53.3 kPa(abs) $= p^*$, the throat pressure is equal to 53.3 kPa(abs) and the duct is choked with $Ma_{th} = 1$. From Fig. D.1, for Ma = 1 we get

$$\frac{T_{th}}{T_0} = 0.83 \quad (4)$$

and

$$\frac{\rho_{th}}{\rho_0} = 0.64 \quad (5)$$

From Eqs. 4 and 5 we obtain

$$T_{th} = (0.83)(288\ K) = 240\ K$$

and

$$\rho_{th} = (0.64)(1.23\ kg/m^3) = 0.79\ kg/m^3$$

Also, from Eqs. 6.29 and E.7 we conclude that

$$V_{th} = Ma_{th}\sqrt{RT_{th}k}$$
$$= (1)\sqrt{[286.9\ J/(kg\cdot K)](240\ K)(1.4)[1(kg\cdot m)/(N\cdot s^2)][1(N\cdot m)/J]} = 310\ m/s$$

Then, from Eq. 1

$$\dot{m} = (0.79\ kg/m^3)(1\times 10^{-4}\ m^2)(310\ m/s) = 0.024\ kg/s \quad \text{(Ans)}$$

The values from Fig. D.1 resulted in answers for mass flowrate that are close to those using the ideal gas equations (see Example 6.11).

The temperature–entropy diagrams remain the same as those provided in the solution of Example 6.11 .

Example 6.13:

The static pressure to stagnation pressure ratio at a point in a flow stream is measured with a Pitot-static tube (see Fig. E6.13) as being equal to 0.82. The stagnation temperature of the fluid is 68 °F.
Determine the flow velocity if the fluid is (a) air, (b) helium.

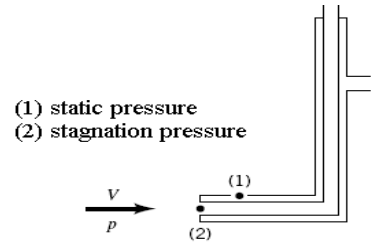

■ FIGURE E 6.13 The Pitot-static tube.

Solution:

We consider both air and helium, flowing as described above, to act as ideal gases with constant specific heats. Then, we can use any of the ideal gas relationships developed in this chapter. To determine the flow velocity, we can combine Eqs. 6.29 and E.7 to obtain

$$V = Ma\sqrt{RTk} \quad (1)$$

By knowing the value of static to stagnation pressure ratio, p/p_0, and the specific heat ratio we can obtain the corresponding Mach number from Eq. E.20 , or for air, from Fig. D.1. Fig. D.1 cannot be used for helium, since k for helium is 1.66 and Fig. D.1 is for $k = 1.4$ only. With Mach number, specific heat ratio, and stagnation temperature known, the value of static temperature can be subsequently ascertained from Eq. E.17 (or Fig. D.1 for air).

(a) For air, $p/p_0 = 0.82$; thus from Fig. D.1,

$$Ma = 0.54 \quad (2)$$

and

$$\frac{T}{T_0} = 0.94 \quad (3)$$

Then, from Eq. 3

$$T = (0.94)[(68 + 460)\ °R] = 496\ °R \quad (4)$$

and using Eqs. 1, 2, and 4 we get

$$V = (0.54)\sqrt{[1.716\times 10^3\ (ft\cdot lb)/(slug\cdot °R)](496\ °R)(1.4)[1\ (slug\cdot ft)/(lb\cdot s^2)]}$$

or

$$V = 590\ ft/s \quad \text{(Ans)}$$

(b) For helium, $p/p_0 = 0.82$ and $k = 1.66$. By substituting these values into Eq. E.20 we get

$$0.82 = \left\{\frac{1}{1 + [(1.66 - 1)/2]\,Ma^2}\right\}^{1.66/(1.66-1)}$$

or

$$Ma = 0.499$$

From Eq. E.17 we obtain

$$\frac{T}{T_0} = \frac{1}{1 + [(k-1)/2]Ma^2}$$

Thus,

$$T = \left\{\frac{1}{1 + [(1.66 - 1)/2](0.499)^2}\right\}[(68 + 460)\ °R] = 488\ °R$$

From Eq. 1 we obtain

$$V = (0.499)\sqrt{[1.242\times 10^4(ft\cdot lb)/(slug\cdot °R)](488\ °R)(1.66)[1(slug\cdot ft)/(lb\cdot s^2)]}$$

or

$$V = 1580\ ft/s \quad \text{(Ans)}$$

Note that the isentropic flow equations and Fig. D.1 for $k = 1.4$ were used presently to describe fluid particle isentropic flow along a pathline in a stagnation process. Even though these equations and graph were developed for one-dimensional duct flows, they can be used for frictionless, adiabatic pathline flows also.

Furthermore, while the Mach numbers calculated above are of similar size for the air and helium flows, the flow speed is much larger for helium than for air because the speed of sound in helium is much larger than it is in air.

Example 6.14:

Air enters subsonically from standard atmosphere and flows isentropically through a choked converging-diverging duct having a circular cross-section area, A, that varies with axial distance from the throat, x, according to the formula $A = 0.1 + x^2$ where A is in square meters and x is in meters. The duct extends from $x = -0.5$ m to $x = +0.5$ m. For this flow situation, sketch the side view of the duct and graph the variation of Mach number, static temperature to stagnation temperature ratio, T/T_0, and static pressure to stagnation pressure ratio, p/p_0, through the duct from $x = -0.5$ m to $x = +0.5$ m. Also show the possible fluid states at $x = -0.5$ m, 0 m, and $+0.5$ m using temperature-entropy coordinates.

Solution:

The side view of the converging-diverging duct is a graph of radius r from the duct axis as a function of axial distance. For a circular flow cross section we have

$$A = \pi r^2 \quad (1)$$

where

$$A = 0.1 + x^2 \quad (2)$$

Thus, combining Eqs. 1 and 2, we have

$$r = \left(\frac{0.1 + x^2}{\pi}\right)^{1/2} \quad (3)$$

and a graph of radius as a function of axial distance can be easily constructed (see Fig. E6.14a).

Since the converging-diverging duct in this example is choked, the throat area is also the critical area, A^*. From Eq. 2 we see that (x = 0 at the throat)

$$A^* = 0.1 \text{ m}^2 \quad (4)$$

For any axial location, from Eqs. 2 and 4 we get

$$\frac{A}{A^*} = \frac{0.1 + x^2}{0.1} \quad (5)$$

Values of A/A^* from Eq. 5 can be used in Eq. 6.61 to calculate corresponding values of Mach number, Ma. For air with $k = 1.4$, we could enter Fig. D.1 with values of A/A^* and read off values of the Mach number. With values of Mach number ascertained, we could use Eqs. E.17 and E.20 to calculate related values of T/T_0 and p/p_0. For air with $k = 1.4$, Fig. D.1 could be entered with A/A^* or Ma to get values of T/T_0 and p/p_0. To solve this example, we elect to use values from Fig. D.1.

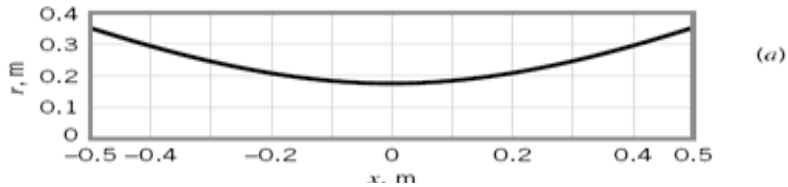

(a)

■ FIGURE E6.14

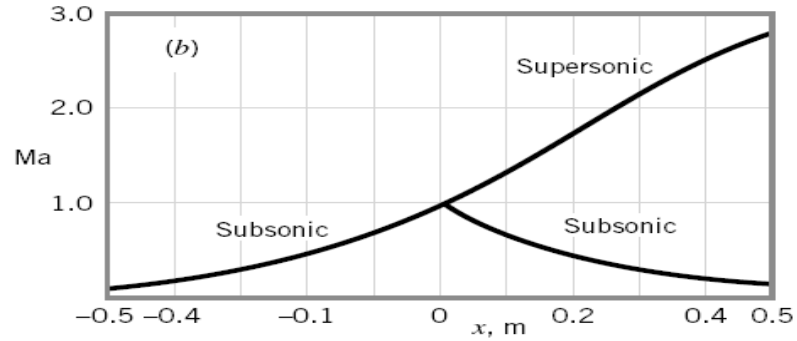

■ FIGURE E6.14 (*Continued*)

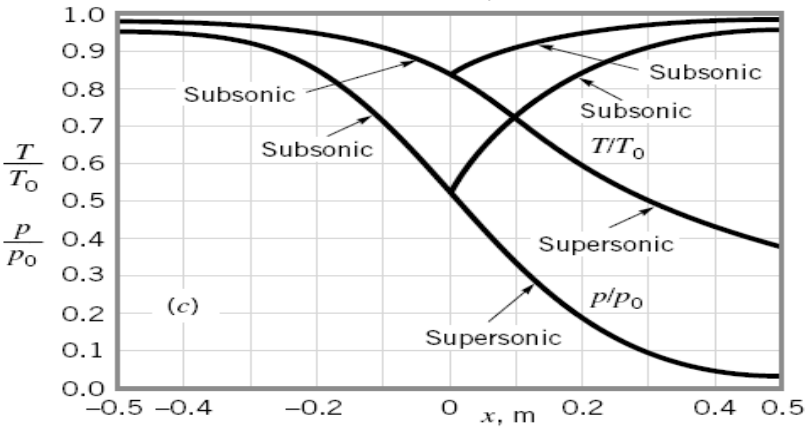

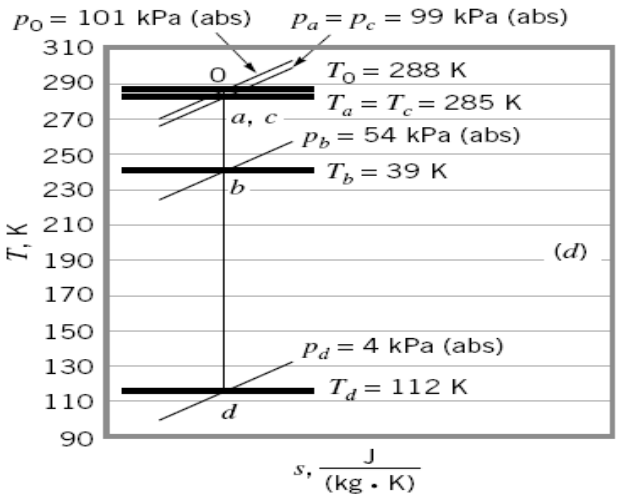

The following table was constructed by using Eqs. 3 and 5 and Fig. D.1.

With the air entering the choked converging-diverging duct subsonically, only one isentropic solution exists for the converging portion of the duct. This solution involves an accelerating flow that becomes sonic (Ma = 1) at the throat of the passage. Two isentropic flow solutions are possible for the diverging portion of the duct—one subsonic, the other supersonic. If the pressure ratio, p/p_0, is set at 0.98 at $x = +0.5$ m (the outlet), the subsonic flow will occur. Alternatively, if p/p_0 is set at 0.04 at $x = +0.5$ m, the supersonic flow field will exist. These conditions are illustrated in Fig. E6.14.. An unchoked subsonic flow through the converging-diverging duct of this example is discussed in Example 11.10. Choked flows involving flows other than the two isentropic flows in the diverging portion of the duct of this example are discussed after Example 6.16 .

x (m)	From Eq. 3, r (m)	From Eq. 5, A/A^*	From Fig. D.1 Ma	From Fig. D.1 T/T_0	From Fig. D.1 p/p_0	State
Subsonic Solution						
−0.5	0.334	3.5	0.17	0.99	0.98	*a*
−0.4	0.288	2.6	0.23	0.99	0.97	
−0.3	0.246	1.9	0.32	0.98	0.93	
−0.2	0.211	1.4	0.47	0.96	0.86	
−0.1	0.187	1.1	0.69	0.91	0.73	
0	0.178	1	1.00	0.83	0.53	*b*
+0.1	0.187	1.1	0.69	0.91	0.73	
+0.2	0.211	1.4	0.47	0.96	0.86	
+0.3	0.246	1.9	0.32	0.98	0.93	
+0.4	0.288	2.6	0.23	0.99	0.97	
+0.5	0.344	3.5	0.17	0.99	0.98	*c*
Supersonic Solution						
+0.1	0.187	1.1	1.37	0.73	0.33	
+0.2	0.211	1.4	1.76	0.62	0.18	
+0.3	0.246	1.9	2.14	0.52	0.10	
+0.4	0.288	2.6	2.48	0.45	0.06	
+0.5	0.334	3.5	2.80	0.39	0.04	*d*

Example 6.15:

Air enters supersonically with T_0 and p_0 equal to standard atmosphere values and flows isentropically through the choked converging-diverging duct described in Example 6.14 . Graph the variation of Mach number, Ma, static temperature to stagnation temperature ratio, T/T_0, and static pressure to stagnation pressure ratio, p/p_0, through the duct from $x = -0.5$ m to $x = +0.5$ m. Also show the possible fluid states at $x = -0.5$ m, 0 m, and +0.5 m by using temperature-entropy coordinates.

Solution:

With the air entering the converging-diverging duct of Example 6.14 supersonically instead of subsonically, a unique isentropic flow solution is obtained for the converging portion of the duct. Now, however, the flow decelerates to the sonic condition at the throat. The two solutions obtained previously in Example 6.14 for the diverging portion are still valid. Since the area variation in the duct is symmetrical with respect to the duct throat, we can use the supersonic flow values obtained from Example 6.14 for the supersonic flow in the converging portion of the duct. The supersonic flow solution for the converging passage is summarized in the following table. The solution values for the entire duct are graphed in Fig. E6.15 .

x (m)	A/A^*	From Fig. D.1 Ma	From Fig. D.1 T/T_0	From Fig. D.1 p/p_0	State
−0.5	3.5	2.8	0.39	0.04	*e*
−0.4	2.6	2.5	0.45	0.06	
−0.3	1.9	2.1	0.52	0.10	
−0.2	1.4	1.8	0.62	0.18	
−0.1	1.1	1.4	0.73	0.33	
0	1	1.0	0.83	0.53	*b*

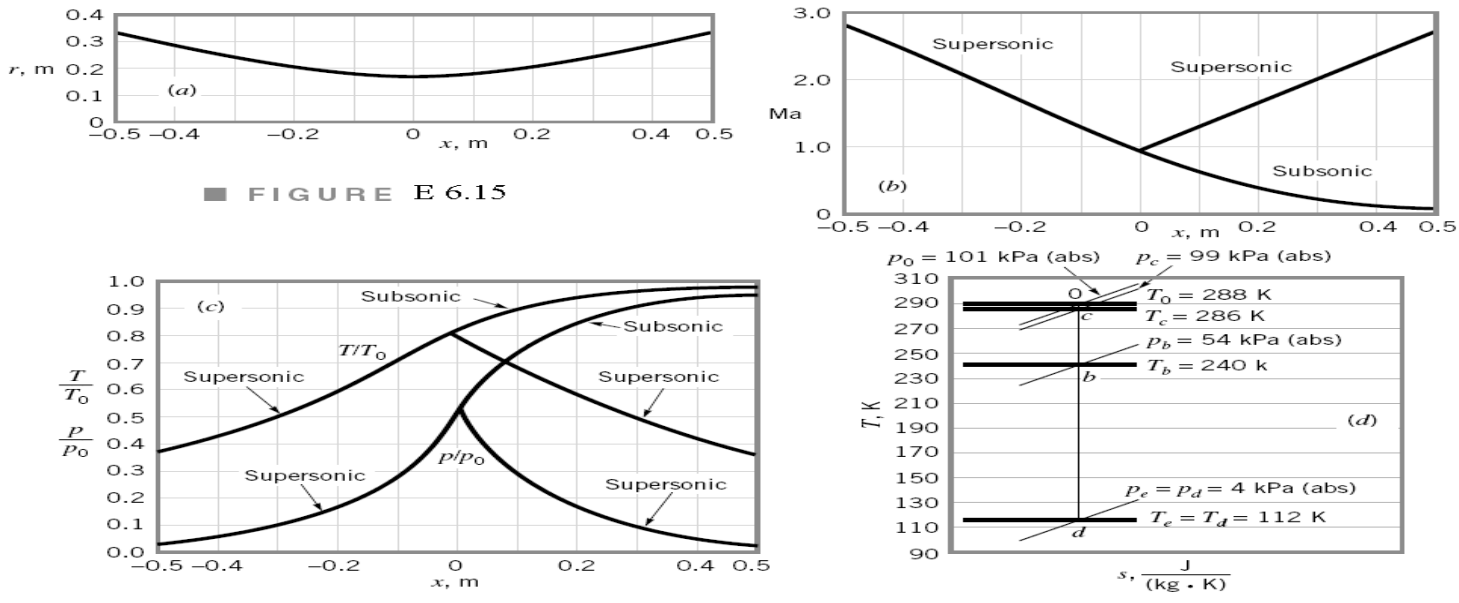

■ FIGURE E 6.15

Example 6.16:

Air flows subsonically and isentropically through the converging-diverging duct of Example 6.14. Graph the variation of Mach number, Ma, static temperature to stagnation temperature ratio, T/T_0, the static pressure to stagnation pressure ratio, p/p_0, through the duct from $x = -0.5$ m to $x = +0.5$ m for Ma $= 0.48$ at $x = 0$ m. Show the corresponding temperature-entropy diagram.

Solution:

Since for this example, Ma $= 0.48$ at $x = 0$ m, the isentropic flow through the converging-diverging duct will be entirely subsonic and not choked. For air ($k = 1.4$) flowing isentropically through the duct, we can use Fig. D.1 for flow field quantities. Entering Fig. D.1 with Ma $= 0.48$ we read off $p/p_0 = 0.85$, $T/T_0 = 0.96$, and $A/A^* = 1.4$. Even though the duct flow is not choked in this example and A^* does not therefore exist physically, it still represents a valid reference. For a given isentropic flow, p_0, T_0, and A^* are constants. Since A at $x = 0$ m is equal to 0.10 m^2 (from Eq. 2 of Example 6.14), A^* for this example is

$$A^* = \frac{A}{(A/A^*)} = \frac{0.10 \text{ m}^2}{1.4} = 0.07 \text{ m}^2 \qquad (1)$$

With known values of duct area at different axial locations, we can calculate corresponding area ratios, A/A^*, knowing $A^* = 0.07$ m^2. Having values of the area ratio, we can use Fig. E.1 and obtain related values of Ma, T/T_0, and p/p_0. The following table summarizes flow quantities obtained in this manner. The results are graphed in Fig. E6.16.

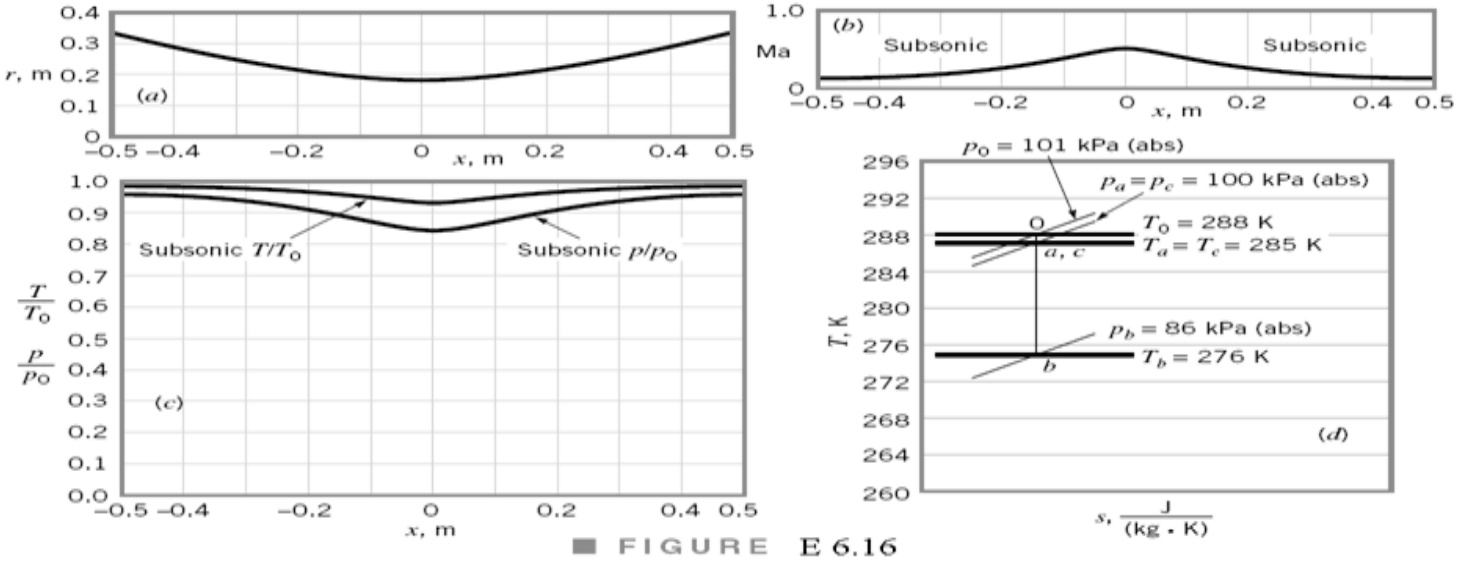

■ FIGURE E 6.16

A more precise solution for the flow of this example could have been obtained with isentropic flow equations by following the steps outlined below.

1. Use Eq. E.20 to get p/p_0 at $x = 0$ knowing k and Ma $= 0.48$.
2. From Eq. 6.61, obtain value of A/A^* at $x = 0$ knowing k and Ma.
3. Determine A^* knowing A and A/A^* at $x = 0$.
4. Determine A/A^* at different axial locations, x.
5. Use Eq. 6.61 and A/A^* from step 4 above to get values of Mach numbers at different axial locations.
6. Use Eqs. E.17 and E.20 and Ma from step 5 above to obtain T/T_0 and p/p_0 at different axial locations, x.

There are an infinite number of subsonic, isentropic flow solutions for the converging-diverging duct considered in this example.

x (m)	Calculated, A/A^*	From Fig. D.1 Ma	From Fig. D.1 T/T_0	From Fig. D.1 p/p_0	State
−0.5	5.0	0.12	0.99	0.99	*a*
−0.4	3.7	0.16	0.99	0.98	
−0.3	2.7	0.23	0.99	0.96	
−0.2	2.0	0.31	0.98	0.94	
−0.1	1.6	0.40	0.97	0.89	
0	1.4	0.48	0.96	0.85	*b*
+0.1	1.6	0.40	0.97	0.89	
+0.2	2.0	0.31	0.98	0.94	
+0.3	2.7	0.23	0.99	0.96	
+0.4	3.7	0.16	0.99	0.98	
+0.5	5.0	0.12	0.99	0.99	*c*

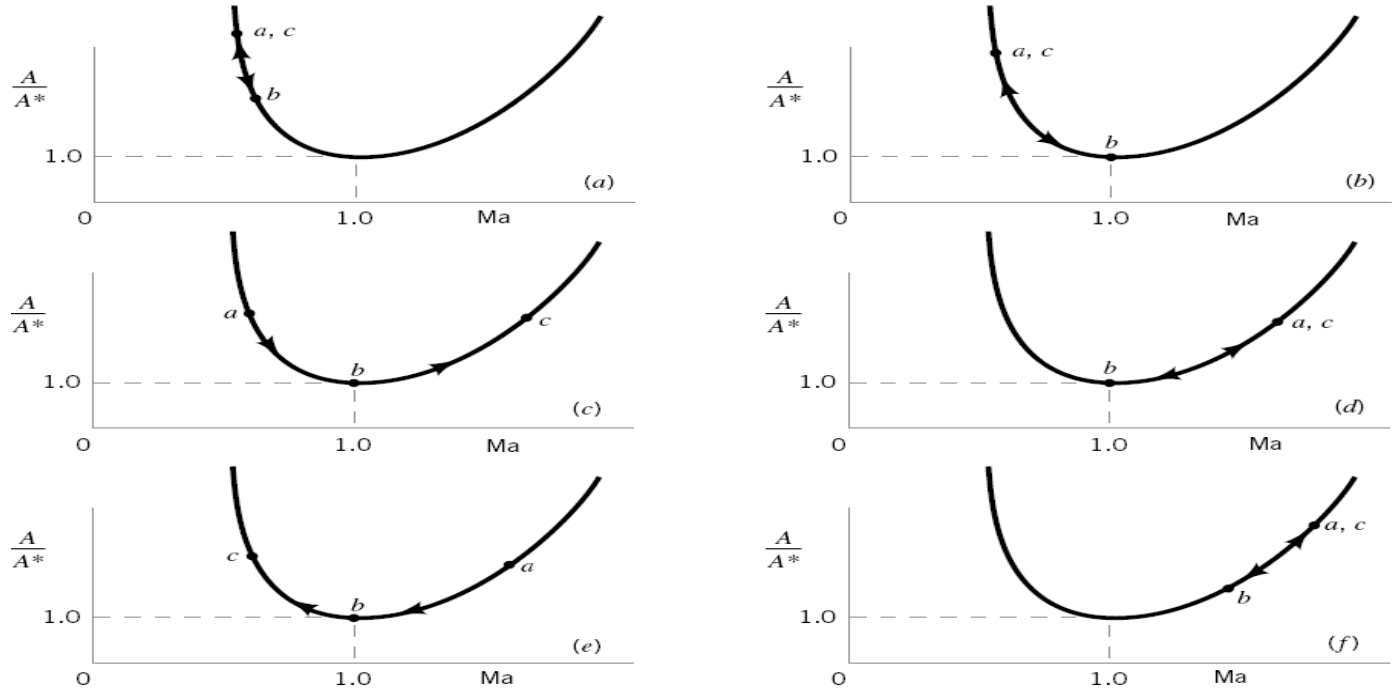

■ FIGURE 6.13 **(*a*) Subsonic to subsonic isentropic flow (not choked). (*b*) Subsonic to subsonic isentropic flow (choked). (*c*) Subsonic to supersonic isentropic flow (choked) (*d*) Supersonic to supersonic isentropic flow (choked). (*e*) Supersonic to subsonic isentropic flow (choked). (*f*) Supersonic to supersonic isentropic flow (not choked).**

The isentropic flow behavior for the converging-diverging duct discussed in Examples 6.14, 6.15, and 6.16 is summarized in the area ratio–Mach number graphs sketched in Fig. 6.13 . The points *a*, *b*, and *c* represent states at axial distance $x = -0.5$ m, 0 m, and $+0.5$ m. In Fig. 6.13 *a*, the isentropic flow through the converging-diverging duct is subsonic without choking at the throat. This situation was discussed in Example 6.16 . Figure 6.13 *b* represents subsonic to subsonic choked flow (Example 6.14) and Fig. 6.13 *c* is for subsonic to supersonic choked flow (also Example 6.14). The states in Fig. 6.13 *d* are related to the supersonic to supersonic choked flow of Example 6.15; the states in Fig. 6.13 *e* are for the supersonic to subsonic choked flow of Example 6.15. Not covered by an example but also possible are the isentropic flow states *a*, *b*, and *c* shown in Fig. 6.13 *f* for supersonic to supersonic flow without choking. These six categories generally represent the possible kinds of isentropic, ideal gas flow through a converging-diverging duct.

For a given stagnation state (i.e., T_0 and p_0 fixed), ideal gas (k = constant), and converging-diverging duct geometry, an infinite number of isentropic subsonic to subsonic (not choked) and supersonic to supersonic (not choked) flow solutions exist. In contrast, the isentropic subsonic to supersonic (choked), subsonic to subsonic (choked), supersonic to subsonic (choked), and supersonic to supersonic (choked) flow solutions are each unique. The

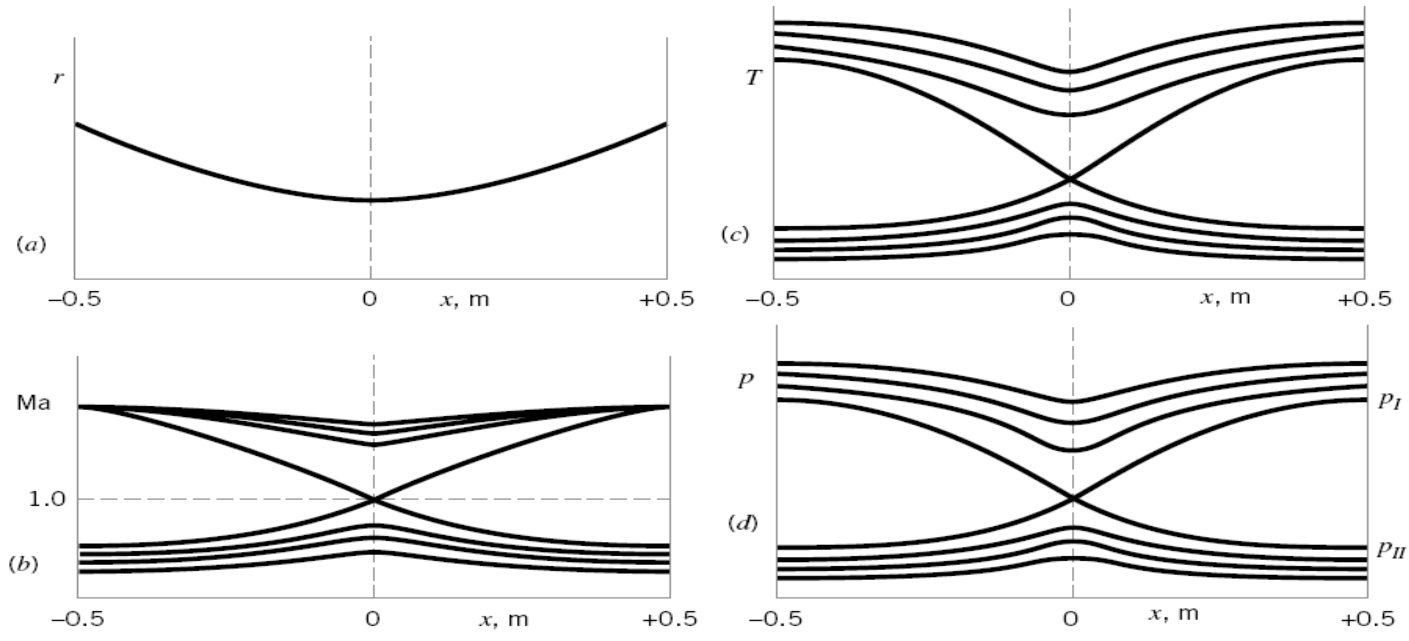

■ FIGURE 6.14 **(*a*) The variation of duct radius with axial distance. (*b*) The variation of Mach number with axial distance. (*c*) The variation of temperature with axial distance. (*d*) The variation of pressure with axial distance.**

above-mentioned isentropic flow solutions are represented in Fig. 6.14 . When the pressure at $x = +0.5$ (exit) is greater than or equal to p_I indicated in Fig. 6.14 *d*, an isentropic flow is possible. When the pressure at $x = +0.5$ is equal to or less than p_{II}, isentropic flows in the duct are possible. However, when the exit pressure is less than p_I and greater than p_{III} as indicated in Fig. 6.15 , isentropic flows are no longer possible in the duct. Determination of the value of p_{III} is discussed in next sections.

Some possible nonisentropic choked flows through our converging-diverging duct are represented in Fig. 6.15 . Each abrupt pressure rise shown within and at the exit of the flow passage occurs across a very thin discontinuity in the flow called a *normal shock wave*. Except for flow across the normal shock wave, the flow is isentropic. The nonisentropic flow equations that describe the changes in fluid properties that take place across a normal shock

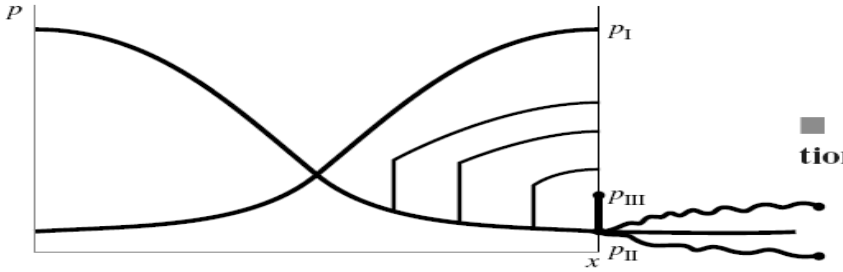

■ FIGURE 6.15 **Shock formation in converging-diverging duct flows.**

wave are developed in Section 6.5 . The less abrupt pressure rise or drop that occurs after the flow leaves the duct is nonisentropic and attributable to three-dimensional *oblique shock waves*. If the pressure rises downstream of the duct exit, the flow is considered *overexpanded*. If the pressure drops downstream of the duct exit, the flow is called *underexpanded*. Further details about over- and underexpanded flows and oblique shock waves are beyond the scope of this text. Interested readers are referred to texts on compressible flows and gas dynamics (for example, Refs. 5, 6, 7, and 8) for additional material on this subject.

6.5 Normal Shock Waves:

6.5.1 The Fixed Normal Shock Wave:

A common irreversibility occurring in supersonic internal or external flows is the normal-shock wave sketched in Fig.6.16. Except at near-vacuum pressures such shock waves are very thin (a few micrometers thick) and approximate a discontinuous change in flow properties. We select a control volume just before and after the wave, as in Fig.6.16.

The analysis is identical to that of Fig. 6.1 ; i.e., a shock wave is a fixed strong pressure wave. To compute all property changes rather than just the wave speed, we use all our basic one-dimensional steady-flow relations, letting section 1 be upstream and section 2 be downstream:

$$\rho_1 V_1 = \rho_2 V_2 = G = \text{const} \qquad (6.66a)$$

$$p_1 - p_2 = \rho_2 V_2^2 - \rho_1 V_1^2 \qquad (6.66b)$$

Energy: $$h_1 + \tfrac{1}{2}V_1^2 = h_2 + \tfrac{1}{2}V_2^2 = h_0 = \text{const} \qquad (6.66c)$$

Perfect gas: $$\frac{p_1}{\rho_1 T_1} = \frac{p_2}{\rho_2 T_2} \qquad (6.66d)$$

Constant c_p: $$h = c_p T \qquad k = \text{const} \qquad (6.66e)$$

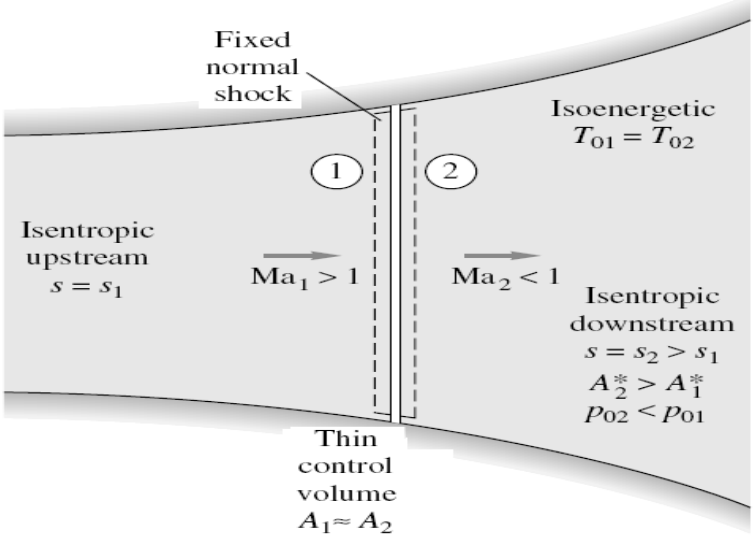

Fig. 6.16 Flow through a fixed normal-shock wave.

Note that we have canceled out the areas $A_1 \approx A_2$, which is justified even in a variable duct section because of the thinness of the wave. The first successful analyses of these normal-shock relations are credited to W. J. M. Rankine (1870) and A. Hugoniot (1887), hence the modern term *Rankine-Hugoniot relations*. If we assume that the upstream conditions (p_1, V_1, ρ_1, h_1, T_1) are known, Eqs. (6.66) are five algebraic relations in the five unknowns (p_2, V_2, ρ_2, h_2, T_2). Because of the velocity-squared term, two solutions are found, and the correct one is determined from the second law of thermodynamics, which requires that $s_2 > s_1$.

The velocities V_1 and V_2 can be eliminated from Eqs. (6.66a) to (6.66c) to obtain the Rankine-Hugoniot relation

$$h_2 - h_1 = \frac{1}{2}(p_2 - p_1)\left(\frac{1}{\rho_2} + \frac{1}{\rho_1}\right) \tag{6.67}$$

This contains only thermodynamic properties and is independent of the equation of state. Introducing the perfect-gas law $h = c_p T = kp/[(k-1)\rho]$, we can rewrite this as

$$\frac{\rho_2}{\rho_1} = \frac{1 + \beta p_2/p_1}{\beta + p_2/p_1} \qquad \beta = \frac{k+1}{k-1} \tag{6.68}$$

We can compare this with the isentropic-flow relation for a very weak pressure wave in a perfect gas

$$\frac{\rho_2}{\rho_1} = \left(\frac{p_2}{p_1}\right)^{1/k} \tag{6.69}$$

Also, the actual change in entropy across the shock can be computed from the perfect-gas relation

$$\frac{s_2 - s_1}{c_v} = \ln\left[\frac{p_2}{p_1}\left(\frac{\rho_1}{\rho_2}\right)^k\right] \tag{6.70}$$

Assuming a given wave strength p_2/p_1, we can compute the density ratio and the entropy change and list them as follows for $k = 1.4$:

$\frac{p_2}{p_1}$	ρ_2/ρ_1		$\frac{s_2 - s_1}{c_v}$
	Eq. (9.51)	Isentropic	
0.5	0.6154	0.6095	−0.0134
0.9	0.9275	0.9275	−0.00005
1.0	1.0	1.0	0.0
1.1	1.00704	1.00705	0.00004
1.5	1.3333	1.3359	0.0027
2.0	1.6250	1.6407	0.0134

We see that the entropy change is negative if the pressure decreases across the shock, which violates the second law. Thus a rarefaction shock is impossible in a perfect gas.[2] We see also that weak-shock waves ($p_2/p_1 \leq 2.0$) are very nearly isentropic.

For a perfect gas all the property ratios across the normal shock are unique functions of k and the upstream Mach number Ma_1. For example, if we eliminate ρ_2 and V_2 from Eqs. (6.66a) to (6.66c) and introduce $h = kp/[(k-1)\rho]$, we obtain

$$\frac{p_2}{p_1} = \frac{1}{k+1}\left[\frac{2\rho_1 V_1^2}{p_1} - (k-1)\right] \tag{6.71}$$

But for a perfect gas $\rho_1 V_1^2/p_1 = kV_1^2/(kRT_1) = k\,\mathrm{Ma}_1^2$, so that Eq. (6.71) is equivalent to

$$\frac{p_2}{p_1} = \frac{1}{k+1}\left[2k\,\mathrm{Ma}_1^2 - (k-1)\right] \tag{6.72}$$

From this equation we see that, for any k, $p_2 > p_1$ only if $\mathrm{Ma}_1 > 1.0$. Thus for flow through a normal-shock wave, the upstream Mach number must be supersonic to satisfy the second law of thermodynamics.

What about the downstream Mach number? From the perfect-gas identity $\rho V^2 = kp\,\mathrm{Ma}^2$, we can rewrite Eq. (6.66b) as

$$\frac{p_2}{p_1} = \frac{1 + k\,\mathrm{Ma}_1^2}{1 + k\,\mathrm{Ma}_2^2} \tag{6.73}$$

which relates the pressure ratio to both Mach numbers. By equating Eqs. (6.72) and (6.73) we can solve for

$$\mathrm{Ma}_2^2 = \frac{(k-1)\,\mathrm{Ma}_1^2 + 2}{2k\,\mathrm{Ma}_1^2 - (k-1)} \tag{6.74}$$

Since Ma_1 must be supersonic, this equation predicts for all $k > 1$ that Ma_2 must be subsonic. Thus a normal-shock wave decelerates a flow almost discontinuously from supersonic to subsonic conditions.

Further manipulation of the basic relations (6.66) for a perfect gas gives additional equations relating the change in properties across a normal-shock wave in a perfect gas

$$\frac{\rho_2}{\rho_1} = \frac{(k+1)\,\mathrm{Ma}_1^2}{(k-1)\,\mathrm{Ma}_1^2 + 2} = \frac{V_1}{V_2}$$

$$\frac{T_2}{T_1} = [2 + (k-1)\,\mathrm{Ma}_1^2]\,\frac{2k\,\mathrm{Ma}_1^2 - (k-1)}{(k+1)^2\,\mathrm{Ma}_1^2} \tag{6.75}$$

$$T_{02} = T_{01}$$

$$\frac{p_{02}}{p_{01}} = \frac{\rho_{02}}{\rho_{01}} = \left[\frac{(k+1)\,\mathrm{Ma}_1^2}{2+(k-1)\,\mathrm{Ma}_1^2}\right]^{k/(k-1)}\left[\frac{k+1}{2k\,\mathrm{Ma}_1^2-(k-1)}\right]^{1/(k-1)}$$

Of additional interest is the fact that the critical, or sonic, throat area A^* in a duct increases across a normal shock

[2] This is true also for most real gases; see Ref. 14, sec. 7.3.

$$\frac{A_2^*}{A_1^*} = \frac{\mathrm{Ma}_2}{\mathrm{Ma}_1}\left[\frac{2+(k-1)\,\mathrm{Ma}_1^2}{2+(k-1)\,\mathrm{Ma}_2^2}\right]^{(1/2)(k+1)/(k-1)} \tag{6.76}$$

All these relations are given in Table B.2 and plotted versus upstream Mach number Ma_1 in Fig.6.17 for $k = 1.4$. We see that pressure increases greatly while temperature and density increase moderately. The effective throat area A^* increases slowly at first and then rapidly. The failure of students to account for this change in A^* is a common source of error in shock calculations.

The stagnation temperature remains the same, but the stagnation pressure and density decrease in the same ratio; i.e., the flow across the shock is adiabatic but nonisentropic. Other basic principles governing the behavior of shock waves can be summarized as follows:

1. The upstream flow is supersonic, and the downstream flow is subsonic.
2. For perfect gases (and also for real fluids except under bizarre thermodynamic conditions) rarefaction shocks are impossible, and only a compression shock can exist.
3. The entropy increases across a shock with consequent decreases in stagnation pressure and stagnation density and an increase in the effective sonic-throat area.
4. Weak shock waves are very nearly isentropic.

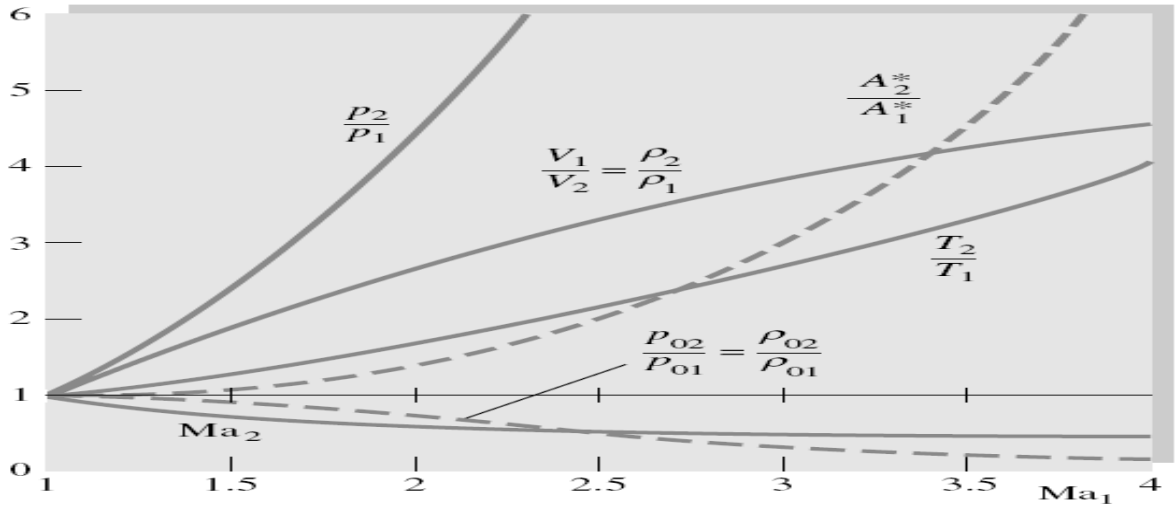

Fig. 6.17 Change in flow properties across a normal-shock wave for $k = 1.4$.

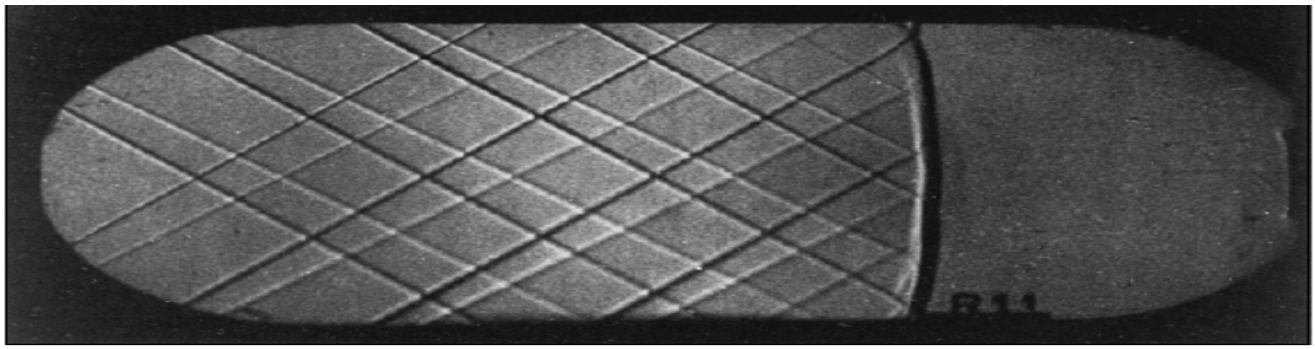

(a)

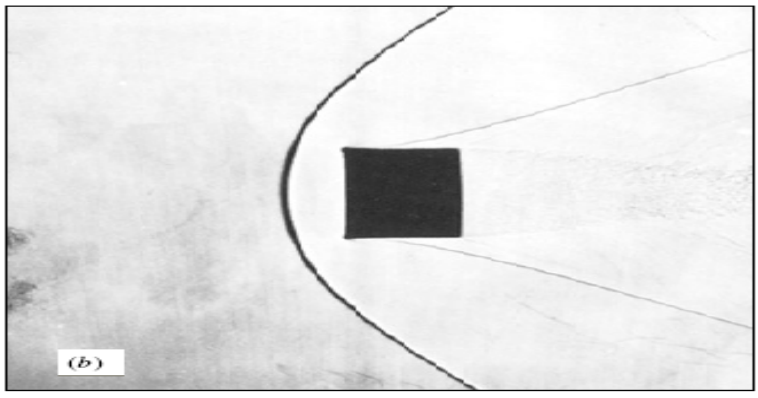

Fig. 6.18 Normal shocks form in both internal and external flows: (*a*) Normal shock in a duct; note the Mach-wave pattern to the left (upstream), indicating supersonic flow. (*Courtesy of U.S. Air Force Arnold Engineering Development Center.*) (*b*) Supersonic flow past a blunt body creates a normal shock at the nose; the apparent shock thickness and body-corner curvature are optical distortions. (*Courtesy of U.S. Army Ballistic Research Laboratory, Aberdeen Proving Ground.*)

Normal-shock waves form in ducts under transient conditions, e.g., shock tubes, and in steady flow for certain ranges of the downstream pressure. Figure 6.18 a shows a normal shock in a supersonic nozzle. Flow is from left to right. The oblique wave pattern to the left is formed by roughness elements on the nozzle walls and indicates that the upstream flow is supersonic. Note the absence of these Mach waves (see Sec. 6.10) in the subsonic flow downstream.

Normal-shock waves occur not only in supersonic duct flows but also in a variety of supersonic external flows. An example is the supersonic flow past a blunt body shown in Fig. 6.18b . The bow shock is curved, with a portion in front of the body which is essentially normal to the oncoming flow. This normal portion of the bow shock satisfies the property-change conditions just as outlined in this section. The flow inside the shock near the body nose is thus subsonic and at relatively high temperature $T_2 > T_1$, and convective heat transfer is especially high in this region.

Each nonnormal portion of the bow shock in Fig. 6.18 b satisfies the oblique-shock relations to be outlined in Sec. 6.9 . Note also the oblique recompression shock on the sides of the body. What has happened is that the subsonic nose flow has accelerated around the corners back to supersonic flow at low pressure, which must then pass through the second shock to match the higher downstream pressure conditions.

Note the fine-grained turbulent wake structure in the rear of the body in Fig. 6.18b . The turbulent boundary layer along the sides of the body is also clearly visible.

The analysis of a complex multidimensional supersonic flow such as in Fig. 6.18 is beyond the scope of this book. For further information see, e.g., Ref. 14, chap. 9, or Ref. 8, chap. 16.

6.5.2 The Moving Normal Shock Wave:

The preceding analysis of the fixed shock applies equally well to the moving shock if we reverse the transformation used in Fig. 6.1 . To make the upstream conditions simulate a still fluid, we move the shock of Fig.6.16 to the left at speed V_1; that is, we fix our coordinates to a control volume moving with the shock. The downstream flow then appears to move to the left at a slower speed $V_1 - V_2$ following the shock. The thermodynamic properties are not changed by this transformation, so that all our Eqs. (6.67) to (6.76) are still valid.

Example 6.17:

Air flows from a reservoir where p=300 kPa and T= 500 K through a throat to section 1 in Fig.E6.17, where there is a normal-shock wave. Compute

(*a*) p_1, (*b*) p_2, (*c*) p_{02}, (*d*) A_2^*, (*e*) p_{03},
(*f*) A_3^*, (*g*) p_3, (*h*) T_{03}, and (*i*) T_3.

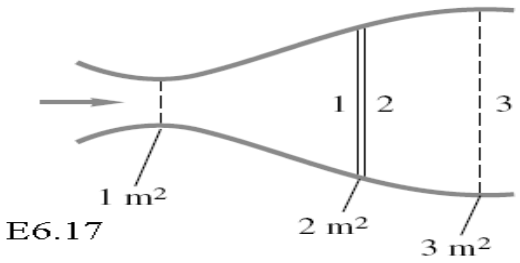

E6.17

Solution

The reservoir conditions are the stagnation properties, which, for assumed one-dimensional adiabatic frictionless flow, hold through the throat up to section 1

$$p_{01} = 300 \text{ kPa} \qquad T_{01} = 500 \text{ K}$$

A shock wave cannot exist unless Ma_1 is supersonic; therefore the flow must have accelerated through a throat which is sonic $A_t = A_1^* = 1 \text{ m}^2$

We can now find the Mach number Ma_1 from the known isentropic area ratio

$$\frac{A_1}{A_1^*} = \frac{2 \text{ m}^2}{1 \text{ m}^2} = 2.0$$

From Eq. (6.65c)

$$\text{Ma}_1 \approx 1 + 1.2(2.0 - 1)^{1/2} = 2.20$$

Further iteration with Eq. (6.62) would give $\text{Ma}_1 = 2.1972$, showing that Eq. (6.65c) gives satisfactory accuracy. The pressure p_1 follows from the isentropic relation (6.45) (or Table B.1)

$$\frac{p_{01}}{p_1} = [1 + 0.2(2.20)^2]^{3.5} = 10.7$$

or

$$p_1 = \frac{300 \text{ kPa}}{10.7} = 28.06 \text{ kPa} \qquad \textit{Ans. (a)}$$

The pressure p_2 is now obtained from Ma_1 and the normal-shock relation (6.72) or Table B.2

$$\frac{p_2}{p_1} = \frac{1}{2.4}[2.8(2.20)^2 - 0.4] = 5.48$$

or

$$p_2 = 5.48(28.06) = 154 \text{ kPa} \qquad \textit{Ans. (b)}$$

In similar manner, for $\text{Ma}_1 = 2.20$, $p_{02}/p_{01} = 0.628$ from Eq. (6.75) and $A_2^*/A_1^* = 1.592$ from

Eq. (6.76), or we can read Table B.2 for these values. Thus

$$p_{02} = 0.628(300 \text{ kPa}) = 188 \text{ kPa} \qquad \textit{Ans. (c)}$$

$$A_2^* = 1.592(1 \text{ m}^2) = 1.592 \text{ m}^2 \qquad \textit{Ans. (d)}$$

The flow from section 2 to 3 is isentropic (but at higher entropy than the flow upstream of the shock). Thus

$$p_{03} = p_{02} = 188 \text{ kPa} \qquad \textit{Ans. (e)}$$

$$A_3^* = A_2^* = 1.592 \text{ m}^2 \qquad \textit{Ans. (f)}$$

Knowing A_3^*, we can now compute p_3 by finding Ma_3 and without bothering to find Ma_2 (which happens to equal 0.547). The area ratio at section 3 is

$$\frac{A_3}{A_3^*} = \frac{3 \text{ m}^2}{1.592 \text{ m}^2} = 1.884$$

Then, since Ma_3 is known to be subsonic because it is downstream of a normal shock, we use Eq. (6.65a) to estimate

$$\text{Ma}_3 \approx \frac{1 + 0.27/(1.884)^2}{1.728(1.884)} = 0.330$$

The pressure p_3 then follows from the isentropic relation (6.45) or Table B.1

$$\frac{p_{03}}{p_3} = [1 + 0.2(0.330)^2]^{3.5} = 1.078$$

or

$$p_3 = \frac{188 \text{ kPa}}{1.078} = 174 \text{ kPa} \qquad \textit{Ans. (g)}$$

Meanwhile, the flow is adiabatic throughout the duct; thus

$$T_{01} = T_{02} = T_{03} = 500 \text{ K} \qquad \textit{Ans. (h)}$$

Therefore, finally, from the adiabatic relation (6.43)

$$\frac{T_{03}}{T_3} = 1 + 0.2(0.330)^2 = 1.022$$

or

$$T_3 = \frac{500 \text{ K}}{1.022} = 489 \text{ K} \qquad \textit{Ans. (i)}$$

Notice that this type of duct-flow problem, with or without a shock wave, requires straightforward application of algebraic perfect-gas relations coupled with a little thought given to which formula is appropriate for the particular situation.

Example 6.18 (on moving shock wave):

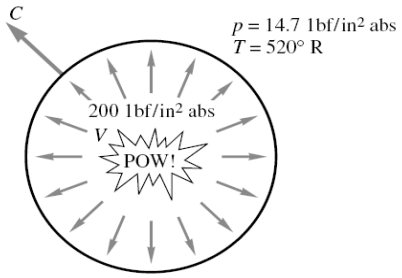

E 6.18

An explosion in air, $k = 1.4$, creates a spherical shock wave propagating radially into still air at standard conditions. At the instant shown in Fig. E 6.18, the pressure just inside the shock is 200 lbf/in^2 absolute. Estimate (*a*) the shock speed C and (*b*) the air velocity V just inside the shock.

Solution

Part (a)

In spite of the spherical geometry the flow across the shock moves normal to the spherical wave-front; hence the normal-shock relations (6.67) to (6.76) apply. Fixing our control volume to the moving shock, we find that the proper conditions to use in Fig. 6.16 are

$$C = V_1 \qquad p_1 = 14.7 \text{ lbf/in}^2 \text{ absolute} \qquad T_1 = 520°\text{R}$$

$$V = V_1 - V_2 \qquad p_2 = 200 \text{ lbf/in}^2 \text{ absolute}$$

The speed of sound outside the shock is $a_1 \approx 49T_1^{1/2} = 1117$ ft/s. We can find Ma_1 from the known pressure ratio across the shock

$$\frac{p_2}{p_1} = \frac{200 \text{ lbf/in}^2 \text{ absolute}}{14.7 \text{ lbf/in}^2 \text{ absolute}} = 13.61$$

From Eq. (6.72) or Table B.2

$$13.61 = \frac{1}{2.4}(2.8 \text{ Ma}_1^2 - 0.4) \qquad \text{or} \qquad \text{Ma}_1 = 3.436$$

Then, by definition of the Mach number,

$$C = V_1 = \text{Ma}_1 a_1 = 3.436(1117 \text{ ft/s}) = 3840 \text{ ft/s} \qquad \textit{Ans. (a)}$$

Part (b)

To find V_2, we need the temperature or sound speed inside the shock. Since Ma_1 is known, from Eq. (6.75) or Table B.2 for $\text{Ma}_1 = 3.436$ we compute $T_2/T_1 = 3.228$. Then

$$T_2 = 3.228T_1 = 3.228(520°\text{R}) = 1679°\text{R}$$

At such a high temperature we should account for non-perfect-gas effects or at least use the gas tables [16], but we won't. Here just estimate from the perfect-gas energy equation (6.40) that

$$V_2^2 = 2c_p(T_1 - T_2) + V_1^2 = 2(6010)(520 - 1679) + (3840)^2 = 815{,}000$$

or

$$V_2 \approx 903 \text{ ft/s}$$

Notice that we did this without bothering to compute Ma_2, which equals 0.454, or $a_2 \approx 49T_2^{1/2} = 2000$ ft/s.

Finally, the air velocity behind the shock is

$$V = V_1 - V_2 = 3840 - 903 \approx 2940 \text{ ft/s} \qquad \textit{Ans. (b)}$$

Thus a powerful explosion creates a brief but intense blast wind as it passes.[3]

---

[3] This is the principle of the *shock-tube wind tunnel*, in which a controlled explosion creates a brief flow at very high Mach number, with data taken by fast-response instruments. See, e.g., Ref. 5, sec. 4.5.

6.6 Operation of Converging and Diverging Nozzles:

By combining the isentropic-flow and normal-shock relations plus the concept of sonic throat choking, we can outline the characteristics of converging and diverging nozzles.

6.6.1 Operation of Converging Nozzles:

First consider the converging nozzle sketched in Fig. 6.19a . There is an upstream reservoir at stagnation pressure p_0. The flow is induced by lowering the downstream outside, or *back*, pressure p_b below p_0, resulting in the sequence of states a to e shown in Fig. 6.19b and c.

For a moderate drop in p_b to states a and b, the throat pressure is higher than the critical value p^* which would make the throat sonic. The flow in the nozzle is subsonic throughout, and the jet exit pressure p_e equals the back pressure p_b. The mass flow is predicted by subsonic isentropic theory and is less than the critical value $\dot{m}_{\max}$, as shown in Fig. 6.19c .

For condition c, the back pressure exactly equals the critical pressure p^* of the throat. The throat becomes sonic, the jet exit flow is sonic, $p_e = p_b$, and the mass flow equals its maximum value from Eq. (6.63). The flow upstream of the throat is subsonic everywhere and predicted by isentropic theory based on the local area ratio $A(x)/A^*$ and Table B.1.

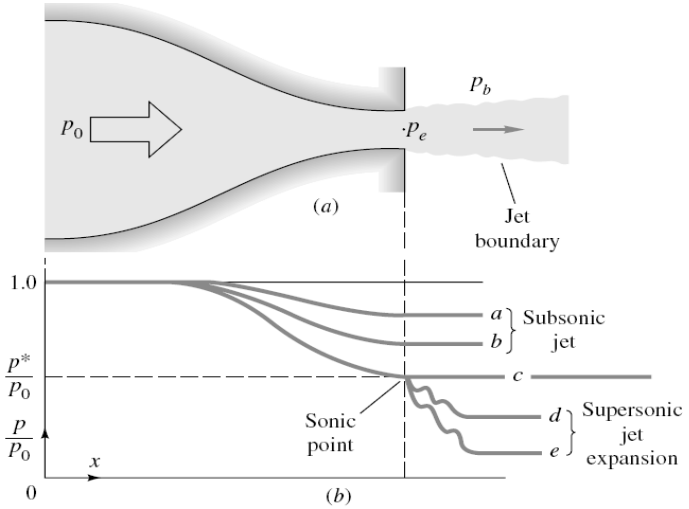

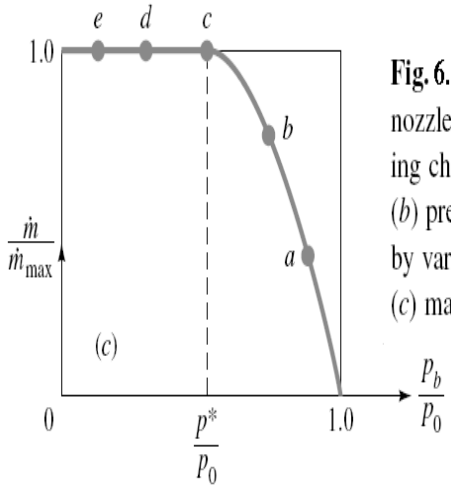

Fig. 6.19 Operation of a converging nozzle: (*a*) nozzle geometry showing characteristic pressures; (*b*) pressure distribution caused by various back pressures; (*c*) mass flow versus back pressure.

Finally, if p_b is lowered further to conditions d or e below p^*, the nozzle cannot respond further because it is choked at its maximum throat mass flow. The throat remains sonic with $p_e = p^*$, and the nozzle-pressure distribution is the same as in state c, as sketched in Fig. 6.19b . The exit jet expands supersonically so that the jet pressure can be reduced from p^* down to p_b. The jet structure is complex and multidimensional and is not shown here. Being supersonic, the jet cannot send any signal upstream to influence the choked flow conditions in the nozzle.

If the stagnation plenum chamber is large or supplemented by a compressor, and if the discharge chamber is larger or supplemented by a vacuum pump, the converging-nozzle flow will be steady or nearly so. Otherwise the nozzle will be blowing down, with p_0 decreasing and p_b increasing, and the flow states will be changing from, say, state e backward to state a. Blowdown calculations are usually made by a quasi-steady analysis based on isentropic steady-flow theory for the instantaneous pressures $p_0(t)$ and $p_b(t)$.

Example 6.19:

A converging nozzle has a throat area of 6 cm^2 and stagnation air conditions of 120 kPa and 400 K. Compute the exit pressure and mass flow if the back pressure is (*a*) 90 kPa and (*b*) 45 kPa. Assume $k = 1.4$.

Solution

From Eq. (6.49) for $k = 1.4$ the critical (sonic) throat pressure is

$$\frac{p^*}{p_0} = 0.5283 \qquad \text{or} \qquad p^* = (0.5283)(120\ \text{kPa}) = 63.4\ \text{kPa}$$

If the back pressure is less than this amount, the nozzle flow is choked.

Part (a)

For $p_b = 90$ kPa $> p^*$, the flow is subsonic, not choked. The exit pressure is $p_e = p_b$. The throat Mach number is found from the isentropic relation (6.52) or Table B.1:

$$\text{Ma}_e^2 = 5\left[\left(\frac{p_0}{p_e}\right)^{2/7} - 1\right] = 5\left[\left(\frac{120}{90}\right)^{2/7} - 1\right] = 0.4283 \qquad \text{Ma}_e = 0.654$$

To find the mass flow, we could proceed with a serial attack on Ma_e, T_e, a_e, V_e, and ρ_e, hence to compute $\rho_e A_e V_e$. However, since the local pressure is known, this part is ideally suited for the dimensionless mass-flow function in Eq. (6.64). With $p_e/p_0 = 90/120 = 0.75$, compute

$$\frac{\dot{m}\sqrt{RT_0}}{Ap_0} = \sqrt{\frac{2(1.4)}{0.4}(0.75)^{2/1.4}[1 - (0.75)^{0.4/1.4}]} = 0.6052$$

hence
$$\dot{m} = 0.6052\frac{(0.0006)(120{,}000)}{\sqrt{287(400)}} = 0.129 \text{ kg/s} \qquad \textit{Ans. (a)}$$

for
$$p_e = p_b = 90 \text{ kPa} \qquad \textit{Ans. (a)}$$

Part (b)

For $p_b = 45$ kPa $< p^*$, the flow is choked, similar to condition d in Fig. 6.19b . The exit pressure is sonic:

$$p_e = p^* = 63.4 \text{ kPa} \qquad \textit{Ans. (b)}$$

The (choked) mass flow is a maximum from Eq. (6.63b):

$$\dot{m} = \dot{m}_{\max} = \frac{0.6847 p_0 A_e}{(RT_0)^{1/2}} = \frac{0.6847(120{,}000)(0.0006)}{[287(400)]^{1/2}} = 0.145 \text{ kg/s} \qquad \textit{Ans. (b)}$$

Any back pressure less than 63.4 kPa would cause this same choked mass flow. Note that the 50 percent increase in exit Mach number, from 0.654 to 1.0, has increased the mass flow only 12 percent, from 0.128 to 0.145 kg/s.

6.6.2 The operation of Converging-Diverging Nozzles:

Now consider the converging-diverging nozzle sketched in Fig. 6.20a . If the back pressure p_b is low enough, there will be supersonic flow in the diverging portion and a variety of shock-wave conditions may occur, which are sketched in Fig. 6.20b . Let the back pressure be gradually decreased.

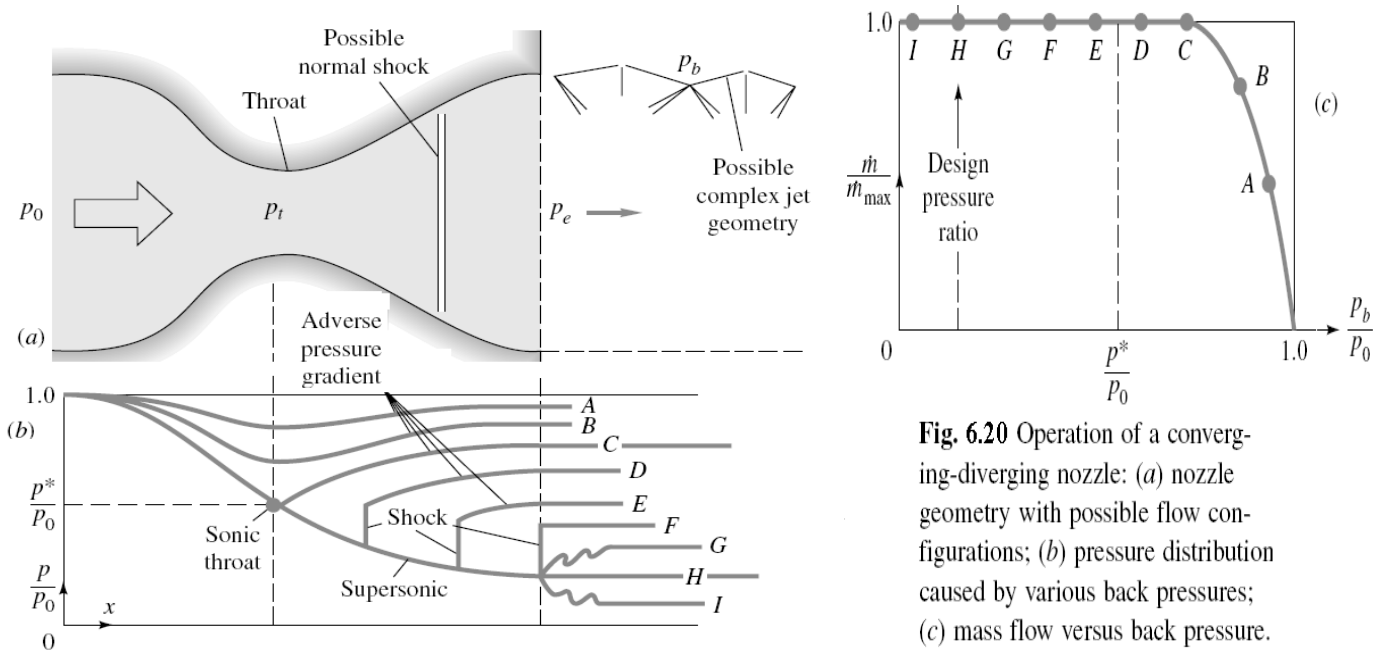

Fig. 6.20 Operation of a converging-diverging nozzle: (*a*) nozzle geometry with possible flow configurations; (*b*) pressure distribution caused by various back pressures; (*c*) mass flow versus back pressure.

For curves A and B in Fig. 6.20b the back pressure is not low enough to induce sonic flow in the throat, and the flow in the nozzle is subsonic throughout. The pressure distribution is computed from subsonic isentropic area-change relations, e.g., Table B.1. The exit pressure $p_e = p_b$, and the jet is subsonic.

For curve C the area ratio A_e/A_t exactly equals the critical ratio A_e/A^* for a subsonic Ma_e in Table B.1. The throat becomes sonic, and the mass flux reaches a maximum in Fig. 6.20c . The remainder of the nozzle flow is subsonic, including the exit jet, and $p_e = p_b$.

Now jump for a moment to curve H. Here p_b is such that p_b/p_0 exactly corresponds to the critical-area ratio A_e/A^* for a *supersonic* Ma_e in Table B.1. The diverging flow is entirely supersonic, including the jet flow, and $p_e = p_b$. This is called the *design pressure ratio* of the nozzle and is the back pressure suitable for operating a supersonic wind tunnel or an efficient rocket exhaust.

Now back up and suppose that p_b lies between curves C and H, which is impossible according to purely isentropic-flow calculations. Then back pressures D to F occur in Fig. 6.20b . The throat remains choked at the sonic value, and we can match $p_e = p_b$ by placing a normal shock at just the right place in the diverging section to cause a *subsonic-diffuser* flow back to the back-pressure condition. The mass flow remains at maximum in Fig. 6.20c . At back pressure F the required normal shock stands in the duct exit. At back pressure G no single normal shock can do the job, and so the flow compresses outside the exit in a complex series of oblique shocks until it matches p_b.

Finally, at back pressure I, p_b is lower than the design pressure H, but the nozzle is choked and cannot respond. The exit flow expands in a complex series of supersonic wave motions until it matches the low back pressure. See, e.g., Ref. 9, sec. 5.4, for further details of these off-design jet-flow configurations.

Note that for p_b less than back pressure C, there is supersonic flow in the nozzle and the throat can receive no signal from the exit behavior. The flow remains choked, and the throat has no idea what the exit conditions are.

Note also that the normal shock-patching idea is idealized. Downstream of the shock the nozzle flow has an adverse pressure gradient, usually leading to wall boundary-layer separation. Blockage by the greatly thickened separated layer interacts strongly with the core flow (recall Fig. 4.21 , part 4) and usually induces a series of weak two-dimensional compression shocks rather than a single one-dimensional normal shock (see, e.g., Ref. 14, pp. 292 and 293, for further details).

Example 6.20:

A converging-diverging nozzle (Fig. 6.20a) has a throat area of 0.002 m^2 and an exit area of 0.008 m^2. Air stagnation conditions are $p_0 = 1000$ kPa and $T_0 = 500$ K. Compute the exit pressure and mass flow for (a) design condition and the exit pressure and mass flow if (b) $p_b \approx 300$ kPa and (c) $p_b \approx 900$ kPa. Assume $k = 1.4$.

Solution

Part (a)

The design condition corresponds to supersonic isentropic flow at the given area ratio $A_e/A_t = 0.008/0.002 = 4.0$. We can find the design Mach number either by iteration of the area-ratio formula (6.62), using EES, or by the curve fit (6.65d)

$$\mathrm{Ma}_{e,\mathrm{design}} \approx [216(4.0) - 254(4.0)^{2/3}]^{1/5} \approx 2.95 \qquad (\text{exact} = 2.9402)$$

The accuracy of the curve fit is seen to be satisfactory. The design pressure ratio follows from Eq. (6.51)

$$\frac{p_0}{p_e} = [1 + 0.2(2.95)^2]^{3.5} = 34.1$$

or

$$p_{e,\mathrm{design}} = \frac{1000 \text{ kPa}}{34.1} = 29.3 \text{ kPa} \qquad \textit{Ans. (a)}$$

Since the throat is clearly sonic at design conditions, Eq. (6.63b) applies

$$\dot{m}_{\mathrm{design}} = \dot{m}_{\max} = \frac{0.6847 p_0 A_t}{(RT_0)^{1/2}} = \frac{0.6847(10^6 \text{ Pa})(0.002 \text{ m}^2)}{[287(500)]^{1/2}} = 3.61 \text{ kg/s} \qquad \textit{Ans. (a)}$$

Part (b)

For $p_b = 300$ kPa we are definitely far below the subsonic isentropic condition C in Fig. 6.20b , but we may even be below condition F with a normal shock in the exit, i.e., in condition G, where oblique shocks occur outside the exit plane. If it is condition G, then $p_e = p_{e,\mathrm{design}} = 29.3$ kPa because no shock has yet occurred. To find out, compute condition F by assuming an exit normal shock with $\mathrm{Ma}_1 = 2.95$, that is, the design Mach number just upstream of the shock. From Eq. (6.72)

$$\frac{p_2}{p_1} = \frac{1}{2.4}[2.8(2.95)^2 - 0.4] = 9.99$$

or

$$p_2 = 9.99 p_1 = 9.99 p_{e,\mathrm{design}} = 293 \text{ kPa}$$

Since this is less than the given $p_b = 300$ kPa, there is a normal shock just upstream of the exit plane (condition E). The exit flow is subsonic and equals the back pressure

$$p_e = p_b = 300 \text{ kPa} \qquad \textit{Ans. (b)}$$

Also

$$\dot{m} = \dot{m}_{\max} = 3.61 \text{ kg/s} \qquad \textit{Ans. (b)}$$

The throat is still sonic and choked at its maximum mass flow.

Part (c)

Finally, for $p_b = 900$ kPa, which is up near condition C, we compute Ma_e and p_e for condition C as a comparison. Again $A_e/A_t = 4.0$ for this condition, with a subsonic Ma_e estimated from the curve-fitted Eq. (6.65a):

$$\mathrm{Ma}_e(C) \approx \frac{1 + 0.27/(4.0)^2}{1.728(4.0)} = 0.147 \qquad (\text{exact} = 0.14655)$$

Then the isentropic exit-pressure ratio for this condition is

$$\frac{p_0}{p_e} = [1 + 0.2(0.147)^2]^{3.5} = 1.0152$$

or

$$p_e = \frac{1000}{1.0152} = 985 \text{ kPa}$$

The given back pressure of 900 kPa is less than this value, corresponding roughly to condition D in Fig. 6.20b. Thus for this case there is a normal shock just downstream of the throat, and the throat is choked

$$p_e = p_b = 900 \text{ kPa} \qquad \dot{m} = \dot{m}_{\max} = 3.61 \text{ kg/s} \qquad \textit{Ans. (c)}$$

For this large exit-area ratio, the exit pressure would have to be larger than 985 kPa to cause a subsonic flow in the throat and a mass flow less than maximum.

6.6.3 The Isentropic Flow Tables:

Similar to fig.D-1, the equations E.17, E.20, E.21 and 6.62 of the isentropic flow of perfect-gas are tabulated below in Table B6.1 (for the case of k=1.4):

Table B6.1 Isentropic Flow of a Perfect Gas, $k = 1.4$

Ma	p/p_0	ρ/ρ_0	T/T_0	A/A^*
0.0	1.0	1.0	1.0	∞
0.02	0.9997	0.9998	0.9999	28.9421
0.04	0.9989	0.9992	0.9997	14.4815
0.06	0.9975	0.9982	0.9993	9.6659
0.08	0.9955	0.9968	0.9987	7.2616
0.1	0.9930	0.9950	0.9980	5.8218
0.12	0.9900	0.9928	0.9971	4.8643
0.14	0.9864	0.9903	0.9961	4.1824
0.16	0.9823	0.9873	0.9949	3.6727
0.18	0.9776	0.9840	0.9936	3.2779
0.2	0.9725	0.9803	0.9921	2.9635
0.22	0.9668	0.9762	0.9904	2.7076
0.24	0.9607	0.9718	0.9886	2.4956
0.26	0.9541	0.9670	0.9867	2.3173
0.28	0.9470	0.9619	0.9846	2.1656
0.3	0.9395	0.9564	0.9823	2.0351
0.32	0.9315	0.9506	0.9799	1.9219
0.34	0.9231	0.9445	0.9774	1.8229
0.36	0.9143	0.9380	0.9747	1.7358
0.38	0.9052	0.9313	0.9719	1.6587
0.4	0.8956	0.9243	0.9690	1.5901
0.42	0.8857	0.9170	0.9659	1.5289
0.44	0.8755	0.9094	0.9627	1.4740
0.46	0.8650	0.9016	0.9594	1.4246
0.48	0.8541	0.8935	0.9559	1.3801
0.5	0.8430	0.8852	0.9524	1.3398
0.52	0.8317	0.8766	0.9487	1.3034
0.54	0.8201	0.8679	0.9449	1.2703
0.56	0.8082	0.8589	0.9410	1.2403
0.58	0.7962	0.8498	0.9370	1.2130
0.6	0.7840	0.8405	0.9328	1.1882
0.62	0.7716	0.8310	0.9286	1.1656
0.64	0.7591	0.8213	0.9243	1.1451
0.66	0.7465	0.8115	0.9199	1.1265
0.68	0.7338	0.8016	0.9153	1.1097
0.7	0.7209	0.7916	0.9107	1.0944
0.72	0.7080	0.7814	0.9061	1.0806
0.74	0.6951	0.7712	0.9013	1.0681
0.76	0.6821	0.7609	0.8964	1.0570
0.78	0.6690	0.7505	0.8915	1.0471
0.8	0.6560	0.7400	0.8865	1.0382
0.82	0.6430	0.7295	0.8815	1.0305
0.84	0.6300	0.7189	0.8763	1.0237
0.86	0.6170	0.7083	0.8711	1.0179
0.88	0.6041	0.6977	0.8659	1.0129
0.9	0.5913	0.6870	0.8606	1.0089
0.92	0.5785	0.6764	0.8552	1.0056
0.94	0.5658	0.6658	0.8498	1.0031
0.96	0.5532	0.6551	0.8444	1.0014
0.98	0.5407	0.6445	0.8389	1.0003
1.0	0.5283	0.6339	0.8333	1.0000
1.02	0.5160	0.6234	0.8278	1.0003
1.04	0.5039	0.6129	0.8222	1.0013
1.06	0.4919	0.6024	0.8165	1.0029
1.08	0.4800	0.5920	0.8108	1.0051
1.1	0.4684	0.5817	0.8052	1.0079
1.12	0.4568	0.5714	0.7994	1.0113
1.14	0.4455	0.5612	0.7937	1.0153
1.16	0.4343	0.5511	0.7879	1.0198
1.18	0.4232	0.5411	0.7822	1.0248
1.2	0.4124	0.5311	0.7764	1.0304
1.22	0.4017	0.5213	0.7706	1.0366
1.24	0.3912	0.5115	0.7648	1.0432
1.26	0.3809	0.5019	0.7590	1.0504
1.28	0.3708	0.4923	0.7532	1.0581
1.3	0.3609	0.4829	0.7474	1.0663
1.32	0.3512	0.4736	0.7416	1.0750
1.34	0.3417	0.4644	0.7358	1.0842
1.36	0.3323	0.4553	0.7300	1.0940
1.38	0.3232	0.4463	0.7242	1.1042
1.4	0.3142	0.4374	0.7184	1.1149
1.42	0.3055	0.4287	0.7126	1.1262
1.44	0.2969	0.4201	0.7069	1.1379
1.46	0.2886	0.4116	0.7011	1.1501
1.48	0.2804	0.4032	0.6954	1.1629
1.5	0.2724	0.3950	0.6897	1.1762
1.52	0.2646	0.3869	0.6840	1.1899
1.54	0.2570	0.3789	0.6783	1.2042
1.56	0.2496	0.3710	0.6726	1.2190
1.58	0.2423	0.3633	0.6670	1.2344
1.6	0.2353	0.3557	0.6614	1.2502
1.62	0.2284	0.3483	0.6558	1.2666
1.64	0.2217	0.3409	0.6502	1.2836
1.66	0.2151	0.3337	0.6447	1.3010
1.68	0.2088	0.3266	0.6392	1.3190
1.7	0.2026	0.3197	0.6337	1.3376
1.72	0.1966	0.3129	0.6283	1.3567
1.74	0.1907	0.3062	0.6229	1.3764
1.76	0.1850	0.2996	0.6175	1.3967
1.78	0.1794	0.2931	0.6121	1.4175
1.8	0.1740	0.2868	0.6068	1.4390
1.82	0.1688	0.2806	0.6015	1.4610
1.84	0.1637	0.2745	0.5963	1.4836
1.86	0.1587	0.2686	0.5910	1.5069
1.88	0.1539	0.2627	0.5859	1.5308
1.9	0.1492	0.2570	0.5807	1.5553
1.92	0.1447	0.2514	0.5756	1.5804
1.94	0.1403	0.2459	0.5705	1.6062
1.96	0.1360	0.2405	0.5655	1.6326
1.98	0.1318	0.2352	0.5605	1.6597
2.0	0.1278	0.2300	0.5556	1.6875
2.02	0.1239	0.2250	0.5506	1.7160
2.04	0.1201	0.2200	0.5458	1.7451
2.06	0.1164	0.2152	0.5409	1.7750
2.08	0.1128	0.2104	0.5361	1.8056
2.1	0.1094	0.2058	0.5313	1.8369
2.12	0.1060	0.2013	0.5266	1.8690
2.14	0.1027	0.1968	0.5219	1.9018
2.16	0.0996	0.1925	0.5173	1.9354
2.18	0.0965	0.1882	0.5127	1.9698
2.2	0.0935	0.1841	0.5081	2.0050
2.22	0.0906	0.1800	0.5036	2.0409
2.24	0.0878	0.1760	0.4991	2.0777
2.56	0.0533	0.1232	0.4328	2.7891
2.58	0.0517	0.1205	0.4289	2.8420
2.6	0.0501	0.1179	0.4252	2.8960
2.62	0.0486	0.1153	0.4214	2.9511
2.64	0.0471	0.1128	0.4177	3.0073
2.66	0.0457	0.1103	0.4141	3.0647
2.68	0.0443	0.1079	0.4104	3.1233
2.7	0.0430	0.1056	0.4068	3.1830
2.72	0.0417	0.1033	0.4033	3.2440
2.74	0.0404	0.1010	0.3998	3.3061
2.76	0.0392	0.0989	0.3963	3.3695
2.78	0.0380	0.0967	0.3928	3.4342
2.8	0.0368	0.0946	0.3894	3.5001
2.82	0.0357	0.0926	0.3860	3.5674
2.84	0.0347	0.0906	0.3827	3.6359
2.86	0.0336	0.0886	0.3794	3.7058
2.88	0.0326	0.0867	0.3761	3.7771
2.9	0.0317	0.0849	0.3729	3.8498
2.92	0.0307	0.0831	0.3696	3.9238
2.94	0.0298	0.0813	0.3665	3.9993
2.96	0.0289	0.0796	0.3633	4.0763
2.98	0.0281	0.0779	0.3602	4.1547
3.0	0.0272	0.0762	0.3571	4.2346
3.02	0.0264	0.0746	0.3541	4.3160
3.04	0.0256	0.0730	0.3511	4.3990
3.06	0.0249	0.0715	0.3481	4.4835
3.08	0.0242	0.0700	0.3452	4.5696
3.1	0.0234	0.0685	0.3422	4.6573
3.12	0.0228	0.0671	0.3393	4.7467
3.14	0.0221	0.0657	0.3365	4.8377
3.16	0.0215	0.0643	0.3337	4.9304
3.18	0.0208	0.0630	0.3309	5.0248
3.2	0.0202	0.0617	0.3281	5.1210
3.22	0.0196	0.0604	0.3253	5.2189
3.24	0.0191	0.0591	0.3226	5.3186
3.26	0.0185	0.0579	0.3199	5.4201
3.28	0.0180	0.0567	0.3173	5.5234
3.3	0.0175	0.0555	0.3147	5.6286
3.32	0.0170	0.0544	0.3121	5.7358

Table B.6.1 (*Cont.*) Isentropic Flow of a Perfect Gas, $k = 1.4$

Ma	p/p_0	ρ/ρ_0	T/T_0	A/A^*
2.26	0.0851	0.1721	0.4947	2.1153
2.28	0.0825	0.1683	0.4903	2.1538
2.3	0.0800	0.1646	0.4859	2.1931
2.32	0.0775	0.1609	0.4816	2.2333
2.34	0.0751	0.1574	0.4773	2.2744
2.36	0.0728	0.1539	0.4731	2.3164
2.38	0.0706	0.1505	0.4688	2.3593
2.4	0.0684	0.1472	0.4647	2.4031
2.42	0.0663	0.1439	0.4606	2.4479
2.44	0.0643	0.1408	0.4565	2.4936
2.46	0.0623	0.1377	0.4524	2.5403
2.48	0.0604	0.1346	0.4484	2.5880
2.5	0.0585	0.1317	0.4444	2.6367
2.52	0.0567	0.1288	0.4405	2.6865
2.54	0.0550	0.1260	0.4366	2.7372
3.64	0.0108	0.0393	0.2740	7.7305
3.66	0.0105	0.0385	0.2718	7.8742
3.68	0.0102	0.0378	0.2697	8.0204
3.7	0.0099	0.0370	0.2675	8.1691
3.72	0.0096	0.0363	0.2654	8.3202
3.74	0.0094	0.0356	0.2633	8.4739
3.76	0.0091	0.0349	0.2613	8.6302
3.78	0.0089	0.0342	0.2592	8.7891
3.8	0.0086	0.0335	0.2572	8.9506
3.82	0.0084	0.0329	0.2552	9.1148
3.84	0.0082	0.0323	0.2532	9.2817
3.86	0.0080	0.0316	0.2513	9.4513
3.88	0.0077	0.0310	0.2493	9.6237
3.9	0.0075	0.0304	0.2474	9.7990
3.92	0.0073	0.0299	0.2455	9.9771
3.94	0.0071	0.0293	0.2436	10.1581
3.96	0.0069	0.0287	0.2418	10.3420
3.98	0.0068	0.0282	0.2399	10.5289
4.0	0.0066	0.0277	0.2381	10.7188
4.02	0.0064	0.0271	0.2363	10.9117
4.04	0.0062	0.0266	0.2345	11.1077
4.06	0.0061	0.0261	0.2327	11.3068
4.08	0.0059	0.0256	0.2310	11.5091
4.1	0.0058	0.0252	0.2293	11.7147
4.12	0.0056	0.0247	0.2275	11.9234
4.14	0.0055	0.0242	0.2258	12.1354
4.16	0.0053	0.0238	0.2242	12.3508
4.18	0.0052	0.0234	0.2225	12.5695
4.2	0.0051	0.0229	0.2208	12.7916
4.22	0.0049	0.0225	0.2192	13.0172
4.24	0.0048	0.0221	0.2176	13.2463
4.26	0.0047	0.0217	0.2160	13.4789
4.28	0.0046	0.0213	0.2144	13.7151
4.3	0.0044	0.0209	0.2129	13.9549
4.32	0.0043	0.0205	0.2113	14.1984
3.34	0.0165	0.0533	0.3095	5.8448
3.36	0.0160	0.0522	0.3069	5.9558
3.38	0.0156	0.0511	0.3044	6.0687
3.4	0.0151	0.0501	0.3019	6.1837
3.42	0.0147	0.0491	0.2995	6.3007
3.44	0.0143	0.0481	0.2970	6.4198
3.46	0.0139	0.0471	0.2946	6.5409
3.48	0.0135	0.0462	0.2922	6.6642
3.5	0.0131	0.0452	0.2899	6.7896
3.52	0.0127	0.0443	0.2875	6.9172
3.54	0.0124	0.0434	0.2852	7.0471
3.56	0.0120	0.0426	0.2829	7.1791
3.58	0.0117	0.0417	0.2806	7.3135
3.6	0.0114	0.0409	0.2784	7.4501
3.62	0.0111	0.0401	0.2762	7.5891
4.34	0.0042	0.0202	0.2098	14.4456
4.36	0.0041	0.0198	0.2083	14.6965
4.38	0.0040	0.0194	0.2067	14.9513
4.4	0.0039	0.0191	0.2053	15.2099
4.42	0.0038	0.0187	0.2038	15.4724
4.44	0.0037	0.0184	0.2023	15.7388
4.46	0.0036	0.0181	0.2009	16.0092
4.48	0.0035	0.0178	0.1994	16.2837
4.5	0.0035	0.0174	0.1980	16.5622
4.52	0.0034	0.0171	0.1966	16.8449
4.54	0.0033	0.0168	0.1952	17.1317
4.56	0.0032	0.0165	0.1938	17.4228
4.58	0.0031	0.0163	0.1925	17.7181
4.6	0.0031	0.0160	0.1911	18.0178
4.62	0.0030	0.0157	0.1898	18.3218
4.64	0.0029	0.0154	0.1885	18.6303
4.66	0.0028	0.0152	0.1872	18.9433
4.68	0.0028	0.0149	0.1859	19.2608
4.7	0.0027	0.0146	0.1846	19.5828
4.72	0.0026	0.0144	0.1833	19.9095
4.74	0.0026	0.0141	0.1820	20.2409
4.76	0.0025	0.0139	0.1808	20.5770
4.78	0.0025	0.0137	0.1795	20.9179
4.8	0.0024	0.0134	0.1783	21.2637
4.82	0.0023	0.0132	0.1771	21.6144
4.84	0.0023	0.0130	0.1759	21.9700
4.86	0.0022	0.0128	0.1747	22.3306
4.88	0.0022	0.0125	0.1735	22.6963
4.9	0.0021	0.0123	0.1724	23.0671
4.92	0.0021	0.0121	0.1712	23.4431
4.94	0.0020	0.0119	0.1700	23.8243
4.96	0.0020	0.0117	0.1689	24.2109
4.98	0.0019	0.0115	0.1678	24.6027
5.0	0.0019	0.0113	0.1667	25.0000

6.6.4 The Normal Shock Wave Tables:

Similar to fig.6.17, all the various equations of the change of the flow properties across the Normal Shock Wave are tabulated below in Table B6.2 (for the case of a perfect gas with k=1.4).

Table B6.2 Normal-Shock Relations for a Perfect Gas, $k = 1.4$

Ma_{n1}	Ma_{n2}	p_2/p_1	$V_1/V_2 = \rho_2/\rho_1$	T_2/T_1	p_{02}/p_{01}	A_2^*/A_1^*
1.0	1.0000	1.0000	1.0000	1.0000	1.0000	1.0000
1.02	0.9805	1.0471	1.0334	1.0132	1.0000	1.0000
1.04	0.9620	1.0952	1.0671	1.0263	0.9999	1.0001
1.06	0.9444	1.1442	1.1009	1.0393	0.9998	1.0002
1.08	0.9277	1.1941	1.1349	1.0522	0.9994	1.0006
1.1	0.9118	1.2450	1.1691	1.0649	0.9989	1.0011
1.12	0.8966	1.2968	1.2034	1.0776	0.9982	1.0018
1.14	0.8820	1.3495	1.2378	1.0903	0.9973	1.0027
1.16	0.8682	1.4032	1.2723	1.1029	0.9961	1.0040
1.18	0.8549	1.4578	1.3069	1.1154	0.9946	1.0055
1.2	0.8422	1.5133	1.3416	1.1280	0.9928	1.0073
1.22	0.8300	1.5698	1.3764	1.1405	0.9907	1.0094
1.24	0.8183	1.6272	1.4112	1.1531	0.9884	1.0118
1.26	0.8071	1.6855	1.4460	1.1657	0.9857	1.0145
1.28	0.7963	1.7448	1.4808	1.1783	0.9827	1.0176
1.3	0.7860	1.8050	1.5157	1.1909	0.9794	1.0211
1.32	0.7760	1.8661	1.5505	1.2035	0.9758	1.0249
1.34	0.7664	1.9282	1.5854	1.2162	0.9718	1.0290
1.36	0.7572	1.9912	1.6202	1.2290	0.9676	1.0335
1.38	0.7483	2.0551	1.6549	1.2418	0.9630	1.0384
1.4	0.7397	2.1200	1.6897	1.2547	0.9582	1.0436
1.42	0.7314	2.1858	1.7243	1.2676	0.9531	1.0492
1.44	0.7235	2.2525	1.7589	1.2807	0.9476	1.0552
1.46	0.7157	2.3202	1.7934	1.2938	0.9420	1.0616
1.48	0.7083	2.3888	1.8278	1.3069	0.9360	1.0684
1.5	0.7011	2.4583	1.8621	1.3202	0.9298	1.0755
1.52	0.6941	2.5288	1.8963	1.3336	0.9233	1.0830
1.54	0.6874	2.6002	1.9303	1.3470	0.9166	1.0910
1.56	0.6809	2.6725	1.9643	1.3606	0.9097	1.0993
1.58	0.6746	2.7458	1.9981	1.3742	0.9026	1.1080
1.6	0.6684	2.8200	2.0317	1.3880	0.8952	1.1171
1.62	0.6625	2.8951	2.0653	1.4018	0.8877	1.1266
1.64	0.6568	2.9712	2.0986	1.4158	0.8799	1.1365
1.66	0.6512	3.0482	2.1318	1.4299	0.8720	1.1468
1.68	0.6458	3.1261	2.1649	1.4440	0.8639	1.1575
1.7	0.6405	3.2050	2.1977	1.4583	0.8557	1.1686
1.72	0.6355	3.2848	2.2304	1.4727	0.8474	1.1801
1.74	0.6305	3.3655	2.2629	1.4873	0.8389	1.1921
1.76	0.6257	3.4472	2.2952	1.5019	0.8302	1.2045
1.78	0.6210	3.5298	2.3273	1.5167	0.8215	1.2173
1.8	0.6165	3.6133	2.3592	1.5316	0.8127	1.2305
1.82	0.6121	3.6978	2.3909	1.5466	0.8038	1.2441
1.84	0.6078	3.7832	2.4224	1.5617	0.7948	1.2582
1.86	0.6036	3.8695	2.4537	1.5770	0.7857	1.2728
1.88	0.5996	3.9568	2.4848	1.5924	0.7765	1.2877
1.9	0.5956	4.0450	2.5157	1.6079	0.7674	1.3032
1.92	0.5918	4.1341	2.5463	1.6236	0.7581	1.3191
1.94	0.5880	4.2242	2.5767	1.6394	0.7488	1.3354
1.96	0.5844	4.3152	2.6069	1.6553	0.7395	1.3522
1.98	0.5808	4.4071	2.6369	1.6713	0.7302	1.3695
2.0	0.5774	4.5000	2.6667	1.6875	0.7209	1.3872
2.02	0.5740	4.5938	2.6962	1.7038	0.7115	1.4054
2.04	0.5707	4.6885	2.7255	1.7203	0.7022	1.4241
2.06	0.5675	4.7842	2.7545	1.7369	0.6928	1.4433
2.08	0.5643	4.8808	2.7833	1.7536	0.6835	1.4630
2.1	0.5613	4.9783	2.8119	1.7705	0.6742	1.4832
2.12	0.5583	5.0768	2.8402	1.7875	0.6649	1.5039
2.14	0.5554	5.1762	2.8683	1.8046	0.6557	1.5252
2.16	0.5525	5.2765	2.8962	1.8219	0.6464	1.5469
2.18	0.5498	5.3778	2.9238	1.8393	0.6373	1.5692
2.2	0.5471	5.4800	2.9512	1.8569	0.6281	1.5920
2.22	0.5444	5.5831	2.9784	1.8746	0.6191	1.6154
2.24	0.5418	5.6872	3.0053	1.8924	0.6100	1.6393
2.26	0.5393	5.7922	3.0319	1.9104	0.6011	1.6638
2.28	0.5368	5.8981	3.0584	1.9285	0.5921	1.6888
2.3	0.5344	6.0050	3.0845	1.9468	0.5833	1.7144
2.32	0.5321	6.1128	3.1105	1.9652	0.5745	1.7406

Table B6.2 (*Cont.*) Normal-Shock Relations for a Perfect Gas, $k = 1.4$

Ma_{n1}	Ma_{n2}	p_2/p_1	$V_1/V_2 = \rho_2/\rho_1$	T_2/T_1	p_{02}/p_{01}	A_2^*/A_1^*
2.34	0.5297	6.2215	3.1362	1.9838	0.5658	1.7674
2.36	0.5275	6.3312	3.1617	2.0025	0.5572	1.7948
2.38	0.5253	6.4418	3.1869	2.0213	0.5486	1.8228
2.4	0.5231	6.5533	3.2119	2.0403	0.5401	1.8514
2.42	0.5210	6.6658	3.2367	2.0595	0.5317	1.8806
2.44	0.5189	6.7792	3.2612	2.0788	0.5234	1.9105
2.46	0.5169	6.8935	3.2855	2.0982	0.5152	1.9410
2.48	0.5149	7.0088	3.3095	2.1178	0.5071	1.9721
2.5	0.5130	7.1250	3.3333	2.1375	0.4990	2.0039
2.52	0.5111	7.2421	3.3569	2.1574	0.4911	2.0364
2.54	0.5092	7.3602	3.3803	2.1774	0.4832	2.0696
2.56	0.5074	7.4792	3.4034	2.1976	0.4754	2.1035
2.58	0.5056	7.5991	3.4263	2.2179	0.4677	2.1381
2.6	0.5039	7.7200	3.4490	2.2383	0.4601	2.1733
2.62	0.5022	7.8418	3.4714	2.2590	0.4526	2.2093
2.64	0.5005	7.9645	3.4937	2.2797	0.4452	2.2461
2.66	0.4988	8.0882	3.5157	2.3006	0.4379	2.2835
2.68	0.4972	8.2128	3.5374	2.3217	0.4307	2.3218
2.7	0.4956	8.3383	3.5590	2.3429	0.4236	2.3608
2.72	0.4941	8.4648	3.5803	2.3642	0.4166	2.4005
2.74	0.4926	8.5922	3.6015	2.3858	0.4097	2.4411
2.76	0.4911	8.7205	3.6224	2.4074	0.4028	2.4825
2.78	0.4896	8.8498	3.6431	2.4292	0.3961	2.5246
2.8	0.4882	8.9800	2.6636	2.4512	0.3895	2.5676
2.82	0.4868	9.1111	3.6838	2.4733	0.3829	2.6115
2.84	0.4854	9.2432	3.7039	2.4955	0.3765	2.6561
2.86	0.4840	9.3762	3.7238	2.5179	0.3701	2.7017
2.88	0.4827	9.5101	3.7434	2.5405	0.3639	2.7481
2.9	0.4814	9.6450	3.7629	2.5632	0.3577	2.7954
2.92	0.4801	9.7808	3.7821	2.5861	0.3517	2.8436
2.94	0.4788	9.9175	3.8012	2.6091	0.3457	2.8927
2.96	0.4776	10.0552	3.8200	2.6322	0.3398	2.9427
2.98	0.4764	10.1938	3.8387	2.6555	0.3340	2.9937
3.0	0.4752	10.3333	3.8571	2.6790	0.3283	3.0456
3.02	0.4740	10.4738	3.8754	2.7026	0.3227	3.0985
3.04	0.4729	10.6152	3.8935	2.7264	0.3172	3.1523
3.06	0.4717	10.7575	3.9114	2.7503	0.3118	3.2072
3.08	0.4706	10.9008	3.9291	2.7744	0.3065	3.2630
3.1	0.4695	11.0450	3.9466	2.7986	0.3012	3.3199
3.12	0.4685	11.1901	3.9639	2.8230	0.2960	3.3778
3.14	0.4674	11.3362	3.9811	2.8475	0.2910	3.4368
3.16	0.4664	11.4832	3.9981	2.8722	0.2860	3.4969
3.18	0.4654	11.6311	4.0149	2.8970	0.2811	3.5580
3.2	0.4643	11.7800	4.0315	2.9220	0.2762	3.6202
3.22	0.4634	11.9298	4.0479	2.9471	0.2715	3.6835
3.24	0.4624	12.0805	4.0642	2.9724	0.2668	3.7480
3.26	0.4614	12.2322	4.0803	2.9979	0.2622	3.8136
3.28	0.4605	12.3848	4.0963	3.0234	0.2577	3.8803
3.3	0.4596	12.5383	4.1120	3.0492	0.2533	3.9483
3.32	0.4587	12.6928	4.1276	3.0751	0.2489	4.0174
3.34	0.4578	12.8482	4.1431	3.1011	0.2446	4.0877
3.36	0.4569	13.0045	4.1583	3.1273	0.2404	4.1593
3.38	0.4560	13.1618	4.1734	3.1537	0.2363	4.2321
3.4	0.4552	13.3200	4.1884	3.1802	0.2322	4.3062
3.42	0.4544	13.4791	4.2032	3.2069	0.2282	4.3815
3.44	0.4535	13.6392	4.2178	3.2337	0.2243	4.4581
3.46	0.4527	13.8002	4.2323	3.2607	0.2205	4.5361
3.48	0.4519	13.9621	4.2467	3.2878	0.2167	4.6154
3.5	0.4512	14.1250	4.2609	3.3151	0.2129	4.6960
3.52	0.4504	14.2888	4.2749	3.3425	0.2093	4.7780
3.54	0.4496	14.4535	4.2888	3.3701	0.2057	4.8614
3.56	0.4489	14.6192	4.3026	3.3978	0.2022	4.9461
3.58	0.4481	14.7858	4.3162	3.4257	0.1987	5.0324
3.6	0.4474	14.9533	4.3296	3.4537	0.1953	5.1200
3.62	0.4467	15.1218	4.3429	3.4819	0.1920	5.2091
3.64	0.4460	15.2912	4.3561	3.5103	0.1887	5.2997
3.66	0.4453	15.4615	4.3692	3.5388	0.1855	5.3918
3.68	0.4446	15.6328	4.3821	3.5674	0.1823	5.4854
3.7	0.4439	15.8050	4.3949	3.5962	0.1792	5.5806
3.72	0.4433	15.9781	4.4075	3.6252	0.1761	5.6773
3.74	0.4426	16.1522	4.4200	3.6543	0.1731	5.7756
3.76	0.4420	16.3272	4.4324	3.6836	0.1702	5.8755
3.78	0.4414	16.5031	4.4447	3.7130	0.1673	5.9770
3.8	0.4407	16.6800	4.4568	3.7426	0.1645	6.0801
3.82	0.4401	16.8578	4.4688	3.7723	0.1617	6.1849
3.84	0.4395	17.0365	4.4807	3.8022	0.1589	6.2915
3.86	0.4389	17.2162	4.4924	3.8323	0.1563	6.3997
3.88	0.4383	17.3968	4.5041	3.8625	0.1536	6.5096
3.9	0.4377	17.5783	4.4156	3.8928	0.1510	6.6213
3.92	0.4372	17.7608	4.5270	3.9233	0.1485	6.7348
3.94	0.4366	17.9442	4.5383	3.9540	0.1460	6.8501
3.96	0.4360	18.1285	4.5494	3.9848	0.1435	6.9672
3.98	0.4355	18.3138	4.5605	4.0158	0.1411	7.0861
4.0	0.4350	18.5000	4.5714	4.0469	0.1388	7.2069

6.7 Flow in a Constant Area Duct (dA=0):

6.7.1 Isentropic Flow in a Constant Area Duct:

For steady, one-dimensional, isentropic flow of ideal gas through a constant-area duct (dA=0 in Fig.6.21), Eq. E.11 suggests that $dV = 0$ or that flow velocity remains constant. With the energy equation (Part (1)) we can conclude that since flow velocity is constant, the fluid enthalpy and thus temperature are also constant for this flow. This information and Eqs. 6.29 and E.7 indicate that the Mach number is constant for this flow also. This being the case, Eqs. E.20 and E.21 tell us that fluid pressure and density also remain unchanged. Thus, we see that a steady, one-dimensional, isentropic flow of an ideal gas does not involve varying velocity or fluid properties unless the flow cross-section area changes.

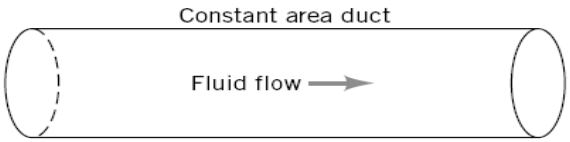

■ FIGURE 6.21 **Constant-area duct flow.**

In Section 6.7.2 we discuss nonisentropic, steady, one-dimensional flows of an ideal gas through a constant-area duct and also a normal shock wave. We learn that friction and/or heat transfer can also accelerate or decelerate a fluid.

6.7.2 Non- Isentropic Flow in a Constant Area Duct:

Actual fluid flows are generally nonisentropic. An important example of nonisentropic flow involves adiabatic (no heat transfer) flow with friction. Flows with heat transfer (diabatic flows) are generally nonisentropic also. In this section we consider the adiabatic flow of an ideal gas through a constant-area duct with friction. This kind of flow is often referred to as *Fanno flow*. We also analyze the diabatic flow of an ideal gas through a constant-area duct without friction (*Rayleigh flow*). The concepts associated with Fanno and Rayleigh flows lead to further discussion of normal shock waves.

Section 6.4 showed the effect of area change on a compressible flow while neglecting friction and heat transfer. We could now add friction and heat transfer to the area change and consider coupled effects, which is done in advanced texts [for example, 8, chap. 8]. Instead, as an elementary introduction, this section treats only the effect of friction, neglecting area change and heat transfer. The basic assumptions are

1. Steady one-dimensional adiabatic flow
2. Perfect gas with constant specific heats
3. Constant-area straight duct
4. Negligible shaft-work and potential-energy changes
5. Wall shear stress correlated by a Darcy friction factor

In effect, we are studying a Moody-type pipe-friction problem but with large changes in kinetic energy, enthalpy, and pressure in the flow.

Consider the elemental duct control volume of area A and length dx in Fig. 6.22 . The area is constant, but other flow properties (p, ρ, T, h, V) may vary with x. Application of the three conservation laws to this control volume gives three differential equations

Continuity:
$$\rho V = \frac{\dot{m}}{A} = G = \text{const}$$

or
$$\frac{d\rho}{\rho} + \frac{dV}{V} = 0 \qquad (6.77a)$$

x momentum:
$$pA - (p + dp)A - \tau_w \pi D\, dx = \dot{m}(V + dV - V)$$

or
$$dp + \frac{4\tau_w dx}{D} + \rho V\, dV = 0 \qquad (6.77b)$$

Energy:
$$h + \tfrac{1}{2}V^2 = h_0 = c_p T_0 = c_p T + \tfrac{1}{2}V^2$$

or
$$c_p\, dT + V\, dV = 0 \qquad (6.77c)$$

Since these three equations have five unknowns—p, ρ, T, V, and τ_w—we need two additional relations. One is the perfect-gas law

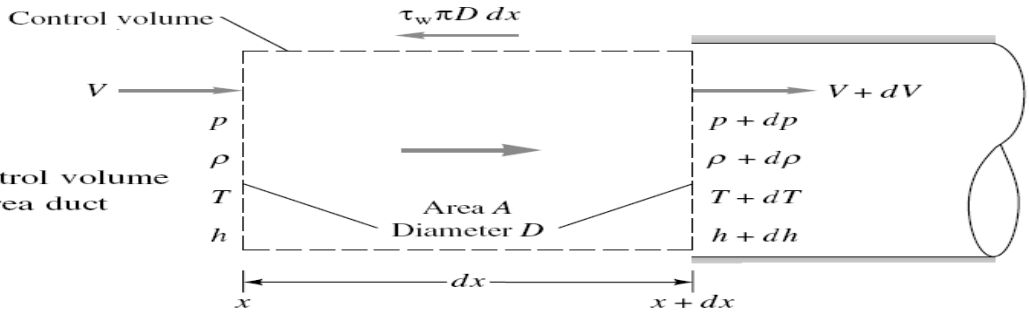

Fig. 6.22 Elemental control volume for flow in a constant-area duct with friction.

$$p = \rho RT \qquad \text{or} \qquad \frac{dp}{p} = \frac{d\rho}{\rho} + \frac{dT}{T} \tag{6.78}$$

To eliminate τ_w as an unknown, it is assumed that wall shear is correlated by a local Darcy friction factor f

$$\tau_w = \tfrac{1}{8} f\rho V^2 = \tfrac{1}{8} fkp\ \mathrm{Ma}^2 \tag{6.79}$$

where the last form follows from the perfect-gas speed-of-sound expression $a^2 = kp/\rho$. In practice, f can be related to the local Reynolds number and wall roughness from, say, the Moody chart, Fig. 2.16 .

Equations (6.77) and (6.78) are first-order differential equations and can be integrated, by using friction-factor data, from any inlet section 1, where p_1, T_1, V_1, etc., are known, to determine $p(x)$, $T(x)$, etc., along the duct. It is practically impossible to eliminate all but one variable to give, say, a single differential equation for $p(x)$, but all equations can be written in terms of the Mach number $\mathrm{Ma}(x)$ and the friction factor, by using the definition of Mach number

$$V^2 = \mathrm{Ma}^2\ kRT$$

or

$$\frac{2\ dV}{V} = \frac{2\ d\,\mathrm{Ma}}{\mathrm{Ma}} + \frac{dT}{T} \tag{6.80}$$

6.7.3 Adiabatic Flow with Friction in a Constant Area Duct (Fanno-Line Flow):

Consider the steady, one-dimensional, and adiabatic flow of an ideal gas through the constant area duct shown in Fig. 6.23 . This is Fanno flow. For the control volume indicated, the energy equation leads to

$$\dot{m}\left[\check{h}_2 - \check{h}_1 + \frac{V_2^2 - V_1^2}{2} + g(z_2 - z_1)\right] = \dot{Q}_{\substack{\text{net}\\ \text{in}}} + \dot{W}_{\substack{\text{shaft}\\ \text{net in}}}$$

0(negligibly small for gas flow); 0(flow is adiabatic); 0(flow is steady throughout)

or

$$\check{h} + \frac{V^2}{2} = \check{h}_0 = \text{constant} \tag{6.81}$$

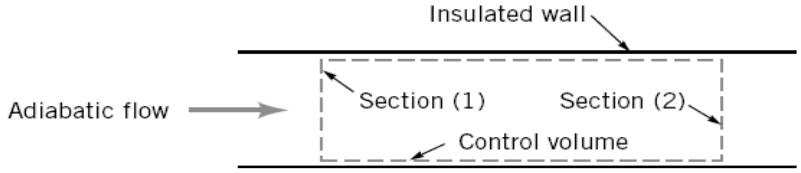

■ FIGURE 6.23 **Adiabatic constant-area flow.**

where h_0 is the stagnation enthalpy. For an ideal gas we gather that

$$\check{h} - \check{h}_0 = c_p(T - T_0) \tag{6.82}$$

so that by combining Eqs. 6.81 and 6.82 we get

$$T + \frac{V^2}{2c_p} = T_0 = \text{constant}$$

or

$$T + \frac{(\rho V)^2}{2c_p\rho^2} = T_0 = \text{constant} \tag{6.83}$$

By substituting the ideal gas equation of state into Eq. 6.83 we obtain

$$T + \frac{(\rho V)^2 T^2}{2c_p(p^2/R^2)} = T_0 = \text{constant} \tag{6.84}$$

From the continuity equation (Eq. E.1) we can conclude that the density-velocity product, ρV, is constant for a given Fanno flow since the area, A, is constant. Also, for a particular Fanno flow, the stagnation temperature, T_0, is fixed. Thus, Eq. 6.84 allows us to calculate values of fluid temperature corresponding to values of fluid pressure in the Fanno flow. We postpone our discussion of how pressure is determined until later.

As with earlier discussions in this chapter, it is helpful to describe Fanno flow with a temperature-entropy diagram. From the second $T\,ds$ relationship, an expression for entropy variation was already derived (Eq. 6.16). If the temperature, T_1, pressure, p_1, and entropy, s_1, at the entrance of the Fanno flow duct are considered as reference values, then Eq. 6.16 yields

$$s - s_1 = c_p \ln \frac{T}{T_1} - R \ln \frac{p}{p_1} \qquad (6.85)$$

Equations 6.84 and 6.85 taken together result in a curve with $T - s$ coordinates as is illustrated in Fig. 6.24 . This curve involves a given gas (c_p and R) with fixed values of stagnation temperature, density-velocity product, and inlet temperature, pressure, and entropy. Curves like the one sketched in Fig. 6.24 are called Fanno lines.

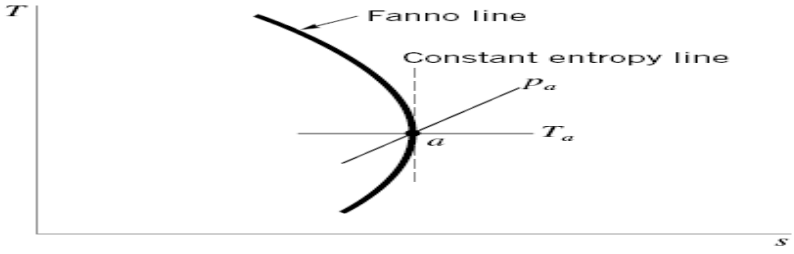

■ **FIGURE 6.24**
The $T-s$ diagram for Fanno flow.

Example 6.21:

Air ($k = 1.4$) enters [section (1)] an insulated, constant cross-section area duct with the following properties: $T_0 = 518.67\ ^\circ\text{R}$, $T_1 = 514.55\ ^\circ\text{R}$, $p_1 = 14.3$ psia
For Fanno flow, determine corresponding values of fluid temperature and entropy change for various values of downstream pressures and plot the related Fanno line.

Solution:

To plot the Fanno line we can use Eq. 6.84

$$T + \frac{(\rho V)^2 T^2}{2c_p p^2/R^2} = T_0 = \text{constant} \qquad (1)$$

and Eq. 6.85

$$s - s_1 = c_p \ln \frac{T}{T_1} - R \ln \frac{p}{p_1} \qquad (2)$$

to construct a table of values of temperature and entropy change corresponding to different levels of pressure in the Fanno flow.

We need values of the ideal gas constant and the specific heat at constant pressure to use in Eqs. 1 and 2. From Table for air $R = 1716\ (\text{ft}\cdot\text{lb})/(\text{slug}\cdot{}^\circ\text{R})$ and $c_p = \dfrac{Rk}{k-1}$

or $$c_p = \frac{[1716\ (\text{ft}\cdot\text{lb})/(\text{slug}\cdot{}^\circ\text{R})](1.4)}{1.4 - 1} = 6006\ (\text{ft}\cdot\text{lb})/(\text{slug}\cdot{}^\circ\text{R}) \qquad (3)$$

From equation of state and speed of sound $\rho V = \dfrac{p}{RT}\text{Ma}\sqrt{RTk}$

and ρV is constant for this flow from continuity and constant A

$$\rho V = \rho_1 V_1 = \frac{p_1}{RT_1}\text{Ma}_1\sqrt{RT_1 k} \qquad (4)$$

But $$\frac{T_1}{T_0} = \frac{514.55\ ^\circ\text{F}}{518.67\ ^\circ\text{R}} = 0.99206$$

and from Eq. E.17 $$\text{Ma}_1 = \sqrt{\left(\frac{1}{0.99202} - 1\right)/.02} = 0.2$$

Thus with Eq. 4

$$\rho V = \frac{(14.3\ \text{psia})(144\ \text{in.}^2/\text{ft}^2)0.2\ \sqrt{(1.4)[1716(\text{ft}\cdot\text{lb})/(\text{slug}\cdot{}^\circ\text{R})](514.55\ ^\circ\text{R})[1(\text{slug}\cdot\text{ft})/(\text{lb}\cdot\text{s}^2)]}}{[1716(\text{ft}\cdot\text{lb})/(\text{slug}\cdot{}^\circ\text{R})](514.55\ ^\circ\text{R})}$$

or $$\rho V = 0.519\ \text{slug}/(\text{ft}^2\cdot\text{s})$$

For $p = 7$ psia we have from Eq. 1

$$T + \frac{[0.519\ \text{slug}/(\text{ft}^2\cdot\text{s})]^2 T^2}{2[6006\ (\text{ft}\cdot\text{lb})/(\text{slug}\cdot{}^\circ\text{R})]\dfrac{(7\ \text{psia})^2(144\ \text{in.}^2/\text{ft}^2)^2}{[1716\ (\text{ft}\cdot\text{lb})/(\text{slug}\cdot{}^\circ\text{R})]^2}} = 518.67\ ^\circ\text{R}$$

or $$6.5 \times 10^{-5} T^2 + T - 518.67 = 0$$

Thus, $$T = 502.3\ ^\circ\text{R} \qquad \textbf{(Ans)}$$

From Eq. 2, we obtain $$s - s_1 = [6006\ (\text{ft}\cdot\text{lb})/(\text{slug}\cdot{}^\circ\text{R})] \ln\left(\frac{502.3\ ^\circ\text{R}}{514.55\ ^\circ\text{R}}\right) - [1716\ (\text{ft}\cdot\text{lb})/(\text{slug}\cdot{}^\circ\text{R})] \ln\left(\frac{7\ \text{psia}}{14.3\ \text{psia}}\right)$$

or $$s - s_1 = 1081\ (\text{ft}\cdot\text{lb})/(\text{slug}\cdot{}^\circ\text{R}) \qquad \textbf{(Ans)}$$

Proceeding as outlined above, we construct the table of values shown below and graphed as the Fanno line in Fig. E 6.21 . The maximum entropy difference occurs at a pressure of 2.62 psia and a temperature of 432.1 °R.

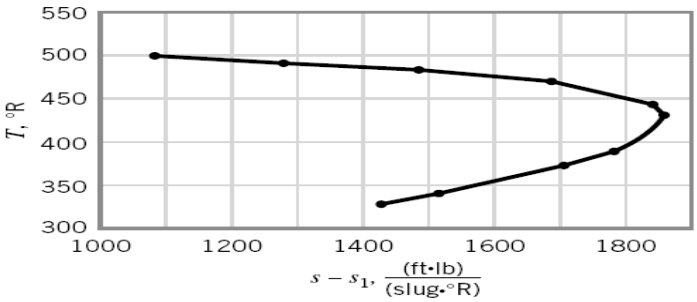

■ FIGURE E 6.21

p (psia)	T (°R)	$s - s_1$ [(ft · lb)/(slug · °R)]
7	502.3	1081
6	496.8	1280
5	488.3	1489
4	474.0	1693
3	447.7	1844
2.62	432.1	1863
2	394.7	1783
1.8	378.1	1706
1.5	347.6	1513
1.4	335.6	1421

6.7.4 General Behavior of Fanno Flow:

By eliminating variables between Eqs. (6.77) to (6.80), we obtain the working relations

$$\frac{dp}{p} = -k\,\mathrm{Ma}^2\,\frac{1 + (k-1)\,\mathrm{Ma}^2}{2(1-\mathrm{Ma}^2)}\,f\frac{dx}{D} \qquad (a)$$

$$\frac{d\rho}{\rho} = -\frac{k\,\mathrm{Ma}^2}{2(1-\mathrm{Ma}^2)}\,f\frac{dx}{D} = -\frac{dV}{V} \qquad (b)$$

$$\frac{dp_0}{p_0} = \frac{d\rho_0}{\rho_0} = -\frac{1}{2}\,k\,\mathrm{Ma}^2\,f\frac{dx}{D} \qquad (c)$$

$$\frac{dT}{T} = -\frac{k(k-1)\,\mathrm{Ma}^4}{2(1-\mathrm{Ma}^2)}\,f\frac{dx}{D} \qquad (d)$$

$$\frac{d\,\mathrm{Ma}^2}{\mathrm{Ma}^2} = k\,\mathrm{Ma}^2\,\frac{1 + \frac{1}{2}(k-1)\,\mathrm{Ma}^2}{1-\mathrm{Ma}^2}\,f\frac{dx}{D} \qquad (e)$$

Property	Subsonic	Supersonic
p	Decreases	Increases
ρ	Decreases	Increases
V	Increases	Decreases
p_0, ρ_0	Decreases	Decreases
T	Decreases	Increases
Ma	Increases	Decreases
Entropy	Increases	Increases

All these except dp_0/p_0 have the factor $1 - \mathrm{Ma}^2$ in the denominator, so that, like the area-change formulas in Fig. 6.10, subsonic and supersonic flow have opposite effects:

We have added to the list above that entropy must increase along the duct for either subsonic or supersonic flow as a consequence of the second law for adiabatic flow. For the same reason, stagnation pressure and density must both decrease.

The key parameter above is the Mach number. Whether the inlet flow is subsonic or supersonic, the duct Mach number always tends downstream toward Ma = 1 because this is the path along which the entropy increases. If the pressure and density are computed from Eqs. (*a*) and (*b*) and the entropy from Eq. (6.70), the result can be plotted in Fig. 6.A versus Mach number for $k = 1.4$. The maximum entropy occurs at Ma = 1, so that the second law requires that the duct-flow properties continually approach the sonic point. Since p_0 and ρ_0 continually decrease along the duct due to the frictional (nonisentropic) losses, they are not useful as reference properties. Instead, the sonic properties p^*, ρ^*, T^*, p_0^*, and ρ_0^* are the appropriate constant reference quantities in adiabatic duct flow. The theory then computes the ratios p/p^*, T/T^*, etc., as a function of local Mach number and the integrated friction effect.

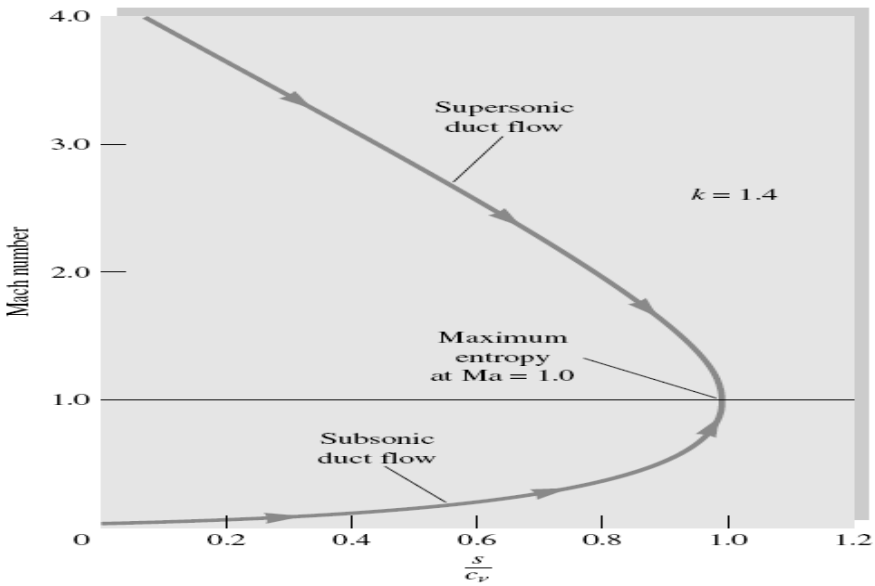

Fig. 6.A Adiabatic frictional flow in a constant-area duct always approaches Ma = 1 to satisfy the second law of thermodynamics. The computed curve is independent of the value of the friction factor.

We can learn more about Fanno lines by further analyzing the equations that describe the physics involved. For example, the second $T\,ds$ equation (Eq. 6.12) is

$$T\,ds = d\check{h} - \frac{dp}{\rho} \qquad (6.12)$$

For an ideal gas $d\check{h} = c_p\,dT$ and $p = \rho RT$

or

$$\frac{dp}{p} = \frac{d\rho}{\rho} + \frac{dT}{T} \qquad (6.86)$$

Thus, consolidating these two relations and Eqs. 6.12 and 6.86 we obtain

$$T\,ds = c_p\,dT - RT\left(\frac{d\rho}{\rho} + \frac{dT}{T}\right) \qquad (6.87)$$

Also, from the continuity equation (Eq. E.1), we get for Fanno flow $\rho V =$ constant or

$$\frac{d\rho}{\rho} = -\frac{dV}{V} \qquad (6.88)$$

Substituting Eq. 6.88 into Eq. 6.87 yields

$$T\,ds = c_p\,dT - RT\left(-\frac{dV}{V} + \frac{dT}{T}\right)$$

or

$$\frac{ds}{dT} = \frac{c_p}{T} - R\left(-\frac{1}{V}\frac{dV}{dT} + \frac{1}{T}\right) \qquad (6.89)$$

By differentiating the energy equation (6.83) obtained earlier, we obtain

$$\frac{dV}{dT} = -\frac{c_p}{V} \qquad (6.90)$$

which, when substituted into Eq. 6.89 , results in

$$\frac{ds}{dT} = \frac{c_p}{T} - R\left(\frac{c_p}{V^2} + \frac{1}{T}\right) \qquad (6.91)$$

By differentiating the energy equation (6.83) obtained earlier, we obtain

$$\frac{dV}{dT} = -\frac{c_p}{V} \qquad (6.90)$$

which, when substituted into Eq. 6.89 , results in

$$\frac{ds}{dT} = \frac{c_p}{T} - R\left(\frac{c_p}{V^2} + \frac{1}{T}\right) \qquad (6.91)$$

The Fanno line in Fig. 6.24 goes through a state (labeled state a) for which $ds/dT = 0$. At this state, we can conclude from Eqs. 6.8 and 6.91 that

$$V_a = \sqrt{RT_a k} \qquad (6.92)$$

However, by comparing Eqs. 6.92 and 6.29 we see that the Mach number at state a is 1. Since the stagnation temperature is the same for all points on the Fanno line [see energy equation (Eq. 6.83)], the temperature at point a is the critical temperature, T^*, for the entire Fanno line. Thus, Fanno flow corresponding to the portion of the Fanno line above the critical temperature must be subsonic, and Fanno flow on the line below T^* must be supersonic.

The second law of thermodynamics states that, based on all past experience, entropy can only remain constant or increase for adiabatic flows. For Fanno flow to be consistent with the second law of thermodynamics, flow can only proceed along the Fanno line toward state a, the critical state. The critical state may or may not be reached by the flow. If it is, the Fanno flow is *choked*. Some examples of Fanno flow behavior are summarized in

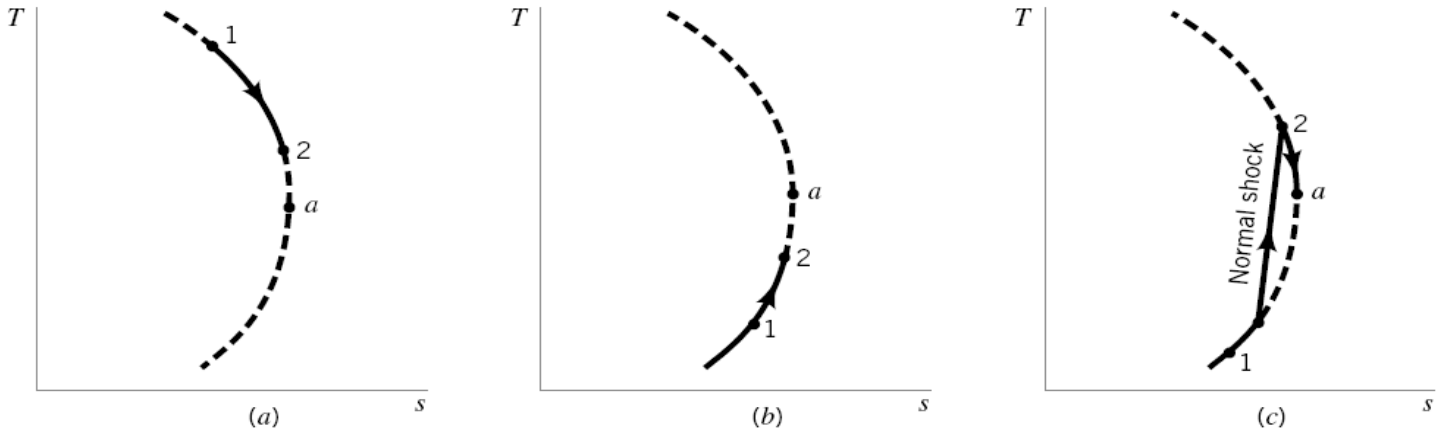

■ **FIGURE 6.25** **(*a*) Subsonic Fanno flow. (*b*) Supersonic Fanno flow. (*c*) Normal shock occurrence in Fanno flow.**

Fig. 6.25 . A case involving subsonic Fanno flow that is accelerated by friction to a higher Mach number without choking is illustrated in Fig. 6.25a . A supersonic flow that is decelerated by friction to a lower Mach number without choking is illustrated in Fig. 6.25b . In Fig. 6.25c , an abrupt change from supersonic to subsonic flow in the Fanno duct is represented. This sudden deceleration occurs across a standing *normal shock wave* that is described in more detail in Section 6.5.

The qualitative aspects of Fanno flow that we have already discussed are summarized in Table 6.A and Fig. 6.26 . To quantify Fanno flow behavior we need to combine a relationship that represents the linear momentum law with the set of equations already derived in this chapter.

If the linear momentum equation (part (2)) is applied to the Fanno flow through the control volume sketched in Fig. 6.27 a , the result is

$$p_1A_1 - p_2A_2 - R_x = \dot{m}(V_2 - V_1)$$

where R_x is the frictional force exerted by the inner pipe wall on the fluid. Since $A_1 = A_2 = A$ and $\dot{m} = \rho AV =$ constant, we obtain

$$p_1 - p_2 - \frac{R_x}{A} = \rho V(V_2 - V_1) \qquad (6.93)$$

TABLE 6.A
Summary of Fanno Flow Behavior

	Flow	
Parameter	**Subsonic Flow**	**Supersonic Flow**
Stagnation temperature	Constant	Constant
Ma	Increases (maximum is 1)	Decreases (minimum is 1)
Friction	Accelerates flow	Decelerates flow
Pressure	Decreases	Increases
Temperature	Decreases	Increases

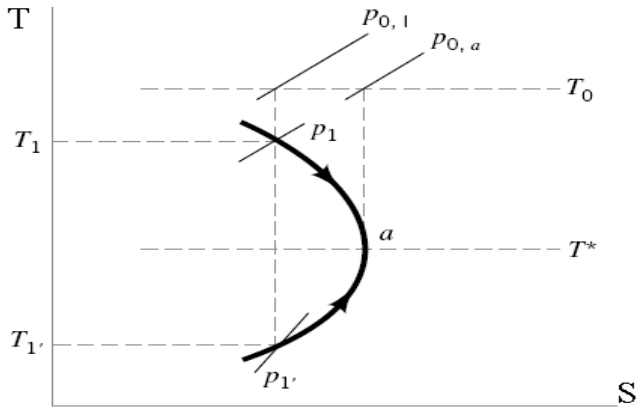

FIGURE 6.26 Fanno flow.

The differential form of Eq. 6.93 , which is valid for Fanno flow through the semi-infinitesimal control volume shown in Fig. 6.27b , is

$$-dp - \frac{\tau_w \pi D\, dx}{A} = \rho V\, dV \qquad (6.94)$$

The wall shear stress, τ_w, is related to the wall friction factor, f, by Eq. 2.54, part 2, as

$$f = \frac{8\tau_w}{\rho V^2} \qquad (6.95)$$

By substituting Eq. 6.95 and $A = \pi D^2/4$ into Eq. 6.94 , we obtain

$$-dp - f\rho \frac{V^2}{2}\frac{dx}{D} = \rho V\, dV \qquad (6.96)$$

or

$$\frac{dp}{p} + \frac{f}{p}\frac{\rho V^2}{2}\frac{dx}{D} + \frac{\rho}{p}\frac{d(V^2)}{2} = 0 \qquad (6.97)$$

Combining the ideal gas equation of state (Eq. 6.1), the ideal gas speed-of-sound equation (Eq. 6.29), and the Mach number definition (Eq. E.7) with Eq. 6.97 leads to

$$\frac{dp}{p} + \frac{fk}{2}\mathrm{Ma}^2\frac{dx}{D} + k\frac{\mathrm{Ma}^2}{2}\frac{d(V^2)}{V^2} = 0 \qquad (6.98)$$

Since $V = \mathrm{Ma}\, c = \mathrm{Ma}\sqrt{RTk}$, then $V^2 = \mathrm{Ma}^2 RTk$

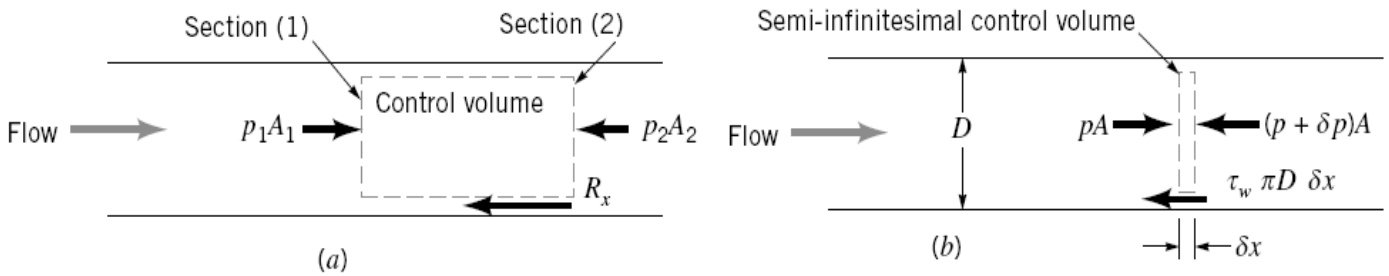

FIGURE 6.27 (a) Finite control volume. (b) Semi-infinitesimal control volume.

or
$$\frac{d(V^2)}{V^2} = \frac{d(\mathrm{Ma}^2)}{\mathrm{Ma}^2} + \frac{dT}{T} \qquad (6.99)$$

The application of the energy equation (part (2)) to Fanno flow gave Eq. 6.83 . If Eq. 6.83 is differentiated and divided by temperature, the result is

$$\frac{dT}{T} + \frac{d(V^2)}{2c_pT} = 0 \qquad (6.100)$$

Substituting Eqs. 6.8 , 6.29 , and E.7 into Eq. 6.100 yields

$$\frac{dT}{T} + \frac{k-1}{2}\mathrm{Ma}^2\,\frac{d(V^2)}{V^2} = 0 \qquad (6.101)$$

which can be combined with Eq. 6.99 to form

$$\frac{d(V^2)}{V^2} = \frac{d(\mathrm{Ma}^2)/\mathrm{Ma}^2}{1 + [(k-1)/2]\mathrm{Ma}^2} \qquad (6.102)$$

We can merge Eqs. 6.86 , 6.88 , and 6.99 to get

$$\frac{dp}{p} = \frac{1}{2}\frac{d(V^2)}{V^2} - \frac{d(\mathrm{Ma}^2)}{\mathrm{Ma}^2} \qquad (6.103)$$

Consolidating Eqs. 6.103 and 6.98 leads to

$$\frac{1}{2}(1 + k\mathrm{Ma}^2)\frac{d(V^2)}{V^2} - \frac{d(\mathrm{Ma}^2)}{\mathrm{Ma}^2} + \frac{fk}{2}\mathrm{Ma}^2\frac{dx}{D} = 0 \qquad (6.104)$$

Finally, incorporating Eq. 6.102 into Eq. 6.104 yields

$$\frac{(1 - \mathrm{Ma}^2)\,d(\mathrm{Ma}^2)}{\{1 + [(k-1)/2]\mathrm{Ma}^2\}k\mathrm{Ma}^4} = f\frac{dx}{D} \qquad (6.105)$$

Equation 6.105 can be integrated from one section to another in a Fanno flow duct. We elect to use the critical (*) state as a reference and to integrate Eq. 6.105 from an upstream state to the critical state. Thus

$$\int_{\mathrm{Ma}}^{\mathrm{Ma}^*=1} \frac{(1 - \mathrm{Ma}^2)\,d(\mathrm{Ma}^2)}{\{1 + [(k-1)/2]\,\mathrm{Ma}^2\}k\mathrm{Ma}^4} = \int_{\ell}^{\ell^*} f\frac{dx}{D} \qquad (6.106)$$

where ℓ is length measured from an arbitrary but fixed upstream reference location to a section in the Fanno flow. For an approximate solution, we can assume that the friction factor is constant at an average value over the integration length, $\ell^* - \ell$. We also consider a constant value of k. Thus, we obtain from Eq. 6.106

$$\boxed{\frac{1}{k}\frac{(1 - \mathrm{Ma}^2)}{\mathrm{Ma}^2} + \frac{k+1}{2k}\ln\left\{\frac{[(k+1)/2]\mathrm{Ma}^2}{1 + [(k-1)/2]\mathrm{Ma}^2}\right\} = \frac{f(\ell^* - \ell)}{D}} \qquad (6.107)$$

For a given gas, values of $f(\ell^* - \ell)/D$ can be tabulated as a function of Mach number for Fanno flow. For example, values of $f(\ell^* - \ell)/D$ for air ($k = 1.4$) Fanno flow are graphed as a function of Mach number in **Fig. D.2** in Appendix D. Note that the critical state does not have to exist in the actual Fanno flow being considered, since for any two sections in a given Fanno flow

$$\boxed{\frac{f(\ell^* - \ell_2)}{D} - \frac{f(\ell^* - \ell_1)}{D} = \frac{f}{D}(\ell_1 - \ell_2)} \qquad (6.108)$$

The sketch in Fig. 6.28 illustrates the physical meaning of Eq. 6.108 .

For a given Fanno flow (constant specific heat ratio, duct diameter, and friction factor) the length of duct required to change the Mach number from Ma_1 to Ma_2 can be determined from Eqs. 6.107 and 6.108 or a graph such as Fig. D.2. To get the values of other fluid properties in the Fanno flow field we need to develop more equations.

By consolidating Eqs. 6.99 and 6.101 we obtain

$$\frac{dT}{T} = -\frac{(k-1)}{2\{1 + [(k-1)/2]\mathrm{Ma}^2\}}\,d(\mathrm{Ma}^2) \qquad (6.109)$$

Integrating Eq. 6.109 from any state upstream in a Fanno flow to the critical (*) state leads to

$$\boxed{\frac{T}{T^*} = \frac{(k+1)/2}{1 + [(k-1)/2]\mathrm{Ma}^2}} \qquad (6.110)$$

$$\frac{V}{V^*} = \frac{\mathrm{Ma}\sqrt{RTk}}{\sqrt{RT^*k}} = \mathrm{Ma}\sqrt{\frac{T}{T^*}} \qquad (6.111)$$

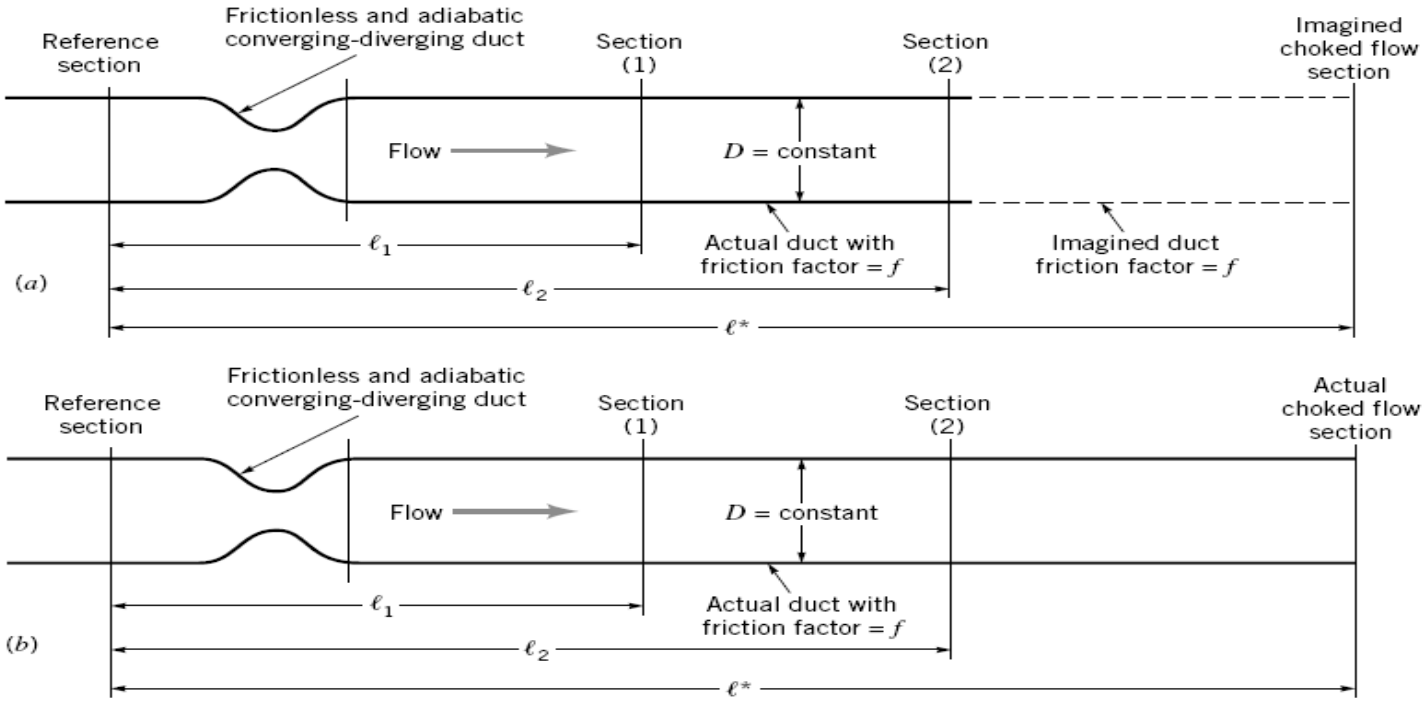

■ FIGURE 6.28 (*a*) Unchoked Fanno flow. (*b*) Choked Fanno flow.

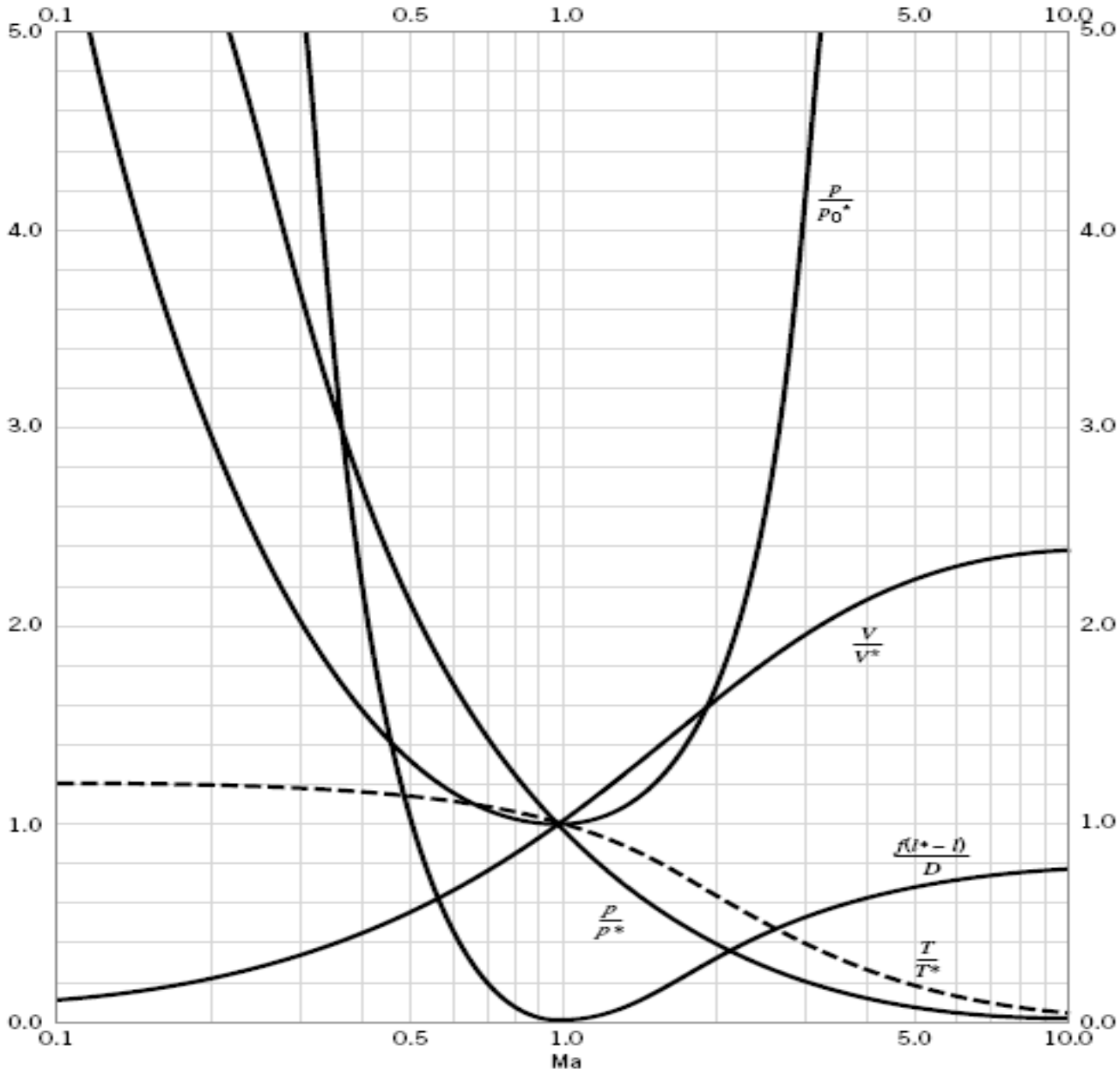

■ FIGURE D.2 **Fanno flow of an ideal gas with $k = 1.4$. (Graph provided by Professor Bruce A. Reichert of Kansas State University.)**

Substituting Eq. 6.110 into Eq. 6.111 yields

$$\frac{V}{V^*} = \left\{\frac{[(k+1)/2]\mathrm{Ma}^2}{1+[(k-1)/2]\mathrm{Ma}^2}\right\}^{1/2} \qquad (6.112)$$

From the continuity equation (Eq. E.1) we get for Fanno flow

$$\frac{\rho}{\rho^*} = \frac{V^*}{V} \qquad (6.113)$$

Combining 6.113 and 6.112 results in

$$\frac{\rho}{\rho^*} = \left\{\frac{1+[(k-1)/2]\mathrm{Ma}^2}{[(k+1)/2]\mathrm{Ma}^2}\right\}^{1/2} \qquad (6.114)$$

The ideal gas equation of state leads to

$$\frac{p}{p^*} = \frac{\rho}{\rho^*}\frac{T}{T^*} \qquad (6.115)$$

and merging Eqs. 6.115 , 6.114 , and 6.110 gives

$$\frac{p}{p^*} = \frac{1}{\mathrm{Ma}}\left\{\frac{(k+1)/2}{1+[(k-1)/2]\mathrm{Ma}^2}\right\}^{1/2} \qquad (6.116)$$

Finally, the stagnation pressure ratio can be written as

$$\frac{p_0}{p_0^*} = \left(\frac{p_0}{p}\right)\left(\frac{p}{p^*}\right)\left(\frac{p^*}{p_0^*}\right) \qquad (6.117)$$

which by use of Eqs. E.20 and 6.116 yields

$$\frac{p_0}{p_0^*} = \frac{1}{\mathrm{Ma}}\left[\left(\frac{2}{k+1}\right)\left(1+\frac{k-1}{2}\mathrm{Ma}^2\right)\right]^{[(k+1)/2(k-1)]} \qquad (6.118)$$

Values of $f(\ell^* - \ell)/D$, T/T^*, V/V^*, p/p^*, and p_0/p_0^* for Fanno flow of air ($k = 1.4$) are graphed as a function of Mach number (using Eqs. 6.108 , 6.110 , 6.112 , 6.116 , and 6.118) in Fig. D.2 The usefulness of Fig. D.2 is illustrated in Examples 6.22, 6.23, and 6.24

Example 6.22:

Standard atmospheric air [$T_0 = 288$ K, $p_0 = 101$ kPa(abs)] is drawn steadily through a frictionless, adiabatic converging nozzle into an adiabatic, constant-area duct as shown in Fig. E6.22a . The duct is 2-m long and has an inside diameter of 0.1 m. The average friction factor for the duct is estimated as being equal to 0.02. What is the maximum mass flowrate through the duct? For this maximum flowrate, determine the values of static temperature, static pressure, stagnation temperature, stagnation pressure, and velocity at the inlet [section (1)] and exit [section (2)] of the constant-area duct. Sketch a temperature-entropy diagram for this flow.

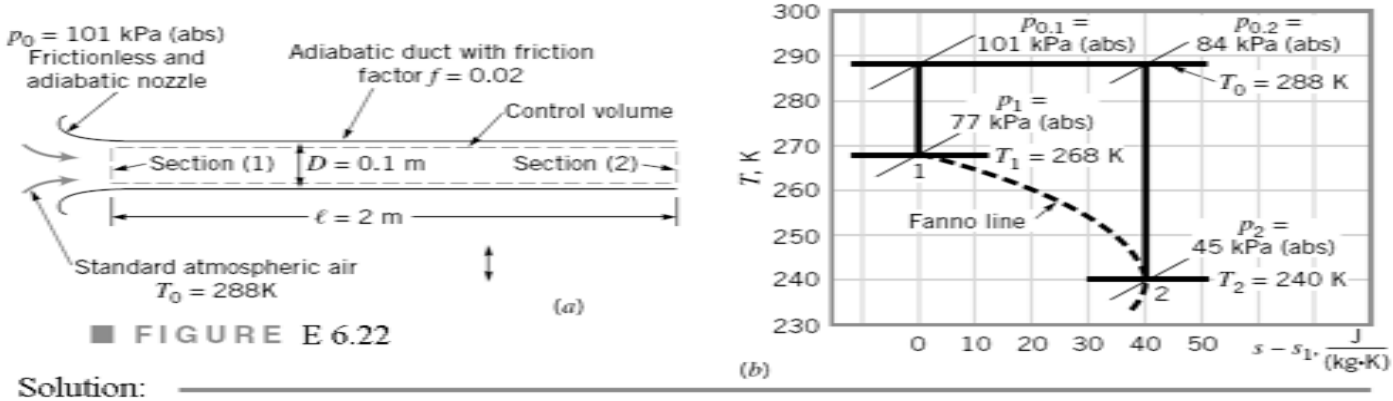

■ FIGURE E 6.22

Solution:

We consider the flow through the converging nozzle to be isentropic and the flow through the constant-area duct to be Fanno flow. A decrease in the pressure at the exit of the constant-area duct (back pressure) causes the mass flowrate through the nozzle and the duct to increase. The flow throughout is subsonic. The maximum flowrate will occur when the back pressure is lowered to the extent that the constant-area duct chokes and the Mach number at the duct exit is equal to 1. Any further decrease of back pressure will not affect the flowrate through the nozzle-duct combination.

For the maximum flowrate condition, the constant-area duct must be choked, and

$$\frac{f(\ell^* - \ell_1)}{D} = \frac{f(\ell_2 - \ell_1)}{D} = \frac{(0.02)(2\text{ m})}{(0.1\text{ m})} = 0.4 \qquad (1)$$

With $k = 1.4$ for air and the above calculated value of $f(\ell^* - \ell_1)/D = 0.4$, we could use Eq. 6.107 to determine a value of Mach number at the entrance of the duct [section (1)]. With $k = 1.4$ and Ma_1 known, we could then rely on Eqs. 6.110 , 6.112 , 6.116 , and 6.118 to obtain values of T_1/T^*, V_1/V^*, p_1/p^*, and $p_{0,1}/p_0^*$. Alternatively, for air ($k = 1.4$), we can use Fig. D.2 with $f(\ell^* - \ell_1)/D = 0.4$ and read off values of Ma_1, T_1/T^*, V_1/V^*, p_1/p^*, and $p_{0,1}/p_0^*$.

The pipe entrance Mach number, Ma_1, also represents the Mach number at the throat (and exit) of the isentropic, converging nozzle. Thus, the isentropic flow equations of Section 6.2 or Fig. D.1 can be used with Ma_1. We use Fig. D.1 in this example.

With Ma_1 known, we can enter Fig. D.1 and get values of T_1/T_0, p_1/p_0, and ρ_1/ρ_0. Through the isentropic nozzle, the values of T_0, p_0, and ρ_0 are each constant, and thus T_1, p_1, and ρ_1 can be readily obtained.

Since T_0 also remains constant through the constant-area duct (see Eq. 6.84), to get T^* Thus,

$$\frac{T^*}{T_0} = \frac{2}{k+1} = \frac{2}{1.4+1} = 0.8333 \qquad \textbf{(2)}$$

Since $T_0 = 288$ K, we get from Eq. 2,

$$T^* = (0.8333)(288\ \text{K}) = 240\ \text{K} = T_2 \qquad \textbf{(3)} \quad \text{(Ans)}$$

With T^* known, we can calculate V^* from Eq. 6.29 as

$$V^* = \sqrt{RT^*k}$$
$$= \sqrt{[(286.9\ \text{J})/(\text{kg}\cdot\text{K})](240\ \text{K})(1.4)[1(\text{kg}\cdot\text{m})/(\text{N}\cdot\text{s}^2)][1(\text{N}\cdot\text{m})/\text{J}]} \qquad \textbf{(4)} \quad \text{(Ans)}$$
$$= 310\ \text{m/s} = V_2$$

Now V_1 can be obtained from V^* and V_1/V^*. Having A_1, ρ_1, and V_1 we can get the mass flowrate from

$$\dot{m} = \rho_1 A_1 V_1 \qquad \textbf{(5)}$$

Values of the other variables asked for can be obtained from the ratios mentioned above.

Entering Fig. D.2 with $f(\ell^* - \ell)/D = 0.4$ we read

$$Ma_1 = 0.63 \quad \textbf{(7)}, \quad \frac{T_1}{T^*} = 1.1 \quad \textbf{(8)}, \quad \frac{V_1}{V^*} = 0.66 \quad \textbf{(9)}, \quad \frac{p_1}{p^*} = 1.7 \quad \textbf{(10)}, \quad \frac{p_{0,1}}{p_0^*} = 1.16 \quad \textbf{(11)}$$

Entering Fig. D.1 with $Ma_1 = 0.63$ we read

$$\frac{T_1}{T_0} = 0.93 \quad \textbf{(12)}, \quad \frac{p_1}{p_{0,1}} = 0.76 \quad \textbf{(13)}, \quad \frac{\rho_1}{\rho_{0,1}} = 0.83 \quad \textbf{(14)}$$

Thus, from Eqs. 4 and 9 we obtain $V_1 = (0.66)(310\ \text{m/s}) = 205\ \text{m/s}$ (Ans)

From Eq. 14 we get $\rho_1 = 0.83\rho_{0,1} = (0.83)(1.23\ \text{kg/m}^3) = 1.02\ \text{kg/m}^3$

and from Eq. 5 we conclude that $\dot{m} = (1.02\ \text{kg/m}^3)\left[\frac{\pi(0.1\ \text{m})^2}{4}\right](206\ \text{m/s}) = 1.65\ \text{kg/s}$ (Ans)

From Eq. 12, it follows that $T_1 = (0.93)(288\ \text{K}) = 268\ \text{K}$ (Ans)

Equation 13 yields $p_1 = (0.76)[101\ \text{kPa (abs)}] = 77\ \text{kPa (abs)}$ (Ans)

The stagnation temperature, T_0, remains constant through this adiabatic flow at a value of

$$T_{0,1} = T_{0,2} = 288\ \text{K} \qquad \text{(Ans)}$$

The stagnation pressure, p_0, at the entrance of the constant-area duct is the same as the constant value of stagnation pressure through the isentropic nozzle. Thus

$$p_{0,1} = 101\ \text{kPa(abs)} \qquad \text{(Ans)}$$

To obtain the duct exit pressure ($p_2 = p^*$) we can use Eqs. 10 and 13. Thus,

$$p_2 = \left(\frac{p^*}{p_1}\right)\left(\frac{p_1}{p_{0,1}}\right)(p_{0,1}) = \left(\frac{1}{1.7}\right)(0.76)[101\ \text{kPa(abs)}] = 45\ \text{kPa(abs)} \qquad \text{(Ans)}$$

For the duct exit stagnation pressure ($p_{0,2} = p_0^*$) we can use Eq. 11 as

$$p_{0,2} = \left(\frac{p_0^*}{p_{0,1}}\right)(p_{0,1}) = \left(\frac{1}{1.2}\right)[101\ \text{kPa(abs)}] = 84\ \text{kPa(abs)} \qquad \text{(Ans)}$$

The stagnation pressure, p_0, decreases in a Fanno flow because of friction.

Use of graphs such as Figs. D.1 and D.2 illustrates the solution of a problem involving Fanno flow. The $T - s$ diagram for this flow is shown in Fig. E. 6.22 b , where the entropy difference, $s_2 - s_1$, is obtained from Eq. 6.16 .

****

Example 6.23:

The duct in Example 6.22 is shortened by 50%, but the duct discharge pressure is maintained at the choked flow value for Example 6.22 , namely, $p_d = 45$ kPa(abs)

Will shortening the duct cause the mass flowrate through the duct to increase or decrease? Assume that the average friction factor for the duct remains constant at a value of $f = 0.02$.

Solution:

We guess that the shortened duct will still choke and check our assumption by comparing p_d with p^*. If $p_d < p^*$, the flow is choked; if not, another assumption has to be made.

For choked flow we can calculate the mass flowrate just as we did for Example 6.22 . For unchoked flow, we will have to devise another strategy.

For choked flow $$\frac{f(\ell^* - \ell_1)}{D} = \frac{(0.02)(1\text{ m})}{0.1\text{ m}} = 0.2$$

and from **Fig. D.2**, we read the values $Ma_1 = 0.70$ and $p_1/p^* = 1.5$. With $Ma_1 = 0.70$, we use Fig. D.1 and get $$\frac{p_1}{p_0} = 0.72$$

Now the duct exit pressure ($p_2 = p^*$) can be obtained from

$$p_2 = p^* = \left(\frac{p^*}{p_1}\right)\left(\frac{p_1}{p_{0,1}}\right)(p_{0,1}) = \left(\frac{1}{1.5}\right)(0.72)[101\text{ kPa(abs)}] = 48.5\text{ kPa(abs)}$$

and we see that $p_d < p^*$. Our assumption of choked flow is justified. The pressure at the exit plane is greater than the surrounding pressure outside the duct exit. The final drop of pressure from 48.5 kPa(abs) to 45 kPa(abs) involves complicated three-dimensional flow downstream of the exit.

To determine the mass flowrate we use $\dot{m} = \rho_1 A_1 V_1$ **(1)**

The density at section (1) is obtained from $$\frac{\rho_1}{\rho_{0,1}} = 0.79$$ **(2)**

which is read in Fig. D.1 for $Ma_1 = 0.7$. Thus,

$$\rho_1 = (0.79)(1.23\text{ kg/m}^3) = 0.97\text{ kg/m}^3$$ **(3)**

We get V_1 from $$\frac{V_1}{V^*} = 0.73$$ **(4)**

from Fig. D.2 for $Ma_1 = 0.7$. The value of V^* is the same as it was in Example 6.22 , namely,

$$V^* = 310\text{ m/s}$$ **(5)**

Thus, from Eqs. 4 and 5 we obtain $$V_1 = (0.73)(310) = 226\text{ m/s}$$ **(6)**

and from Eqs. 1, 3, and 6 we get

$$\dot{m} = (0.97\text{ kg/m}^3)\left[\frac{\pi(0.1\text{m})^2}{4}\right](226\text{ m/s}) = 1.73\text{ kg/s}$$ **(Ans)**

The mass flowrate associated with a shortened tube is larger than the mass flowrate for the longer tube, $\dot{m} = 1.65$ kg/s. This trend is general for subsonic Fanno flow. For the same upstream stagnation state and downstream pressure, the mass flowrate for the Fanno flow will decrease with increase in length of duct for subsonic flow. Equivalently, if the length of the duct remains the same but the wall friction is increased, the mass flowrate will decrease.

****

Example 6.24:

If the same flowrate obtained in Example 6.22 ($\dot{m} = 1.65$ kg/s) is desired through the shortened duct of Example 6.23 ($\ell_2 - \ell_1 = 1$ m), determine the Mach number at the exit of the duct, M_2, and the back pressure, p_2, required. Assume f remains constant at a value of 0.02.

Solution:

Since the mass flowrate of Example 6.22 is desired, the Mach number and other properties at the entrance of the constant-area duct remain at the values determined in Example 6.22 . Thus, from Example 6.22 , $Ma_1 = 0.63$ and from **Fig. D.2** $$\frac{f(\ell^* - \ell_1)}{D} = 0.4$$

For this example, $$\frac{f(\ell_2 - \ell_1)}{D} = \frac{f(\ell^* - \ell_1)}{D} - \frac{f(\ell^* - \ell_2)}{D}$$

or $$\frac{(0.02)(1\text{ m})}{0.1\text{ m}} = 0.4 - \frac{f(\ell^* - \ell_2)}{D}$$

so that $$\frac{f(\ell^* - \ell_2)}{D} = 0.2$$ **(1)**

By using the value from Eq. 1 and Fig. D.2, we get $Ma_2 = 0.70$ **(Ans)**

and $$\frac{p_2}{p^*} = 1.5$$ **(2)**

We obtain p_2 from $$p_2 = \left(\frac{p_2}{p^*}\right)\left(\frac{p^*}{p_1}\right)\left(\frac{p_1}{p_{0,1}}\right)(p_{0,1})$$

where p_2/p^* is given in Eq. 2 and p^*/p_1, $p_1/p_{0,1}$, and $p_{0,1}$ are the same as they were in Example 6.22 . Thus,

$$p_2 = (1.5)\left(\frac{1}{1.7}\right)(0.76)[101 \text{ kPa(abs)}] = 68.0 \text{ kPa(abs)} \quad \textbf{(Ans)}$$

A larger back pressure [68.0 kPa(abs)] than the one associated with choked flow through a Fanno duct [45 kPa(abs)] will maintain the same flowrate through a shorter Fanno duct with the same friction coefficient. The flow through the shorter duct is not choked. It would not be possible to maintain the same flowrate through a Fanno duct longer than the choked one with the same friction coefficient, regardless of what back pressure is used.

****

6.7.5 Further Analysis and Examples of Fanno-Flow:

Let us consider only the length of the constant area duct in Fig.6.28 (i.e., without the length of the nozzle attached to it). So in Eq.6.106 the lower limit of the integration on the R.H.S. starts at x =0 (i.e., $l = 0$). Equation 6.106 now becomes:

$$\int_0^{L^*} f\frac{dx}{D} = \int_{\text{Ma}^2}^{1.0} \frac{1 - \text{Ma}^2}{k\,\text{Ma}^4[1 + \frac{1}{2}(k-1)\,\text{Ma}^2]}\,d\,\text{Ma}^2 \tag{6.119}$$

The upper limit is the sonic point, whether or not it is actually reached in the duct flow. The lower limit is arbitrarily placed at the position $x = 0$, where the Mach number is Ma. The result of the integration is

$$\frac{\bar{f}L^*}{D} = \frac{1 - \text{Ma}^2}{k\,\text{Ma}^2} + \frac{k+1}{2k}\ln\frac{(k+1)\,\text{Ma}^2}{2 + (k-1)\,\text{Ma}^2} \tag{6.120}$$

where $\bar{f}$ is the average friction factor between 0 and L^*. In practice, an average f is always assumed, and no attempt is made to account for the slight changes in Reynolds number along the duct. For noncircular ducts, D is replaced by the hydraulic diameter $D_h = (4 \times \text{area})/\text{perimeter}$.

Equation (6.120) is tabulated versus Mach number in Table B.3. The length L^* is the length of duct required to develop a duct flow from Mach number Ma to the sonic point. Many problems involve short ducts which never become sonic, for which the solution uses the differences in the tabulated "maximum," or sonic, length. For example, the length ΔL required to develop from Ma_1 to Ma_2 is given by

$$\bar{f}\frac{\Delta L}{D} = \left(\frac{\bar{f}L^*}{D}\right)_1 - \left(\frac{\bar{f}L^*}{D}\right)_2 \tag{6.121}$$

This avoids the need for separate tabulations for short ducts.

It is recommended that the friction factor $\bar{f}$ be estimated from the Moody chart (Fig. 2.16) for the average Reynolds number and wall-roughness ratio of the duct. Available data [20] on duct friction for compressible flow show good agreement with the Moody chart for subsonic flow, but the measured data in supersonic duct flow are up to 50 percent less than the equivalent Moody friction factor.

Formulas for other flow properties along the duct are derived from Eqs. (a to e) in sec. 6.7.4 Equation (*e*) can be used to eliminate $f\,dx/D$ from each of the other relations, giving, for example, dp/p as a function only of Ma and $d\,\text{Ma}^2/\text{Ma}^2$. For convenience in tabulating the results, each expression is then integrated all the way from (p, Ma) to the sonic point (p^*, 1.0). The integrated results are

$$\frac{p}{p^*} = \frac{1}{\text{Ma}}\left[\frac{k+1}{2 + (k-1)\,\text{Ma}^2}\right]^{1/2} \tag{6.122a}$$

$$\frac{\rho}{\rho^*} = \frac{V^*}{V} = \frac{1}{\text{Ma}}\left[\frac{2 + (k-1)\,\text{Ma}^2}{k+1}\right]^{1/2} \tag{6.122b}$$

$$\frac{T}{T^*} = \frac{a^2}{a^{*2}} = \frac{k+1}{2 + (k-1)\,\text{Ma}^2} \tag{6.122c}$$

$$\frac{p_0}{p_0^*} = \frac{\rho_0}{\rho_0^*} = \frac{1}{\text{Ma}}\left[\frac{2 + (k-1)\,\text{Ma}^2}{k+1}\right]^{(1/2)(k+1)/(k-1)} \tag{6.122d}$$

All these ratios are also tabulated in Table B.3. For finding changes between points Ma_1 and Ma_2 which are not sonic, products of these ratios are used. For example,

$$\frac{p_2}{p_1} = \frac{p_2}{p^*}\frac{p^*}{p_1} \tag{6.123}$$

since p^* is a constant reference value for the flow.

Table B6.3 (Fanno-flow) Adiabatic Frictional Flow in a Constant-Area Duct for $k = 1.4$

Ma	$\bar{f}L^*/D$	p/p^*	T/T^*	$\rho^*/\rho = V/V^*$	p_o/p_o^*
0.0	∞	∞	1.2000	0.0	∞
0.02	1778.4500	54.7701	1.1999	0.0219	28.9421
0.04	440.3520	27.3817	1.1996	0.0438	14.4815
0.06	193.0310	18.2508	1.1991	0.0657	9.6659
0.08	106.7180	13.6843	1.1985	0.0876	7.2616
0.1	66.9216	10.9435	1.1976	0.1094	5.8218
0.12	45.4080	9.1156	1.1966	0.1313	4.8643
0.14	32.5113	7.8093	1.1953	0.1531	4.1824
0.16	24.1978	6.8291	1.1939	0.1748	3.6727
0.18	18.5427	6.0662	1.1923	0.1965	3.2779
0.2	14.5333	5.4554	1.1905	0.2182	2.9635
0.22	11.5961	4.9554	1.1885	0.2398	2.7076
0.24	9.3865	4.5383	1.1863	0.2614	2.4956
0.26	7.6876	4.1851	1.1840	0.2829	2.3173
0.28	6.3572	3.8820	1.1815	0.3043	2.1656
0.3	5.2993	3.6191	1.1788	0.3257	2.0351
0.32	4.4467	3.3887	1.1759	0.3470	1.9219
0.34	3.7520	3.1853	1.1729	0.3682	1.8229
0.36	3.1801	3.0042	1.1697	0.3893	1.7358
0.38	2.7054	2.8420	1.1663	0.4104	1.6587
0.4	2.3085	2.6958	1.1628	0.4313	1.5901
0.42	1.9744	2.5634	1.1591	0.4522	1.5289
0.44	1.6915	2.4428	1.1553	0.4729	1.4740
0.46	1.4509	2.3326	1.1513	0.4936	1.4246
0.48	1.2453	2.2313	1.1471	0.5141	1.3801
0.5	1.0691	2.1381	1.1429	0.5345	1.3398
0.52	0.9174	2.0519	1.1384	0.5548	1.3034
0.54	0.7866	1.9719	1.1339	0.5750	1.2703
0.56	0.6736	1.8975	1.1292	0.5951	1.2403
0.58	0.5757	1.8282	1.1244	0.6150	1.2130
0.6	0.4908	1.7634	1.1194	0.6348	1.1882
0.62	0.4172	1.7026	1.1143	0.6545	1.1656
0.64	0.3533	1.6456	1.1091	0.6740	1.1451
0.66	0.2979	1.5919	1.1038	0.6934	1.1265
0.68	0.2498	1.5413	1.0984	0.7127	1.1097
0.7	0.2081	1.4935	1.0929	0.7318	1.0944
0.72	0.1721	1.4482	1.0873	0.7508	1.0806
0.74	0.1411	1.4054	1.0815	0.7696	1.0681
0.76	0.1145	1.3647	1.0757	0.7883	1.0570
0.78	0.0917	1.3261	1.0698	0.8068	1.0471
0.8	0.0723	1.2893	1.0638	0.8251	1.0382
0.82	0.0559	1.2542	1.0578	0.8433	1.0305
0.84	0.0423	1.2208	1.0516	0.8614	1.0237
0.86	0.0310	1.1889	1.0454	0.8793	1.0179
0.88	0.0218	1.1583	1.0391	0.8970	1.0129
0.9	0.0145	1.1291	1.0327	0.9146	1.0089
0.92	0.0089	1.1011	1.0263	0.9320	1.0056
0.94	0.0048	1.0743	1.0198	0.9493	1.0031
0.96	0.0021	1.0485	1.0132	0.9663	1.0014
0.98	0.0005	1.0238	1.0066	0.9833	1.0003
1.0	0.0000	1.0000	1.0000	1.0000	1.0000
1.02	0.0005	0.9771	0.9933	1.0166	1.0003
1.04	0.0018	0.9551	0.9866	1.0330	1.0013
1.06	0.0038	0.9338	0.9798	1.0492	1.0029
1.08	0.0066	0.9133	0.9730	1.0653	1.0051
1.1	0.0099	0.8936	0.9662	1.0812	1.0079
1.12	0.0138	0.8745	0.9593	1.0970	1.0113
1.14	0.0182	0.8561	0.9524	1.1126	1.0153
1.16	0.0230	0.8383	0.9455	1.1280	1.0198
1.18	0.0281	0.8210	0.9386	1.1432	1.0248
1.2	0.0336	0.8044	0.9317	1.1583	1.0304
1.22	0.0394	0.7882	0.9247	1.1732	1.0366
1.24	0.0455	0.7726	0.9178	1.1879	1.0432
1.26	0.0517	0.7574	0.9108	1.2025	1.0504
1.28	0.0582	0.7427	0.9038	1.2169	1.0581
1.3	0.0648	0.7285	0.8969	1.2311	1.0663
1.32	0.0716	0.7147	0.8899	1.2452	1.0750
1.34	0.0785	0.7012	0.8829	1.2591	1.0842
1.36	0.0855	0.6882	0.8760	1.2729	1.0940
1.38	0.0926	0.6755	0.8690	1.2864	1.1042
1.4	0.0997	0.6632	0.8621	1.2999	1.1149
1.42	0.1069	0.6512	0.8551	1.3131	1.1262
1.44	0.1142	0.6396	0.8482	1.3262	1.1379
1.46	0.1215	0.6282	0.8413	1.3392	1.1501
1.48	0.1288	0.6172	0.8344	1.3520	1.1629
1.5	0.1361	0.6065	0.8276	1.3646	1.1762

Table B6.3 (Fanno-flow) Adiabatic Frictional Flow in a Constant-Area Duct for $k = 1.4$

Ma	$\bar{f}L^*/D$	p/p^*	T/T^*	$\rho^*/\rho = V/V^*$	p_o/p_o^*
1.52	0.1433	0.5960	0.8207	1.3770	1.1899
1.54	0.1506	0.5858	0.8139	1.3894	1.2042
1.56	0.1579	0.5759	0.8071	1.4015	1.2190
1.58	0.1651	0.5662	0.8004	1.4135	1.2344
1.6	0.1724	0.5568	0.7937	1.4254	1.2502
1.62	0.1795	0.5476	0.7869	1.4371	1.2666
1.64	0.1867	0.5386	0.7803	1.4487	1.2836
1.66	0.1938	0.5299	0.7736	1.4601	1.3010
1.68	0.2008	0.5213	0.7670	1.4713	1.3190
1.7	0.2078	0.5130	0.7605	1.4825	1.3376
1.72	0.2147	0.5048	0.7539	1.4935	1.3567
1.74	0.2216	0.4969	0.7474	1.5043	1.3764
1.76	0.2284	0.4891	0.7410	1.5150	1.3967
1.78	0.2352	0.4815	0.7345	1.5256	1.4175
1.8	0.2419	0.4741	0.7282	1.5360	1.4390
1.82	0.2485	0.4668	0.7218	1.5463	1.4610
1.84	0.2551	0.4597	0.7155	1.5564	1.4836
1.86	0.2616	0.4528	0.7093	1.5664	1.5069
1.88	0.2680	0.4460	0.7030	1.5763	1.5308
1.9	0.2743	0.4394	0.6969	1.5861	1.5553
1.92	0.2806	0.4329	0.6907	1.5957	1.5804
1.94	0.2868	0.4265	0.6847	1.6052	1.6062
1.96	0.2929	0.4203	0.6786	1.6146	1.6326
1.98	0.2990	0.4142	0.6726	1.6239	1.6597
2.0	0.3050	0.4082	0.6667	1.6330	1.6875
2.02	0.3109	0.4024	0.6608	1.6420	1.7160
2.04	0.3168	0.3967	0.6549	1.6509	1.7451
2.06	0.3225	0.3911	0.6491	1.6597	1.7750
2.08	0.3282	0.3856	0.6433	1.6683	1.8056
2.1	0.3339	0.3802	0.6376	1.6769	1.8369
2.12	0.3394	0.3750	0.6320	1.6853	1.8690
2.14	0.3449	0.3698	0.6263	1.6936	1.9018
2.16	0.3503	0.3648	0.6208	1.7018	1.9354
2.18	0.3556	0.3598	0.6152	1.7099	1.9698
2.2	0.3609	0.3549	0.6098	1.7179	2.0050
2.22	0.3661	0.3502	0.6043	1.7258	2.0409
2.24	0.3712	0.3455	0.5989	1.7336	2.0777
2.26	0.3763	0.3409	0.5936	1.7412	2.1153
2.28	0.3813	0.3364	0.5883	1.7488	2.1538
2.3	0.3862	0.3320	0.5831	1.7563	2.1931
2.32	0.3911	0.3277	0.5779	1.7637	2.2333
2.34	0.3959	0.3234	0.5728	1.7709	2.2744
2.36	0.4006	0.3193	0.5677	1.7781	2.3164
2.38	0.4053	0.3152	0.5626	1.7852	2.3593
2.4	0.4099	0.3111	0.5576	1.7922	2.4031
2.42	0.4144	0.3072	0.5527	1.7991	2.4479
2.44	0.4189	0.3033	0.5478	1.8059	2.4936
2.46	0.4233	0.2995	0.5429	1.8126	2.5403
2.48	0.4277	0.2958	0.5381	1.8192	2.5880
2.5	0.4320	0.2921	0.5333	1.8257	2.6367
2.52	0.4362	0.2885	0.5286	1.8322	2.6865
2.54	0.4404	0.2850	0.5239	1.8386	2.7372
2.56	0.4445	0.2815	0.5193	1.8448	2.7891
2.58	0.4486	0.2781	0.5147	1.8510	2.8420
2.6	0.4526	0.2747	0.5102	1.8571	2.8960
2.62	0.4565	0.2714	0.5057	1.8632	2.9511
2.64	0.4604	0.2682	0.5013	1.8691	3.0073
2.66	0.4643	0.2650	0.4969	1.8750	3.0647
2.68	0.4681	0.2619	0.4925	1.8808	3.1233
2.7	0.4718	0.2588	0.4882	1.8865	3.1830
2.72	0.4755	0.2558	0.4839	1.8922	3.2440
2.74	0.4791	0.2528	0.4797	1.8978	3.3061
2.76	0.4827	0.2498	0.4755	1.9033	3.3695
2.78	0.4863	0.2470	0.4714	1.9087	3.4342

Table B6.3 (Fanno-flow) Adiabatic Frictional Flow in a Constant-Area Duct for $k = 1.4$

Ma	$\bar{f}L^*/D$	p/p^*	T/T^*	$\rho^*/\rho = V/V^*$	p_0/p_0^*
2.8	0.4898	0.2441	0.4673	1.9140	3.5001
2.82	0.4932	0.2414	0.4632	1.9193	3.5674
2.84	0.4966	0.2386	0.4592	1.9246	3.6359
2.86	0.5000	0.2359	0.4552	1.9297	3.7058
2.88	0.5033	0.2333	0.4513	1.9348	3.7771
2.9	0.5065	0.2307	0.4474	1.9398	3.8498
2.92	0.5097	0.2281	0.4436	1.9448	3.9238
2.94	0.5129	0.2256	0.4398	1.9497	3.9993
2.96	0.5160	0.2231	0.4360	1.9545	4.0763
2.98	0.5191	0.2206	0.4323	1.9593	4.1547
3.0	0.5222	0.2182	0.4286	1.9640	4.2346
3.02	0.5252	0.2158	0.4249	1.9686	4.3160
3.04	0.5281	0.2135	0.4213	1.9732	4.3989
3.06	0.5310	0.2112	0.4177	1.9777	4.4835
3.08	0.5339	0.2090	0.4142	1.9822	4.5696
3.1	0.5368	0.2067	0.4107	1.9866	4.6573
3.12	0.5396	0.2045	0.4072	1.9910	4.7467
3.14	0.5424	0.2024	0.4038	1.9953	4.8377
3.16	0.5451	0.2002	0.4004	1.9995	4.9304
3.18	0.5478	0.1981	0.3970	2.0037	5.0248
3.2	0.5504	0.1961	0.3937	2.0079	5.1210
3.22	0.5531	0.1940	0.3904	2.0120	5.2189
3.24	0.5557	0.1920	0.3872	2.0160	5.3186
3.26	0.5582	0.1901	0.3839	2.0200	5.4201
3.28	0.5607	0.1881	0.3807	2.0239	5.5234
3.3	0.5632	0.1862	0.3776	2.0278	5.6286
3.32	0.5657	0.1843	0.3745	2.0317	5.7358
3.34	0.5681	0.1825	0.3714	2.0355	5.8448
3.36	0.5705	0.1806	0.3683	2.0392	5.9558
3.38	0.5729	0.1788	0.3653	2.0429	6.0687
3.4	0.5752	0.1770	0.3623	2.0466	6.1837
3.42	0.5775	0.1753	0.3594	2.0502	6.3007
3.44	0.5798	0.1736	0.3564	2.0537	6.4198
3.46	0.5820	0.1718	0.3535	2.0573	6.5409
3.48	0.5842	0.1702	0.3507	2.0607	6.6642
3.5	0.5864	0.1685	0.3478	2.0642	6.7896
3.52	0.5886	0.1669	0.3450	2.0676	6.9172
3.54	0.5907	0.1653	0.3422	2.0709	7.0471
3.56	0.5928	0.1637	0.3395	2.0743	7.1791
3.58	0.5949	0.1621	0.3368	2.0775	7.3135
3.6	0.5970	0.1616	0.3341	2.0808	7.4501
3.62	0.5990	0.1590	0.3314	2.0840	7.5891
3.64	0.6010	0.1575	0.3288	2.0871	7.7305
3.66	0.6030	0.1560	0.3262	2.0903	7.8742
3.68	0.6049	0.1546	0.3236	2.0933	8.0204
3.7	0.6068	0.1531	0.3210	2.0964	8.1691
3.72	0.6087	0.1517	0.3185	2.0994	8.3202
3.74	0.6106	0.1503	0.3160	2.1024	8.4739
3.76	0.6125	0.1489	0.3135	2.1053	8.6302
3.78	0.6143	0.1475	0.3111	2.1082	8.7891
3.8	0.6161	0.1462	0.3086	2.1111	8.9506
3.82	0.6179	0.1449	0.3062	2.1140	9.1148
3.84	0.6197	0.1436	0.3039	2.1168	9.2817
3.86	0.6214	0.1423	0.3015	2.1195	9.4513
3.88	0.6231	0.1410	0.2992	2.1223	9.6237
3.9	0.6248	0.1397	0.2969	2.1250	9.7990
3.92	0.6265	0.1385	0.2946	2.1277	9.9771
3.94	0.6282	0.1372	0.2923	2.1303	10.1581
3.96	0.6298	0.1360	0.2901	2.1329	10.3420
3.98	0.6315	0.1348	0.2879	2.1355	10.5289
4.0	0.6331	0.1336	0.2857	2.1381	10.7188

Example 6.25:

Air flows subsonically in an adiabatic 2-cm-diameter duct. The average friction factor is 0.024. What length of duct is necessary to accelerate the flow from $\text{Ma}_1 = 0.1$ to $\text{Ma}_2 = 0.5$? What additional length will accelerate it to $\text{Ma}_3 = 1.0$? Assume $k = 1.4$.

Solution

Equation 6.121 applies, with values of $\bar{f}L^*/D$ computed from Eq.6.120 or read from Table B6.3 :

$$\bar{f}\frac{\Delta L}{D} = \frac{0.024\ \Delta L}{0.02\ \text{m}} = \left(\frac{\bar{f}L^*}{D}\right)_{\text{Ma}=0.1} - \left(\frac{\bar{f}L^*}{D}\right)_{\text{Ma}=0.5}$$

$$= 66.9216 - 1.0691 = 65.8525$$

Thus
$$\Delta L = \frac{65.8525(0.02\ \text{m})}{0.024} = 55\ \text{m} \qquad \textit{Ans. (a)}$$

The additional length $\Delta L'$ to go from Ma = 0.5 to Ma = 1.0 is taken directly from Table B6.3

$$f\frac{\Delta L'}{D} = \left(\frac{fL^*}{D}\right)_{\text{Ma}=0.5} = 1.0691$$

or
$$\Delta L' = L^*_{\text{Ma}=0.5} = \frac{1.0691(0.02\ \text{m})}{0.024} = 0.9\ \text{m} \qquad \textit{Ans. (b)}$$

This is typical of these calculations: It takes 55 m to accelerate up to Ma = 0.5 and then only 0.9 m more to get all the way up to the sonic point.

****

Example 6.26:

For the duct flow of Example 6.25 assume that, at $\text{Ma}_1 = 0.1$, we have $p_1 = 600$ kPa and $T_1 = 450$ K. At section 2 farther downstream, $\text{Ma}_2 = 0.5$. Compute (*a*) p_2, (*b*) T_2, (*c*) V_2, and (*d*) p_{02}.

Solution

As preliminary information we can compute V_1 and p_{01} from the given data:

$$V_1 = \text{Ma}_1\, a_1 = 0.1[(1.4)(287)(450)]^{1/2} = 0.1(425\ \text{m/s}) = 42.5\ \text{m/s}$$

$$p_{01} = p_1(1 + 0.2\ \text{Ma}_1^2)^{3.5} = (600\ \text{kPa})[1 + 0.2(0.1)^2]^{3.5} = 604\ \text{kPa}$$

Now enter Table B6.3or Eqs. 6.122 to find the following property ratios:

Section	Ma	p/p^*	T/T^*	V/V^*	p_0/p_0^*
1	0.1	10.9435	1.1976	0.1094	5.8218
2	0.5	2.1381	1.1429	0.5345	1.3399

Use these ratios to compute all properties downstream:

$$p_2 = p_1\frac{p_2/p^*}{p_1/p^*} = (600\ \text{kPa})\frac{2.1381}{10.9435} = 117\ \text{kPa} \qquad \textit{Ans. (a)}$$

$$T_2 = T_1\frac{T_2/T^*}{T_1/T^*} = (450\ \text{K})\frac{1.1429}{1.1976} = 429\ \text{K} \qquad \textit{Ans. (b)}$$

$$V_2 = V_1\frac{V_2/V^*}{V_1/V^*} = (42.5\ \text{m/s})\frac{0.5345}{0.1094} = 208\ \frac{\text{m}}{\text{s}} \qquad \textit{Ans. (c)}$$

$$p_{02} = p_{01}\frac{p_{02}/p_0^*}{p_{01}/p_0^*} = (604\ \text{kPa})\frac{1.3399}{5.8218} = 139\ \text{kPa} \qquad \textit{Ans. (d)}$$

Note the 77 percent reduction in stagnation pressure due to friction. The formulas are seductive, so check your work by other means. For example, check $p_{02} = p_2(1 + 0.2\ \text{Ma}_2^2)^{3.5}$.

6.7.6 Choking of Fanno-Flow Due to friction:

The theory here predicts that for adiabatic frictional flow in a constant-area duct, no matter what the inlet Mach number Ma_1 is, the flow downstream tends toward the sonic point. There is a certain duct length $L^*(\text{Ma}_1)$ for which the exit Mach number will be exactly unity. The duct is then choked.

But what if the actual length L is greater than the predicted "maximum" length L^*? Then the flow conditions must change, and there are two classifications.

Subsonic inlet. If $L > L^*(\text{Ma}_1)$, the flow slows down until an inlet Mach number Ma_2 is reached such that $L = L^*(\text{Ma}_2)$. The exit flow is sonic, and the mass flow has been reduced by *frictional choking*. Further increases in duct length will continue to decrease the inlet Ma and mass flow.

Supersonic inlet. From Table B6.3 we see that friction has a very large effect on supersonic duct flow. Even an infinite inlet Mach number will be reduced to sonic conditions in only 41 diameters for $\bar{f} = 0.02$. Some typical numerical values are shown in Fig. 6.29 , assuming an inlet Ma = 3.0 and $\bar{f} = 0.02$. For this condition $L^* = 26$ diameters. If L is increased beyond $26D$, the flow will not choke but a normal shock will form at just the right place for the subsequent subsonic frictional flow to become sonic exactly at the exit. Figure 6.29 shows two examples, for $L/D = 40$ and 53. As the length increases, the required normal shock moves upstream until, for Fig. 6.29 , the shock is at the inlet for $L/D = 63$. Further increase in L causes the shock to move upstream of

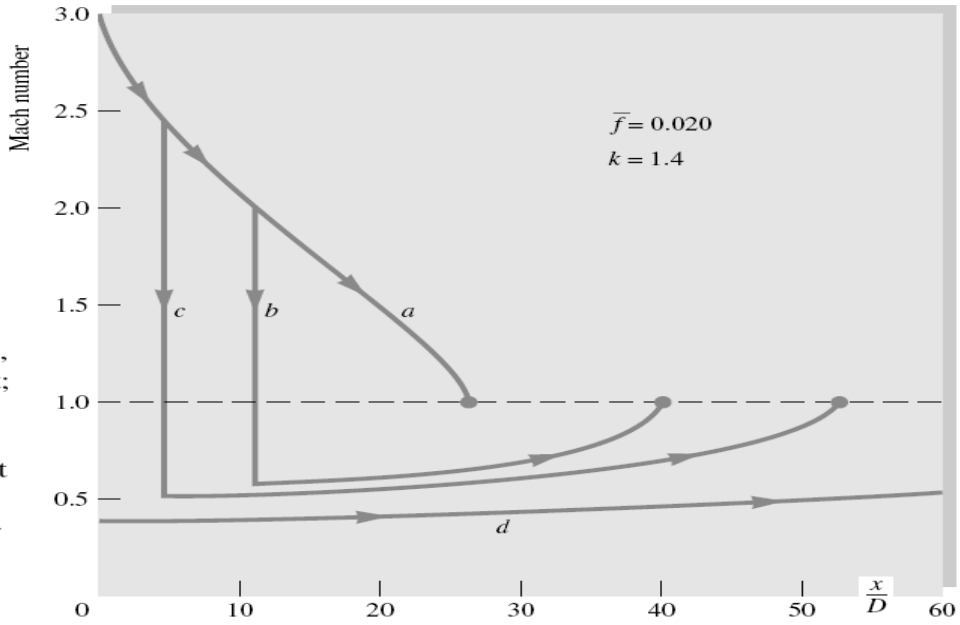

Fig. 6.29 Behavior of duct flow with a nominal supersonic inlet condition Ma = 3.0: (*a*) $L/D \leq 26$, flow is supersonic throughout duct; (*b*) $L/D = 40 > L^*/D$, normal shock at Ma = 2.0 with subsonic flow then accelerating to sonic exit point; (*c*) $L/D = 53$, shock must now occur at Ma = 2.5; (*d*) $L/D > 63$, flow must be entirely subsonic and choked at exit.

the inlet into the supersonic nozzle feeding the duct. Yet the mass flow is still the same as for the very short duct, because presumably the feed nozzle still has a sonic throat. Eventually, a very long duct will cause the feed-nozzle throat to become choked, thus reducing the duct mass flow. Thus supersonic friction changes the flow pattern if $L > L^*$ but does not choke the flow until L is much larger than L^*.

Example 6.27:

Air enters a 3-cm-diameter duct at $p_0 = 200$ kPa, $T_0 = 500$ K, and $V_1 = 100$ m/s. The friction factor is 0.02. Compute (*a*) the maximum duct length for these conditions, (*b*) the mass flow if the duct length is 15 m, and (*c*) the reduced mass flow if $L = 30$ m.

Solution

Part (a)

First compute $$T_1 = T_0 - \frac{\frac{1}{2}V_1^2}{c_p} = 500 - \frac{\frac{1}{2}(100 \text{ m/s})^2}{1005 \text{ m}^2/(\text{s}^2 \cdot \text{K})} = 500 - 5 = 495 \text{ K}$$

$$a_1 = (kRT_1)^{1/2} \approx 20(495)^{1/2} = 445 \text{ m/s}$$

Thus $$\text{Ma}_1 = \frac{V_1}{a_1} = \frac{100}{445} = 0.225$$

For this Ma_1, from Eq. 6.120 or interpolation in Table B6.3

$$\frac{\bar{f}L^*}{D} = 11.0$$

The maximum duct length possible for these inlet conditions is

$$L^* = \frac{(\bar{f}L^*/D)D}{\bar{f}} = \frac{11.0(0.03 \text{ m})}{0.02} = 16.5 \text{ m} \qquad \textit{Ans. (a)}$$

Part (b)

The given $L = 15$ m is less than L^*, and so the duct is not choked and the mass flow follows from inlet conditions

$$\rho_{01} = \frac{p_{01}}{RT_0} = \frac{200{,}000 \text{ Pa}}{287(500 \text{ K})} = 1.394 \text{ kg/m}^3$$

$$\rho_1 = \frac{\rho_{01}}{[1 + 0.2(0.225)^2]^{2.5}} = \frac{1.394}{1.0255} = 1.359 \text{ kg/m}^3$$

whence $$\dot{m} = \rho_1 A V_1 = (1.359 \text{ kg/m}^3)\left[\frac{\pi}{4}(0.03 \text{ m})^2\right](100 \text{ m/s})$$

$$= 0.0961 \text{ kg/s} \qquad \textit{Ans. (b)}$$

Part (c)

Since $L = 30$ m is greater than L^*, the duct must choke back until $L = L^*$, corresponding to a lower inlet Ma_1:

$$L^* = L = 30 \text{ m}$$

$$\frac{\bar{f}L^*}{D} = \frac{0.02(30 \text{ m})}{0.03 \text{ m}} = 20.0$$

It is difficult to interpolate for $fL/D = 20$ in Table B6.3 and impossible to invert Eq. 6.120 for the Mach number without laborious iteration. But it is a breeze for EES to solve Eq. 6.120 for the Mach number, using the following three statements:

```
k = 1.4
fLD = 20
fLD = (1 - Ma^2)/k/Ma^2 + (k + 1)/2/k*LN((k + 1)*Ma^2/(2 + (k - 1)*Ma^2))
```

Simply specify Ma < 1 in the Variable Information menu and EES cheerfully reports

$$\text{Ma}_{choked} = 0.174 \quad (23 \text{ percent less})$$

$$T_{1,new} = \frac{T_0}{1 + 0.2(0.174)^2} = 497 \text{ K}$$

$$a_{1,new} \approx 20(497 \text{ K})^{1/2} = 446 \text{ m/s}$$

$$V_{1,new} = \text{Ma}_1 a_1 = 0.174(446) = 77.6 \text{ m/s}$$

$$\rho_{1,new} = \frac{\rho_{01}}{[1 + 0.2(0.174)^2]^{2.5}} = 1.373 \text{ kg/m}^3$$

$$\dot{m}_{new} = \rho_1 A V_1 = 1.373\left[\frac{\pi}{4}(0.03)^2\right](77.6)$$

$$= 0.0753 \text{ kg/s} \quad (22 \text{ percent less}) \qquad \textit{Ans. (c)}$$

6.8 Isothermal Flow with Friction:

The adiabatic frictional-flow assumption is appropriate to high-speed flow in short ducts. For flow in long ducts, e.g., natural-gas pipelines, the gas state more closely approximates an isothermal flow. The analysis is the same except that the isoenergetic energy equation (6.77c) is replaced by the simple relation

$$T = \text{const} \qquad dT = 0 \tag{6.124}$$

Again it is possible to write all property changes in terms of the Mach number. Integration of the Mach-number–friction relation yields

$$\frac{\bar{f}L_{\max}}{D} = \frac{1 - k\,\text{Ma}^2}{k\,\text{Ma}^2} + \ln(k\,\text{Ma}^2) \tag{6.125}$$

which is the isothermal analog of Eq. (6.120) for adiabatic flow.

This friction relation has the interesting result that $L_{\max}$ becomes zero not at the sonic point but at $\text{Ma}_{crit} = 1/k^{1/2} = 0.845$ if $k = 1.4$. The inlet flow, whether subsonic or supersonic, tends downstream toward this limiting Mach number $1/k^{1/2}$. If the tube length L is greater than $L_{\max}$ from Eq. 6.125 , a subsonic flow will choke back to a smaller Ma_1 and mass flow and a supersonic flow will experience a normal-shock adjustment similar to Fig. 6.29 .

The exit isothermal choked flow is not sonic , and so the use of the asterisk is inappropriate. Let p', ρ', and V' represent properties at the choking point $L = L_{\max}$. Then the isothermal analysis leads to the following Mach-number relations for the flow properties:

$$\frac{p}{p'} = \frac{1}{\text{Ma}\,k^{1/2}} \qquad \frac{V}{V'} = \frac{\rho'}{\rho} = \text{Ma}\,k^{1/2} \tag{6.126}$$

The complete analysis and some examples are given in advanced texts [for example, 8, sec. 6.4].

6.8.1 Mass Flow for a Given Pressure Drop in Isothermal Flow:

An interesting by-product of the isothermal analysis is an explicit relation between the pressure drop and duct mass flow. This is a common problem which requires numerical iteration for adiabatic flow, as outlined below. In isothermal flow, we may substitute $dV/V = -dp/p$ and $V^2 = G^2/[p/(RT)]^2$ in Eq. (6.80) to obtain

$$\frac{2p\,dp}{G^2RT} + f\frac{dx}{D} - \frac{2\,dp}{p} = 0$$

Since G^2RT is constant for isothermal flow, this may be integrated in closed form between $(x, p) = (0, p_1)$ and (L, p_2):

$$G^2 = \left(\frac{\dot{m}}{A}\right)^2 = \frac{p_1^2 - p_2^2}{RT[\bar{f}L/D + 2\ln(p_1/p_2)]} \tag{6.127}$$

Thus mass flow follows directly from the known end pressures, without any use of Mach numbers or tables.

The writer does not know of any direct analogy to Eq. (6.127) for adiabatic flow. However, a useful adiabatic relation, involving velocities instead of pressures, is derived in several textbooks [5, p. 212; 34, p. 418]:

$$V_1^2 = \frac{a_0^2[1 - (V_1/V_2)^2]}{k\bar{f}L/D + (k+1)\ln(V_2/V_1)} \tag{6.128}$$

where $a_0 = (kRT_0)^{1/2}$ is the stagnation speed of sound, constant for adiabatic flow. We assign the proof of this as a problem exercise. This may be combined with continuity for constant duct area $V_1/V_2 = \rho_2/\rho_1$, plus the following combination of adiabatic energy and the perfect-gas relation:

$$\frac{V_1}{V_2} = \frac{p_2}{p_1}\frac{T_1}{T_2} = \frac{p_2}{p_1}\left[\frac{2a_0^2 - (k-1)V_1^2}{2a_0^2 - (k-1)V_2^2}\right] \tag{6.129}$$

If we are given the end pressures, neither V_1 nor V_2 will likely be known in advance. Here, if EES is not available, we suggest only the following simple procedure. Begin with $a_0 \approx a_1$ and the bracketed term in Eq. 6.129 approximately equal to 1.0. Solve Eq. 6.129 for a first estimate of V_1/V_2, and use this value in Eq. 6.128 to get a better estimate of V_1. Use V_1 to improve your estimate of a_0, and repeat the procedure. The process should converge in a few iterations.

Equations 6.127 and 6.128 have one flaw: With the Mach number eliminated, the frictional choking phenomenon is not directly evident. Therefore, assuming a subsonic inlet flow, one should check the exit Mach number Ma_2 to ensure that it is not greater than $1/k^{1/2}$ for isothermal flow or greater than 1.0 for adiabatic flow. We illustrate both adiabatic and isothermal flow with the following example.

Example 6.28:

Air enters a pipe of 1-cm diameter and 1.2-m length at $p_1 = 220$ kPa and $T_1 = 300$ K. If $\bar{f} = 0.025$ and the exit pressure is $p_2 = 140$ kPa, estimate the mass flow for (*a*) isothermal flow and (*b*) adiabatic flow.

Solution

Part (a) For isothermal flow Eq. 6.127 applies without iteration:

$$\frac{\bar{f}L}{D} + 2\ln\frac{p_1}{p_2} = \frac{(0.025)(1.2\text{ m})}{0.01\text{ m}} + 2\ln\frac{220}{140} = 3.904$$

$$G^2 = \frac{(220{,}000\text{ Pa})^2 - (140{,}000\text{ Pa})^2}{[287\text{ m}^2/(\text{s}^2\cdot\text{K})](300\text{ K})(3.904)} = 85{,}700 \qquad \text{or} \qquad G = 293\text{ kg/(s}\cdot\text{m}^2)$$

Since $A = (\pi/4)(0.01\text{ m})^2 = 7.85\text{ E-5 m}^2$, the isothermal mass flow estimate is

$$\dot{m} = GA = (293)(7.85\text{ E-5}) \approx 0.0230\text{ kg/s} \qquad \textit{Ans. (a)}$$

Check that the exit Mach number is not choked:

$$\rho_2 = \frac{p_2}{RT} = \frac{140{,}000}{(287)(300)} = 1.626\text{ kg/m}^3 \qquad V_2 = \frac{G}{\rho_2} = \frac{293}{1.626} = 180\text{ m/s}$$

or

$$\mathrm{Ma}_2 = \frac{V_2}{\sqrt{kRT}} = \frac{180}{[1.4(287)(300)]^{1/2}} = \frac{180}{347} \approx 0.52$$

This is well below choking, and the isothermal solution is accurate.

Part (b)

For adiabatic flow, we can iterate by hand, in the time-honored fashion, using Eqs. 6.128 and 6.129 plus the definition of stagnation speed of sound. A few years ago the author would have done just that, laboriously. However, EES makes handwork and manipulation of equations unnecessary, although careful programming and good guesses are required. If we ignore superfluous output such as T_2 and V_2, 13 statements are appropriate. First, spell out the given physical properties (in SI units):

```
k = 1.4
P1 = 220000
P2 = 140000
T1 = 300
```

Next, apply the adiabatic friction relations, Eqs. 6.120 and 6.121, to both points 1 and 2:

```
fLD1 = (1 - Ma1^2)/k/Ma1^2+(k+1)/2/k*LN((k+1)*Ma1^2/(2+(k-1)*Ma1^2))
fLD2 = (1 - Ma2^2)/k/Ma2^2+(k+1)/2/k*LN((k+1)*Ma2^2/(2+(k-1)*Ma2^2))
DeltafLD = 0.025*1.2/0.01
fLD1 = fLD2 + DeltafLD
```

Then apply the pressure-ratio formula 6.122a to both points 1 and 2:

```
P1/Pstar = ((k+1)/(2+(k-1)*Ma1^2))^0.5/Ma1
P2/Pstar = ((k+1)/(2+(k-1)*Ma2^2))^0.5/Ma2
```

These are *adiabatic* relations, so we need not further spell out quantities such as T_0 or a_0 unless we want them as additional output.

The above 10 statements are a closed algebraic system, and EES will solve them for Ma_1 and Ma_2. However, the problem asks for mass flow, so we complete the system:

```
V1 = Ma1*sqrt(1.4*287*T1)
Rho1 = P1/287/T1
Mdot = Rho1*(pi/4*0.01^2)*V1
```

If we apply no constraints, EES reports "cannot solve", because its default allows all variables to lie between $-\infty$ and $+\infty$. So we enter Variable Information and constrain Ma_1 and Ma_2 to lie between 0 and 1 (subsonic flow). EES still complains that it "cannot solve" but hints that "better guesses are needed". Indeed, the default guesses for EES variables are normally 1.0, too large for the Mach numbers. Guess the Mach numbers equal to 0.8 or even 0.5, and EES still complains, for a subtle reason: Since $f\Delta L/D = 0.025(1.2/0.01) = 3.0$, Ma_1 can be no larger than 0.36 (see Table B6.3). Finally, then, we guess Ma_1 and $Ma_2 = 0.3$ or 0.4, and EES happily reports the solution:

$$Ma_1 = 0.3343 \qquad Ma_2 = 0.5175 \qquad \frac{fL}{D_1} = 3.935 \qquad \frac{fL}{D_2} = 0.9348$$

$$p^* = 67{,}892 \text{ Pa} \qquad \dot{m} = \mathbf{0.0233\ kg/s} \qquad \textit{Ans. (b)}$$

Though the programming is complicated, the EES approach is superior to hand iteration and, of course, we can save this program for use again with new data.

==========

6.9 Frictionless Flow with Heat Transfer (Rayliegh Flow):

Consider the steady, one-dimensional, and frictionless flow of an ideal gas through the constant-area duct with heat transfer illustrated in Fig. 6.30. This is *Rayleigh flow*. Application of the linear momentum equation (Part (1)) to the Rayleigh flow through the finite control volume sketched in Fig. 6.30 results in

$$p_1A_1 + \dot{m}V_1 = p_2A_2 + \dot{m}V_2 + \underbrace{R_x}_{0 \text{ (frictionless flow)}}$$

or

$$p + \frac{(\rho V)^2}{\rho} = \text{constant} \qquad (6.119)$$

Use of the ideal gas equation of state in Eq. 6.119 leads to

$$p + \frac{(\rho V)^2 RT}{p} = \text{constant} \qquad (6.120)$$

Since the flow cross-sectional area remains constant for Rayleigh flow, from the continuity equation (Eq. E.1) we conclude that $\rho V = \text{constant}$

For a given Rayleigh flow, the constant in Eq. 6.120, the density–velocity product, ρV, and the ideal gas constant are all fixed. Thus, Eq. 6.120 can be used to determine values of fluid temperature corresponding to the local pressure in a Rayleigh flow.

To construct a temperature-entropy diagram for a given Rayleigh flow, we can use Eq. 6.85, which was developed earlier from the second $T\,ds$ relationship. Equations 6.120 and 6.85 can be solved simultaneously to obtain the curve sketched in Fig. 6.31. Curves like the one in Fig. 6.31 are called *Rayleigh lines*.

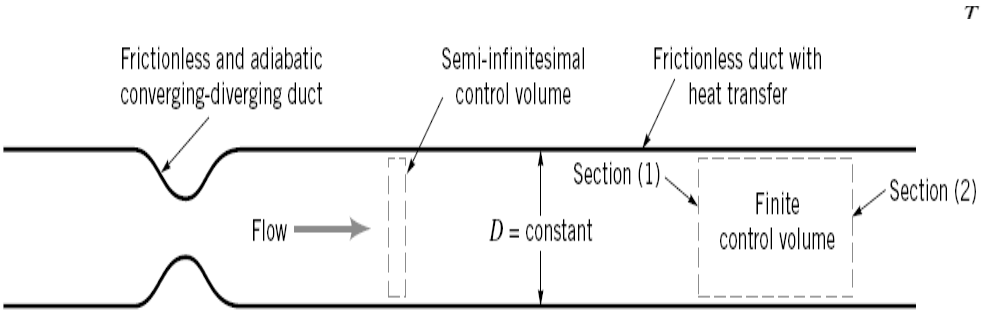

FIGURE 6.30 Rayleigh flow.

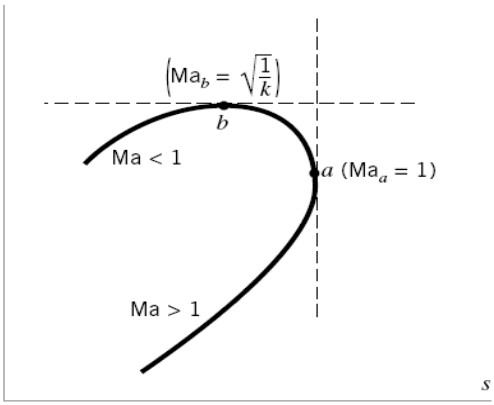

FIGURE 6.31 Rayleigh line.

an amount of heat δQ is added (or removed) to each incremental mass δm passing through. With no friction or area change, the control-volume conservation relations are quite simple:

Continuity: $$\rho_1 V_1 = \rho_2 V_2 = G = \text{const} \qquad (a)$$

x momentum: $$p_1 - p_2 = G(V_2 - V_1) \qquad (b)$$

Energy: $$\dot{Q} = \dot{m}(h_2 + \tfrac{1}{2}V_2^2 - h_1 - \tfrac{1}{2}V_1^2)$$

or $$q = \frac{\dot{Q}}{\dot{m}} = \frac{\delta Q}{\delta m} = h_{02} - h_{01} \qquad (c)$$

The heat transfer results in a change in stagnation enthalpy of the flow. We shall not specify exactly how the heat is transferred—combustion, nuclear reaction, evaporation, condensation, or wall heat exchange—but simply that it happened in amount q between 1 and 2. We remark, however, that wall heat exchange is not a good candidate for the theory because wall convection is inevitably coupled with wall friction, which we neglected.

To complete the analysis, we use the perfect-gas and Mach-number relations

$$\frac{p_2}{\rho_2 T_2} = \frac{p_1}{\rho_1 T_1} \qquad h_{02} - h_{01} = c_p(T_{02} - T_{01})$$
$$\frac{V_2}{V_1} = \frac{\text{Ma}_2\, a_2}{\text{Ma}_1\, a_1} = \frac{\text{Ma}_2}{\text{Ma}_1}\left(\frac{T_2}{T_1}\right)^{1/2} \qquad (d)$$

For a given heat transfer $q = \delta Q/\delta m$ or, equivalently, a given change $h_{02} - h_{01}$, Eqs. (a, b, c, and d) can be solved algebraically for the property ratios p_2/p_1, Ma_2/Ma_1, etc., between inlet and outlet. Note that because the heat transfer allows the entropy to either increase or decrease, the second law imposes no restrictions on these solutions.

Before writing down these property-ratio functions, we illustrate the effect of heat transfer in Fig. 6.31A,which shows T_0 and T versus Mach number in the duct. Heating increases T_0, and cooling decreases it. The maximum possible T_0 occurs at Ma = 1.0, and we see that heating, whether the inlet is subsonic or supersonic, drives the duct Mach number toward unity. This is analogous to the effect of friction in the previous section. The temperature of a perfect gas increases from Ma = 0 up to Ma = $1/k^{1/2}$ and then decreases. Thus there is a peculiar—or at least unexpected—region where heat-

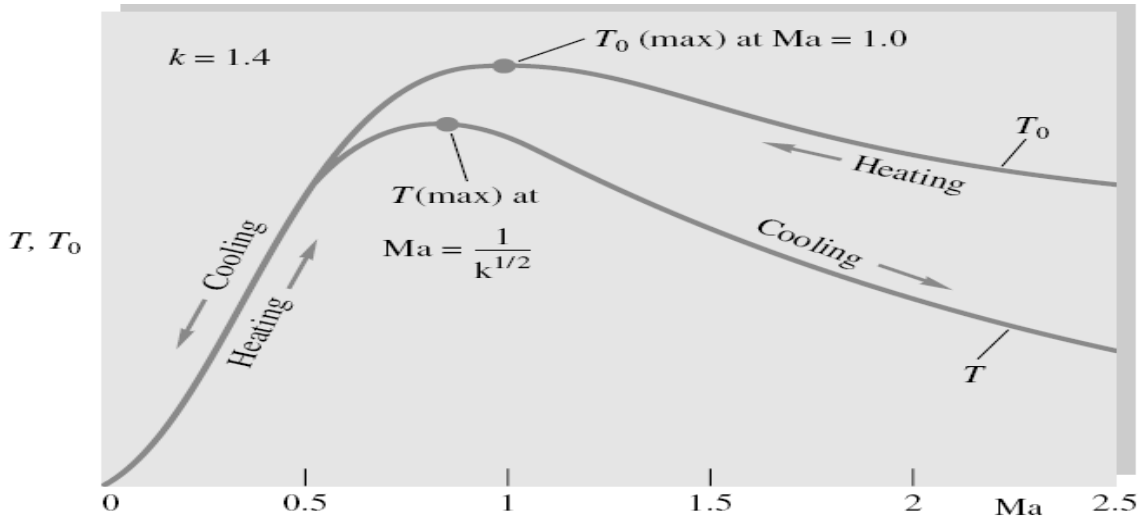

Fig. 6.31A Effect of heat transfer on Mach number.

ing (increasing T_0) actually decreases the gas temperature, the difference being reflected in a large increase of the gas kinetic energy. For $k = 1.4$ this peculiar area lies between Ma = 0.845 and Ma = 1.0 (interesting but not very useful information).

The complete list of the effects of simple T_0 change on flow properties is as follows:

	Heating		Cooling	
	Subsonic	Supersonic	Subsonic	Supersonic
T_0	Increases	Increases	Decreases	Decreases
Ma	Increases	Decreases	Decreases	Increases
p	Decreases	Increases	Increases	Decreases
ρ	Decreases	Increases	Increases	Decreases
V	Increases	Decreases	Decreases	Increases
p_0	Decreases	Decreases	Increases	Increases
s	Increases	Increases	Decreases	Decreases
T	*	Increases	†	Decreases

*Increases up to Ma $= 1/k^{1/2}$ and decreases thereafter.
†Decreases up to Ma $= 1/k^{1/2}$ and increases thereafter.

Probably the most significant item on this list is the stagnation pressure p_0, which always decreases during heating whether the flow is subsonic or supersonic. Thus heating does increase the Mach number of a flow but entails a loss in effective pressure recovery.

Example 6.29:

Air ($k = 1.4$) enters [section (1)] a frictionless, constant flow cross-section area duct with the following properties (the same as in Example 6.21):

$T_0 = 518.67\ ^\circ\text{R}$ $T_1 = 514.55\ ^\circ\text{R}$ $p_1 = 14.3$ psia

For Rayleigh flow, determine corresponding values of fluid temperature and entropy change for various levels of downstream pressure and plot the related Rayleigh line.

Solution:

To plot the Rayleigh line asked for, use Eq. 6.120

$$p + \frac{(\rho V)^2 RT}{p} = \text{constant} \tag{1}$$

and Eq. 6.85

$$s - s_1 = c_p \ln \frac{T}{T_1} - R \ln \frac{p}{p_1} \tag{2}$$

to construct a table of values of temperature and entropy change corresponding to different levels of pressure downstream in a Rayleigh flow.

Use the value of ideal gas constant for air from Table 1.7 $R = 1716\ (\text{ft} \cdot \text{lb})/(\text{slug} \cdot {}^\circ\text{R})$ and the value of specific heat a constant pressure for air from Example 6.21 , namely,

$$c_p = 6006\ (\text{ft} \cdot \text{lb})/(\text{slug} \cdot {}^\circ\text{R})$$

Also, from Example 6.21 , $\rho V = 0.519$ slug/(ft^2 · s). For the given inlet [section (1)] conditions, we get from Eq. 1

$$p + \frac{(\rho V)^2 RT}{p} = 14.3 \text{ psia} + \frac{[0.519 \text{ slug}/(\text{ft}^2 \cdot \text{s})]^2 [1716\ (\text{ft} \cdot \text{lb})/(\text{slug} \cdot {}^\circ\text{R})](514.55\ {}^\circ\text{R})}{(144 \text{ in.}^2/\text{ft}^2)^2\ 14.3 \text{ psia}} = \text{constant}$$

or

$$p + \frac{(\rho V)^2 RT}{p} = 15.10 \text{ psia} = \text{constant} \tag{3}$$

From Eq. 3, with the downstream pressure $p = 13.5$ psia, we obtain

$$13.5 \text{ psia} + \frac{[0.519 \text{ slug}/(\text{ft}^2/\text{s})]^2 [1716\ (\text{ft} \cdot \text{lb})/(\text{slug} \cdot {}^\circ\text{R})]T}{(144 \text{ in.}^2/\text{ft}^2)^2\ 13.5 \text{ psia}} = 15.10 \text{ psia}$$

or

$$T = 969\ ^\circ\text{R}$$

From Eq. 2 with the downstream pressure $p = 13.5$ psia and temperature $T = 969\ ^\circ$R we get

$$s - s_1 = [6006\ (\text{ft} \cdot \text{lb})/(\text{slug} \cdot {}^\circ\text{R})] \ln\left(\frac{969\ {}^\circ\text{R}}{514.55\ {}^\circ\text{R}}\right) - [1716\ (\text{ft} \cdot \text{lb})/(\text{slug} \cdot {}^\circ\text{R})] \ln\left(\frac{13.5 \text{ psia}}{14.3 \text{ psia}}\right)$$

$$s - s_1 = 3900\ (\text{ft} \cdot \text{lb})/(\text{slug} \cdot {}^\circ\text{R})$$

By proceeding as outlined above, we can construct the table of values shown below and graph the Rayleigh line of Fig. E6.29 .

p (psia)	T (°R)	$s - s_1$ [(ft · lb)/(slug · °R)]
13.5	969	3,900
12.5	1459	6,490
11.5	1859	8,089
10.5	2168	9,168
9.0	2464	10,202
8.0	2549	10,607
7.6	2558	10,716
7.5	2558	10,739
7.0	2544	10,825
6.3	2488	10,872
6.0	2450	10,863
5.5	2369	10,810
5.0	2266	10,707
4.5	2140	10,544
4.0	1992	10,315
2.0	1175	8,335
1.0	633	5,809

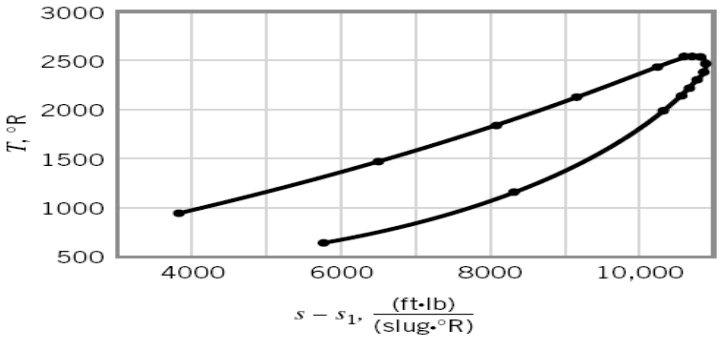

■ FIGURE **E6.29**

At point a on the Rayleigh line of Fig. 6.31 , $ds/dT = 0$. To determine the physical importance of point a, we analyze further some of the governing equations. By differentiating the linear momentum equation for Rayleigh flow (Eq. 6.119) we obtain

$$dp = -\rho V\, dV$$

or

$$\frac{dp}{\rho} = -V\, dV \qquad (6.121)$$

Combining Eq. 6.121 with the second $T\,ds$ equation (Eq. 6.12) leads to

$$T\, ds = d\check{h} + V\, dV \qquad (6.122)$$

For an ideal gas $d\check{h} = c_p\, dT$. Thus, substituting into Eq. 6.122 gives

$$T\, ds = c_p\, dT + V\, dV$$

or

$$\frac{ds}{dT} = \frac{c_p}{T} + \frac{V}{T}\frac{dV}{dT} \qquad (6.123)$$

Consolidation of Eqs. 6.123 , 6.121 (linear momentum), 6.86 (differentiated equation of state), and 6.88 (continuity) leads to

$$\frac{ds}{dT} = \frac{c_p}{T} + \frac{V}{T}\frac{1}{[(T/V) - (V/R)]} \qquad (6.124)$$

Hence, at state a where $ds/dT = 0$, Eq. 6.124 reveals that

$$V_a = \sqrt{RT_a k} \qquad (6.125)$$

Comparison of Eqs. 6.125 and 6.29 tells us that the Mach number at state a is equal to 1.

$$\mathrm{Ma}_a = 1 \qquad (6.126)$$

At point b on the Rayleigh line of Fig. 6.31 , $dT/ds = 0$. From Eq. 6.124 we get

$$\frac{dT}{ds} = \frac{1}{ds/dT} = \frac{1}{(c_p/T) + (V/T)[(T/V) - (V/R)]^{-1}}$$

which for $dT/ds = 0$ (point b) gives

$$\mathrm{Ma}_b = \sqrt{\frac{1}{k}} \qquad (6.127)$$

The flow at point b is subsonic ($\mathrm{Ma}_b < 1.0$). Recall that $k > 1$ for any gas.

To learn more about Rayleigh flow, we need to consider the energy equation in addition to the equations already used. Application of the energy equation (Part (2)) to the Rayleigh flow through the finite control volume of Fig. 6.30 yields

$$\dot{m}\left[\check{h}_2 - \check{h}_1 + \frac{V_2^2 - V_1^2}{2} + g(z_2 - z_1)\right] = \dot{Q}_{\substack{\text{net}\\ \text{in}}} + \dot{W}_{\substack{\text{shaft}\\ \text{net in}}}$$

0(negligibly small for gas flow) 0(flow is steady throughout)

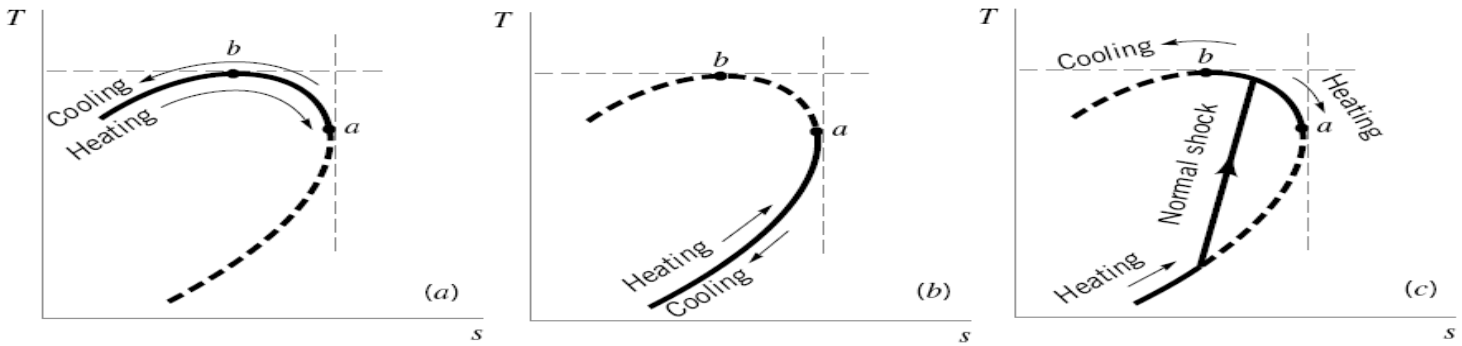

■ FIGURE **6.32** **(*a*) Subsonic Rayleigh flow. (*b*) Supersonic Rayleigh flow. (*c*) Normal shock in a Rayleigh flow.**

TABLE 6.2
Summary of Rayleigh Flow Characteristics

	Heating	Cooling
Ma $<$ 1	Acceleration	Deceleration
Ma $>$ 1	Deceleration	Acceleration

or in differential form for Rayleigh flow through the semi-infinitesimal control volume of Fig. 6.30

$$d\check{h} + V\,dV = \delta q \qquad (6.128)$$

where δq is the heat transfer per unit mass of fluid in the semi-infinitesimal control volume.

By using $d\check{h} = c_p\,dT = Rk\,dT/(k-1)$ in Eq. 6.128, we obtain

$$\frac{dV}{V} = \frac{\delta q}{c_p T}\left[\frac{V}{T}\frac{dT}{dV} + \frac{V^2(k-1)}{kRT}\right]^{-1} \qquad (6.129)$$

Thus, by combining Eqs. 6.29 (ideal gas speed of sound), E.7 (Mach number), 6.1 and 6.86 (ideal gas equation of state), 6.88 (continuity), and 6.121 (linear momentum) with Eq. 6.129 (energy) we get

$$\frac{dV}{V} = \frac{\delta q}{c_p T}\frac{1}{(1-\mathrm{Ma}^2)} \qquad (6.130)$$

With the help of Eq. 6.130, we see clearly that when the Rayleigh flow is subsonic (Ma $<$ 1), fluid heating ($\delta q > 0$) increases fluid velocity while fluid cooling ($\delta q < 0$) decreases fluid velocity. When Rayleigh flow is supersonic (Ma $>$ 1), fluid heating decreases fluid velocity and fluid cooling increases fluid velocity.

The second law of thermodynamics states that, based on experience, entropy increases with heating and decreases with cooling. With this additional insight provided by the conservation of energy principle and the second law of thermodynamics, we can say more about the Rayleigh line in Fig. 6.31. A summary of the qualitative aspects of Rayleigh flow is outlined in Table 6.2 and Fig. 6.32. Along the upper portion of the line, which includes point b, the flow is subsonic. Heating the fluid results in flow acceleration to a maximum Mach number of 1 at point a. Note that between points b and a along the Rayleigh line, heating the fluid results in a temperature decrease and cooling the fluid leads to a temperature increase. This trend is not surprising if we consider the stagnation temperature and fluid velocity changes that occur between points a and b when the fluid is heated or cooled. Along the lower portion of the Rayleigh curve the flow is supersonic. Rayleigh flows may or may not be choked. The amount of heating or cooling involved determines what will happen in a specific instance. As with Fanno flows, an abrupt deceleration from supersonic flow to subsonic flow across a normal shock wave can also occur in Rayleigh flows.

To quantify Rayleigh flow behavior we need to develop appropriate forms of the governing equations. We elect to use the state of the Rayleigh flow fluid at point a of Fig. 6.31 as the reference state. As shown earlier, the Mach number at point a is 1. Even though the Rayleigh flow being considered may not choke and state a is not achieved by the flow, this reference state is useful.

If we apply the linear momentum equation (Eq. 6.119) to Rayleigh flow between any upstream section and the section, actual or imagined, where state a is attained, we get

$$p + \rho V^2 = p_a + \rho_a V_a^2$$

or

$$\frac{p}{p_a} + \frac{\rho V^2}{p_a} = 1 + \frac{\rho_a}{p_a}V_a^2 \qquad (6.131)$$

By substituting the ideal gas equation of state into Eq. 6.131 and making use of the ideal gas speed-of-sound equation (Eq. 6.29) and the definition of Mach number (Eq. E.7), we obtain

$$\boxed{\frac{p}{p_a} = \frac{1+k}{1+k\mathrm{Ma}^2}} \qquad (6.132)$$

From the ideal gas equation of state we conclude that

$$\frac{T}{T_a} = \frac{p}{p_a}\frac{\rho_a}{\rho} \qquad (6.133)$$

Conservation of mass (Eq. E.1) with constant A gives

$$\frac{\rho_a}{\rho} = \frac{V}{V_a} \qquad (6.134)$$

which when combined with Eqs. 6.29 (ideal gas speed of sound) and E.7 (Mach number definition) gives

$$\frac{\rho_a}{\rho} = \mathrm{Ma}\sqrt{\frac{T}{T_a}} \qquad (6.135)$$

Combining Eqs. 6.133 and 6.135 leads to

$$\frac{T}{T_a} = \left(\frac{p}{p_a}\mathrm{Ma}\right)^2 \qquad (6.136)$$

which when combined with Eq. 6.132 gives

$$\boxed{\frac{T}{T_a} = \left[\frac{(1+k)\mathrm{Ma}}{1+k\mathrm{Ma}^2}\right]^2} \qquad (6.137)$$

From Eqs. 6.134, 6.135, and 6.137 we see that

$$\frac{\rho_a}{\rho} = \frac{V}{V_a} = \mathrm{Ma}\left[\frac{(1 + k)\mathrm{Ma}}{1 + k\mathrm{Ma}^2}\right] \qquad (6.138)$$

The energy equation (Part (1)) tells us that because of the heat transfer involved in Rayleigh flows, the stagnation temperature varies. We note that

$$\frac{T_0}{T_{0,a}} = \left(\frac{T_0}{T}\right)\left(\frac{T}{T_a}\right)\left(\frac{T_a}{T_{0,a}}\right) \qquad (6.139)$$

We can use Eq. E.17 (developed earlier for steady, isentropic, ideal gas flow) to evaluate T_0/T and T_a/T_{0a} because these two temperature ratios, by definition of the stagnation state, involve isentropic processes. Equation 6.137 can be used for T/T_a. Thus, consolidating Eqs. 6.139, E.17, and 6.137 we obtain

$$\frac{T_0}{T_{0,a}} = \frac{2(k + 1)\mathrm{Ma}^2\left(1 + \dfrac{k - 1}{2}\mathrm{Ma}^2\right)}{(1 + k\mathrm{Ma}^2)^2} \qquad (6.140)$$

Finally, we observe that

$$\frac{p_0}{p_{0,a}} = \left(\frac{p_0}{p}\right)\left(\frac{p}{p_a}\right)\left(\frac{p_a}{p_{0,a}}\right) \qquad (6.141)$$

We can use Eq. E.20 developed earlier for steady, isentropic, ideal gas flow to evaluate p_0/p and $p_a/p_{0,a}$ because these two pressure ratios, by definition, involve isentropic processes. Equation 6.132 can be used for p/p_a. Together, Eqs. E.20, 6.132, and 6.141 give

$$\frac{p_0}{p_{0a}} = \frac{(1 + k)}{(1 + k\mathrm{Ma}^2)}\left[\left(\frac{2}{k + 1}\right)\left(1 + \frac{k - 1}{2}\mathrm{Ma}^2\right)\right]^{k/(k-1)} \qquad (6.142)$$

Values of p/p_a, T/T_a, ρ_a/ρ, or V/V_a, $T_0/T_{0,a}$, and $p_0/p_{0,a}$ are graphed in Fig. D.3 of Appendix D as a function of Mach number for Rayleigh flow of air ($k = 1.4$). The values in Fig. D.3 were calculated from Eqs. 6.132, 6.137, 6.138, 6.140, and 6.142. The usefulness of Fig. D.3 is illustrated in Example 6.30.

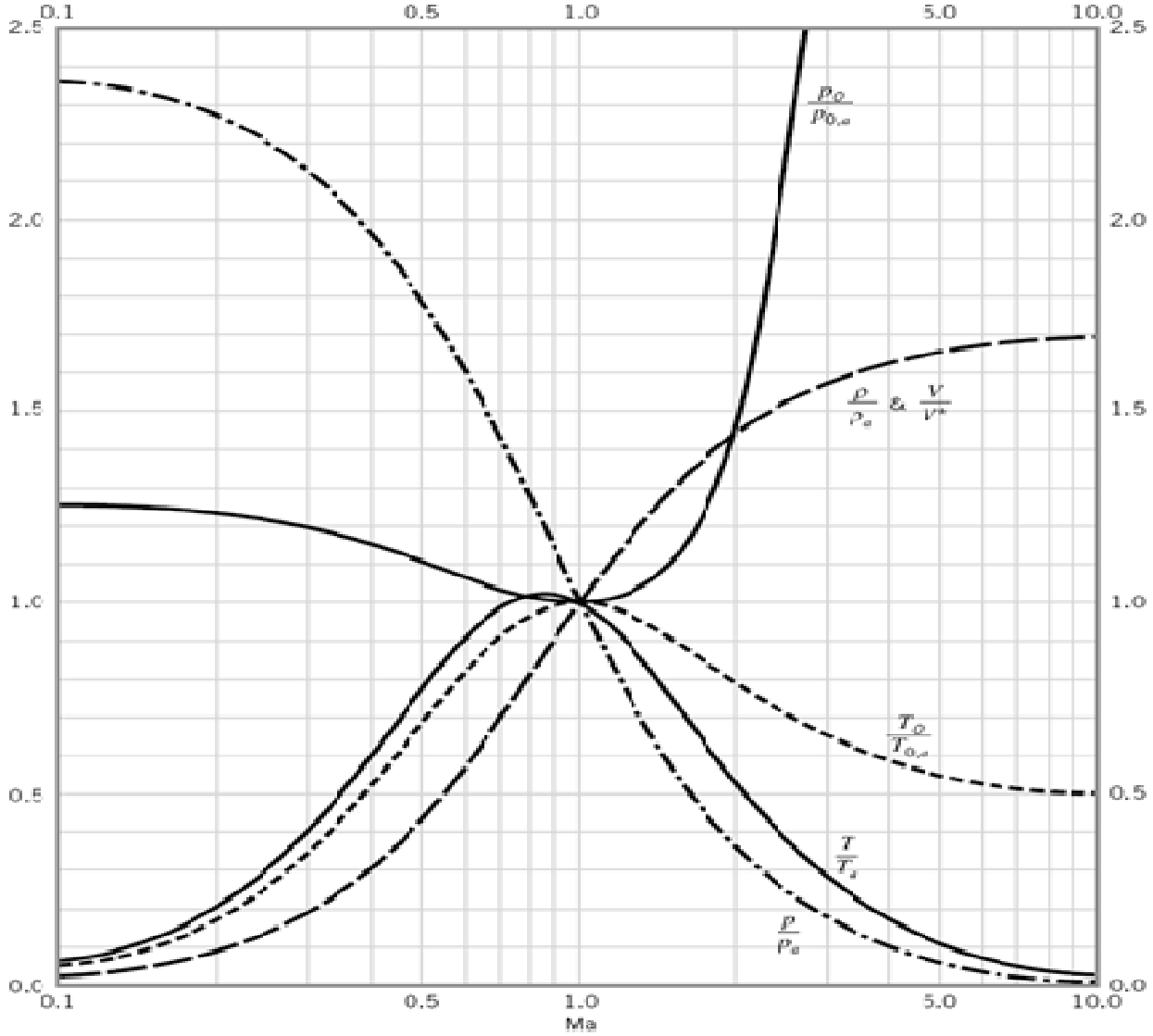

■ FIGURE D.3 **Rayleigh flow of an ideal gas with $k = 1.4$. (Graph provided by Professor Bruce A. Reichert of Kansas State University.)**

The information in Table 6.2 shows us that subsonic Rayleigh flow accelerates when heated and decelerates when cooled. Supersonic Rayleigh flow behaves just opposite to subsonic Rayleigh flow; it decelerates when heated and accelerates when cooled. Using Fig. D.3 for air ($k = 1.4$), state whether velocity, Mach number, static temperature, stagnation temperature, static pressure, and stagnation pressure increase or decrease as subsonic and supersonic Rayleigh flow is (a) heated, (b) cooled.

Solution:

Acceleration occurs when V/V_a in Fig. D.3 increases. For deceleration, V/V_a decreases. From **Fig. D.3** and Table 6.2 the following chart can be constructed.

	Heating		**Cooling**	
	Subsonic	**Supersonic**	**Subsonic**	**Supersonic**
V	Increase	Decrease	Decrease	Increase
Ma	Increase	Decrease	Decrease	Increase
T	Increase for $0 \le \text{Ma} \le \sqrt{1/k} = 0.845$ Decrease for $\sqrt{1/k} \le \text{Ma} \le 1$	Increase	Decrease for $0 \le \text{Ma} \le \sqrt{1/k} = 0.845$ Increase for $\sqrt{1/k} \le \text{Ma} \le 1$	Decrease
T_0	Increase	Increase	Decrease	Decrease
p	Decrease	Increase	Increase	Decrease
p_0	Decrease	Decrease	Increase	Increase

From the Rayleigh flow trends summarized in the table above, we note that heating affects Rayleigh flows much like friction affects Fanno flows. Heating and friction both accelerate subsonic flows and decelerate supersonic flows. More importantly, both heating and friction cause the stagnation pressure to decrease. Since stagnation pressure loss is considered undesirable in terms of fluid mechanical efficiency, heating a fluid flow must be accomplished with this loss in mind.

==========

6.9.1 The Mach-Number Relations and Tables of The Rayleigh-Flow:

Similar to the behavior of Fanno-flow, we note that the maximum entropy is found at point (a) on Figs.6.31 and 6.32 where the value of Mach Number $(\text{Ma})_a = 1$ (eq. 6.126). So the flow is sonic at point (a). If we consider point (a) as a reference point and write down all the Mach-Number relations of the Rayleigh-flow, we get:

For convenience, we specify that the outlet section is sonic, Ma =1, Point (a) on Fig.6.31 with reference properties T_0^*, T^*, p^*, ρ^*, V^*, and p_0^*. The inlet is assumed to be at arbitrary Mach number Ma. Equations (a, b, c, and d) then take the following form:

$$\frac{T_0}{T_0^*} = \frac{(k+1)\,\text{Ma}^2\,[2 + (k-1)\,\text{Ma}^2]}{(1 + k\,\text{Ma}^2)^2} \tag{6.143a}$$

$$\frac{T}{T^*} = \frac{(k+1)^2\,\text{Ma}^2}{(1 + k\,\text{Ma}^2)^2} \tag{6.143b}$$

$$\frac{p}{p^*} = \frac{k+1}{1 + k\,\text{Ma}^2} \tag{6.143c}$$

$$\frac{V}{V^*} = \frac{\rho^*}{\rho} = \frac{(k+1)\,\text{Ma}^2}{1 + k\,\text{Ma}^2} \tag{6.143d}$$

$$\frac{p_0}{p_0^*} = \frac{k+1}{1 + k\,\text{Ma}^2}\left[\frac{2 + (k-1)\,\text{Ma}^2}{k+1}\right]^{k/(k-1)} \tag{6.143e}$$

These formulas are all tabulated versus Mach number in Table B6.4. The tables are very convenient if inlet properties Ma_1, V_1, etc., are given but are somewhat cumbersome if the given information centers on T_{01} and T_{02}. Let us illustrate with an example.

Table B6.4 Rayleigh-flow:Frictionless Duct Flow with Heat Transfer for $k = 1.4$

Ma	T_0/T_0^*	p/p^*	T/T^*	$\rho^*/\rho = V/V^*$	p_0/p_0^*
0.0	0.0	2.4000	0.0	0.0	1.2679
0.02	0.0019	2.3987	0.0023	0.0010	1.2675
0.04	0.0076	2.3946	0.0092	0.0038	1.2665
0.06	0.0171	2.3800	0.0205	0.0086	1.2647
0.08	0.0302	2.3787	0.0362	0.0152	1.2623
0.1	0.0468	2.3669	0.0560	0.0237	1.2591
0.12	0.0666	2.3526	0.0797	0.0339	1.2554
0.14	0.0895	2.3359	0.1069	0.0458	1.2510
0.16	0.1151	2.3170	0.1374	0.0593	1.2461
0.18	0.1432	2.2959	0.1708	0.0744	1.2406
0.2	0.1736	2.2727	0.2066	0.0909	1.2346
0.22	0.2057	2.2477	0.2445	0.1088	1.2281
0.24	0.2395	2.2209	0.2841	0.1279	1.2213
0.26	0.2745	2.1925	0.3250	0.1482	1.2140
0.28	0.3104	2.1626	0.3667	0.1696	1.2064
0.3	0.3469	2.1314	0.4089	0.1918	1.1985
0.32	0.3837	2.0991	0.4512	0.2149	1.1904
0.34	0.4206	2.0657	0.4933	0.2388	1.1822
0.36	0.4572	2.0314	0.5348	0.2633	1.1737
0.38	0.4935	1.9964	0.5755	0.2883	1.1652
0.4	0.5290	1.9608	0.6151	0.3137	1.1566
0.42	0.5638	1.9247	0.6535	0.3395	1.1480
0.44	0.5975	1.8882	0.6903	0.3656	1.1394
0.46	0.6301	1.8515	0.7254	0.3918	1.1308
0.48	0.6614	1.8147	0.7587	0.4181	1.1224
0.5	0.6914	1.7778	0.7901	0.4444	1.1141
0.52	0.7199	1.7409	0.8196	0.4708	1.1059
0.54	0.7470	1.7043	0.8469	0.4970	1.0979
0.56	0.7725	1.6678	0.8723	0.5230	1.0901
0.58	0.7965	1.6316	0.8955	0.5489	1.0826
0.6	0.8189	1.5957	0.9167	0.5745	1.0753
0.62	0.8398	1.5603	0.9358	0.5998	1.0682
0.64	0.8592	1.5253	0.9530	0.6248	1.0615
0.66	0.8771	1.4908	0.9682	0.6494	1.0550
0.68	0.8935	1.4569	0.9814	0.6737	1.0489
0.7	0.9085	1.4235	0.9929	0.6975	1.0431
0.72	0.9221	1.3907	1.0026	0.7209	1.0376
0.74	0.9344	1.3585	1.0106	0.7439	1.0325
0.76	0.9455	1.3270	1.0171	0.7665	1.0278
0.78	0.9553	1.2961	1.0220	0.7885	1.0234
0.8	0.9639	1.2658	1.0255	0.8101	1.0193
0.82	0.9715	1.2362	1.0276	0.8313	1.0157
0.84	0.9781	1.2073	1.0285	0.8519	1.0124
0.86	0.9836	1.1791	1.0283	0.8721	1.0095
0.88	0.9883	1.1515	1.0269	0.8918	1.0070
0.9	0.9921	1.1246	1.0245	0.9110	1.0049
0.92	0.9951	1.0984	1.0212	0.9297	1.0031
0.94	0.9973	1.0728	1.0170	0.9480	1.0017
0.96	0.9988	1.0479	1.0121	0.9658	1.0008
0.98	0.9997	1.0236	1.0064	0.9831	1.0002
1.0	1.0000	1.0000	1.0000	1.0000	1.0000
1.02	0.9997	0.9770	0.9930	1.0164	1.0002
1.04	0.9989	0.9546	0.9855	1.0325	1.0008
1.06	0.9977	0.9327	0.9776	1.0480	1.0017
1.08	0.9960	0.9115	0.9691	1.0632	1.0031
1.1	0.9939	0.8909	0.9603	1.0780	1.0049
1.12	0.9915	0.8708	0.9512	1.0923	1.0070
1.14	0.9887	0.8512	0.9417	1.1063	1.0095
1.16	0.9856	0.8322	0.9320	1.1198	1.0124
1.18	0.9823	0.8137	0.9220	1.1330	1.0157
1.2	0.9787	0.7958	0.9118	1.1459	1.0194
1.22	0.9749	0.7783	0.9015	1.1584	1.0235
1.24	0.9709	0.7613	0.8911	1.1705	1.0279
1.26	0.9668	0.7447	0.8805	1.1823	1.0328
1.28	0.9624	0.7287	0.8699	1.1938	1.0380
1.3	0.9580	0.7130	0.8592	1.2050	1.0437
1.32	0.9534	0.6978	0.8484	1.2159	1.0497
1.34	0.9487	0.6830	0.8377	1.2264	1.0561
1.36	0.9440	0.6686	0.8269	1.2367	1.0629
1.38	0.9391	0.6546	0.8161	1.2467	1.0701
1.4	0.9343	0.6410	0.8054	1.2564	1.0777
1.42	0.9293	0.6278	0.7947	1.2659	1.0856
1.44	0.9243	0.6149	0.7840	1.2751	1.0940
1.46	0.9193	0.6024	0.7735	1.2840	1.1028
1.48	0.9143	0.5902	0.7629	1.2927	1.1120
1.5	0.9093	0.5783	0.7525	1.3012	1.1215
1.52	0.9042	0.5668	0.7422	1.3095	1.1315
1.54	0.8992	0.5555	0.7319	1.3175	1.1419
1.56	0.8942	0.5446	0.7217	1.3253	1.1527
1.58	0.8892	0.5339	0.7117	1.3329	1.1640
1.6	0.8842	0.5236	0.7017	1.3403	1.1756
1.62	0.8792	0.5135	0.6919	1.3475	1.1877
1.64	0.8743	0.5036	0.6822	1.3546	1.2002
1.66	0.8694	0.4940	0.6726	1.3614	1.2131
1.68	0.8645	0.4847	0.6631	1.3681	1.2264

Table B6.4 Rayleigh-flow: Frictionless Duct Flow with Heat Transfer for $k = 1.4$

Ma	T_0/T_0^*	p/p^*	T/T^*	$\rho^*/\rho = V/V^*$	p_0/p_0^*
1.7	0.8597	0.4756	0.6538	1.3746	1.2402
1.72	0.8549	0.4668	0.6445	1.3809	1.2545
1.74	0.8502	0.4581	0.6355	1.3870	1.2692
1.76	0.8455	0.4497	0.6265	1.3931	1.2843
1.78	0.8409	0.4415	0.6176	1.3989	1.2999
1.8	0.8363	0.4335	0.6089	1.4046	1.3159
1.82	0.8317	0.4257	0.6004	1.4102	1.3324
1.84	0.8273	0.4181	0.5919	1.4156	1.3494
1.86	0.8228	0.4107	0.5836	1.4209	1.3669
1.88	0.8185	0.4035	0.5754	1.4261	1.3849
1.9	0.8141	0.3964	0.5673	1.4311	1.4033
1.92	0.8099	0.3895	0.5594	1.4360	1.4222
1.94	0.8057	0.3828	0.5516	1.4408	1.4417
1.96	0.8015	0.3763	0.5439	1.4455	1.4616
1.98	0.7974	0.3699	0.5364	1.4501	1.4821
2.0	0.7934	0.3636	0.5289	1.4545	1.5031
2.02	0.7894	0.3575	0.5216	1.4589	1.5246
2.04	0.7855	0.3516	0.5144	1.4632	1.5467
2.06	0.7816	0.3458	0.5074	1.4673	1.5693
2.08	0.7778	0.3401	0.5004	1.4714	1.5924
2.1	0.7741	0.3345	0.4936	1.4753	1.6162
2.12	0.7704	0.3291	0.4868	1.4792	1.6404
2.14	0.7667	0.3238	0.4802	1.4830	1.6653
2.16	0.7631	0.3186	0.4737	1.4867	1.6908
2.18	0.7596	0.3136	0.4673	1.4903	1.7168
2.2	0.7561	0.3086	0.4611	1.4938	1.7434
2.22	0.7527	0.3038	0.4549	1.4973	1.7707
2.24	0.7493	0.2991	0.4488	1.5007	1.7986
2.26	0.7460	0.2945	0.4428	1.5040	1.8271
2.28	0.7428	0.2899	0.4370	1.5072	1.8562
2.3	0.7395	0.2855	0.4312	1.5104	1.8860
2.32	0.7364	0.2812	0.4256	1.5134	1.9165
2.34	0.7333	0.2769	0.4200	1.5165	1.9476
2.36	0.7302	0.2728	0.4145	1.5194	1.9794
2.38	0.7272	0.2688	0.4091	1.5223	2.0119
2.4	0.7242	0.2648	0.4038	1.5252	2.0451
2.42	0.7213	0.2609	0.3986	1.5279	2.0789
2.44	0.7184	0.2571	0.3935	1.5306	2.1136
2.46	0.7156	0.2534	0.3885	1.5333	2.1489
2.48	0.7128	0.2497	0.3836	1.5359	2.1850
2.5	0.7101	0.2462	0.3787	1.5385	2.2218
2.52	0.7074	0.2427	0.3739	1.5410	2.2594
2.54	0.7047	0.2392	0.3692	1.5434	2.2978
2.56	0.7021	0.2359	0.3646	1.5458	2.3370
2.58	0.6995	0.2326	0.3601	1.5482	2.3770
2.6	0.6970	0.2294	0.3556	1.5505	2.4177
2.62	0.6945	0.2262	0.3512	1.5527	2.4593
2.64	0.6921	0.2231	0.3469	1.5549	2.5018
2.66	0.6896	0.2201	0.3427	1.5571	2.5451
2.68	0.6873	0.2171	0.3385	1.5592	2.5892
2.7	0.6849	0.2142	0.3344	1.5613	2.6343
2.72	0.6826	0.2113	0.3304	1.5634	2.6802
2.74	0.6804	0.2085	0.3264	1.5654	2.7270
2.76	0.6781	0.2058	0.3225	1.5673	2.7748
2.78	0.6761	0.2030	0.3186	1.5693	2.8235
2.8	0.6738	0.2004	0.3149	1.5711	2.8731
2.82	0.6717	0.1978	0.3111	1.5730	2.9237
2.84	0.6696	0.1953	0.3075	1.5748	2.9752
2.86	0.6675	0.1927	0.3039	1.5766	3.0278
2.88	0.6655	0.1903	0.3004	1.5784	3.0813
2.9	0.6635	0.1879	0.2969	1.5801	3.1359
2.92	0.6615	0.1855	0.2934	1.5818	3.1914
2.94	0.6596	0.1832	0.2901	1.5834	3.2481
2.96	0.6577	0.1809	0.2868	1.5851	3.3058
2.98	0.6558	0.1787	0.2835	1.5867	3.3646
3.0	0.6540	0.1765	0.2803	1.5882	3.4245
3.02	0.6522	0.1743	0.2771	1.5898	3.4854
3.04	0.6504	0.1722	0.2740	1.5913	3.5476
3.06	0.6486	0.1701	0.2709	1.5928	3.6108
3.08	0.6469	0.1681	0.2679	1.5942	3.6752
3.1	0.6452	0.1660	0.2650	1.5957	3.7408
3.12	0.6435	0.1641	0.2620	1.5971	3.8076
3.14	0.6418	0.1621	0.2592	1.5985	3.8756
3.16	0.6402	0.1602	0.2563	1.5998	3.9449
3.18	0.6386	0.1583	0.2535	1.6012	4.0154
3.2	0.6370	0.1565	0.2508	1.6025	4.0871
3.22	0.6354	0.1547	0.2481	1.6038	4.1602
3.24	0.6339	0.1529	0.2454	1.6051	4.2345
3.26	0.6324	0.1511	0.2428	1.6063	4.3101
3.28	0.6309	0.1494	0.2402	1.6076	4.3871
3.3	0.6294	0.1477	0.2377	1.6088	4.4655
3.32	0.6280	0.1461	0.2352	1.6100	4.5452
3.34	0.6265	0.1444	0.2327	1.6111	4.6263
3.36	0.6251	0.1428	0.2303	1.6123	4.7089

Table B6.4 Rayleigh-flow: Frictionless Duct Flow with Heat Transfer for $k = 1.4$

Ma	T_0/T_0^*	p/p^*	T/T^*	$\rho^*/\rho = V/V^*$	p_0/p_0^*
3.38	0.6237	0.1412	0.2279	1.6134	4.7929
3.4	0.6224	0.1397	0.2255	1.6145	4.8783
3.42	0.6210	0.1381	0.2232	1.6156	4.9652
3.44	0.6197	0.1366	0.2209	1.6167	5.0536
3.46	0.6184	0.1351	0.2186	1.6178	5.1435
3.48	0.6171	0.1337	0.2164	1.6188	5.2350
3.5	0.6158	0.1322	0.2142	1.6198	5.3280
3.52	0.6145	0.1308	0.2120	1.6208	5.4226
3.54	0.6133	0.1294	0.2099	1.6218	5.5188
3.56	0.6121	0.1280	0.2078	1.6228	5.6167
3.58	0.6109	0.1267	0.2057	1.6238	5.7162
3.6	0.6097	0.1254	0.2037	1.6247	5.8173
3.62	0.6085	0.1241	0.2017	1.6257	5.9201
3.64	0.6074	0.1228	0.1997	1.6266	6.0247
3.66	0.6062	0.1215	0.1977	1.6275	6.1310
3.68	0.6051	0.1202	0.1958	1.6284	6.2390
3.7	0.6040	0.1190	0.1939	1.6293	6.3488
3.72	0.6029	0.1178	0.1920	1.6301	6.4605
3.74	0.6018	0.1166	0.1902	1.6310	6.5739
3.76	0.6008	0.1154	0.1884	1.6318	6.6893
3.78	0.5997	0.1143	0.1866	1.6327	6.8065
3.8	0.5987	0.1131	0.1848	1.6335	6.9256
3.82	0.5977	0.1120	0.1830	1.6343	7.0466
3.84	0.5967	0.1109	0.1813	1.6351	7.1696
3.86	0.5957	0.1098	0.1796	1.6359	7.2945
3.88	0.5947	0.1087	0.1779	1.6366	7.4215
3.9	0.5937	0.1077	0.1763	1.6374	7.5505
3.92	0.5928	0.1066	0.1746	1.6381	7.6816
3.94	0.5918	0.1056	0.1730	1.6389	7.8147
3.96	0.5909	0.1046	0.1714	1.6396	7.9499
3.98	0.5900	0.1036	0.1699	1.6403	8.0873
4.0	0.5891	0.1026	0.1683	1.6410	8.2269

Example 6.31:

A fuel-air mixture, approximated as air with $k = 1.4$, enters a duct combustion chamber at $V_1 = 75$ m/s, $p_1 = 150$ kPa, and $T_1 = 300$ K. The heat addition by combustion is 900 kJ/kg of mixture. Compute (*a*) the exit properties V_2, p_2, and T_2 and (*b*) the total heat addition which would have caused a sonic exit flow.

Solution

Part (a)

First compute $T_{01} = T_1 + V_1^2/(2c_p) = 300 + (75)^2/[2(1005)] = 303$ K. Then compute the change in stagnation temperature of the gas: $q = c_p(T_{02} - T_{01})$

or
$$T_{02} = T_{01} + \frac{q}{c_p} = 303 \text{ K} + \frac{900{,}000 \text{ J/kg}}{1005 \text{ J/(kg} \cdot \text{K)}} = 1199 \text{ K}$$

We have enough information to compute the initial Mach number:

$$a_1 = \sqrt{kRT_1} = [1.4(287)(300)]^{1/2} = 347 \text{ m/s} \qquad \text{Ma}_1 = \frac{V_1}{a_1} = \frac{75}{347} = 0.216$$

For this Mach number, use Eq. (6.143a) or Table B6.4 to find the sonic value T^*_0:

At $\text{Ma}_1 = 0.216$: $\dfrac{T_{01}}{T_0^*} \approx 0.1992$ or $T_0^* = \dfrac{303 \text{ K}}{0.1992} \approx 1521$ K

Then the stagnation temperature ratio at section 2 is $T_{02}/T_0^* = 1199/1521 = 0.788$, which corresponds in Table B6.4 to a Mach number $\text{Ma}_2 \approx 0.573$.

Now use Table B6.4 at Ma_1 and Ma_2 to tabulate the desired property ratios.

Section	Ma	V/V^*	p/p^*	T/T^*
1	0.216	0.1051	2.2528	0.2368
2	0.573	0.5398	1.6442	0.8876

The exit properties are computed by using these ratios to find state 2 from state 1:

$$V_2 = V_1 \frac{V_2/V^*}{V_1/V^*} = (75 \text{ m/s}) \frac{0.5398}{0.1051} = 385 \text{ m/s}$$

$$p_2 = p_1 \frac{p_2/p^*}{p_1/p^*} = (150 \text{ kPa}) \frac{1.6442}{2.2528} = 109 \text{ kPa} \qquad \textit{Ans. (a)}$$

$$T_2 = T_1 \frac{T_2/T^*}{T_1/T^*} = (300 \text{ K}) \frac{0.8876}{0.2368} = 1124 \text{ K} \qquad \textit{Ans. (a)}$$

Part (b)

The maximum allowable heat addition would drive the exit Mach number to unity:

$$T_{02} = T_0^* = 1521 \text{ K}$$

$$q_{\max} = c_p(T_0^* - T_{01}) = [1005 \text{ J/(kg} \cdot \text{K)}](1521 - 303 \text{ K}) \approx 1.22 \text{ E6 J/kg} \qquad \textit{Ans. (b)}$$

6.9.2 The Choking of Rayleigh-Flow Due to Simple Heating:

Equation (6.143a) and Table B6.4 indicate that the maximum possible stagnation temperature in simple heating corresponds to T_0^*, or the sonic exit Mach number. Thus, for given inlet conditions, only a certain maximum amount of heat can be added to the flow, for example, 1.22 MJ/kg in Example 6.31 . For a subsonic inlet there is no theoretical limit on heat addition: The flow chokes more and more as we add more heat, with the inlet velocity approaching zero. For supersonic flow, even if Ma_1 is infinite, there is a finite ratio $T_{01}/T_0^* = 0.4898$ for $k = 1.4$. Thus if heat is added without limit to a supersonic flow, a normal-shock-wave adjustment is required to accommodate the required property changes.

In subsonic flow there is no theoretical limit to the amount of cooling allowed: The exit flow just becomes slower and slower, and the temperature approaches zero. In supersonic flow only a finite amount of cooling can be allowed before the exit flow approaches infinite Mach number, with $T_{02}/T_0^* = 0.4898$ and the exit temperature equal to zero. There are very few practical applications for supersonic cooling.

Example 6.32:

What happens to the inlet flow in Example 6.31 if the heat addition is increased to 1400 kJ/kg and the inlet pressure and stagnation temperature are fixed? What will be the subsequent decrease in mass flow?

Solution

For $q = 1400$ kJ/kg, the exit will be choked at the stagnation temperature

$$T_0^* = T_{01} + \frac{q}{c_p} = 303 + \frac{1.4 \text{ E6 J/kg}}{1005 \text{ J/(kg} \cdot \text{K)}} \approx 1696 \text{ K}$$

This is higher than the value $T_0^* = 1521$ K in Example 6.31, so we know that condition 1 will have to choke down to a lower Mach number. The proper value is found from the ratio $T_{01}/T_0^* = 303/1696 = 0.1787$. From Table B6.4 or Eq. (6.143) for this condition, we read the new, lowered entrance Mach number: $\text{Ma}_{1,\text{new}} \approx 0.203$. With T_{01} and p_1 known, the other inlet properties follow from this Mach number:

$$T_1 = \frac{T_{01}}{1 + 0.2 \text{ Ma}_1^2} = \frac{303}{1 + 0.2(0.203)^2} = 301 \text{ K}$$

$$a_1 = \sqrt{kRT_1} = [1.4(287)(301)]^{1/2} = 348 \text{ m/s}$$

$$V_1 = \text{Ma}_1 \, a_1 = (0.202)(348 \text{ m/s}) = 70 \text{ m/s}$$

$$\rho_1 = \frac{p_1}{RT_1} = \frac{150{,}000}{(287)(301)} = 1.74 \text{ kg/m}^3$$

Finally, the new lowered mass flow per unit area is

$$\frac{\dot{m}_{\text{new}}}{A} = \rho_1 V_1 = (1.74 \text{ kg/m}^3)(70 \text{ m/s}) = 122 \text{ kg/(s} \cdot \text{m}^2)$$

This is 7 percent less than in Example 6.31, due to choking by excess heat addition.

6.9.3 Relation Between Normal Shock Wave and The Fanno and Rayleigh Flows:

As mentioned earlier, normal shock waves can occur in supersonic flows through converging-diverging and constant-area ducts. Past experience suggests that normal shock waves involve deceleration from a supersonic flow to a subsonic flow, a pressure rise, and an increase of entropy. We found also that normal shock waves may happen in supersonic constant area duct flow as discussed before. We showed that choking of any supersonic flow must lead to occuring of a normal shock wave (for the Fanno-flow, Isothermal-flow, and the Rayleigh-flow). In this section we shall deive in details the normal shock wave equations given before in Sec.6.5.

To develop the equations that verify this observed behavior of flows across a normal shock, we apply first principles to the flow through a control volume that completely surrounds a normal shock wave (see Fig. 6.33). We consider the normal shock and thus the control volume to be infinitesimally thin and stationary.

For steady flow through the control volume of Fig. 6.33 , the conservation of mass principle yields $\rho V = \text{constant}$ (6.144)

because the flow cross-sectional area remains essentially constant within the infinitesimal

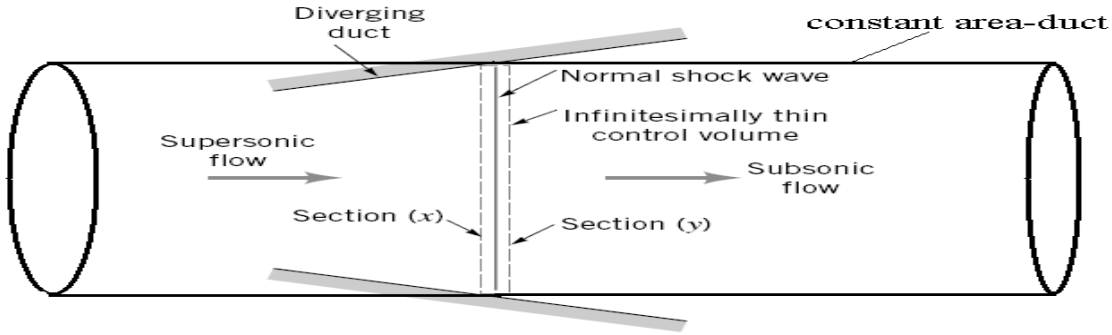

■ FIGURE **6.33** Normal shock control volume.

thickness of the normal shock. Note that Eq. 6.144 is identical to the continuity equation used for Fanno and Rayleigh flows considered earlier.

The friction force acting on the contents of the infinitesimally thin control volume surrounding the normal shock is considered to be negligibly small. Also for ideal gas flow, the effect of gravity is neglected. Thus, the linear momentum equation (Part (2)) describing steady gas flow through the control volume of Fig. 6.33 is $p + \rho V^2 = \text{constant}$

or for an ideal gas for which $p = \rho RT$, $$p + \frac{(\rho V)^2 RT}{p} = \text{constant} \qquad (6.145)$$

Equation 6.145 is the same as the linear momentum equation for Rayleigh flow, which was derived earlier (Eq. 6.120).

For the control volume containing the normal shock, no shaft work is involved and the heat transfer is assumed negligible. Thus, the energy equation (Part (2)) can be applied to steady gas flow through the control volume of Fig. 6.33 to obtain

$$\check{h} + \frac{V^2}{2} = \check{h}_0 = \text{constant}$$

or, for an ideal gas, since $\check{h} - \check{h}_0 = c_p(T - T_0)$ and $p = \rho RT$

$$T + \frac{(\rho V)^2 T^2}{2c_p(p^2/R^2)} = T_0 = \text{constant} \qquad (6.146)$$

Equation 6.146 is identical to the energy equation for Fanno flow analyzed earlier (Eq.6.84).

The $T\,ds$ relationship previously used for ideal gas flow (Eq. 6.16) is valid for the flow through the normal shock (Fig. 6.33) because it (Eq. 6.16) is an ideal gas property relationship.

From the analyses in the previous paragraphs, it is apparent that the steady flow of an ideal gas across a normal shock is governed by some of the same equations used for describing Fanno and Rayleigh flows (energy equation for Fanno flows and momentum equation for Rayleigh flow). Thus, for a given density-velocity product (ρV), gas (R,k), and conditions at the inlet of the normal shock (T_x, p_x, and s_x), the conditions downstream of the shock (state y) will be on both a Fanno line and a Rayleigh line that pass through the inlet state (state x), as is illustrated in Fig. 6.34 . To conform with common practice we designate

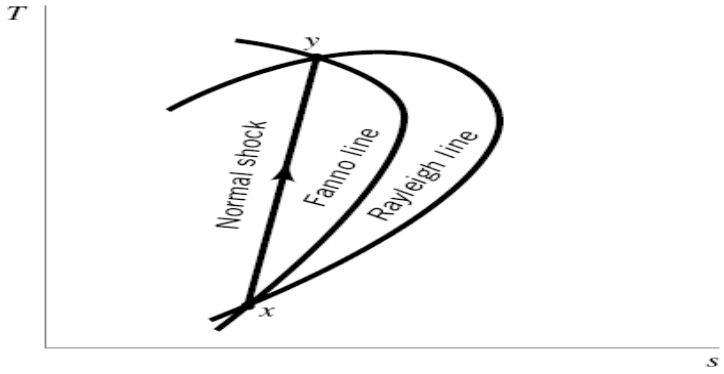

■ **FIGURE 6.34** The relationship between a normal shock and Fanno and Rayleigh lines.

the states upstream and downstream of the normal shock with x and y instead of numerals 1 and 2. The Fanno and Rayleigh lines describe more of the flow field than just in the vicinity of the normal shock when Fanno and Rayleigh flows are actually involved (solid lines in Figs. 6.35a and 6.35b). Otherwise, these lines (dashed lines in Figs. 6.35a, 6.35b, and 6.35c) are useful mainly as a way to better visualize how the governing equations combine to yield a solution to the normal shock flow problem.

The second law of thermodynamics requires that entropy must increase across a normal shock wave. This law and sketches of the Fanno line and Rayleigh line intersections, like those of Figs. 6.34 and 6.35, persuade us to conclude that flow across a normal shock can only proceed from supersonic to subsonic flow. Similarly, in open-channel flows the flow across a hydraulic jump proceeds from supercritical to subcritical conditions.

Since the states upstream and downstream of a normal shock wave are represented by the supersonic and subsonic intersections of actual and/or imagined Fanno and Rayleigh lines, we should be able to use equations developed earlier for Fanno and Rayleigh flows to quantify normal shock flow. For example, for the Rayleigh line of Fig. 6.35b

$$\frac{p_y}{p_x} = \left(\frac{p_y}{p_a}\right)\left(\frac{p_a}{p_x}\right) \qquad (6.147)$$

But from Eq. 6.132 for Rayleigh flow we get

$$\frac{p_y}{p_a} = \frac{1 + k}{1 + k\mathrm{Ma}_y^2} \qquad (6.148)$$

and

$$\frac{p_x}{p_a} = \frac{1 + k}{1 + k\mathrm{Ma}_x^2} \qquad (6.149)$$

Thus, by combining Eqs. 6.147, 6.148, and 6.149 we get

$$\boxed{\frac{p_y}{p_x} = \frac{1 + k\mathrm{Ma}_x^2}{1 + k\mathrm{Ma}_y^2}} \qquad (6.150)$$

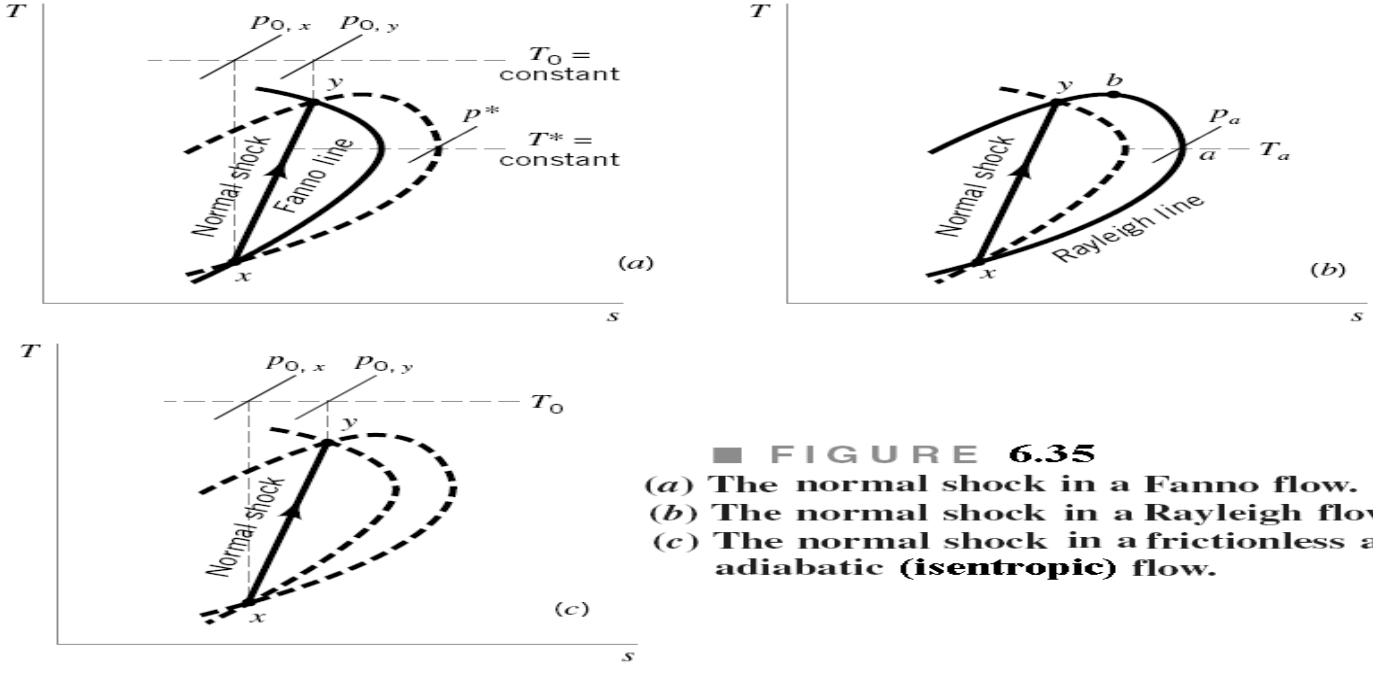

■ **FIGURE 6.35**
(a) The normal shock in a Fanno flow.
(b) The normal shock in a Rayleigh flow.
(c) The normal shock in a frictionless and adiabatic (isentropic) flow.

Equation 6.150 can also be derived starting with

$$\frac{p_y}{p_x} = \left(\frac{p_y}{p^*}\right)\left(\frac{p^*}{p_x}\right)$$

and using the Fanno flow equation (Eq. 6.116)

$$\frac{p}{p^*} = \frac{1}{\text{Ma}}\left\{\frac{(k+1)/2}{1+[(k-1)/2]\text{Ma}^2}\right\}^{1/2}$$

As might be expected, Eq. 6.150 can be obtained directly from the linear momentum equation

$$p_x + \rho_x V_x^2 = p_y + \rho_y V_y^2$$

since $\rho V^2/p = V^2/RT = kV^2/RTk = k\,\text{Ma}^2$.

For the Fanno flow of Fig. 6.35a,

$$\frac{T_y}{T_x} = \left(\frac{T_y}{T^*}\right)\left(\frac{T^*}{T_x}\right) \qquad (6.151)$$

From Eq. 6.110 for Fanno flow we get

$$\frac{T_y}{T^*} = \frac{(k+1)/2}{1+[(k-1)/2]\text{Ma}_y^2} \qquad (6.152)$$

and

$$\frac{T_x}{T^*} = \frac{(k+1)/2}{1+[(k-1)/2]\text{Ma}_x^2} \qquad (6.153)$$

A consolidation of Eqs. 6.151 , 6.152 , and 6.153 gives

$$\boxed{\frac{T_y}{T_x} = \frac{1+[(k-1)/2]\text{Ma}_x^2}{1+[(k-1)/2]\text{Ma}_y^2}} \qquad (6.154)$$

We seek next to develop an equation that will allow us to determine the Mach number downstream of the normal shock, Ma_y, when the Mach number upstream of the normal shock, Ma_x, is known. From the ideal gas equation of state, we can form

$$\frac{p_y}{p_x} = \left(\frac{T_y}{T_x}\right)\left(\frac{\rho_y}{\rho_x}\right) \qquad (6.155)$$

Using the continuity equation $\rho_x V_x = \rho_y V_y$

with Eq. 6.155 we obtain

$$\frac{p_y}{p_x} = \left(\frac{T_y}{T_x}\right)\left(\frac{V_x}{V_y}\right) \qquad (6.156)$$

When combined with the Mach number definition (Eq. E.7) and the ideal gas speed-of-sound equation (Eq. 6.29), Eq. 6.156 becomes

$$\frac{p_y}{p_x} = \left(\frac{T_y}{T_x}\right)^{1/2}\left(\frac{\text{Ma}_x}{\text{Ma}_y}\right) \qquad (6.157)$$

Thus, Eqs. 6.157 and 6.154 lead to

$$\frac{p_y}{p_x} = \left\{\frac{1+[(k-1)/2]\text{Ma}_x^2}{1+[(k-1)/2]\text{Ma}_y^2}\right\}^{1/2}\frac{\text{Ma}_x}{\text{Ma}_y} \qquad (6.158)$$

which can be merged with Eq. 6.150 to yield

$$\boxed{\text{Ma}_y^2 = \frac{\text{Ma}_x^2 + [2/(k-1)]}{[2k/(k-1)]\text{Ma}_x^2 - 1}} \qquad (6.159)$$

Thus, we can use Eq. 6.159 to calculate values of Mach number downstream of a normal shock from a known Mach number upstream of the shock. As suggested by Fig. 6.35 , to have a normal shock we must have $\text{Ma}_x > 1$. From Eq. 6.159 we find that $\text{Ma}_y < 1$.

If we combine Eqs. 6.159 and 6.150 , we get

$$\boxed{\frac{p_y}{p_x} = \frac{2k}{k+1}\text{Ma}_x^2 - \frac{k-1}{k+1}} \qquad (6.160)$$

which allows us to calculate the pressure ratio across a normal shock from a known upstream Mach number. Similarly, taking Eqs. 6.159 and 6.154 together we obtain

$$\boxed{\frac{T_y}{T_x} = \frac{\{1+[(k-1)/2]\text{Ma}_x^2\}\{[2k/(k-1)]\text{Ma}_x^2 - 1\}}{\{(k+1)^2/[2(k-1)]\}\text{Ma}_x^2}} \qquad (6.161)$$

From the continuity equation (Eq. E.1), we have for flow across a normal shock

$$\frac{\rho_y}{\rho_x} = \frac{V_x}{V_y} \qquad (6.162)$$

and from the ideal gas equation of state

$$\frac{\rho_y}{\rho_x} = \left(\frac{p_y}{p_x}\right)\left(\frac{T_x}{T_y}\right) \qquad (6.163)$$

Thus, by combining Eqs. 6.162 , 6.163 , 6.160 , and 6.161, we get

$$\boxed{\frac{\rho_y}{\rho_x} = \frac{V_x}{V_y} = \frac{(k+1)\text{Ma}_x^2}{(k-1)\text{Ma}_x^2 + 2}} \qquad (6.164)$$

TABLE 6.3
Summary of Normal Shock Wave Characteristics

Variable	Change Across Normal Shock Wave
Mach number	Decrease
Static pressure	Increase
Stagnation pressure	Decrease
Static temperature	Increase
Stagnation temperature	Constant
Density	Increase
Velocity	Decrease

The stagnation pressure ratio across the shock can be determined by combining

$$\frac{p_{0,y}}{p_{0,x}} = \left(\frac{p_{0,y}}{p_y}\right)\left(\frac{p_y}{p_x}\right)\left(\frac{p_x}{p_{0,x}}\right) \qquad (6.165)$$

with Eqs. E.20 , E.10 , and 6.160 to get

$$\frac{p_{0,y}}{p_{0,x}} = \frac{\left(\frac{k+1}{2}\mathrm{Ma}_x^2\right)^{k/(k-1)}\left(1+\frac{k-1}{2}\mathrm{Ma}_x^2\right)^{k/(1-k)}}{\left(\frac{2k}{k+1}\mathrm{Ma}_x^2-\frac{k-1}{k+1}\right)^{1/(k-1)}} \qquad (6.166)$$

Fig. D.4 in Appendix D graphs values of downstream Mach numbers, Ma_y, pressure ratio, p_y/p_x, temperature ratio, T_y/T_x, density ratio, ρ_y/ρ_x or velocity ratio, V_x/V_y, and stagnation pressure ratio, $p_{0,y}/p_{0,x}$, as a function of upstream Mach number, Ma_x, for the steady flow across a normal shock wave of an ideal gas having a specific heat ratio $k = 1.4$. These values were calculated from Eqs. 6.159 , 6.160 , 6.161 , 6.164 , and 6.166.

Important trends associated with the steady flow of an ideal gas across a normal shock wave can be determined by studying Fig. D.4. These trends are summarized in Table 6.3 .

Examples 6.33 and 6.34 illustrate how Fig. D.4 can be used to solve fluid flow problems involving normal shock waves.

Example 6.33:

Designers involved with fluid mechanics work hard at minimizing loss of available energy in their designs. Adiabatic, frictionless flows involve no loss in available energy. Entropy remains constant for these idealized flows. Adiabatic flows with friction involve available energy loss and entropy increase. Generally, larger entropy increases imply larger losses. For normal shocks, show that the stagnation pressure drop (and thus loss) is larger for higher Mach numbers.

Solution:

We assume that air ($k = 1.4$) behaves as a typical gas and use Fig. D.4 to respond to the above-stated requirements. Since

$$1 - \frac{p_{0,y}}{p_{0,x}} = \frac{p_{0,x} - p_{0,y}}{p_{0,x}}$$

we can construct the following table with values of $p_{0,y}/p_{0,x}$ from Fig. D.4.

When the Mach number of the flow entering the shock is low, say $\mathrm{Ma}_x = 1.2$, the flow across the shock is nearly isentropic and the loss in stagnation pressure is small. However, at larger Mach numbers, the entropy change across the normal shock rises dramatically and the stagnation pressure drop across the shock is appreciable. If a shock occurs at $\mathrm{Ma}_x = 2.5$, only about 50% of the upstream stagnation pressure is recovered.

In devices where supersonic flows occur, for example, high-performance aircraft engine inlet ducts and high-speed wind tunnels, designers attempt to prevent shock formation, or if shocks must occur, they design the flow path so that shocks are positioned where they are weak (small Mach number).

Ma_x	$p_{0,y}/p_{0,x}$	$\frac{p_{0,x}-p_{0,y}}{p_{0,x}}$
1.0	1.0	0
1.2	0.99	0.01
1.5	0.93	0.07
2.0	0.72	0.28
2.5	0.50	0.50
3.0	0.33	0.67
3.5	0.21	0.79
4.0	0.14	0.86
5.0	0.06	0.94

Ma_x	p_y/p_x
1.0	1.0
1.2	1.5
1.5	2.5
2.0	4.5
3.0	10
4.0	18
5.0	29

Of interest also is the static pressure rise that occurs across a normal shock. These static pressure ratios, p_y/p_x, obtained from Fig. D.4 are shown in the table above for a few Mach numbers. For a developing boundary layer, any pressure rise in the flow direction is considered as an adverse pressure gradient that can possibly cause flow separation. Thus, shock–boundary layer interactions are of great concern to designers of high-speed flow devices.

Example 6.34:

A total pressure probe is inserted into a supersonic air flow. A shock wave forms just upstream of the impact hole and head as illustrated in Fig. E6.34 . The probe measures a total pressure of 60 psia. The stagnation temperature at the probe head is 1000 °R. The static pressure upstream of the shock is measured with a wall tap to be 12 psia. From these data determine the Mach number and velocity of the flow.

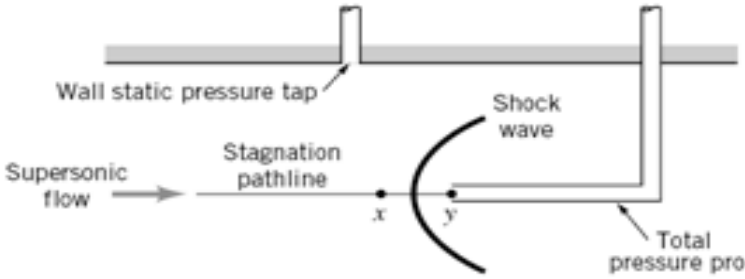

■ FIGURE E6.34

Solution:

We assume that the flow along the stagnation pathline is isentropic except across the shock. Also, the shock is treated as a normal shock. Thus, in terms of the data we have

$$\frac{p_{0,y}}{p_x} = \left(\frac{p_{0,y}}{p_{0,x}}\right)\left(\frac{p_{0,x}}{p_x}\right) \tag{1}$$

where $p_{0,y}$ is the stagnation pressure measured by the probe, and p_x is the static pressure measured by the wall tap. The stagnation pressure upstream of the shock, $p_{0,x}$, is not measured. Combining Eqs. 1, 6.166 , and E.20 we obtain

$$\frac{p_{0,y}}{p_x} = \frac{\{[(k+1)/2]\mathrm{Ma}_x^2\}^{k/(k-1)}}{\{[2k/(k+1)]\mathrm{Ma}_x^2 - [(k-1)/(k+1)]\}^{1/(k-1)}} \tag{2}$$

which is called the *Rayleigh Pitot-tube formula*. Values of $p_{0,y}/p_x$ from Eq. 2 are considered important enough to be included in Fig. D.4 for $k = 1.4$. Thus, for $k = 1.4$ and

$$\frac{p_{0,y}}{p_x} = \frac{60 \text{ psia}}{12 \text{ psia}} = 5$$

we use Fig. D.4 to ascertain that $\mathrm{Ma}_x = 1.9$ (Ans)

To determine the flow velocity we need to know the static temperature upstream of the shock, since Eqs. 6.29 and E.7 can be used to yield

$$V_x = Ma_x c_x = \mathrm{Ma}_x \sqrt{\mathrm{RT}_x k} \tag{3}$$

The stagnation temperature downstream of the shock was measured and found to be

$$T_{0,y} = 1000\ ^\circ\mathrm{R}$$

Since the stagnation temperature remains constant across a normal shock (see Eq. 6.146),

$$T_{0,x} = T_{0,y} = 1000\ ^\circ\mathrm{R}$$

For the isentropic flow upstream of the shock, Eq. E.17 or Fig. D.1 can be used. For $\mathrm{Ma}_x = 1.9$,

$$\frac{T_x}{T_{0,x}} = 0.59$$

or

$$T_x = (0.59)(1000\ ^\circ\mathrm{R}) = 590\ ^\circ\mathrm{R}$$

With Eq. 3 we obtain

$$V_x = 1.87\sqrt{[1716(\mathrm{ft}\cdot\mathrm{lb})/(\mathrm{slug}\cdot{}^\circ\mathrm{R})](590\ ^\circ\mathrm{R})(1.4)[1(\mathrm{slug}\cdot\mathrm{ft})/(\mathrm{lb}\cdot\mathrm{s}^2)]} = 2200 \text{ ft/s} \quad \textbf{(Ans)}$$

Application of the incompressible flow Pitot tube results would give highly inaccurate results because of the large pressure and density changes involved.

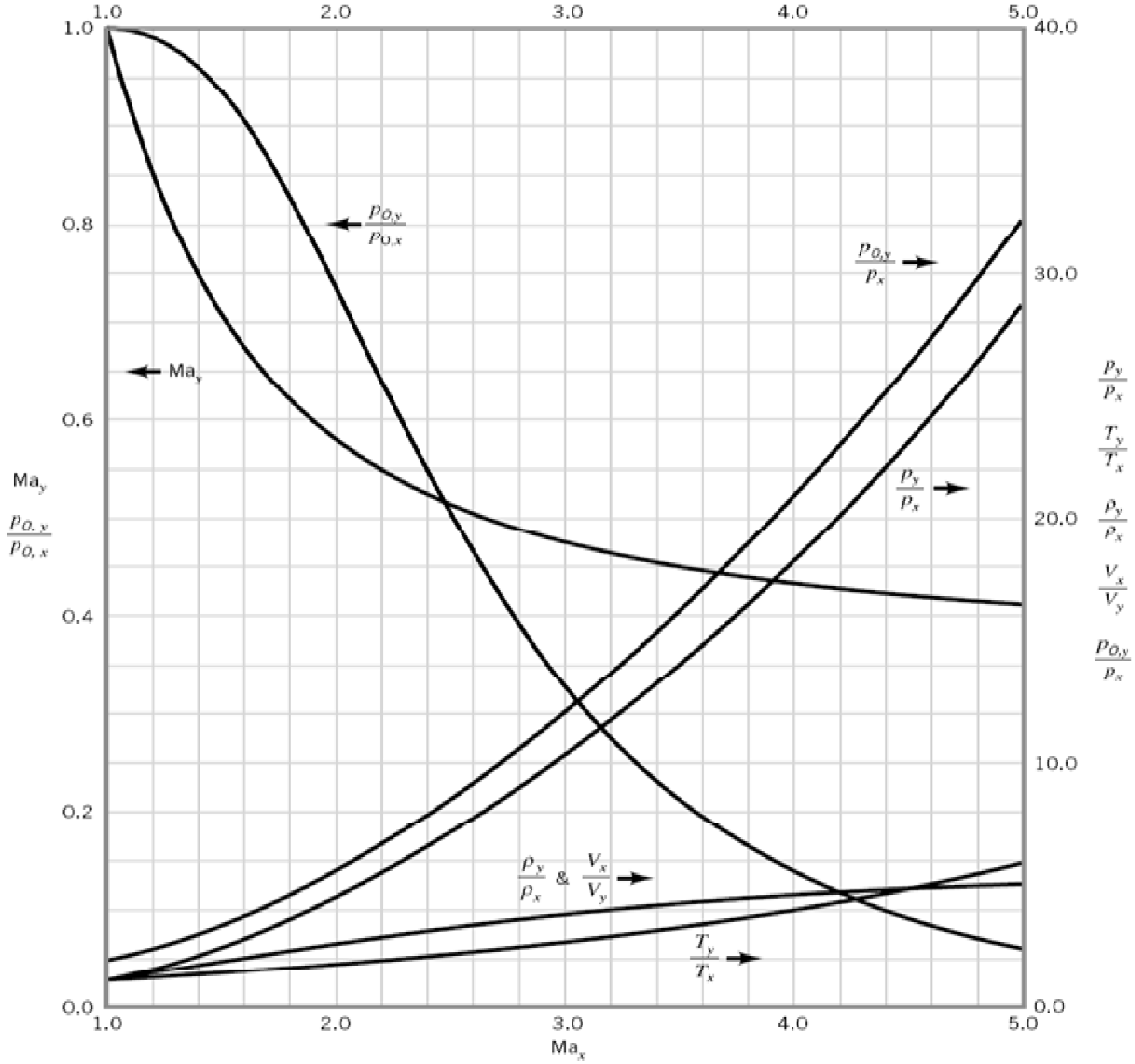

■ FIGURE D.4 **Normal shock flow of an ideal gas with $k = 1.4$. (Graph provided by Professor Bruce A. Reichert of Kansas State University.)**

Example 6.35:

Determine, for the converging-diverging duct of Example 6.14 , the ratio of back pressure to inlet stagnation pressure, $p_{\mathrm{III}}/p_{0,x}$ (see Fig. 6.15), that will result in a standing normal shock at the exit ($x = +0.5$ m) of the duct. What value of the ratio of back pressure to inlet stagnation pressure would be required to position the shock at $x = +0.3$ m? Show related temperature-entropy diagrams for these flows.

Solution:

For supersonic, isentropic flow through the nozzle to just upstream of the standing normal shock at the duct exit, we have from the table of Example 6.14 at $x = +0.5$ m

$$\mathrm{Ma}_x = 2.8$$

and

$$\frac{p_x}{p_{0,x}} = 0.04$$

From Fig. D.4 for $\mathrm{Ma}_x = 2.8$ we obtain $\dfrac{p_y}{p_x} = 9.0$

Thus,

$$\frac{p_y}{p_{0,x}} = \left(\frac{p_y}{p_x}\right)\left(\frac{p_x}{p_{0,x}}\right) = (9.0)(0.04) = 0.36 = \frac{p_{\mathrm{III}}}{p_{0,x}} \qquad \text{(Ans)}$$

When the ratio of duct back pressure to inlet stagnation pressure, $p_{III}/p_{0,x}$, is set equal to 0.36, the air will accelerate through the converging-diverging duct to a Mach number of 2.8 at the duct exit. The air will subsequently decelerate to a subsonic flow across a normal shock at the duct exit. The stagnation pressure ratio across the normal shock, $p_{0,y}/p_{0,x}$, is 0.38 (Fig. D.4 for $M_x = 2.8$). A considerable amount of available energy is lost across the shock.

For a normal shock at $x = +0.3$ m, we note from the table of Example 6.14 that $\text{Ma}_x = 2.14$ and

$$\frac{p_x}{p_{0,x}} = 0.10 \tag{1}$$

From Fig. D.4 for $\text{Ma}_x = 2.14$ we obtain $p_y/p_x = 5.2$, $\text{Ma}_y = 0.56$ and

$$\frac{p_{0,y}}{p_{0,x}} = 0.66 \tag{2}$$

From Fig. D.1 for $\text{Ma}_y = 0.56$ we get

$$\frac{A_y}{A^*} = 1.24 \tag{3}$$

For $x = +0.3$ m, the ratio of duct exit area to local area (A_2/A_y) is, using the area equation from Example 6.14,

$$\frac{A_2}{A_y} = \frac{0.1 + (0.5)^2}{0.1 + (0.3)^2} = 1.842 \tag{4}$$

Using Eqs. 3 and 4 we get

$$\frac{A_2}{A^*} = \left(\frac{A_y}{A^*}\right)\left(\frac{A_2}{A_y}\right) = (1.24)(1.842) = 2.28$$

Note that for the isentropic flow upstream of the shock, $A^* = 0.10$ m^2 (the actual throat area), while for the isentropic flow downstream of the shock, $A^* = A_2/2.28 = 0.35$ m$^2/2.28 = 0.15$ m^2. With $A_2/A^* = 2.28$ we use Fig. D.1 and find $\text{Ma}_2 = 0.26$ and

$$\frac{p_2}{p_{0,y}} = 0.95 \tag{5}$$

Combining Eqs. 2 and 5 we obtain

$$\frac{p_2}{p_{0,x}} = \left(\frac{p_2}{p_{0,y}}\right)\left(\frac{p_{0,y}}{p_{0,x}}\right) = (0.95)(0.66) = 0.63 \quad \textbf{(Ans)}$$

When the back pressure, p_2, is set equal to 0.63 times the inlet stagnation pressure, $p_{0,x}$, the normal shock will be positioned at $x = +0.3$ m. Note that $p_2/p_{0,x} = 0.63$ is less than the value of this ratio for subsonic isentropic flow through the converging-diverging duct, $p_2/p_0 = 0.98$ (from Example 6.14) and is larger than $p_{III}/p_{0,x} = 0.36$, for duct flow with a normal shock at the exit (see Fig. 6.15). Also the stagnation pressure ratio with the shock at $x = +0.3$ m, $p_{0,y}/p_{0,x} = 0.66$, is much greater than the stagnation pressure ratio, 0.38, when the shock occurs at the exit ($x = +0.5$ m) of the duct. The corresponding $T - s$ diagrams are shown in Figs. E6.35a and E6.35b.

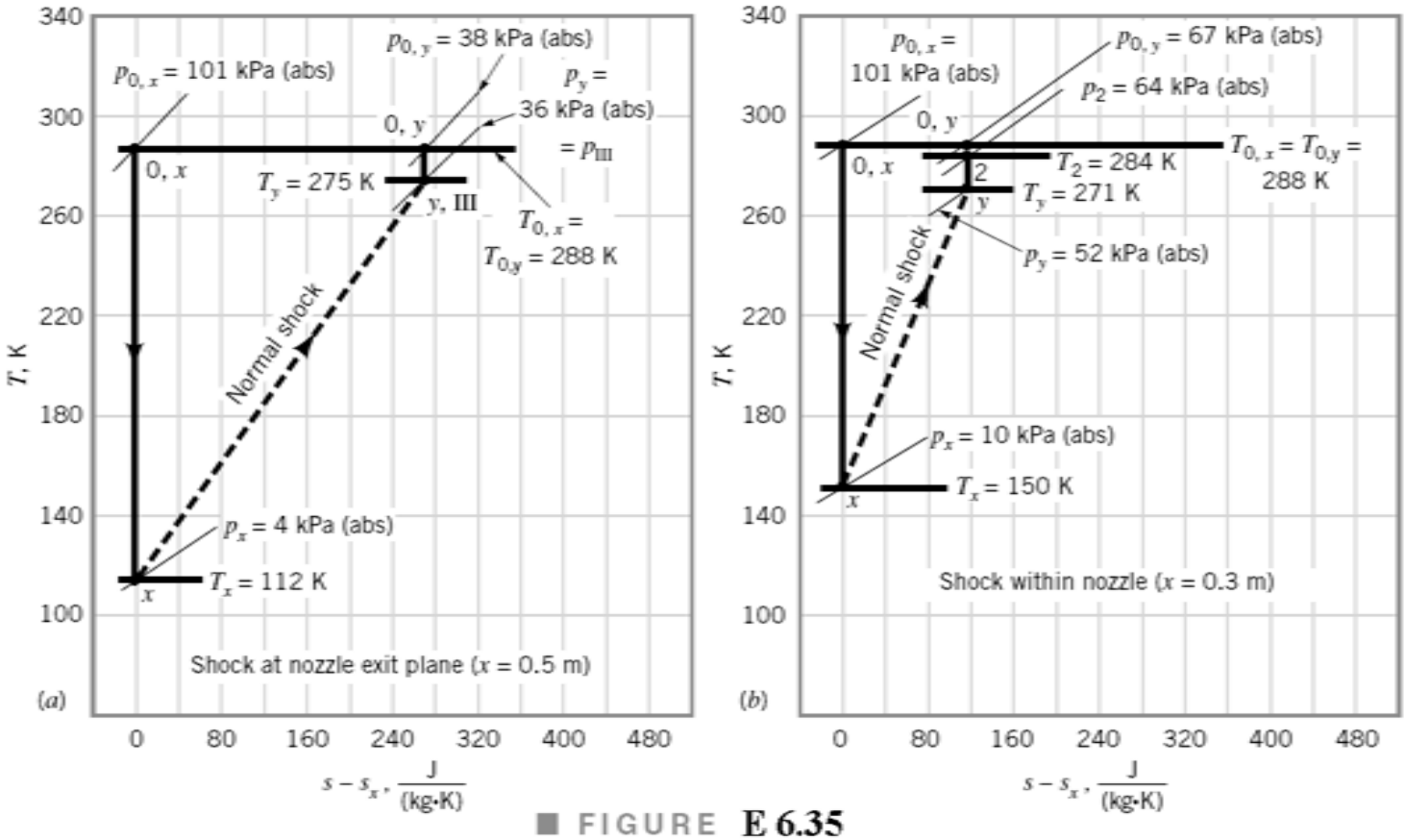

■ FIGURE E 6.35

6.9.4 Analogy Between Compressible and Open-Channel Flows

During a first course in fluid mechanics, students rarely study both open-channel flows and compressible flows. This is unfortunate because these two kinds of flows are strikingly similar in several ways. Furthermore, the analogy between open-channel and compressible flows is useful because important two-dimensional compressible flow phenomena can be simply and inexpensively demonstrated with a shallow, open-channel flow field in a *ripple tank* or *water table*.

The propagation of weak pressure pulses (sound waves) in a compressible flow can be considered to be comparable to the movement of small amplitude waves on the surface of an open-channel flow. In each case—two-dimensional compressible flow and open-channel flow—the influence of flow velocity on wave pattern is similar. When the flow velocity is less than the wave speed, wave fronts can move upstream of the wave source and the flow is subsonic (compressible flow) or subcritical (open-channel flow). When the flow velocity is equal to the wave speed, wave fronts cannot move upstream of the wave source and the flow is sonic (compressible flow) or critical (open-channel flow). When the flow velocity is greater than the wave speed, the flow is supersonic (compressible flow) or supercritical (open-channel flow). Normal shocks can occur in supersonic compressible flows. Hydraulic jumps can occur in supercritical open-channel flows. Comparison of the characteristics of normal shocks and hydraulic jumps suggests a strong resemblance and thus analogy between the two phenomena.

For compressible flows a meaningful dimensionless variable is the Mach number, where

$$\mathrm{Ma} = \frac{V}{c} \qquad (\text{E.7})$$

In open-channel flows, an important dimensionless variable is the Froude number, where

$$\mathrm{Fr} = \frac{V_{oc}}{\sqrt{gy}} \qquad (6.167)$$

The velocity of the channel flow is V_{oc}, the acceleration of gravity is g, and the depth of the flow is y. Since the speed of a small amplitude wave on the surface of an open-channel flow, c_{oc}, is

$$c_{oc} = \sqrt{gy} \qquad (6.168)$$

we conclude that

$$\mathrm{Fr} = \frac{V_{oc}}{c_{oc}} \qquad (6.169)$$

From Eqs. E.7 and 6.169 we see the similarity between Mach number (compressible flow) and Froude number (open-channel flow).

For compressible flow, the continuity equation is

$$\rho A V = \text{constant} \qquad (6.170)$$

where V is the flow velocity, ρ is the fluid density, and A is the flow cross-section area. For an open-channel flow, conservation of mass leads to

$$ybV_{oc} = \text{constant} \qquad (6.171)$$

where V_{oc} is the flow velocity, and y and b are the depth and width of the open-channel flow. Comparing Eqs. 6.170 and 6.171 we note that if flow velocities are considered similar and flow area, A, and channel width, b, are considered similar, then compressible flow density, ρ, is analogous to open-channel flow depth, y.

It should be pointed out that the similarity between Mach number and Froude number is generally not exact. If compressible flow and open-channel flow velocities are considered to be similar, then it follows that for Mach number and Froude number similarity the wave speeds c and c_{oc} must also be similar.

From the development of the equation for the speed of sound in an ideal gas (see Eqs. 6.27 and 6.28) we have for the compressible flow

$$c = \sqrt{(\text{constant})\, k\rho^{k-1}} \qquad (6.172)$$

From Eqs. 6.172 and 6.168 , we see that if y is to be similar to ρ as suggested by comparing Eq. 6.170 and 6.171 , then k should be equal to 2. Typically $k = 1.4$ or 1.67, not 2. This limitation to exactness is, however, usually not serious enough to compromise the benefits of the analogy between compressible and open-channel flows.

6.10 Two-Dimensional Supersonic Flow:

Up to this point we have considered only one-dimensional compressible-flow theories. This illustrated many important effects, but a one-dimensional world completely loses sight of the wave motions which are so characteristic of supersonic flow. The only "wave motion" we could muster in a one-dimensional theory was the normal-shock wave, which amounted only to a flow discontinuity in the duct.

6.10.1 The Mach Waves:

When we add a second dimension to the flow, wave motions immediately become apparent if the flow is supersonic. Figure 6.36 shows a celebrated graphical construction which appears in every fluid-mechanics textbook and was first presented by Ernst Mach in 1887. The figure shows the pattern of pressure disturbances (sound waves) sent out by a small particle moving at speed U through a still fluid whose sound velocity is a.

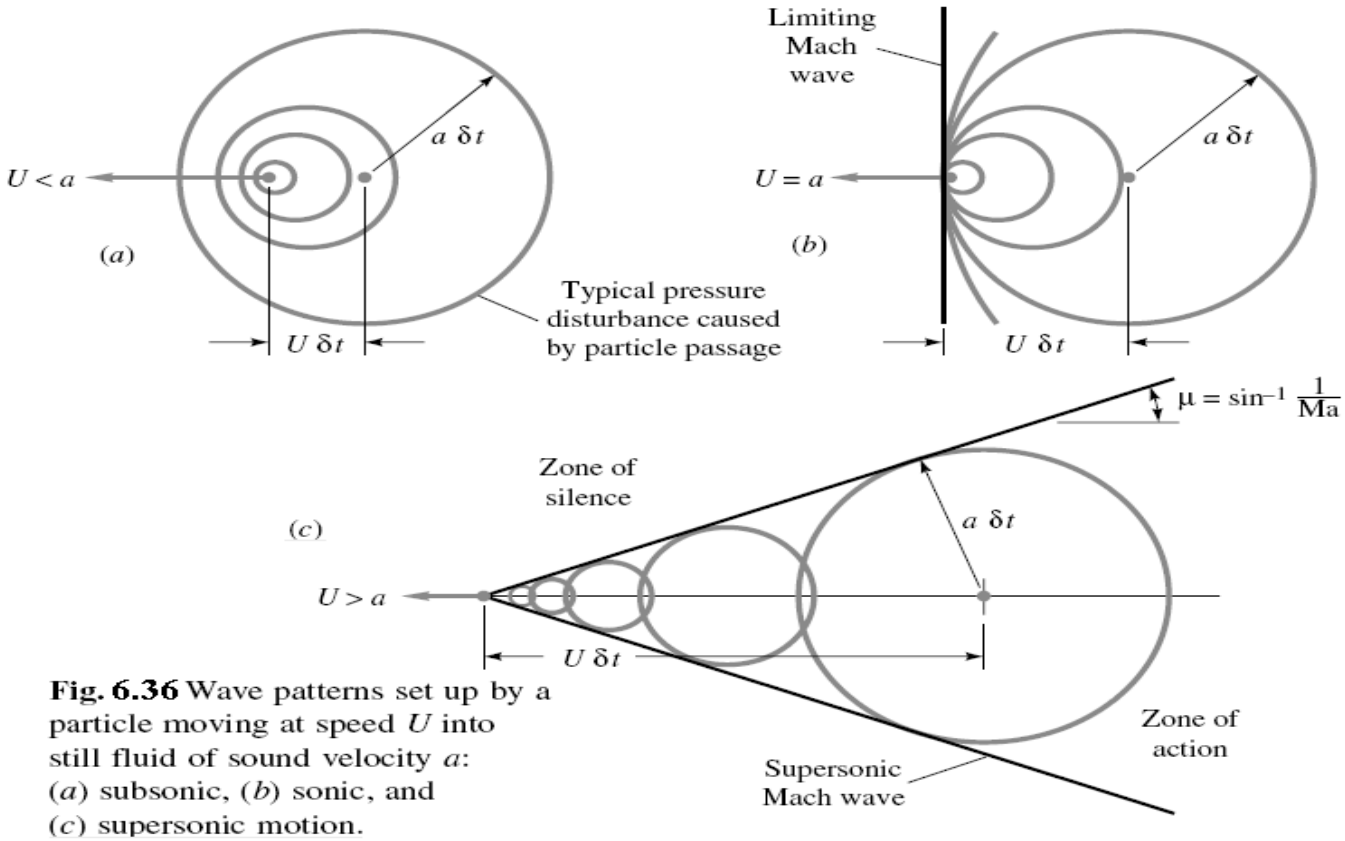

Fig. 6.36 Wave patterns set up by a particle moving at speed U into still fluid of sound velocity a: (a) subsonic, (b) sonic, and (c) supersonic motion.

As the particle moves, it continually crashes against fluid particles and sends out spherical sound waves emanating from every point along its path. A few of these spherical disturbance fronts are shown in Fig. 6.36 . The behavior of these fronts is quite different according to whether the particle speed is subsonic or supersonic.

In Fig. 6.36a , the particle moves subsonically, $U < a$, $\text{Ma} = U/a < 1$. The spherical disturbances move out in all directions and do not catch up with one another. They move well out in front of the particle also, because they travel a distance $a\ \delta t$ during the time interval δt in which the particle has moved only $U\ \delta t$. Therefore a subsonic body motion makes its presence felt everywhere in the flow field: You can "hear" or "feel" the pressure rise of an oncoming body before it reaches you. This is apparently why that pigeon in the road, without turning around to look at you, takes to the air and avoids being hit by your car.

At sonic speed, $U = a$, Fig. 6.36b , the pressure disturbances move at exactly the speed of the particle and thus pile up on the left at the position of the particle into a sort of "front locus," which is now called a *Mach wave*, after Ernst Mach. No disturbance reaches beyond the particle. If you are stationed to the left of the particle, you cannot "hear" the oncoming motion. If the particle blew its horn, you couldn't hear that either: A sonic car can sneak up on a pigeon.

In supersonic motion, $U > a$, the lack of advance warning is even more pronounced. The disturbance spheres cannot catch up with the fast-moving particle which created them. They all trail behind the particle and are tangent to a conical locus called the *Mach cone*. From the geometry of Fig. 6.36c the angle of the Mach cone is seen to be

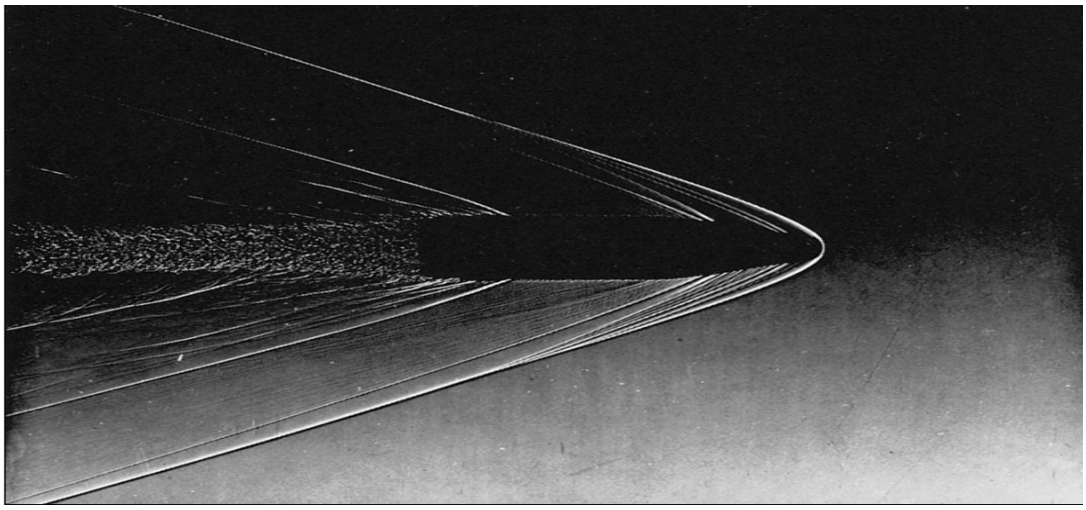

Fig. 6.37 Supersonic wave pattern emanating from a projectile moving at Ma ≈ 2.0. The heavy lines are oblique-shock waves and the light lines Mach waves (*Courtesy of U.S. Army Ballistic Research Laboratory, Aberdeen Proving Ground.*)

$$\mu = \sin^{-1}\frac{a}{U}\frac{\delta t}{\delta t} = \sin^{-1}\frac{a}{U} = \sin^{-1}\frac{1}{\text{Ma}} \tag{6.1173}$$

The higher the particle Mach number, the more slender the Mach cone; for example, μ is 30° at Ma = 2.0 and 11.5° at Ma = 5.0. For the limiting case of sonic flow, Ma = 1, μ = 90°; the Mach cone becomes a plane front moving with the particle, in agreement with Fig. 6.36b .

You cannot "hear" the disturbance caused by the supersonic particle in Fig. 6.36c until you are in the *zone of action* inside the Mach cone. No warning can reach your ears if you are in the *zone of silence* outside the cone. Thus an observer on the ground beneath a supersonic airplane does not hear the *sonic boom* of the passing cone until the plane is well past.

The Mach wave need not be a cone: Similar waves are formed by a small disturbance of any shape moving supersonically with respect to the ambient fluid. For example, the "particle" in Fig. 6.36c could be the leading edge of a sharp flat plate, which would form a Mach wedge of exactly the same angle μ. Mach waves are formed by small roughnesses or boundary-layer irregularities in a supersonic wind tunnel or at the surface of a supersonic body. Look again at Fig. 6.18c: Mach waves are clearly visible along the body surface downstream of the recompression shock, especially at the rear corner. Their angle is about 30°, indicating a Mach number of about 2.0 along this surface. A more complicated system of Mach waves emanates from the supersonic projectile in Fig. 6.37 . The Mach angles change, indicating a variable supersonic Mach number along the body surface. There are also several stronger oblique-shock waves formed along the surface.

EXAMPLE 6.36

An observer on the ground does not hear the sonic boom caused by an airplane moving at 5-km altitude until it is 9 km past her. What is the approximate Mach number of the plane? Assume a small disturbance and neglect the variation of sound speed with altitude.

Solution

A finite disturbance like an airplane will create a finite-strength oblique-shock wave whose angle will be somewhat larger than the Mach-wave angle μ and will curve downward due to the variation in atmospheric sound speed. If we neglect these effects, the altitude and distance are a measure of μ, as seen in Fig. E6.36 . Thus

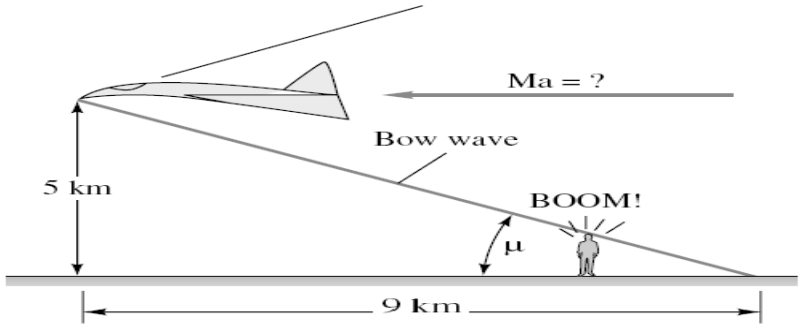

E 6.36

$$\tan\mu = \frac{5\text{ km}}{9\text{ km}} = 0.5556 \qquad \text{or} \qquad \mu = 29.05°$$

Hence, from Eq. (6.173),

$$\text{Ma} = \csc\mu = 2.06 \qquad \textit{Ans.}$$

6.10.2 The Oblique shock Waves:

Figures 6.18 and 6.37 and our earlier discussion all indicate that a shock wave can form at an oblique angle to the oncoming supersonic stream. Such a wave will deflect the stream through an angle θ, unlike the normal-shock wave, for which the downstream flow is in the same direction. In essence, an oblique shock is caused by the necessity for a supersonic stream to turn through such an angle. Examples could be a finite wedge at the leading edge of a body and a ramp in the wall of a supersonic wind tunnel.

The flow geometry of an oblique shock is shown in Fig. 6.38 . As for the normal shock of Fig.6.16, state 1 denotes the upstream conditions and state 2 is downstream. The shock angle has an arbitrary value β, and the downstream flow V_2 turns at an angle θ which is a function of β and state 1 conditions. The upstream flow is always supersonic, but the downstream Mach number $\text{Ma}_2 = V_2/a_2$ may be subsonic, sonic, or supersonic, depending upon the conditions.

It is convenient to analyze the flow by breaking it up into normal and tangential components with respect to the wave, as shown in Fig. 6.38 . For a thin control volume

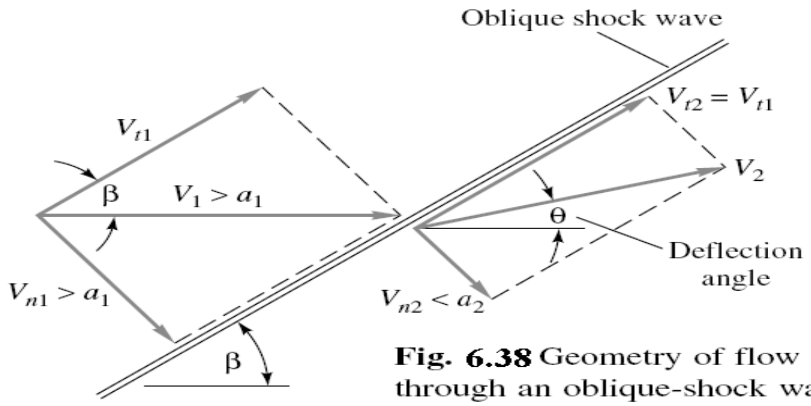

Fig. 6.38 Geometry of flow through an oblique-shock wave.

just encompassing the wave, we can then derive the following integral relations, canceling out $A_1 = A_2$ on each side of the wave:

Continuity: $$\rho_1 V_{n1} = \rho_2 V_{n2} \tag{6.174a}$$

Normal momentum: $$p_1 - p_2 = \rho_2 V_{n2}^2 - \rho_1 V_{n1}^2 \tag{6.174b}$$

Tangential momentum: $$0 = \rho_1 V_{n1}(V_{t2} - V_{t1}) \tag{6.174c}$$

Energy: $$h_1 + \tfrac{1}{2}V_{n1}^2 + \tfrac{1}{2}V_{t1}^2 = h_2 + \tfrac{1}{2}V_{n2}^2 + \tfrac{1}{2}V_{t2}^2 = h_0 \tag{6.174d}$$

We see from Eq.(6.174c) that there is no change in tangential velocity across an oblique shock

$$V_{t2} = V_{t1} = V_t = \text{const} \tag{6.175}$$

Thus tangential velocity has as its only effect the addition of a constant kinetic energy $\frac{1}{2}V_t^2$ to each side of the energy equation(6.174d). We conclude that Eqs. (6.174) are identical to the normal-shock relations (6.66) , with V_1 and V_2 replaced by the normal components V_{n1} and V_{n2}. All the various relations from Sec. 6.5 can be used to compute properties of an oblique-shock wave. The trick is to use the "normal" Mach numbers in place of Ma_1 and Ma_2:

$$\text{Ma}_{n1} = \frac{V_{n1}}{a_1} = \text{Ma}_1 \sin\beta \qquad \text{and} \qquad \text{Ma}_{n2} = \frac{V_{n2}}{a_2} = \text{Ma}_2 \sin(\beta - \theta) \tag{6.176}$$

Then, for a perfect gas with constant specific heats, the property ratios across the oblique shock are the analogs of Eqs. (6.72) to (6.75) with Ma_1 replaced by Ma_{n1}:

$$\frac{p_2}{p_1} = \frac{1}{k+1}\left[2k\,\text{Ma}_1^2 \sin^2\beta - (k-1)\right] \tag{6.177a}$$

$$\frac{\rho_2}{\rho_1} = \frac{\tan\beta}{\tan(\beta - \theta)} = \frac{(k+1)\,\text{Ma}_1^2 \sin^2\beta}{(k-1)\,\text{Ma}_1^2 \sin^2\beta + 2} = \frac{V_{n1}}{V_{n2}} \tag{6.177b}$$

$$\frac{T_2}{T_1} = \left[2 + (k-1)\,\text{Ma}_1^2 \sin^2\beta\right]\frac{2k\,\text{Ma}_1^2 \sin^2\beta - (k-1)}{(k+1)^2\,\text{Ma}_1^2 \sin^2\beta} \tag{6.177c}$$

$$T_{02} = T_{01} \tag{6.177d}$$

$$\frac{p_{02}}{p_{01}} = \left[\frac{(k+1)\,\mathrm{Ma}_1^2 \sin^2\beta}{2 + (k-1)\,\mathrm{Ma}_1^2 \sin^2\beta}\right]^{k/(k-1)} \left[\frac{k+1}{2k\,\mathrm{Ma}_1^2 \sin^2\beta - (k-1)}\right]^{1/(k-1)} \tag{6.177e}$$

$$\mathrm{Ma}_{n2}^2 = \frac{(k-1)\,\mathrm{Ma}_{n1}^2 + 2}{2k\,\mathrm{Ma}_{n1}^2 - (k-1)} \tag{6.177f}$$

All these are tabulated in the normal-shock Table B6.2. If you wondered why that table listed the Mach numbers as Ma_{n1} and Ma_{n2}, it should be clear now that the table is also valid for the oblique-shock wave.

Thinking all this over, we realize by hindsight that an oblique-shock wave is the flow pattern one would observe by running along a normal-shock wave (Fig. 6.16) at a constant tangential speed V_t. Thus the normal and oblique shocks are related by a galilean, or inertial, velocity transformation and therefore satisfy the same basic equations.

If we continue with this run-along-the-shock analogy, we find that the deflection angle θ increases with speed V_t up to a maximum and then decreases. From the geometry of Fig. 6.38 the deflection angle is given by

$$\theta = \tan^{-1}\frac{V_t}{V_{n2}} - \tan^{-1}\frac{V_t}{V_{n1}} \tag{6.178}$$

If we differentiate θ with respect to V_t and set the result equal to zero, we find that the maximum deflection occurs when $V_t/V_{n1} = (V_{n2}/V_{n1})^{1/2}$. We can substitute this back into Eq. (6.178) to compute

$$\theta_{\max} = \tan^{-1} r^{1/2} - \tan^{-1} r^{-1/2} \qquad r = \frac{V_{n1}}{V_{n2}} \tag{6.179}$$

For example, if $\mathrm{Ma}_{n1} = 3.0$, from Table B6.2 we find that $V_{n1}/V_{n2} = 3.8571$, the square root of which is 1.9640. Then Eq. (6.179) predicts a maximum deflection of $\tan^{-1} 1.9640 - \tan^{-1}(1/1.9640) = 36.03°$. The deflection is quite limited even for infinite Ma_{n1}: From Table B6.2 for this case $V_{n1}/V_{n2} = 6.0$, and we compute from Eq. (6.179) that $\theta_{\max} = 45.58°$.

This limited-deflection idea and other facts become more evident if we plot some of the solutions of Eqs. (6.177). For given values of V_1 and a_1, assuming as usual that $k = 1.4$, we can plot all possible solutions for V_2 downstream of the shock. Figure 6.39 does this in velocity-component coordinates V_x and V_y, with x parallel to V_1. Such a plot is called a *hodograph*. The heavy dark line which looks like a fat airfoil is the locus, or *shock polar*, of all physically possible solutions for the given Ma_1. The two dashed-line fishtails are solutions which increase V_2; they are physically impossible because they violate the second law.

Examining the shock polar in Fig. 6.39 , we see that a given deflection line of small angle θ crosses the polar at two possible solutions: the *strong* shock, which greatly decelerates the flow, and the *weak* shock, which causes a much milder deceleration. The flow downstream of the strong shock is always subsonic, while that of the weak shock is usually supersonic but occasionally subsonic if the deflection is large. Both types of shock occur in practice. The weak shock is more prevalent, but the strong shock will occur if there is a blockage or high-pressure condition downstream.

Since the shock polar is only of finite size, there is a maximum deflection $\theta_{\max}$, shown in Fig. 6.39 , which just grazes the upper edge of the polar curve. This verifies the kinematic discussion which led to Eq. (6.179). What happens if a supersonic flow is forced to deflect through an angle greater than $\theta_{\max}$? The answer is illustrated in Fig. 9.40 for flow past a wedge-shaped body.

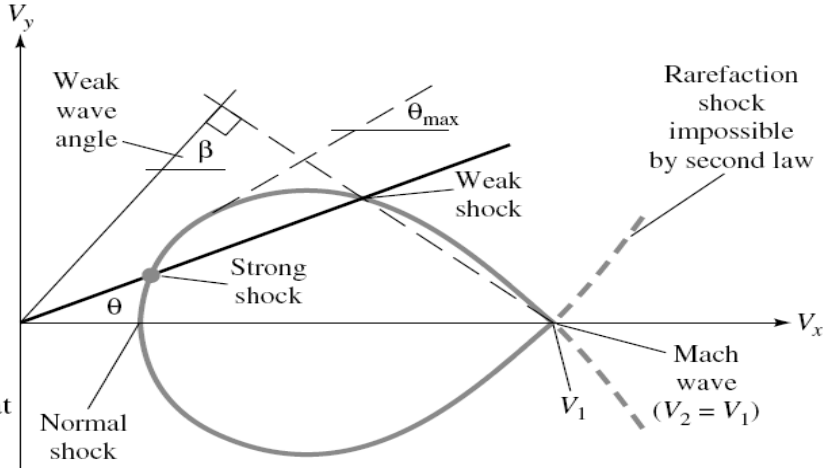

Fig. 6.39 The oblique-shock polar hodograph, showing double solutions (strong and weak) for small deflection angle and no solutions at all for large deflection.

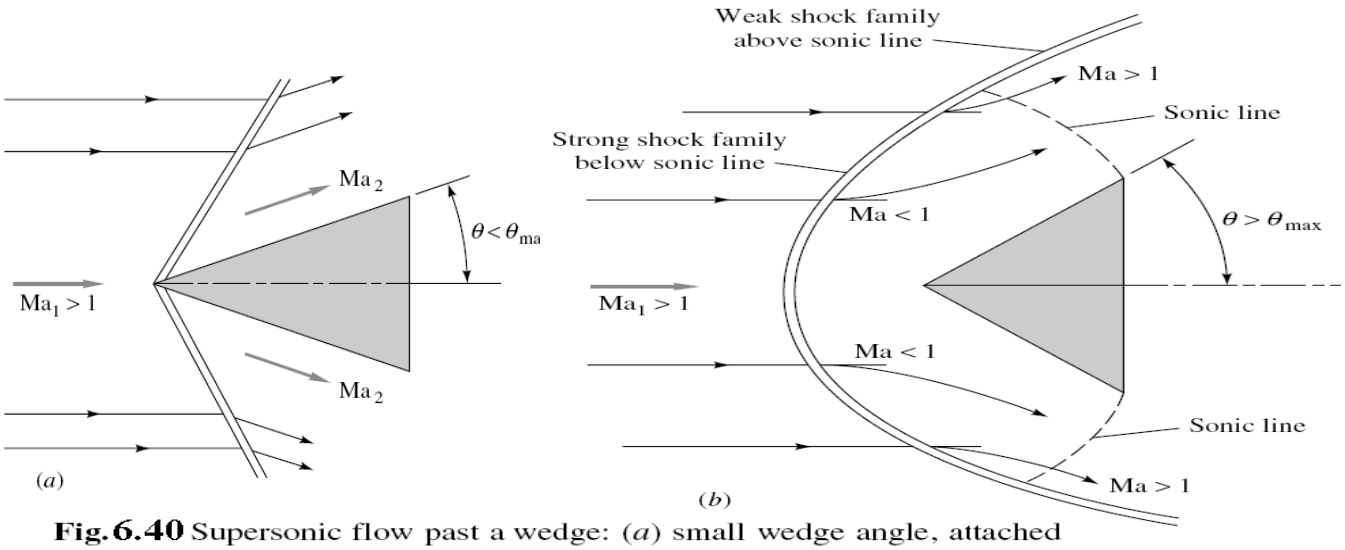

Fig. 6.40 Supersonic flow past a wedge: (*a*) small wedge angle, attached oblique shock forms; (*b*)large wedge angle, attached shock not possible, broad curved detached shock forms.

In Fig. 6.40a the wedge half-angle θ is less than θ_{max}, and thus an oblique shock forms at the nose of wave angle β just sufficient to cause the oncoming supersonic stream to deflect through the wedge angle θ. Except for the usually small effect of boundary-layer growth (see, e.g., Ref. 19, sec. 7–5.2), the Mach number Ma_2 is constant along the wedge surface and is given by the solution of Eqs. (6.177). The pressure, density, and temperature along the surface are also nearly constant, as predicted by Eqs. (6.177). When the flow reaches the corner of the wedge, it expands to higher Mach number and forms a wake (not shown) similar to that in Fig. 6.18 .

In Fig. 6.40b the wedge half-angle is greater than θ_{max}, and an attached oblique shock is impossible. The flow cannot deflect at once through the entire angle θ_{max}, yet somehow the flow must get around the wedge. A detached curve shock wave forms in front of the body, discontinuously deflecting the flow through angles smaller than θ_{max}.

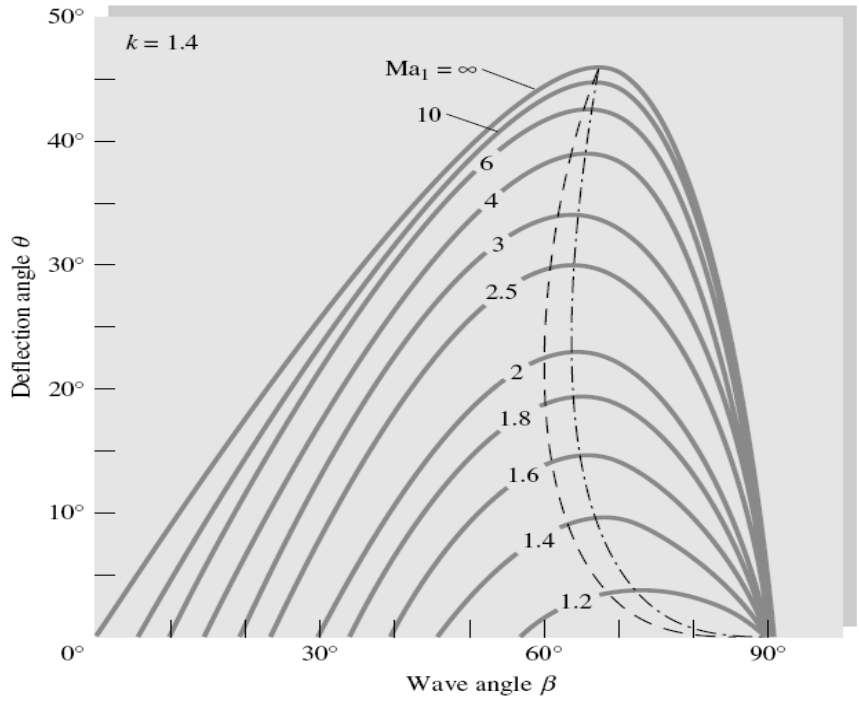

Fig. 6.41 Oblique-shock deflection versus wave angle for various upstream Mach numbers, $k = 1.4$: dash-dot curve, locus of θ_{max}, divides strong (right) from weak (left) shocks; dashed curve, locus of sonic points, divides subsonic Ma_2 (right) from supersonic Ma_2 (left).

The flow then curves, expands, and deflects subsonically around the wedge, becoming sonic and then supersonic as it passes the corner region. The flow just inside each point on the curved shock exactly satisfies the oblique-shock relations (6.177) for that particular value of β and the given Ma_1. Every condition along the curved shock is a point on the shock polar of Fig. 6.39 . Points near the front of the wedge are in the strong-shock family, and points aft of the sonic line are in the weak-shock family. The analysis of detached shock waves is extremely complex, and experimentation is usually needed, e.g., the shadowgraph optical technique of Fig. 6.18 .

The complete family of oblique-shock solutions can be plotted or computed from Eqs.(6.177). For a given k, the wave angle β varies with Ma_1 and θ, from Eq.(6.177b). By using a trigonometric identity for tan $(\beta - \theta)$ this can be rewritten in the more convenient form

$$\tan\,\theta = \frac{2\,\cot\,\beta\,(Ma_1^2\,\sin^2\,\beta - 1)}{Ma_1^2\,(k + \cos\,2\beta) + 2} \tag{6.180}$$

All possible solutions of Eq.(6.180) for $k = 1.4$ are shown in Fig. 6.41. For deflections $\theta < \theta_{max}$ there are two solutions: a weak shock (small β) and a strong shock (large β), as expected. All points along the dash-dot line for θ_{max} satisfy Eq.(6.179). A dashed line has been added to show where Ma_2 is exactly sonic. We see that there is a narrow region near maximum deflection where the weak-shock downstream flow is subsonic.

For zero deflections ($\theta = 0$) the weak-shock family satisfies the wave-angle relation

$$\beta = \mu = \sin^{-1}\,\frac{1}{Ma_1} \tag{6.181}$$

Thus weak shocks of vanishing deflection are equivalent to Mach waves. Meanwhile the strong shocks all converge at zero deflection to the normal-shock condition $\beta = 90°$.

Two additional oblique-shock charts are given in App. B, where Fig. B.1 gives the downstream Mach number Ma_2 and Fig. B.2 the pressure ratio p_2/p_1, each plotted as a function of Ma_1 and θ. Additional graphs, tables, and computer programs are given in Refs. 24 and 25.

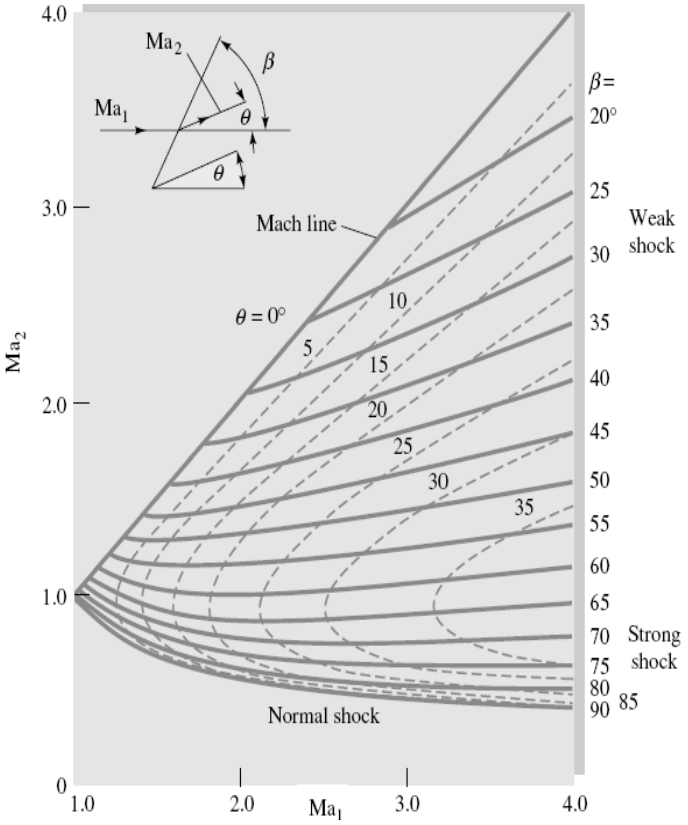

Fig. B.1 Mach number downstream of an oblique shock for $k = 1.4$.

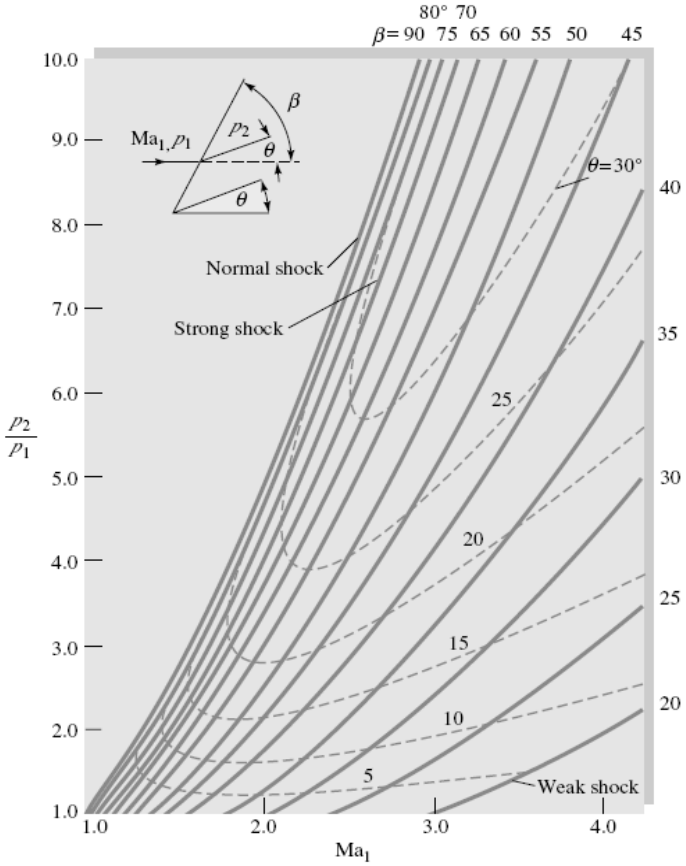

Fig. B.2 Pressure ratio downstream of an oblique shock for $k = 1.4$.

6.10.3 Very Weak Shock Waves:

For any finite θ the wave angle β for a weak shock is greater than the Mach angle μ. For small θ Eq. (6.180) can be expanded in a power series in tan θ with the following linearized result for the wave angle:

$$\sin\,\beta = \sin\,\mu + \frac{k+1}{4\,\cos\,\mu}\,\tan\,\theta + \cdots + \mathcal{O}(\tan^2\,\theta) + \cdots \tag{6.182}$$

For Ma_1 between 1.4 and 20.0 and deflections less than 6° this relation predicts β to within 1° for a weak shock. For larger deflections it can be used as a useful initial guess for iterative solution of Eq.(6.180).

Other property changes across the oblique shock can also be expanded in a power series for small deflection angles. Of particular interest is the pressure change from Eq. (6.177a), for which the linearized result for a weak shock is

$$\frac{p_2 - p_1}{p_1} = \frac{k\,Ma_1^2}{(Ma_1^2 - 1)^{1/2}}\,\tan\,\theta + \cdots + \mathcal{O}(\tan^2\,\theta) + \cdots \tag{6.183}$$

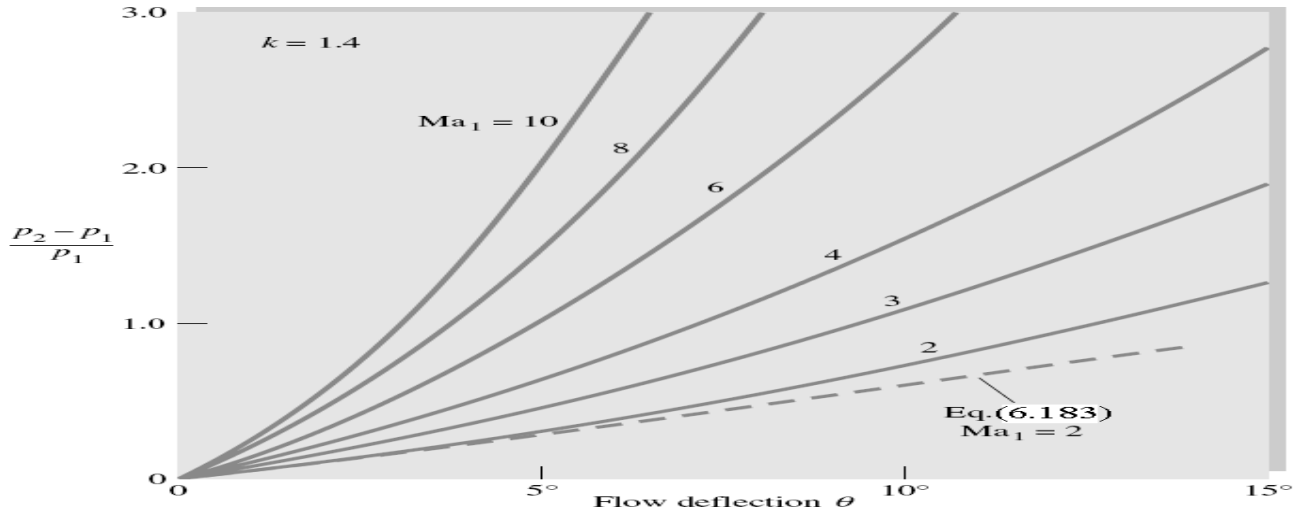

Fig. 6.42 Pressure jump across a weak oblique-shock wave from Eq. (6.177a) for $k = 1.4$. For very small deflections Eq. (6.183) applies.

The differential form of this relation is used in the next section to develop a theory for supersonic expansion turns. Figure 6.42 shows the exact weak-shock pressure jump computed from Eq. (6.177a). At very small deflections the curves are linear with slopes given by Eq. (6.183).

Finally, it is educational to examine the entropy change across a very weak shock. Using the same power-series expansion technique, we can obtain the following result for small flow deflections:

$$\frac{s_2 - s_1}{c_p} = \frac{(k^2 - 1)\mathrm{Ma}_1^6}{12(\mathrm{Ma}_1^2 - 1)^{3/2}} \tan^3 \theta + \cdots + \mathcal{O}(\tan^4 \theta) + \cdots \qquad (6.184)$$

The entropy change is cubic in the deflection angle θ. Thus weak shock waves are very nearly isentropic, a fact which is also used in the next section.

EXAMPLE 6.37

Air at Ma = 2.0 and $p = 10$ lbf/in^2 absolute is forced to turn through 10° by a ramp at the body surface. A weak oblique shock forms as in Fig. E6.37. For $k = 1.4$ compute from exact oblique-shock theory (*a*) the wave angle β, (*b*) Ma_2, and (*c*) p_2. Also use the linearized theory to estimate (*d*) β and (*e*) p_2.

Solution

With $\mathrm{Ma}_1 = 2.0$ and $\theta = 10°$ known, we can estimate $\beta \approx 40° \pm 2°$ from Fig. 6.41. For more (hand calculated) accuracy, we have to solve Eq. 6.180 by iteration. Or we can program Eq. 6.180 in EES with six statements (in SI units, with angles in degrees):

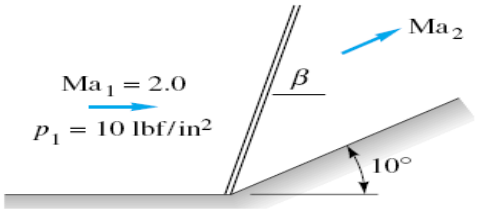

E 6.37

```
Ma = 2.0
k = 1.4
Theta = 10
Num = 2*(Ma^2*SIN(Beta)^2 - 1)/TAN(Beta)
Denom = Ma^2*(k + COS(2*Beta)) + 2
Theta = ARCTAN(Num/Denom)
```

Specify that Beta > 0 and EES promptly reports an accurate result:

$$\beta = 39.32° \qquad \textit{Ans. (a)}$$

The normal Mach number upstream is thus

$$\mathrm{Ma}_{n1} = \mathrm{Ma}_1 \sin \beta = 2.0 \sin 39.32° = 1.267$$

With Ma_{n1} we can use the normal-shock relations (Table B6.2) or Fig. 6.17 or Eqs. (6.73) to (6.75) to compute

$$\mathrm{Ma}_{n2} = 0.8031 \qquad \frac{p_2}{p_1} = 1.707$$

Thus the downstream Mach number and pressure are

$$\mathrm{Ma}_2 = \frac{\mathrm{Ma}_{n2}}{\sin(\beta - \theta)} = \frac{0.8031}{\sin(39.32° - 10°)} = 1.64 \qquad \textit{Ans. (b)}$$

$$p_2 = (10 \text{ lbf/in}^2 \text{ absolute})(1.707) = 17.07 \text{ lbf/in}^2 \text{ absolute} \qquad \textit{Ans. (c)}$$

Notice that the computed pressure ratio agrees with Figs. 6.42 and B.2.

For the linearized theory the Mach angle is $\mu = \sin^{-1}(1/2.0) = 30°$. Equation (6.182) then estimates that

$$\sin\beta \approx \sin 30° + \frac{2.4\tan 10°}{4\cos 30°} = 0.622$$

or $$\beta \approx 38.5° \qquad \textit{Ans. (d)}$$

Equation (6.183) estimates that

$$\frac{p_2}{p_1} \approx 1 + \frac{1.4(2)^2\tan 10°}{(2^2-1)^{1/2}} = 1.57$$

or $$p_2 \approx 1.57(10\ \text{lbf/in}^2\ \text{absolute}) \approx 15.7\ \text{lbf/in}^2\ \text{absolute} \qquad \textit{Ans. (e)}$$

These are reasonable estimates in spite of the fact that 10° is really not a "small" flow deflection.

6.10.4 Prandtl-Merer Expansion Waves:

The oblique-shock solution of Sec.6.10.2 is for a finite compressive deflection θ which obstructs a supersonic flow and thus decreases its Mach number and velocity. The present section treats gradual changes in flow angle which are primarily *expansive*; i.e., they widen the flow area and increase the Mach number and velocity. The property changes accumulate in infinitesimal increments, and the linearized relations (6.182) and (6.183) are used. The local flow deflections are infinitesimal, so that the flow is nearly isentropic according to Eq.(6.184).

Figure 6.43 shows four examples, one of which (Fig. 6.43c) fails the test for gradual changes. The gradual compression of Fig. 6.43a is essentially isentropic, with a smooth increase in pressure along the surface, but the Mach angle decreases along the surface and the waves tend to coalesce farther out into an oblique-shock wave. The gradual expansion of Fig. 6.43b causes a smooth isentropic increase of Mach number and velocity along the surface, with diverging Mach waves formed.

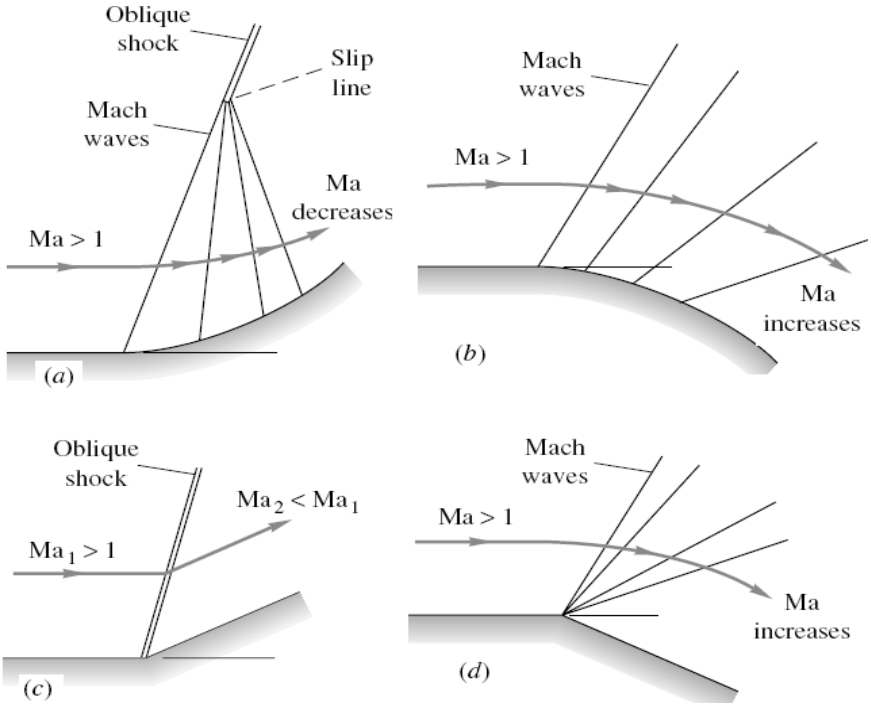

Fig.6.43
Some examples of supersonic expansion and compression: (*a*) gradual isentropic compression on a concave surface, Mach waves coalesce farther out to form oblique shock; (*b*) gradual isentropic expansion on convex surface, Mach waves diverge; (*c*) sudden compression, nonisentropic shock forms; (*d*) sudden expansion, centered isentropic fan of Mach waves forms.

The sudden compression of Fig. 6.43c cannot be accomplished by Mach waves: An oblique shock forms, and the flow is nonisentropic. This could be what you would see if you looked at Fig. 6.43a from far away. Finally, the sudden expansion of Fig. 6.43d is isentropic and forms a fan of centered Mach waves emanating from the corner. Note that the flow on any streamline passing through the fan changes smoothly to higher Mach number and velocity. In the limit as we near the corner the flow expands almost discontinuously at the surface. The cases in Fig. 6.43 *a*, *b*, and *d* can all be handled by the Prandtl-Meyer supersonic-wave theory of this section, first formulated by Ludwig Prandtl and his student Theodor Meyer in 1907 to 1908.

Note that none of this discussion makes sense if the upstream Mach number is subsonic, since Mach wave and shock wave patterns cannot exist in subsonic flow.

6.10.5 The Prandtl-Merer Perfect-Gas Function:

Consider a small, nearly infinitesimal flow deflection $d\theta$ such as occurs between the first two Mach waves in Fig. 6.43a . From Eqs. (6.182) and (6.183) we have, in the limit,

$$\beta \approx \mu = \sin^{-1} \frac{1}{\text{Ma}} \tag{6.185a}$$

$$\frac{dp}{p} \approx \frac{k\ \text{Ma}^2}{(\text{Ma}^2 - 1)^{1/2}}\, d\theta \tag{6.185b}$$

Since the flow is nearly isentropic, we have the frictionless differential momentum equation for a perfect gas

$$dp = -\rho V\, dV = -kp\ \text{Ma}^2 \frac{dV}{V} \tag{6.186}$$

Combining Eqs. (6.185a) and (6.186) to eliminate dp, we obtain a relation between turning angle and velocity change

$$d\theta = -(\text{Ma}^2 - 1)^{1/2} \frac{dV}{V} \tag{6.187}$$

This can be integrated into a functional relation for finite turning angles if we can relate V to Ma. We do this from the definition of Mach number

$$V = \text{Ma}\ a$$

or

$$\frac{dV}{V} = \frac{d\ \text{Ma}}{\text{Ma}} + \frac{da}{a} \tag{6.188}$$

Finally, we can eliminate da/a because the flow is isentropic and hence a_0 is constant for a perfect gas

$$a = a_0[1 + \tfrac{1}{2}(k - 1)\ \text{Ma}^2]^{-1/2}$$

or

$$\frac{da}{a} = \frac{-\frac{1}{2}(k - 1)\ \text{Ma}\ d\ \text{Ma}}{1 + \frac{1}{2}(k - 1)\ \text{Ma}^2} \tag{6.189}$$

Eliminating dV/V and da/a from Eqs. (6.1.87) to (6.189), we obtain a relation solely between turning angle and Mach number

$$d\theta = -\frac{(\text{Ma}^2 - 1)^{1/2}}{1 + \frac{1}{2}(k - 1)\ \text{Ma}^2} \frac{d\ \text{Ma}}{\text{Ma}} \tag{6.190}$$

Before integrating this expression, we note that the primary application is to expansions, i.e., increasing Ma and decreasing θ. Therefore, for convenience, we define the Prandtl-Meyer angle $\omega(\text{Ma})$ which increases when θ decreases and is zero at the sonic point

$$d\omega = -d\theta \qquad \omega = 0 \quad \text{at} \quad \text{Ma} = 1 \tag{6.191}$$

Thus we integrate Eq. (6.190) from the sonic point to any value of Ma

$$\int_0^{\omega} d\omega = \int_1^{\text{Ma}} \frac{(\text{Ma}^2 - 1)^{1/2}}{1 + \frac{1}{2}(k - 1)\ \text{Ma}^2} \frac{d\ \text{Ma}}{\text{Ma}} \tag{6.192}$$

The integrals are evaluated in closed form, with the result, in radians,

$$\omega(\text{Ma}) = K^{1/2} \tan^{-1} \left(\frac{\text{Ma}^2 - 1}{K}\right)^{1/2} - \tan^{-1} (\text{Ma}^2 - 1)^{1/2} \tag{6.193}$$

where

$$K = \frac{k + 1}{k - 1}$$

This is the *Prandtl-Meyer supersonic expansion function*, which is plotted in Fig. 6.44 and tabulated in Table B.5 for $k = 1.4$, $K = 6$. The angle ω changes rapidly at first and then levels off at high Mach number to a limiting value as $\text{Ma} \longrightarrow \infty$:

$$\omega_{\max} = \frac{\pi}{2} (K^{1/2} - 1) = 130.45^\circ \qquad \text{if} \qquad k = 1.4 \tag{6.194}$$

Thus a supersonic flow can expand only through a finite turning angle before it reaches infinite Mach number, maximum velocity, and zero temperature.

Gradual expansion or compression between finite Mach numbers Ma_1 and Ma_2, neither of which is unity, is computed by relating the turning angle $\Delta\omega$ to the difference in Prandtl-Meyer angles for the two conditions

$$\Delta\omega_{1 \to 2} = \omega(\text{Ma}_2) - \omega(\text{Ma}_1) \tag{6.195}$$

The change $\Delta\omega$ may be either positive (expansion) or negative (compression) as long as the end conditions lie in the supersonic range. Let us illustrate with an example.

EXAMPLE 6.38

Air ($k = 1.4$) flows at $\text{Ma}_1 = 3.0$ and $p_1 = 200$ kPa. Compute the final downstream Mach number and pressure for (*a*) an expansion turn of 20° and (*b*) a gradual compression turn of 20°.

Solution

Part (a)

The isentropic stagnation pressure is $p_0 = p_1[1 + 0.2(3.0)^2]^{3.5} = 7347$ kPa and this will be the same at the downstream point. For $\text{Ma}_1 = 3.0$ we find from Table B.5 or Eq. (6.193) that $\omega_1 = 49.757^\circ$. The flow expands to a new condition such that

$$\omega_2 = \omega_1 + \Delta\omega = 49.757^\circ + 20^\circ = 69.757^\circ$$

Linear interpolation in Table B.5 is quite accurate, yielding $\text{Ma}_2 \approx 4.32$. Inversion of Eq. (6.193) to find Ma when ω is given, is impossible without iteration. Once again, our friend EES easily handles Eq. (6.193) with four statements (angles specified in degrees):

```
k = 1.4
C = ((k+1)/(k - 1))^0.5
Omega = 69.757
Omega = C*ARCTAN((Ma^2-1)^0.5/C) - ARCTAN((Ma^2-1)^0.5)
```

Specify that Ma > 1, and EES readily reports an accurate result:[6]

$$\mathrm{Ma}_2 = 4.32 \qquad \textit{Ans. (a)}$$

The isentropic pressure at this new condition is

$$p_2 = \frac{p_0}{[1 + 0.2(4.32)^2]^{3.5}} = \frac{7347}{230.1} = 31.9 \text{ kPa} \qquad \textit{Ans. (a)}$$

[6]The author saves these little programs for further use, giving them names such as *Prandtl-Meyer*.

Part (b)

The flow compresses to a lower Prandtl-Meyer angle

$$\omega_2 = 49.757^\circ - 20^\circ = 29.757^\circ$$

Again from Eq.(6.193), Table B.5, or EES we compute that

Again from Eq.(6.193) Table B.5, or EES we compute that

$$\mathrm{Ma}_2 = 2.125 \qquad \textit{Ans. (b)}$$

$$p_2 = \frac{p_0}{[1 + 0.2(2.125)^2]^{3.5}} = \frac{7347}{9.51} = 773 \text{ kPa} \qquad \textit{Ans. (b)}$$

Similarly, density and temperature changes are computed by noticing that T_0 and ρ_0 are constant for isentropic flow.

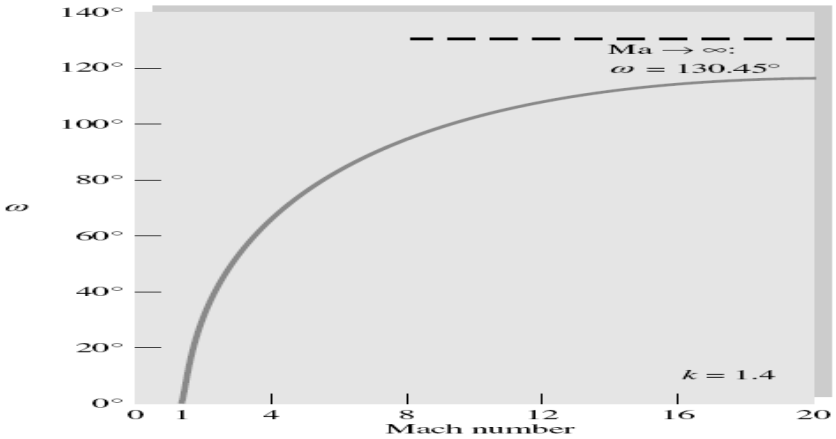

Fig, 6.44 The Prandtl-Meyer supersonic expansion from Eq.(6.193) for $k = 1.4$.

Table B.5 Prandtl-Meyer Supersonic Expansion Function for $k = 1.4$

Ma	ω, deg	Ma	ω, deg	Ma	ω, deg	Ma	ω, deg
1.00	0.0						
1.05	0.49	3.05	50.71	5.05	77.38	7.05	91.23
1.10	1.34	3.10	51.65	5.10	77.84	7.10	91.49
1.15	2.38	3.15	52.57	5.15	78.29	7.15	91.75
1.20	3.56	3.20	53.47	5.20	78.73	7.20	92.00
1.25	4.83	3.25	54.35	5.25	79.17	7.25	92.24
1.30	6.17	3.30	55.22	5.30	79.60	7.30	92.49
1.35	7.56	3.35	56.07	5.35	80.02	7.35	92.73
1.40	8.99	3.40	56.91	5.40	80.43	7.40	92.97
1.45	10.44	3.45	57.73	5.45	80.84	7.45	93.21
1.50	11.91	3.50	58.53	5.50	81.24	7.50	93.44
1.55	13.38	3.55	59.32	5.55	81.64	7.55	93.67
1.60	14.86	3.60	60.09	5.60	82.03	7.60	93.90
1.65	16.34	3.65	60.85	5.65	82.42	7.65	94.12
1.70	17.81	3.70	61.60	5.70	82.80	7.70	94.34
1.75	19.27	3.75	62.33	5.75	83.17	7.75	94.56
1.80	20.73	3.80	63.04	5.80	83.54	7.80	94.78
1.85	22.16	3.85	63.75	5.85	83.90	7.85	95.00
1.90	23.59	3.90	64.44	5.90	84.26	7.90	95.21
1.95	24.99	3.95	65.12	5.95	84.61	7.95	95.42
2.00	26.38	4.00	65.78	6.00	84.96	8.00	95.62
2.05	27.75	4.05	66.44	6.05	85.30	8.05	95.83
2.10	29.10	4.10	67.08	6.10	85.63	8.10	96.03
2.15	30.43	4.15	67.71	6.15	85.97	8.15	96.23
2.20	31.73	4.20	68.33	6.20	86.29	8.20	96.43
2.25	33.02	4.25	68.94	6.25	86.62	8.25	96.63
2.30	34.28	4.30	69.54	6.30	86.94	8.30	96.82
2.35	35.53	4.35	70.13	6.35	87.25	8.35	97.01
2.40	36.75	4.40	70.71	6.40	87.56	8.40	97.20
2.45	37.95	4.45	71.27	6.45	87.87	8.45	97.39
2.50	39.12	4.50	71.83	6.50	88.17	8.50	97.57
2.55	40.28	4.55	72.38	6.55	88.47	8.55	97.76
2.60	41.41	4.60	72.92	6.60	88.76	8.60	97.94
2.65	42.53	4.65	73.45	6.65	89.05	8.65	98.12
2.70	43.62	4.70	73.97	6.70	89.33	8.70	98.29
2.75	44.69	4.75	74.48	6.75	89.62	8.75	98.47
2.80	45.75	4.80	74.99	6.80	89.90	8.80	98.64
2.85	46.78	4.85	75.48	6.85	90.17	8.85	98.81
2.90	47.79	4.90	75.97	6.90	90.44	8.90	98.98
2.95	48.78	4.95	76.45	6.95	90.71	8.95	99.15
3.00	49.76	5.00	76.92	7.00	90.97	9.00	99.32

6.10.6 Applications to Supersonic Airfoils:

The oblique-shock and Prandtl-Meyer expansion theories can be used to patch together a number of interesting and practical supersonic flow fields. This marriage, called *shock expansion theory*, is limited by two conditions: (1) Except in rare instances the flow must be supersonic throughout, and (2) the wave pattern must not suffer interference from waves formed in other parts of the flow field.

A very successful application of shock expansion theory is to supersonic airfoils. Figure 6.45 shows two examples, a flat plate and a diamond-shaped foil. In contrast to subsonic-flow designs (Part (3)), these airfoils must have sharp leading edges, which form attached oblique shocks or expansion fans. Rounded supersonic leading edges would cause detached bow shocks, as in Fig. 6.37 or 6.40b, greatly increasing the drag and lowering the lift.

In applying shock expansion theory, one examines each surface turning angle to see whether it is an expansion ("opening up") or compression (obstruction) to the surface flow. Figure 6.45a shows a flat-plate foil at an angle of attack. There is a leading-edge shock on the lower edge with flow deflection $\theta = \alpha$, while the upper edge has an expansion fan with increasing Prandtl-Meyer angle $\Delta\omega = \alpha$. We compute p_3 with expansion theory and p_2 with oblique-shock theory. The force on the plate is thus $F = (p_2 - p_3)Cb$, where C is the chord length and b the span width (assuming no wingtip effects). This force is normal to the plate, and thus the lift force normal to the stream is $L = F\cos\alpha$, and the drag parallel to the stream is $D = F\sin\alpha$. The dimensionless coefficients C_L and C_D have the same definitions as in low-speed flow, Eq. (7.66), except that the perfect-gas-law identity $\frac{1}{2}\rho V^2 \equiv \frac{1}{2}kp\ \mathrm{Ma}^2$ is very useful here Part (5)

$$C_L = \frac{L}{\frac{1}{2}kp_\infty\ \mathrm{Ma}_\infty^2\ bC} \qquad C_D = \frac{D}{\frac{1}{2}kp_\infty\ \mathrm{Ma}_\infty^2\ bC} \tag{6.196}$$

The typical supersonic lift coefficient is much smaller than the subsonic value $C_L \approx 2\pi\alpha$, but the lift can be very large because of the large value of $\frac{1}{2}\rho V^2$ at supersonic speeds.

At the trailing edge in Fig. 6.45a , a shock and fan appear in reversed positions and bend the two flows back so that they are parallel in the wake and have the same pressure. They do not have quite the same velocity because of the unequal shock strengths on the upper and lower surfaces; hence a vortex sheet trails behind the wing. This is very interesting, but in the theory you ignore the trailing-edge pattern entirely, since it does not affect the surface pressures: The supersonic surface flow cannot "hear" the wake disturbances.

The diamond foil in Fig. 6.45b adds two more wave patterns to the flow. At this particular α less than the diamond half-angle, there are leading-edge shocks on both surfaces, the upper shock being much weaker. Then there are expansion fans on each shoulder of the diamond: The Prandtl-Meyer angle change $\Delta\omega$ equals the sum of the leading-edge and trailing-edge diamond half-angles. Finally, the trailing-edge pattern is similar to that of the flat plate (6.45a) and can be ignored in the calculation. Both lower-surface pressures p_2 and p_4 are greater than their upper counterparts, and the lift is nearly that of the flat plate. There is an additional drag due to thickness, because p_4 and p_5 on the trailing surfaces are lower than their counterparts p_2 and p_3. The diamond drag is greater than the flat-plate drag, but this must be endured in practice to achieve a wing structure strong enough to hold these forces.

The theory sketched in Fig. 6.45 is in good agreement with measured supersonic lift and drag as long as the Reynolds number is not too small (thick boundary layers) and the Mach number not too large (hypersonic flow). It turns out that for large Re_C and moderate supersonic Ma_∞ the boundary layers are thin and separation seldom occurs, so that the shock expansion theory, although frictionless, is quite successful. Let us look now at an example.

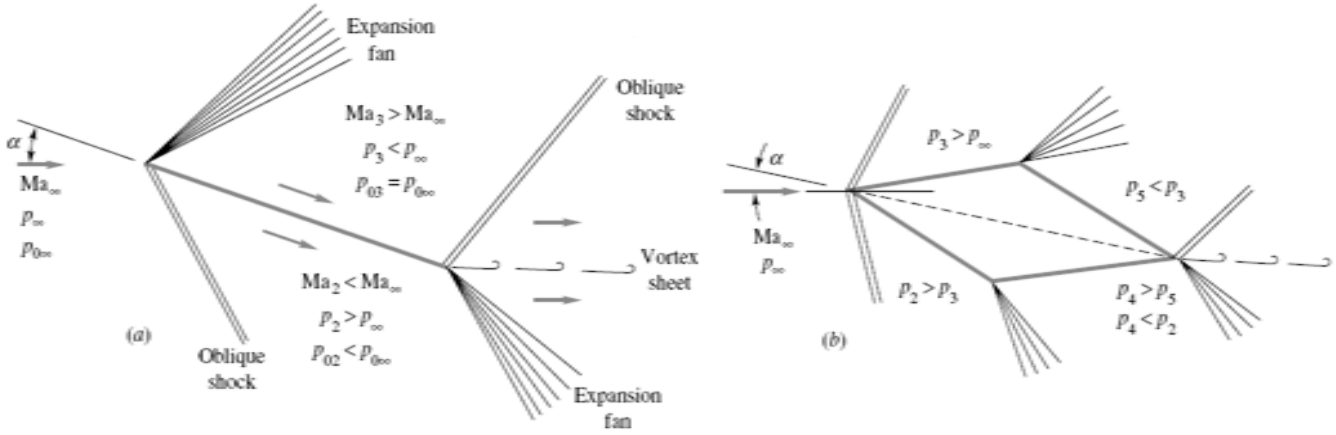

Fig. 6.45 Supersonic airfoils: (*a*) flat plate, higher pressure on lower surface, drag due to small downstream component of net pressure force; (*b*) diamond foil, higher pressures on both lower surfaces, additional drag due to body thickness.

EXAMPLE 6.39

A flat-plate airfoil with $C = 2$ m is immersed at $\alpha = 8°$ in a stream with $Ma_\infty = 2.5$ and $p_\infty = 100$ kPa. Compute (*a*) C_L and (*b*) C_D, and compare with low-speed airfoils. Compute (*c*) lift and (*d*) drag in newtons per unit span width.

Solution

Instead of using a lot of space outlining the detailed oblique-shock and Prandtl-Meyer expansion computations, we list all pertinent results in Fig. E6.39 on the upper and lower surfaces. Using the theories of Secs. 6.9 and 6.10, you should verify every single one of the calculations in Fig. E6.39 to make sure that all details of shock expansion theory are well understood.

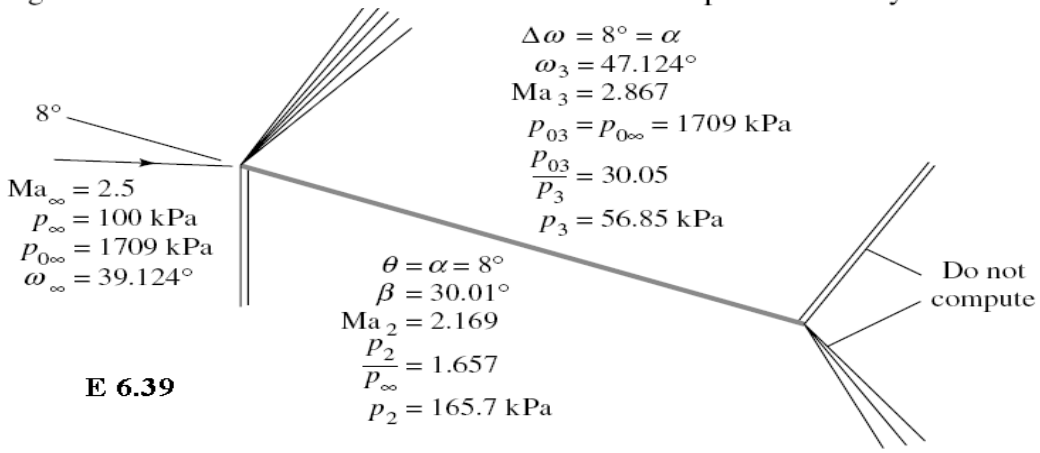

E 6.39

The important final results are p_2 and p_3, from which the total force per unit width on the plate is

$$F = (p_2 - p_3)bC = (165.7 - 56.85)(\text{kPa})(1\text{ m})(2\text{ m}) = 218\text{ kN}$$

The lift and drag per meter width are thus

$$L = F\cos 8° = 216\text{ kN} \qquad \textit{Ans. (c)}$$

$$D = F\sin 8° = 30\text{ kN} \qquad \textit{Ans. (d)}$$

These are very large forces for only 2 m^2 of wing area.

From Eq. (6.196) the lift coefficient is

$$C_L = \frac{216\text{ kN}}{\frac{1}{2}(1.4)(100\text{ kPa})(2.5)^2(2\text{ m}^2)} = 0.246 \qquad \textit{Ans. (a)}$$

The comparable low-speed coefficient from Part (3) is $C_L = 2\pi \sin 8° = 0.874$, which is 3.5 times larger.

From Eq. 6.196 the drag coefficient is

$$C_D = \frac{30\text{ kN}}{\frac{1}{2}(1.4)(100\text{ kPa})(2.5)^2(2\text{ m}^2)} = 0.035 \qquad \textit{Ans. (b)}$$

From Fig. 6.47 for the NACA 0009 airfoil C_D at $\alpha = 8°$ is about 0.009, or about 4 times smaller.

Notice that this supersonic theory predicts a finite drag in spite of assuming frictionless flow with infinite wing aspect ratio. This is called *wave drag*, and we see that the d'Alembert paradox of zero body drag does not occur in supersonic flow.

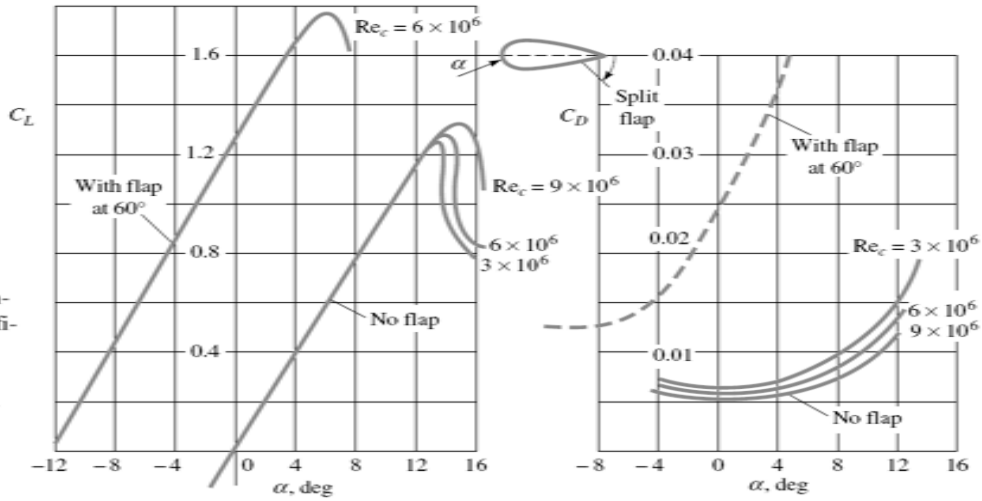

Fig. 6.47 Lift and drag of a symmetric NACA 0009 airfoil of infinite span, including effect of a split-flap deflection. Note that roughness can increase C_D from 100 to 300 percent.

6.10.7 The Thin Airfoil Theory:

In spite of the simplicity of the flat-plate geometry, the calculations in Example 6.39 were laborious. In 1925 Ackeret [21] developed simple yet effective expressions for the lift, drag, and center of pressure of supersonic airfoils, assuming small thickness and angle of attack.

The theory is based on the linearized expression (6.183), where tan $\theta \approx$ surface deflection relative to the free stream and condition 1 is the free stream, $\text{Ma}_1 = \text{Ma}_\infty$. For the flat-plate airfoil, the total force F is based on

$$\frac{p_2 - p_3}{p_\infty} = \frac{p_2 - p_\infty}{p_\infty} - \frac{p_3 - p_\infty}{p_\infty}$$

$$= \frac{k\ \text{Ma}_\infty^2}{(\text{Ma}_\infty^2 - 1)^{1/2}} [\alpha - (-\alpha)] \qquad (6.197)$$

Substitution into Eq. (6.196) gives the linearized lift coefficient for a supersonic flat-plate airfoil

$$C_L \approx \frac{(p_2 - p_3)bC}{\frac{1}{2}kp_\infty\ \text{Ma}_\infty^2\ bC} \approx \frac{4\alpha}{(\text{Ma}_\infty^2 - 1)^{1/2}} \qquad (6.198)$$

Computations for diamond and other finite-thickness airfoils show no first-order effect of thickness on lift. Therefore Eq. (6.198) is valid for any sharp-edged supersonic thin airfoil at a small angle of attack.

The flat-plate drag coefficient is

$$C_D = C_L \tan \alpha \approx C_L \alpha \approx \frac{4\alpha^2}{(\text{Ma}_\infty^2 - 1)^{1/2}} \qquad (6.199)$$

However, the thicker airfoils have additional thickness drag. Let the chord line of the airfoil be the x-axis, and let the upper-surface shape be denoted by $y_u(x)$ and the lower profile by $y_l(x)$. Then the complete Ackeret drag theory (see, e.g., Ref. 8, sec. 14.6, for details) shows that the additional drag depends on the mean square of the slopes of the upper and lower surfaces, defined by

$$\overline{y'^2} = \frac{1}{C} \int_0^C \left(\frac{dy}{dx}\right)^2 dx \qquad (6.200)$$

The final expression for drag [8, p. 442] is

$$C_D \approx \frac{4}{(\text{Ma}_\infty^2 - 1)^{1/2}} \left[\alpha^2 + \frac{1}{2}(\overline{y_u'^2} + \overline{y_l'^2})\right] \qquad (6.201)$$

These are all in reasonable agreement with more exact computations, and their extreme simplicity makes them attractive alternatives to the laborious but accurate shock expansion theory. Consider the following example.

EXAMPLE 6.40

Repeat parts (*a*) and (*b*) of Example 6.39, using the linearized Ackeret theory.

Solution

From Eqs. (6.198) and (6.199) we have, for $\text{Ma}_\infty = 2.5$ and $\alpha = 8° = 0.1396$ rad,

$$C_L \approx \frac{4(0.1396)}{(2.5^2 - 1)^{1/2}} = 0.244 \qquad C_D = \frac{4(0.1396)^2}{(2.5^2 - 1)^{1/2}} = 0.034 \qquad \textit{Ans.}$$

These are less than 3 percent lower than the more exact computations of Example 6.39.

A further result of the Ackeret linearized theory is an expression for the position x_{CP} of the center of pressure (CP) of the force distribution on the wing:

$$\frac{x_{CP}}{C} = 0.5 + \frac{S_u - S_l}{2\alpha C^2} \qquad (6.202)$$

where S_u is the cross-sectional area between the upper surface and the chord and S_l is the area between the chord and the lower surface. For a symmetric airfoil ($S_l = S_u$) we

obtain $x_{CP} = 0.5C$ at the half-chord point, in contrast with the low-speed airfoil result of Part (3), where x_{CP} is at the quarter-chord.

The difference in difficulty between the simple Ackeret theory and shock expansion theory is even greater for a thick airfoil, as the following example shows.

EXAMPLE 6.41

By analogy with Example 6.39 analyze a diamond, or double-wedge, airfoil of 2° half-angle and $C = 2$ m at $\alpha = 8°$ and $\text{Ma}_\infty = 2.5$. Compute C_L and C_D by (*a*) shock expansion theory and (*b*) Ackeret theory. Pinpoint the difference from Example 6.39.

Solution

Part (a)

Again we omit the details of shock expansion theory and simply list the properties computed on each of the four airfoil surfaces in Fig. E6.41. Assume $p_\infty = 100$ kPa. There are both a force F normal to the chord line and a force P parallel to the chord. For the normal force the pressure difference on the front half is $p_2 - p_3 = 186.4 - 65.9 = 120.5$ kPa, and on the rear half it is $p_4 - p_5 = 146.9 - 48.1 = 98.1$ kPa. The average pressure difference is $\frac{1}{2}(120.5 + 98.1) = 109.3$ kPa, so that the normal force is

$$F = (109.3 \text{ kPa})(2 \text{ m}^2) = 218.6 \text{ kN}$$

For the chordwise force P the pressure difference on the top half is $p_3 - p_5 = 65.9 - 48.8 = 17.1$ kPa, and on the bottom half it is $p_2 - p_4 = 186.4 - 146.9 = 39.5$ kPa. The average difference is $\frac{1}{2}(17.1 + 39.5) = 28.3$ kPa, which when multiplied by the frontal area (maximum thickness times 1-m width) gives

$$P = (28.3 \text{ kPa})(0.07 \text{ m})(1 \text{ m}) = 2.0 \text{ kN}$$

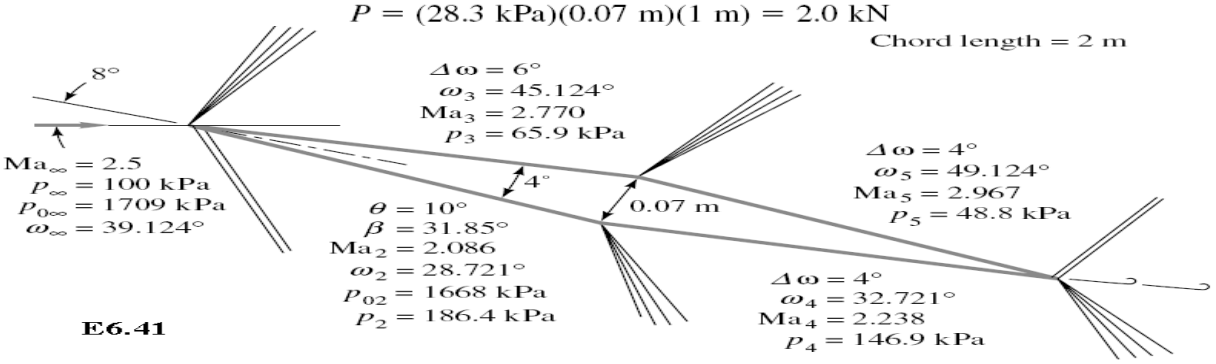

Both F and P have components in the lift and drag directions. The lift force normal to the free stream is

$$L = F \cos 8° - P \sin 8° = 216.2 \text{ kN}$$

and

$$D = F \sin 8° + P \cos 8° = 32.4 \text{ kN}$$

For computing the coefficients, the denominator of Eq. (6.196) is the same as in Example 6.39: $\frac{1}{2}kp_\infty \text{Ma}_\infty^2 bC = \frac{1}{2}(1.4)(100 \text{ kPa})(2.5)^2(2 \text{ m}^2) = 875$ kN. Thus, finally, shock expansion theory predicts

$$C_L = \frac{216.2 \text{ kN}}{875 \text{ kN}} = 0.247 \qquad C_D = \frac{32.4 \text{ kN}}{875 \text{ kN}} = 0.0370 \qquad \textit{Ans. (a)}$$

Part (b)

Meanwhile, by Ackeret theory, C_L is the same as in Example 6.40:

$$C_L = \frac{4(0.1396)}{(2.5^2 - 1)^{1/2}} = 0.244 \qquad \textit{Ans. (b)}$$

This is 1 percent less than the shock expansion result above. For the drag we need the mean-square slopes from Eq. (6.200)

$$\overline{y_u'^2} = \overline{y_l'^2} = \tan^2 2° = 0.00122$$

Then Eq. (6.201) predicts the linearized result

$$C_D = \frac{4}{(2.5^2 - 1)^{1/2}} [(0.1396)^2 + \tfrac{1}{2}(0.00122 + 0.00122)] = 0.0362 \qquad \textit{Ans. (b)}$$

This is 2 percent lower than shock expansion theory predicts. We could judge Ackeret theory to be "satisfactory." Ackeret theory predicts $p_2 = 167$ kPa (−11 percent), $p_3 = 60$ kPa (−9 percent), $p_4 = 140$ kPa (−5 percent), and $p_5 = 33$ kPa (−6 percent).

6.10.8 Three-Dimensional Supersonic Flow:

We have gone about as far as we can go in an introductory treatment of compressible flow. Of course, there is much more, and you are invited to study further in the references at the end of the chapter.

Three-dimensional supersonic flows are highly complex, especially if they concern blunt bodies, which therefore contain embedded regions of subsonic and transonic flow, e.g., Fig. 6.18. Some flows, however, yield to accurate theoretical treatment such as flow past a cone at zero incidence, as shown in Fig. 6.46. The exact theory of cone flow is discussed in advanced texts [for example, 8, chap. 17], and

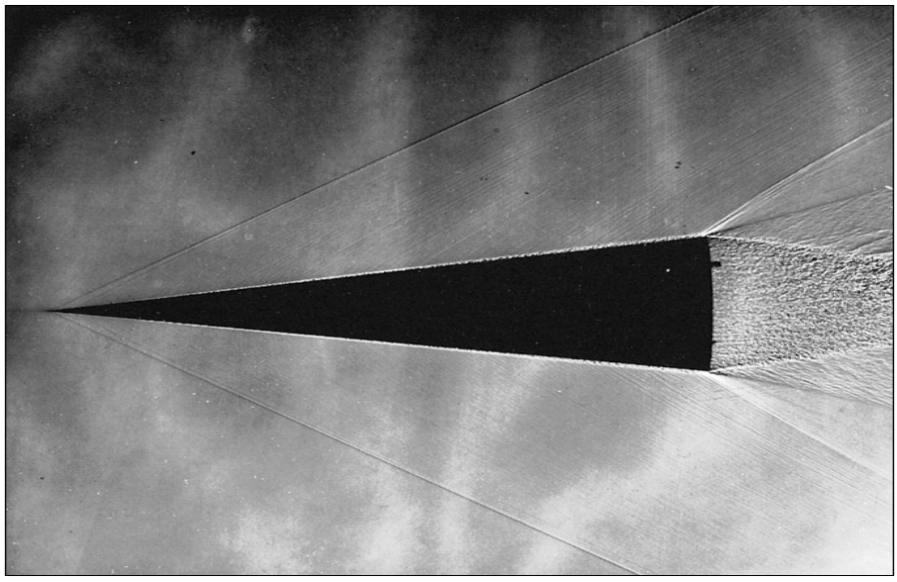

Fig. 6.46 Shadowgraph of flow past an 8° half-angle cone at $Ma_\infty = 2.0$. The turbulent boundary layer is clearly visible. The Mach lines curve slightly, and the Mach number varies from 1.98 just inside the shock to 1.90 at the surface. *(Courtesy of U.S. Army Ballistic Research Center, Aberdeen Proving Ground.)*

extensive tables of such solutions have been published [22, 23]. There are similarities between cone flow and the wedge flows illustrated in Fig. 6.40 : an attached oblique shock, a thin turbulent boundary layer, and an expansion fan at the rear corner. However, the conical shock deflects the flow through an angle less than the cone half-angle, unlike the wedge shock. As in the wedge flow, there is a maximum cone angle above which the shock must detach, as in Fig. 6.40b . For $k = 1.4$ and $Ma_\infty = \infty$, the maximum cone half-angle for an attached shock is about 57°, compared with the maximum wedge angle of 45.6° (see Ref. 23).

For more complicated body shapes one usually resorts to experimentation in a supersonic wind tunnel. Figure 6.48 shows a wind-tunnel study of supersonic flow past a model of an interceptor aircraft. The many junctions and wingtips and shape changes make theoretical analysis very difficult. Here the surface-flow patterns, which indicate boundary-layer development and regions of flow separation, have been visualized by the smearing of oil drops placed on the model surface before the test.

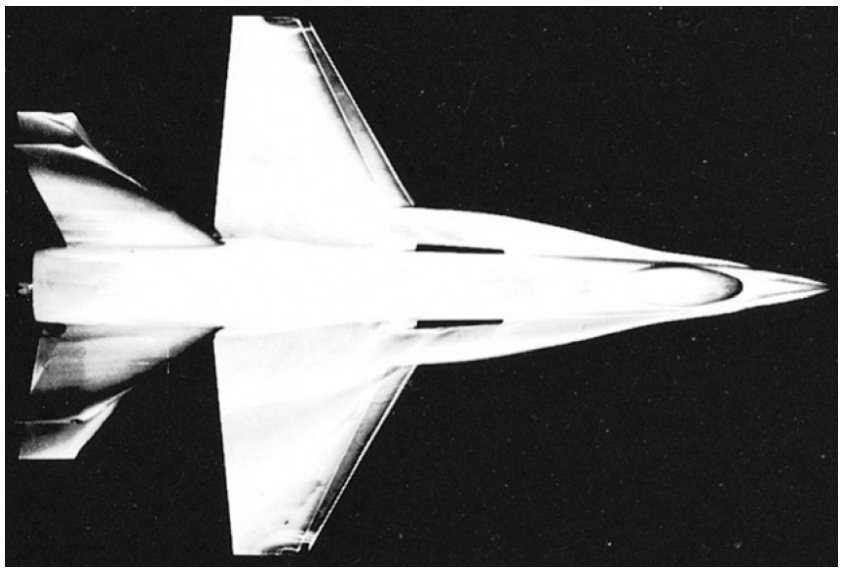

Fig. 6.48 Wind-tunnel test of the Cobra P-530 supersonic interceptor. The surface flow patterns are visualized by the smearing of oil droplets. *(Courtesy of Northrop Corp.)*

As we shall see in the next chapter, there is an interesting analogy between gas-dynamic shock waves and the surface water waves which form in an open-channel flow. Chapter 11 of Ref. 14 explains how a water channel can be used in an inexpensive simulation of supersonic-flow experiments.

Reusable Hypersonic Launch Vicles:

Having achieved reliable supersonic flight with both military and commercial aircraft, the next step is probably to develop a hypersonic vehicle that can achieve orbit, yet be retrieved. Presently the United States employs the Space Shuttle, where only the manned vehicle is retrieved, the very expensive giant rocket boosters being lost. In 1996, NASA selected Lockheed-Martin to develop the X-33, the first smaller-scale step toward a retrievable single-stage-to-orbit (SSTO) vehicle, to be called the VentureStar [36].

The X-33, shown in an artist's rendering in Fig. 6.49 , will be 20 m long, about half the size of the VentureStar, and it will be *suborbital*. It will take off vertically, rise to a height of 73 km, and coast back to earth at a steep (stressful) angle. Such a flight will test many new plans for the VentureStar [37], such as metallic tiles, titanium components, graphite composite fuel tanks, high-voltage control actuators, and Rocketdyne's novel "aerospike" rocket nozzles. If successful, the VentureStar 39 m long and weigh 9.7 MN, of which 88 percent (965 tons!) will be propellant r will be

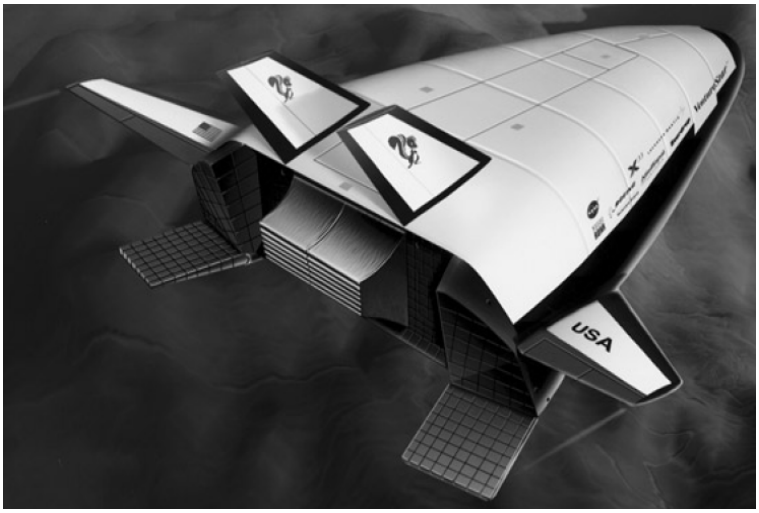

Fig. 6.49 The X-33 is a half-size suborbital test version of the VentureStar, which is planned as an orbital, low-cost retrievable space vehicle. It takes off vertically but then uses its lifting shape to glide back to earth and land horizontally [36, 37]*(Courtesy of Lockheed Martin Corp.)*

and only 2.7 percent (260 kN) will be payload. The dream is that the X-33 and VentureStar and their progeny will lead to an era of routine, low-cost space travel appropriate to the new millennium.

Summary:

This chapter is a brief introduction to a very broad subject, compressible flow, sometimes called *gas dynamics*. The primary parameter is the Mach number Ma = V/a, which is large and causes the fluid density to vary significantly. This means that the continuity and momentum equations must be coupled to the energy relation and the equation of state to solve for the four unknowns (p, ρ, T, $\mathbf{V}$).

The chapter reviews the thermodynamic properties of an ideal gas and derives a formula for the speed of sound of a fluid. The analysis is then simplified to one-dimensional steady adiabatic flow without shaft work, for which the stagnation enthalpy of the gas is constant. A further simplification to isentropic flow enables formulas to be derived for high-speed gas flow in a variable-area duct. This reveals the of back pressure on the performance of converging-diverging nozzles.

To illustrate nonisentropic flow conditions, there is a brief study of constant-area duct flow with friction and with heat transfer, both of which lead to choking of the exit flow.

The chapter ends with a discussion of two-dimensional supersonic flow, where oblique-shock waves and Prandtl-Meyer (isentropic) expansion waves appear. With a proper combination of shocks and expansions one can analyze supersonic airfoils.

Oral Exam Questions of Gas Dynamics

1- Find what is wrong in each of the following statements and then re-write the full correct statement (you can also add a T-S diagram to show the correct meaning) :

a) In Gas Dynamics, we define Mach number in a C-D nozzle as a constant thermodynamic property which is equal to (a/V) where a is the vector of the gas velocity.
b) In Gas Dynamics, we have to assume that Mach number is ≥ 0.3 all the time and assume also that the speed of sound through all gases is equal to 342 m/s all the time.
c) If air velocity in C-D nozzle is less than 0.3 speed of sound we must assume the flow is isentropic and incompressible and must assume also that the air is a thermal perfect gas.
d) The speed of sound in a subsonic air flow in C-D nozzle remains constant if the flow is accelerated to a supersonic flow because we assume air is a thermal perfect gas.
e) In Fanno-Line flow in a converging nozzle, the flow is isentropic and the exit properties must be sonic properties for any value of back pressure and any length of the nozzle.

2- Define the physical meaning and the mathematical equation for calculating the speed of sound, a, in any gas. What are the assumptions we make to get that equation? Can we calculate the speed of sound for a gas if it is moving at M=1 or it is moving at M>1?

3- Find what is wrong in each of the following statements and then re-write the full correct statement (you can also add a T-S diagram to show the correct meaning) :

a) We can not define the speed of sound for any incompressible flow because the density is must assumed to be constant and because the Mach Number is less than 0.3.
b) We can define the speed of sound, a, for air only and we have to assume the speed of sound a scalar quantity because it moves in the x-direction only.
c) For an incompressible flow, the speed of sound is defined as propagation of huge pressure pulse through isothermal fluid where friction and heat transfer are neglected.
d) All fluids at the same temperature must have the same speed of sound because the speed of sound is a function of the temperature only.
e) In Rayliegh-Line flow in a converging nozzle, the flow is isentropic and the exit properties must be sonic properties for any back pressure and any length of the nozzle.

4- Given that $dA/A = (1-M^2)(dp/\rho V^2) = -(1-M^2)(dV/V)$, Show that the converging-diverging nozzle is the only possible shape though which a gas may be accelerated smoothly from subsonic flow to supersonic flow without violating any of the gas dynamics relations. (use any needed equations and sketches).

5- Define the physical meaning of the speed sound. If we found that $a^2=(\partial p/\partial \rho)$, show that the speed of sound in a thermally perfect gas is $a = \sqrt{\gamma RT}$ (if we assume that sound waves are propagating isntropically). Prove that the speed of sound in a thermally perfect gas is $a = \sqrt{RT}$ (if we assume sound waves are propagating isothermally not isntropically). Which value is more accurate: ($a = \sqrt{\gamma RT}$) or ($a = \sqrt{RT}$) ? why ?

6- What is the "Mach Cone"? Define the physical meaning and the mathematical equation for calculating the half angle, α, of that cone. Can we see the Mach cone in a liquid or in an incompressible fluid ?

7- Define the physical meaning and the mathematical equations for the total isentropic stagnation properties (P_o, T_o, h_o, etc) and the critical isentropic properties (P*, T* , h* ,etc). Show both types of properties on T-S chart if the flow is subsonic and if it is supersonic.

8- Discuss, using the mass conservation, both the physical meaning and the mathematical relations which describe the chocking (الإختناق) in a variable area channel. Where may chocking take place? and How? What are the conditions that must exist to have a chocking? What are the possible flow conditions downstream of the chocked area?

9- Find what is wrong in each of the following statements and then re-write the full correct statement (you can also add a T-S diagram to show the correct meaning) :

a) All stagnation isentropic conditions (P_o, T_o, h_o, etc) of any subsonic flow must change if the flow becomes sonic or supersonic through an isentropic process.
b) All stagnation isentropic conditions (P_o, T_o, h_o, etc) of any subsonic flow must change if the flow becomes sonic or supersonic through a non-isentropic process.
c) All critical isentropic conditions (P*, T*, h*, etc) of any subsonic flow must change if the flow becomes sonic or supersonic through an isentropic process.
d) All critical isentropic conditions (P*, T*, h*, etc) of any subsonic flow must change if the flow becomes sonic or supersonic through a non-isentropic process.
e) In Rayliegh-Line flow in a converging nozzle, the flow is isentropic and the exit properties must be sonic properties for any back pressure and any length of the nozzle.

10- What is the temperature, density, ρ, pressure, p, and speed of sound, a, on the nose of a supersonic fighter flying at a Mach number of M=2 through air at 273K and 0.7 bar.

11- Find what is wrong in each of the following statements and then re-write the full correct statement (you can also add a T-S diagram to show the correct meaning) :

a) All perfect gases of the same value of γ will have the same stagnation conditions (P_o , T_o , h_o , …etc) and also the same critical conditions (P* , T* , h* , …etc).
b) Two perfect gases with different values of γ can not have the same stagnation conditions (P_o , T_o , h_o , …etc) and also the same critical conditions (P* , T* , h* , …etc).
c) In calculating reference stagnation properties (P_o, T_o, h_o, etc) we get an adiabatic decrease in both of gas temperature and density but we get an increase in the gas pressure.
d) Inside the Mach Cone created by the subsonic flow of an airplane, the speed of sound must be constant because we assume air is a thermal perfect gas.
e) In Fanno-Line flow in a converging nozzle, the flow is isentropic and the exit properties must be sonic properties for any back pressure and any length of the nozzle.

12- Air from a large tank flows at M=0.5 through a conduit of a cross-sectional area of 65cm^2. The conditions in the tank are 340 kPa, abs. and 10 ^oC. Calculate the properties, P, T, ρ, a, and the mass flow rate through that cross-section of the conduit.

13- Find what is wrong in each of the following statements and then re-write the full correct statement (you can also add a T-S diagram to show the correct meaning) :

a) During an isentropic subsonic expansion in a diffuser, the stagnation conditions (P_o, T_o & ρ_o) and also the critical conditions (P*, T*, ρ*) must remain constant.
b) During a non-isentropic subsonic expansion in a diffuser, the stagnation conditions (P_o, T_o & ρ_o) and also the critical conditions (P*, T*, ρ*) must remain constant.

c) During an isentropic subsonic compression in a nozzle, the stagnation conditions (P_o, T_o & ρ_o) and also the critical conditions (P*, T*, ρ*) must remain constant.
d) During a non-isentropic subsonic compression in a nozzle, the stagnation conditions (P_o, T_o & ρ_o) and also the critical conditions (P*, T*, ρ*) must remain constant.
e) In Fanno-Line flow in a converging nozzle, the flow is isentropic and the exit properties must be sonic properties for any back pressure and any length of the nozzle.

14- Air in a large reservoir at 8.5 bar abs. and 26 ^oC is allowed to escape through a channel at a rate of 2.25 kg/s. Find the Mach number, velocity and area at a point in the channel where the pressure is 5.8 bar abs.

15- Find what is wrong in each of the following statements and then re-write the full correct statement (you can also add a T-S diagram to show the correct meaning) :

a) During an isentropic compression in a converging nozzle, the flow must be subsonic along the nozzle but the exit conditions must be sonic conditions.
b) During a non-isentropic expansion in a converging-diverging nozzle, the flow must be subsonic along all the nozzle length including the nozzle throat area.
c) The only method to increase the flow rate through the nozzle throat after its chocking is to decrease the nozzle throat area.
d) For a fixed nozzle throat area, the critical conditions (P*, T*, ρ*) will be fixed values which can not be changed.
e) In Fanno-Line flow in a converging nozzle, the flow is isentropic and the exit properties must be sonic properties for any back pressure and any length of the nozzle.

16- At a certain point in a channel, Helium is flowing at M=2 and 2 bar abs. At a point further downstream, the pressure is 1 bar abs. Assuming isentropic flow through the channel, determine the Mach number at the second point (take γ=1.67).

17- Discuss in details all the operation conditions for a converging nozzle for all the possible values of back pressure in the range from P_o down to a back pressure less than the design one. Show the chocking case and the under expansion case on the T-S diagram and show the variation of the mass flow rate for all possible operation conditions.

18- At one point on a streamline in airflow the velocity, absolute pressure, and temperature are 30 m/s, 35 kPa, and 150 ^oC resp. The process along the streamline is assumed isentropic; calculate the pressure and temperature at a second point where the velocity is 150 m/s.

19- Given that $dA/A = (1-M^2)(dp/\rho V^2) = -(1-M^2)(dV/V)$, show, using any needed equations and sketches, what is the relation between the value of the Mach number and both of the nozzle or the diffuser shape for the subsonic and supersonic flow regimes.
Show that the converging-diverging nozzle is the only possible shape though which a gas may be accelerated smoothly from subsonic flow to supersonic flow without violating any of the gas dynamics relations.

20- A bullet was shot at a speed of 280 m/s in a stagnant air at 273 K and 0.98 bar abs. Calculate the total pressure at the bullet tip if air is considered incompressible and if it is considered compressible. Do same if the bullet speed was 700m/s. Comment on results!

21- Discuss in details how can chocking (الإختناق) take place in a converging nozzle. What are all the flow properties at the exit plane of the nozzle? How can we increase the mass flow rate more than the maximum at the chocking conditions? (plot T-S for all cases).

22- Pitot tube in a wind tunnel gives a static reading of 0.6 bar vacuum and a stagnation pressure of 0.1 bar gauge. If the stagnation temperature is 363 K, what will be the air velocity upstream of the Pitot tube.

23- For the flow in a variable area duct, discuss and plot the relation between **A/A^*** and the Mach number M for any perfect gas and for γ=1.4. What is the origin of this relation? Show the physical meaning of A^* and where it is located in a variable area duct. How can we get, physically, two possible values for M for the same value of A/A^* ?

24- Atmospheric air at 101.3 kPa abs. and 15 ^oC is accelerated isentropically. What are its velocity, pressure, temperature, and density when the velocity reaches the speed of sound.

25- For the flow in a variable area duct, discuss and plot the relation between **A^*/A** and the Mach number M for any perfect gas and for γ=1.4. What is the relation between A^*/A and chocking of the flow. Show the physical meaning of A^* and where it is located in the duct ? How can we get, physically, two possible values for M for the same value of A^*/A?

26- Air flows into a frictionless passage. The speed of the air increases in the direction of the flow. At station (1) the static temperature is 450K, static pressure is 2 bar abs., and the velocity is 200m/s. At station (2) the velocity is equal to the speed of sound. Calculate the static temperature, static pressure, velocity, and the density at station (2).

27- Plot and Discuss the mathematical meaning and physical meaning for these relations:

$$M \approx \frac{1+0.27(A/A^*)^{-2}}{1.728(A/A^*)} \quad .....for.subsonic.flow...\gamma = 1.4...and \longrightarrow 1.34 < A/A^* < \infty$$

$$M \approx 1-0.88\{\ln(A/A^*)\}^{0.45} \quad .....for.subsonic.flow...\gamma = 1.4...and \longrightarrow 1.0 < A/A^* < 1.34$$

$$M \approx 1+1.2(A/A^*-1)^{1/2} \quad .....for.supersonic.flow...\gamma = 1.4...and \longrightarrow 1.0 < A/A^* < 2.9$$

$$M \approx \left[216(A/A^*)-254(A/A^*)^{2/3}\right]^{1/5} \quad .....for.supersonic.flow...\gamma = 1.4...and \longrightarrow 2.9 < A/A^* < \infty$$

28- Air flows isentropically in a channel. At section (1), M_1=0.3, A_1=0.001m^2, P_1=650 kPa, T_1= 62 ^oC. At section (2), M_2=0.8. Sketch the channel shape, plot the T-S diagram and find A_2, P_{o2}, and all static properties at section (2).

29- Discuss in details the operation of a converging nozzle for all possible values of back pressure from $P_b = P_o$ to $P_b < P^*$. Plot the T-S diagram and also all possible pressure distributions along the nozzle. Show how do the flow rate and exit pressure depend on P_b?

30- It is required to expand air from P_o=200 kPa and T_o=500K through a throat to an exit Mach number of 2.5. If the desired mass flow rate is 3 kg/s, Find the throat area A*, the exit conditions A_2, P_2, T_2, and V_2. Assume an isentropic flow.

31-Discuss in details the physical meaning of the Normal Shock Wave. Show where and How it may take place? What are the flow conditions that must exist for the N.S.W. to take place? What are the flow conditions upstream and downstream the N.S.W.? Plot the T-S diagram for the process of the N.S.W.

32- What is the temperature, density, ρ, pressure, p, and speed of sound, a, on the nose of a supersonic fighter flying at a Mach number of M=2 through air at 273K and 0.7 bar.

33- Discuss in details the operation of a converging-diverging nozzle for all possible values of back pressure from $P_b = P_o$ to $P_b < P_d$, where P_d is the design pressure for supersonic exit. Plot the T-S diagram and also all possible pressure distributions along the nozzle. Show how do the flow rate and exit pressure depend on P_b? Show all possible locations of the Normal shock Wave as the back pressure is reduced.

34- Air at 10 bar abs., and 300K issues from a reservoir through a converging nozzle of 10 mm exit diameter. Assuming isentropic flow, calculate the mass flow rate and exit Mach number if the back pressure is 2 bar abs.

---

(35) The Rayliegh Line flow has the following properties (*select one statement only*):

a- adiabatic frictionless flow in a constant area duct with subsonic inlet conditions.
b- frictionless air flow in constant area duct with max. stagnation temperature at $M=\gamma^{-0.5}$
c- isentropic flow in a constant area duct with heating at constant stagnation temperature.
d- Isothermal air flow in a duct with maximum stagnation temperature at M=1.
e- Non of the above but the following: (*state five properties for Rayliegh Line flow*).

---

(36) Nitrogen (with $\gamma = 1.35$) flows subsonically in an adiabatic 2.54 cm diameter duct. The inlet conditions are: $M_1 = 0.1$, $P_1 = 2$ bar and $T_1 = 350$ K. The average friction factor may be assumed to be f = 0.024. (a) What type of flow is this? Find the length of the duct that is necessary to accelerate the flow to $M_2 = 0.5$, (b) Find the conditions P_2 , T_2 , V_2 and P_{o2} at section (2). Plot the T-S diagram for this flow. (use the following equations):

$$\frac{\bar{f}.L^*}{D} = \frac{1-M^2}{\gamma M^2} + \frac{\gamma+1}{2\gamma}\ln\left[\frac{(\gamma+1)M^2}{2+(\gamma-1)M^2}\right] \quad \text{.....,} \quad \frac{\bar{f}.\Delta L}{D} = \left(\frac{\bar{f}.L^*_1}{D}\right) - \left(\frac{\bar{f}.L^*_2}{D}\right)$$

$$\frac{T}{T^*} = \frac{a^2}{a^{*2}} = \frac{\gamma+1}{2+(\gamma-1)M^2} \quad \text{.....,} \quad \frac{P}{P^*} = \frac{1}{M}\left[\frac{\gamma+1}{2+(\gamma-1)M^2}\right]^{1/2}$$

$$\frac{\rho}{\rho^*} = \frac{V^*}{V} = \frac{1}{M}\left[\frac{2+(\gamma-1)M^2}{\gamma+1}\right]^{1/2} \quad \text{.....,} \quad \frac{P_o}{P_o^*} = \frac{\rho_o}{\rho_o^*} = \frac{1}{M}\left[\frac{2+(\gamma-1)M^2}{\gamma+1}\right]^{\frac{\gamma+1}{2(\gamma-1)}}$$

---

(37) The Fanno-Line flow has the following properties (*select one statement only*):

f- adiabatic frictionless flow in a constant area duct with subsonic inlet conditions.
g- frictionless air flow in constant area duct with max. stagnation temperature at $M=\gamma^{-0.5}$
h- isentropic flow in a constant area duct with heating at constant stagnation temperature.
i- Isothermal air flow in a duct with maximum stagnation temperature at M=1.
j- Non of the above but the following: (*state five properties for Rayliegh Line flow*).

---

(38) An industrial gas (with γ=1.4 and R=350 J/kg.K) flows with a negligible friction through a 0.1 m2 consant area duct. At the inlet section: V1= 53.7m/s, T1= 300 K, P1= 1.5 bar (abs.). The gas is heated along the duct so that the exit pressure is found to be P2 = 1.1175 bar (abs.) What type of flow is this? (a) Find stagnation conditions T_{O1} , P_{O1} & the Mach number M_1 at the inlet section. (b) Without using any tables find the exit conditions: V_2 , ρ_2, T_2 , M_2 , and T_{O2} , P_{O2}. (c)Find total amount of heat transferred to the gas in Kw,(Plot T-S diagram).

$$\frac{T_o}{T_o^*}=\frac{(\gamma+1)M^2\left[2+(\gamma-1)M^2\right]}{(1+\gamma.M^2)^2}\ldots\ldots\ldots,\frac{T}{T^*}=\frac{(\gamma+1)^2.M^2}{\left(1+\gamma.M^2\right)^2}\ldots\ldots\ldots\ldots\ldots,\frac{P}{P^*}=\frac{\gamma+1}{1+\gamma.M^2}$$

$$\frac{V}{V^*}=\frac{\rho^*}{\rho}=\frac{(\gamma+1)M^2}{1+\gamma.M^2}\ldots\ldots\ldots\ldots\ldots\ldots\ldots\ldots,\frac{P_o}{P_o^*}=\frac{\gamma+1}{1+\gamma.M^2}.\left[\frac{2+(\gamma-1)M^2}{\gamma+1}\right]^{\frac{\gamma}{\gamma-1}}$$

---

(39) The Fanno-Line flow has the following properties (*select one statement only*):

k- adiabatic frictionless flow in a constant area duct with subsonic inlet conditions.

l- frictionless air flow in constant area duct with max. stagnation temperature at M= $\gamma^{-0.5}$

m- isentropic flow in constant area duct with heating at constant stagnation temperature.

n- Isothermal air flow in a duct with maximum stagnation temperature at M=1.

o- Non of the above but the following: (*state five properties for Rayliegh Line flow*).

---

(40) Natural gas of molecular weight 18 and γ =1.35 is to be pumped through a pipe of 80 cm internal diameter connecting two compressor stations 70 km apart. At the upstream station, the pressure is 7 bar and at the downstream station, the pressure is 0.7 bar. Assuming that there is sufficient heat transfer through the pipe wall to keep the local static gas temperature at 40 oC everywhere along the flow, find: (a) the inlet and exit Mach number for the maximum mass flow rate in the pipe. (b) the maximum mass flow rate in the pipe in kg/sec. (c) the coefficient of friction associated with this pipe length. Plot the T-S diagram.

$$\frac{\bar{f}.L_{\max}}{D}=\frac{1-\gamma M^2}{\gamma M^2}+\ln(\gamma M^2).....,\frac{P_1}{P'}=\frac{1}{M_1.\gamma^{0.5}}.....,\frac{V_1}{V'}=\frac{\rho'}{\rho_1}=M_1.\gamma^{0.5}$$

$$\frac{P_1}{P_2}=\frac{\rho_1}{\rho_2}=\frac{V_2}{V_1}=\frac{M_2}{M_1}.....,G^2=(\dot{m}/A)^2=\frac{P_1^2-P_2^2}{R.T\left[(\bar{f}.L/D)+2\ln(P_1/P_2)\right]}$$

****

Word Problems

W .1 Notice from Table 6.1 that (*a*) water and mercury and (*b*) aluminum and steel have nearly the same speeds of sound, yet the second of the two materials is much denser. Can you account for this oddity? Can molecular theory explain it?

W .2 When an object approaches you at Ma = 0.8, you can hear it, according to Fig. 6.36a. But would there be a Doppler shift? For example, would a musical tone seem to you to have a higher or a lower pitch?

W .3 The subject of this chapter is commonly called *gas dynamics*. But can liquids not perform in this manner? Using water as an example, make a rule-of-thumb estimate of the pressure level needed to drive a water flow at velocities comparable to the sound speed.

W .4 Suppose a gas is driven at compressible subsonic speeds by a large pressure drop, p_1 to p_2. Describe its behavior on an appropriately labeled Mollier chart for (*a*) frictionless flow in a converging nozzle and (*b*) flow with friction in a long duct.

W .5 Describe physically what the "speed of sound" represents. What kind of pressure changes occur in air sound waves during ordinary conversation?

W .6 Give a physical description of the phenomenon of choking in a converging-nozzle gas flow. Could choking happen even if wall friction were not negligible?

W .7 Shock waves are treated as discontinuities here, but they actually have a very small finite thickness. After giving it some thought, sketch your idea of the distribution of gas velocity, pressure, temperature, and entropy through the inside of a shock wave.

W .8 Describe how an observer, running along a normal-shock wave at finite speed V, will see what appears to be an oblique-shock wave. Is there any limit to the running speed?

One-dimensional compressible-flow problems have become quite popular on the FE Exam, especially in the afternoon sessions. In the following problems, assume one-dimensional flow of ideal air, $R = 287$ J/(kg·K) and $k = 1.4$.

FE .1 For steady isentropic flow, if the absolute temperature increases 50 percent, by what ratio does the static pressure increase?
(*a*) 1.12, (*b*) 1.22, (*c*) 2.25, (*d*) 2.76, (*e*) 4.13

FE .2 For steady isentropic flow, if the density doubles, by what ratio does the static pressure increase?
(*a*) 1.22, (*b*) 1.32, (*c*) 1.44, (*d*) 2.64, (*e*) 5.66

FE .3 A large tank, at 500 K and 200 kPa, supplies isentropic airflow to a nozzle. At section 1, the pressure is only 120 kPa. What is the Mach number at this section?
(*a*) 0.63, (*b*) 0.78, (*c*) 0.89, (*d*) 1.00, (*e*) 1.83

FE .4 In Prob. FE .3 what is the temperature at section 1?
(*a*) 300 K, (*b*) 408 K, (*c*) 417 K, (*d*) 432 K, (*e*) 500 K

FE .7 If the exit Mach number in Fig. FE .6 is 2.2, what is the exit area?
(*a*) 0.10 m^2, (*b*) 0.12 m^2, (*c*) 0.15 m^2, (*d*) 0.18 m^2, (*e*) 0.22 m^2

FE .8 If there are no shock waves and the pressure at one duct section in Fig. FE .6 is 55.5 kPa, what is the velocity at that section?
(*a*) 166 m/s, (*b*) 232 m/s, (*c*) 554 m/s, (*d*) 706 m/s, (*e*) 774 m/s

FE .5 In Prob. FE .3, if the area at section 1 is 0.15 m^2, what is the mass flow?
(*a*) 38.1 kg/s, (*b*) 53.6 kg/s, (*c*) 57.8 kg/s, (*d*) 67.8 kg/s, (*e*) 77.2 kg/s

FE .6 For steady isentropic flow, what is the maximum possible mass flow through the duct in Fig. FE .6?
(*a*) 9.5 kg/s, (*b*) 15.1 kg/s, (*c*) 26.2 kg/s, (*d*) 30.3 kg/s, (*e*) 52.4 kg/s

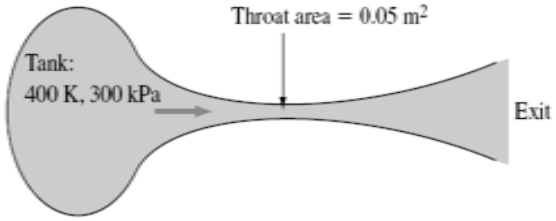

FE .6

FE .9 If, in Fig. FE .6, there is a normal shock wave at a section where the area is 0.07 m^2, what is the air density just upstream of that shock?
(*a*) 0.48 kg/m^3, (*b*) 0.78 kg/m^3, (*c*) 1.35 kg/m^3, (*d*) 1.61 kg/m^3, (*e*) 2.61 kg/m^3

FE .10 In Prob. FE .9, what is the Mach number just downstream of the shock wave?
(*a*) 0.42, (*b*) 0.55, (*c*) 0.63, (*d*) 1.00, (*e*) 1.76

Comprehensive Problems

C .1 The converging-diverging nozzle sketched in Fig. C9.1 is designed to have a Mach number of 2.00 at the exit plane (assuming the flow remains nearly isentropic). The flow travels from tank *a* to tank *b*, where tank *a* is much larger than tank *b*. (*a*) Find the area at the exit A_e and the back pressure p_b which will allow the system to operate at design conditions. (*b*) As time goes on, the back pressure will grow, since the second tank slowly fills up with more air. Since tank *a* is huge, the flow in the nozzle will remain the same, however, until a normal shock wave appears at the exit plane. At what back pressure will this occur? (*c*) If tank *b* is held at constant temperature, $T = 20°C$, estimate how long it will take for the flow to go from design conditions to the condition of part (*b*), i.e., with a shock wave at the exit plane.

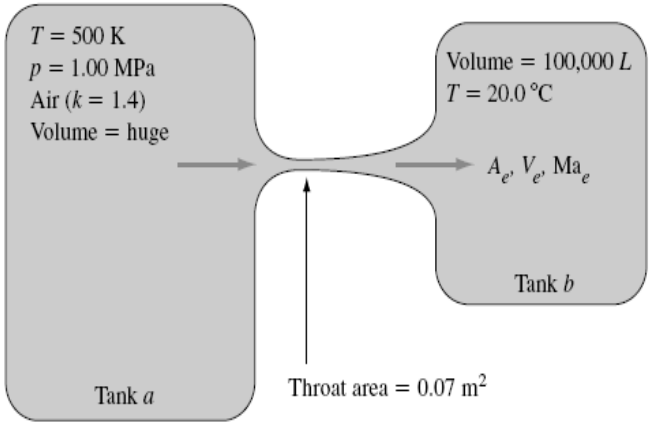

C .1

C .2 Two large air tanks, one at 400 K and 300 kPa and the other at 300 K and 100 kPa, are connected by a straight tube 6 m long and 5 cm in diameter. The average friction factor is 0.0225. Assuming adiabatic flow, estimate the mass flow through the tube.

***C .3** Figure C9.3 shows the exit of a converging-diverging nozzle, where an oblique-shock pattern is formed. In the exit plane, which has an area of 15 cm^2, the air pressure is 16 kPa and the temperature is 250 K. Just outside the exit shock, which makes an angle of 50° with the exit plane, the temperature is 430 K. Estimate (*a*) the mass flow, (*b*) the throat area, (*c*) the turning angle of the exit flow, and, in the tank supplying the air, (*d*) the pressure and (*e*) the temperature.

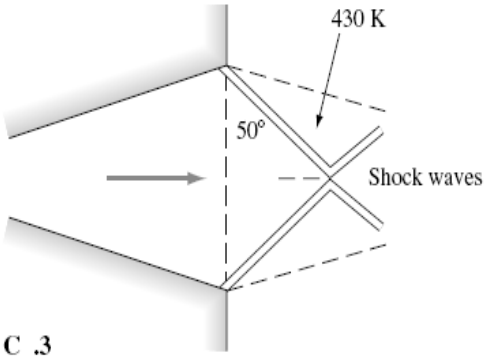

C .3

Problems on Part (6)

Most of the problems herein are fairly straightforward. More difficult or open-ended assignments are labeled with an asterisk. Problems labeled with an EES icon will benefit from the use of the Engineering Equations Solver (EES), while problems labeled with a computer icon may require the use of a computer. The standard end-of-chapter problems .1 to .157 (categorized in the problem list below) are given after word problems W .1 to W .8, fundamentals of engineering exam problems FE .1 to FE .10, comprehensive problems C .1 to C .3

Problem distribution

Section	Topic	Problems
1	Introduction	1– 9
2	The speed of sound	10– 18
3	Adiabatic and isentropic flow	19– 33
4	Isentropic flow with area changes	34– 53
5	The normal-shock wave	54– 62
6	Converging and diverging nozzles	63– 85
7	Duct flow with friction	86– 107
8	Frictionless duct flow with heat transfer	108– 115
9	Mach waves	116– 121
9	The oblique-shock wave	122– 139
10	Prandtl-Meyer expansion waves	140– 147
10	Supersonic airfoils	148– 157

P .1 An ideal gas flows adiabatically through a duct. At section 1, $p_1 = 140$ kPa, $T_1 = 260°C$, and $V_1 = 75$ m/s. Farther downstream, $p_2 = 30$ kPa and $T_2 = 207°C$. Calculate V_2 in m/s and $s_2 - s_1$ in J/(kg · K) if the gas is (*a*) air, $k = 1.4$, and (*b*) argon, $k = 1.67$.

P .2 Solve Prob. .1 if the gas is steam. Use two approaches: (*a*) an ideal gas from Table A.4 and (*b*) real gas data from the steam tables [15].

P .3 If 8 kg of oxygen in a closed tank at 200°C and 300 kPa is heated until the pressure rises to 400 kPa, calculate (*a*) the new temperature, (*b*) the total heat transfer, and (*c*) the change in entropy.

P .4 Compressibility effects become important when the Mach number exceeds approximately 0.3. How fast can a two-dimensional cylinder travel in sea-level standard air before compressibility becomes important *somewhere* in its vicinity?

P .5 Steam enters a nozzle at 377°C, 1.6 MPa, and a steady speed of 200 m/s and accelerates isentropically until it exits at saturation conditions. Estimate the exit velocity and temperature.

P .6 Is it possible for the steam in Prob. .5 to continue accelerating until it exits with a moisture content of 12 percent? If so, estimate the new exit velocity and temperature.

P .7 Carbon dioxide ($k = 1.28$) enters a constant-area duct at 400°F, 100 lbf/in^2 absolute, and 500 ft/s. Farther downstream the properties are $V_2 = 1000$ ft/s and $T_2 = 900°F$. Compute (*a*) p_2, (*b*) the heat added between sections, (*c*) the entropy change between sections, and (*d*) the mass flow per unit area. *Hint:* This problem requires the continuity equation.

P .8 Atmospheric air at 20°C enters and fills an insulated tank which is initially evacuated. Using a control-volume analysis from Eq. (3.63), compute the tank air temperature when it is full.

P .9 Liquid hydrogen and oxygen are burned in a combustion chamber and fed through a rocket nozzle which exhausts at $V_{exit} = 1600$ m/s to an ambient pressure of 54 kPa. The nozzle exit diameter is 45 cm, and the jet exit density is 0.15 kg/m^3. If the exhaust gas has a molecular weight of 18, estimate (*a*) the exit gas temperature, (*b*) the mass flow, and (*c*) the thrust developed by the rocket.

P .10 A certain aircraft flies at the same Mach number regardless of its altitude. Compared to its speed at 12,000-m standard altitude, it flies 127 km/h faster at sea level. Determine its Mach number.

P .11 At 300°C and 1 atm, estimate the speed of sound of (*a*) nitrogen, (*b*) hydrogen, (*c*) helium, (*d*) steam, and (*e*) $^{238}UF_6$ ($k \approx 1.06$).

P .12 Assume that water follows Eq. (1.19) with $n \approx 7$ and $B \approx 3000$. Compute the bulk modulus (in kPa) and the speed of sound (in m/s) at (*a*) 1 atm and (*b*) 1100 atm (the deepest part of the ocean). (*c*) Compute the speed of sound at 20°C and 9000 atm and compare with the measured value of 2650 m/s (A. H. Smith and A. W. Lawson, *J. Chem. Phys.*, vol. 22, 1954, p. 351).

P .13 From Prob. 1.33, mercury data fit Eq. (1.19) with $n \approx 6$ and $B \approx 41{,}000$. Estimate (*a*) the bulk modulus and (*b*) the speed of sound of mercury at 2500 atm and compare with Table .1.

P .14 Assume steady adiabatic flow of a perfect gas. Show that the energy equation (21), when plotted as speed of sound versus velocity, forms an ellipse. Sketch this ellipse; label the intercepts and the regions of subsonic, sonic, and supersonic flow; and determine the ratio of the major and minor axes.

P .15 A weak pressure wave (sound wave) with a pressure change $\Delta p = 40$ Pa propagates through air at 20°C and 1 atm. Estimate (*a*) the density change, (*b*) the temperature change, and (*c*) the velocity change across the wave.

P .16 A weak pressure pulse Δp propagates through still air. Discuss the type of reflected pulse which occurs and the boundary conditions which must be satisfied when the

wave strikes normal to, and is reflected from, (*a*) a solid wall and (*b*) a free liquid surface.

P .17 A submarine at a depth of 800 m sends a sonar signal and receives the reflected wave back from a similar submerged object in 15 s. Using Prob. .12 as a guide, estimate the distance to the other object.

***P .18** The properties of a dense gas (high pressure and low temperature) are often approximated by van der Waals' equation of state [17, 18]:

$$p = \frac{\rho RT}{1 - b_1\rho} - a_1\rho^2$$

where constants a_1 and b_1 can be found from the critical temperature and pressure

$$a_1 = \frac{27R^2T_c^2}{64p_c} = 9.0 \times 10^5 \text{ lbf} \cdot \text{ft}^4/\text{slug}^2$$

for air, and

$$b_1 = \frac{RT_c}{8p_c} = 0.65 \text{ ft}^3/\text{slug}$$

for air. Find an analytic expression for the speed of sound of a van der Waals gas. Assuming $k = 1.4$, compute the speed of sound of air in ft/s at −100°F and 20 atm for (*a*) a perfect gas and (*b*) a van der Waals gas. What percentage higher density does the van der Waals relation predict?

P .19 The Concorde aircraft flies at Ma ≈ 2.3 at 11-km standard altitude. Estimate the temperature in °C at the front stagnation point. At what Mach number would it have a front stagnation-point temperature of 450°C?

P .20 A gas flows at $V = 200$ m/s, $p = 125$ kPa, and $T = 200$°C. For (*a*) air and (*b*) helium, compute the maximum pressure and the maximum velocity attainable by expansion or compression.

P .21 Air expands isentropically through a duct from $p_1 = 125$ kPa and $T_1 = 100$°C to $p_2 = 80$ kPa and $V_2 = 325$ m/s. Compute (*a*) T_2, (*b*) Ma_2, (*c*) T_0, (*d*) p_0, (*e*) V_1, and (f) Ma_1.

P .22 Given the pitot stagnation temperature and pressure and the static-pressure measurements in Fig. P .22, estimate the air velocity V, assuming (*a*) incompressible flow and (*b*) compressible flow.

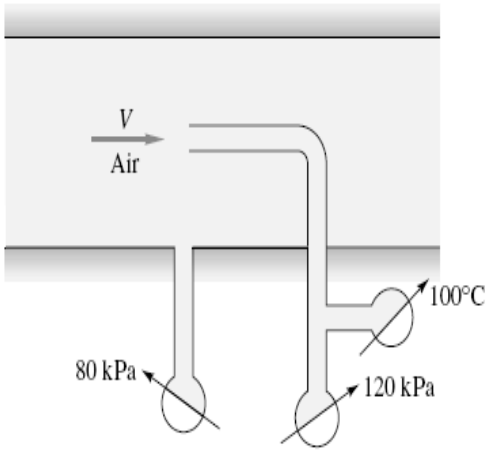

P .22

P .23 A large rocket engine delivers hydrogen at 1500°C and 3 MPa, $k = 1.41$, $R = 4124$ J/(kg·K), to a nozzle which exits with gas pressure equal to the ambient pressure of 54 kPa. Assuming isentropic flow, if the rocket thrust is 2 MN, what is (*a*) the exit velocity and (*b*) the mass flow of hydrogen?

P .24 For low-speed (nearly incompressible) gas flow, the stagnation pressure can be computed from Bernoulli's equation

$$p_0 = p + \frac{1}{2}\rho V^2$$

(*a*) For higher subsonic speeds, show that the isentropic relation (9.28*a*) can be expanded in a power series as follows:

$$p_0 \approx p + \frac{1}{2}\rho V^2\left(1 + \frac{1}{4}\text{Ma}^2 + \frac{2-k}{24}\text{Ma}^4 + \cdots\right)$$

(*b*) Suppose that a pitot-static tube in air measures the pressure difference $p_0 - p$ and uses the Bernoulli relation, with stagnation density, to estimate the gas velocity. At what Mach number will the error be 4 percent?

P .25 If it is known that the air velocity in the duct is 750 ft/s, use the mercury-manometer measurement in Fig. P .25 to estimate the static pressure in the duct in lbf/in^2 absolute.

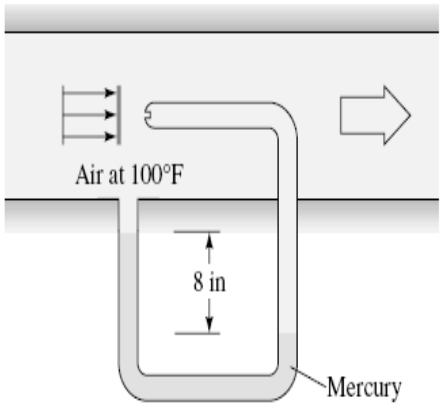

P .25

P .26 Show that for isentropic flow of a perfect gas if a pitot-static probe measures p_0, p, and T_0, the gas velocity can be calculated from

$$V^2 = 2c_pT_0\left[1 - \left(\frac{p}{p_0}\right)^{(k-1)/k}\right]$$

What would be a source of error if a shock wave were formed in front of the probe?

P .27 In many problems the sonic (*) properties are more useful reference values than the stagnation properties. For isentropic flow of a perfect gas, derive relations for p/p^*,

T/T^*, and ρ/ρ^* as functions of the Mach number. Let us help by giving the density-ratio formula:

$$\frac{\rho}{\rho^*} = \left[\frac{k+1}{2+(k-1)\,\mathrm{Ma}^2}\right]^{1/(k-1)}$$

P .28 A large vacuum tank, held at 60 kPa absolute, sucks sea-level standard air through a converging nozzle whose throat diameter is 3 cm. Estimate (*a*) the mass-flow rate through the nozzle and (*b*) the Mach number at the throat.

P .29 Steam from a large tank, where $T = 400°C$ and $p = 1$ MPa, expands isentropically through a nozzle until, at a section of 2-cm diameter, the pressure is 500 kPa. Using the steam tables [15], estimate (*a*) the temperature, (*b*) the velocity, and (*c*) the mass flow at this section. Is the flow subsonic?

P .30 Air flows in a duct of diameter 5 cm. At one section, $T_0 = 300°C$, $p = 120$ kPa, and $\dot{m} = 0.4$ kg/s. Estimate, at this section, (*a*) V, (*b*) Ma, and (*c*) ρ_0.

P .31 Air flows adiabatically through a duct. At one section $V_1 = 400$ ft/s, $T_1 = 200°F$, and $p_1 = 35$ lbf/in^2 absolute, while farther downstream $V_2 = 1100$ ft/s and $p_2 = 18$ lbf/in^2 absolute. Compute (*a*) Ma_2, (*b*) $U_{\max}$, and (*c*) p_{02}/p_{01}.

P .32 The large compressed-air tank in Fig. P .32 exhausts from a nozzle at an exit velocity of 235 m/s. The mercury manometer reads $h = 30$ cm. Assuming isentropic flow, compute the pressure (*a*) in the tank and (*b*) in the atmosphere. (*c*) What is the exit Mach number?

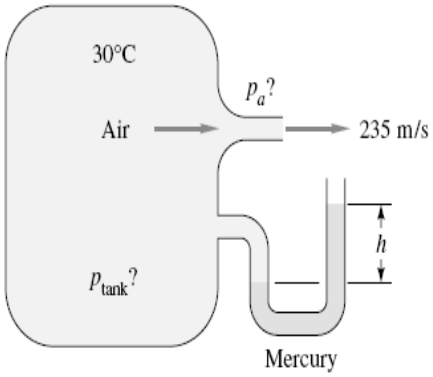

P .32

P .33 Air flows isentropically from a reservoir, where $p = 300$ kPa and $T = 500$ K, to section 1 in a duct, where $A_1 = 0.2$ m^2 and $V_1 = 550$ m/s. Compute (*a*) Ma_1, (*b*) T_1, (*c*) p_1, (*d*) $\dot{m}$, and (*e*) A^*. Is the flow choked?

P .34 Steam in a tank at 450°F and 100 lbf/in^2 absolute exhausts through a converging nozzle of 0.1-in^2 throat area to a 1-atm environment. Compute the initial mass flow (*a*) for an ideal gas and (*b*) from the steam tables [15].

P .35 Helium, at $T_0 = 400$ K, enters a nozzle isentropically. At section 1, where $A_1 = 0.1$ m^2, a pitot-static arrangement (see Fig. P .25) measures stagnation pressure of 150 kPa and static pressure of 123 kPa. Estimate (*a*) Ma_1, (*b*) mass flow $\dot{m}$, (*c*) T_1, and (*d*) A^*.

P .36 An air tank of volume 1.5 m^3 is initially at 800 kPa and 20°C. At $t = 0$, it begins exhausting through a converging nozzle to sea-level conditions. The throat area is 0.75 cm^2. Estimate (*a*) the initial mass flow in kg/s, (*b*) the time required to blow down to 500 kPa, and (*c*) the time at which the nozzle ceases being choked.

P .37 Make an exact control-volume analysis of the blowdown process in Fig. P .37, assuming an insulated tank with negligible kinetic and potential energy within. Assume critical flow at the exit, and show that both p_0 and T_0 decrease during blowdown. Set up first-order differential equations for $p_0(t)$ and $T_0(t)$, and reduce and solve as far as you can.

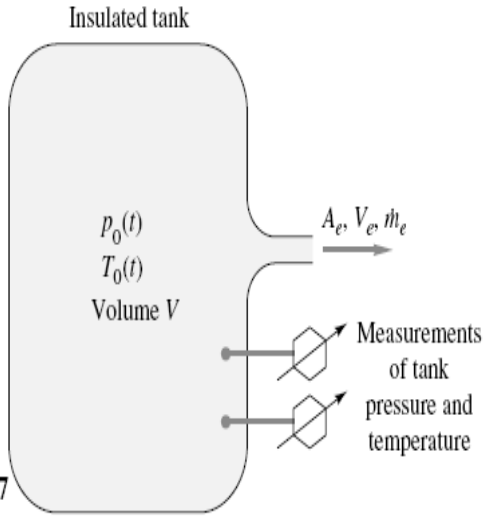

P .37

P .38 Prob. .37 makes an ideal senior project or combined laboratory and computer problem, as described in Ref. 30, sec. 8.6. In Bober and Kenyon's lab experiment, the tank had a volume of 0.0352 ft^3 and was initially filled with air at 50 lb/in^2 gage and 72°F. Atmospheric pressure was 14.5 lb/in^2 absolute, and the nozzle exit diameter was 0.05 in. After 2 s of blowdown, the measured tank pressure was 20 lb/in^2 gage and the tank temperature was −5°F. Compare these values with the theoretical analysis of Prob. 9.37.

P .39 Consider isentropic flow in a channel of varying area, from section 1 to section 2. We know that $\mathrm{Ma}_1 = 2.0$ and desire that the velocity ratio V_2/V_1 be 1.2. Estimate (*a*) Ma_2 and (*b*) A_2/A_1. (*c*) Sketch what this channel looks like. For example, does it converge or diverge? Is there a throat?

P9.40 Air, with stagnation conditions of 800 kPa and 100°C, expands isentropically to a section of a duct where $A_1 = 20$ cm^2 and $p_1 = 47$ kPa. Compute (*a*) Ma_1, (*b*) the throat area, and (*c*) $\dot{m}$. At section 2 between the throat and section 1, the area is 9 cm^2. (*d*) Estimate the Mach number at section 2.

P .41 Air, with a stagnation pressure of 100 kPa, flows through the nozzle in Fig. P .41, which is 2 m long and has an area variation approximated by

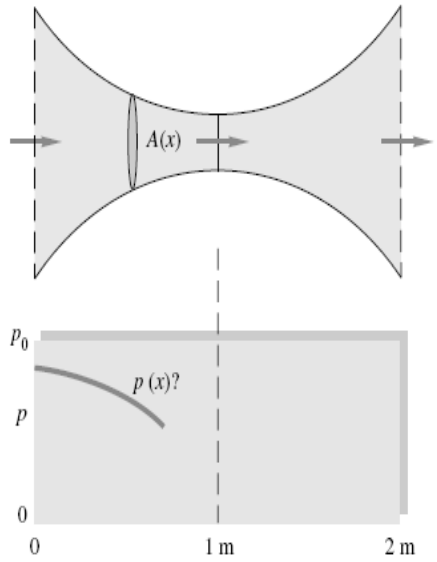

P .41

$$A \approx 20 - 20x + 10x^2$$

with A in cm^2 and x in m. It is desired to plot the complete family of isentropic pressures $p(x)$ in this nozzle, for the range of inlet pressures $1 < p(0) < 100$ kPa. Indicate those inlet pressures which are not physically possible and discuss briefly. If your computer has an online graphics routine, plot at least 15 pressure profiles; otherwise just hit the highlights and explain.

P .42 A bicycle tire is filled with air at an absolute pressure of 169.12 kPa, and the temperature inside is 30.0°C. Suppose the valve breaks, and air starts to exhaust out of the tire into the atmosphere (p_a = 100 kPa absolute and T_a = 20.0°C). The valve exit is 2.00 mm in diameter and is the smallest cross-sectional area of the entire system. Frictional losses can be ignored here, i.e., one-dimensional isentropic flow is a reasonable assumption. (*a*) Find the Mach number, velocity, and temperature at the exit plane of the valve (initially). (*b*) Find the initial mass-flow rate out of the tire. (*c*) Estimate the velocity at the exit plane using the incompressible Bernoulli equation. How well does this estimate agree with the "exact" answer of part (*a*)? Explain.

P .43 Air flows isentropically through a duct with T_0 = 300°C. At two sections with identical areas of 25 cm^2, the pressures are p_1 = 120 kPa and p_2 = 60 kPa. Determine (*a*) the mass flow, (*b*) the throat area, and (*c*) Ma_2.

P .44 In Prob. we knew nothing about compressible flow at the time, so we merely assumed exit conditions p_2 and T_2 and computed V_2 as an application of the continuity equation. Suppose that the throat diameter is 3 in. For the given stagnation conditions in the rocket chamber in Fig. P and assuming k = 1.4 and a molecular weight of 26, compute the actual exit velocity, pressure, and temperature according to one-dimensional theory. If p_a = 14.7 lbf/in^2 absolute, compute the thrust from the analysis of Prob. 3.68. This thrust is entirely independent of the stagnation temperature (check this by changing T_0 to 2000°R if you like). Why?

P .45 At a point upstream of the throat of a converging-diverging nozzle the properties are V_1 = 200 m/s, T_1 = 300 K, and p_1 = 125 kPa. If the exit flow is supersonic, compute, from isentropic theory, (*a*) $\dot{m}$ and (*b*) A_1. The throat area is 35 cm^2.

P .46 If the author did not falter, the results of Prob. .43 are (*a*) 0.671 kg/s, (*b*) 23.3 cm^2, and (*c*) 1.32. Do not tell your friends who are still working on Prob. .43. Consider a control volume which encloses the nozzle between these two 25-cm^2 sections. If the pressure outside the duct is 1 atm, determine the total force acting on this section of nozzle.

P .47 In wind-tunnel testing near Mach 1, a small area decrease caused by model blockage can be important. Suppose the test section area is 1 m^2, with unblocked test conditions Ma = 1.10 and T = 20°C. What model area will first cause the test section to choke? If the model cross section is 0.004 m^2 (0.4 percent blockage), what percentage change in test-section velocity results?

P .48 A force F = 1100 N pushes a piston of diameter 12 cm through an insulated cylinder containing air at 20°C, as in Fig. P .48. The exit diameter is 3 mm, and p_a = 1 atm. Estimate (*a*) V_e, (*b*) V_p, and (*c*) $\dot{m}_e$.

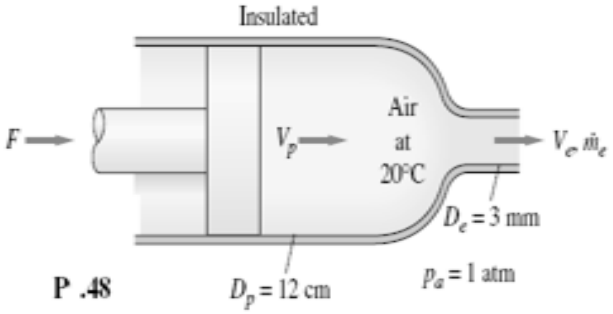

P .48

P .49 Air expands through a nozzle and exits supersonically. The throat area is 10 cm^2, and the throat pressure is 100 kPa. Find the pressure on either side of the throat where the duct area is 24 cm^2.

P .50 Argon expands isentropically in a converging nozzle whose entrance conditions are D_1 = 10 cm, p_1 = 150 kPa, T_1 = 100°C, and $\dot{m}$ = 1 kg/s. The flow discharges smoothly to an ambient pressure of 101 kPa. (*a*) What is the exit diameter of the nozzle? (*b*) How much further can the ambient pressure be reduced before it affects the inlet mass flow?

P .51 Air, at stagnation conditions of 500 K and 200 kPa, flows through a nozzle. At section 1, where the area is 12 cm^2,

the density is 0.32 kg/m^3. Assuming isentropic flow, (*a*) find the mass flow. (*b*) Is the flow choked? If so, estimate A^*. Also estimate (*c*) p_1 and (*d*) Ma_1.

P .52 A converging-diverging nozzle exits smoothly to sea-level standard atmosphere. It is supplied by a 40-m^3 tank initially at 800 kPa and 100°C. Assuming isentropic flow in the nozzle, estimate (*a*) the throat area and (*b*) the tank pressure after 10 s of operation. The exit area is 10 cm^2.

P .53 Air flows steadily from a reservoir at 20°C through a nozzle of exit area 20 cm^2 and strikes a vertical plate as in Fig. P .53. The flow is subsonic throughout. A force of 135 N is required to hold the plate stationary. Compute (*a*) V_e, (*b*) Ma_e, and (*c*) p_0 if p_a = 101 kPa.

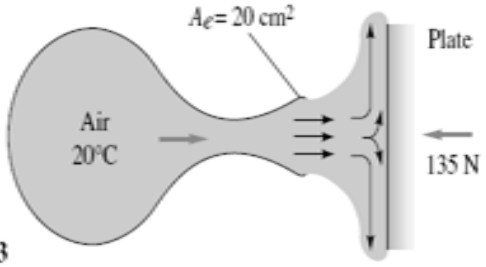

P .53

P .54 For flow of air through a normal shock the upstream conditions are V_1 = 600 m/s, T_{01} = 500 K, and p_{01} = 700 kPa. Compute the downstream conditions Ma_2, V_2, T_2, p_2, and p_{02}.

P .55 Air, supplied by a reservoir at 450 kPa, flows through a converging-diverging nozzle whose throat area is 12 cm^2. A normal shock stands where A_1 = 20 cm^2. (*a*) Compute the pressure just downstream of this shock. Still farther downstream, at A_3 = 30 cm^2, estimate (*b*) p_3, (*c*) A_3^*, and (*d*) Ma_3.

P .56 Air from a reservoir at 20°C and 500 kPa flows through a duct and forms a normal shock downstream of a throat of area 10 cm^2. By an odd coincidence it is found that the stagnation pressure downstream of this shock exactly equals the throat pressure. What is the area where the shock wave stands?

P .57 Air flows from a tank through a nozzle into the standard atmosphere, as in Fig. P .57. A normal shock stands in the exit of the nozzle, as shown. Estimate (*a*) the pressure in the tank and (*b*) the mass flow.

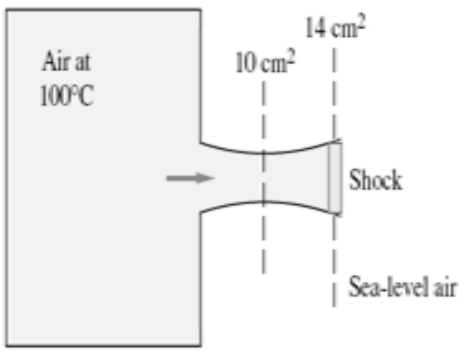

P .57

P .58 Argon (Table A.4) approaches a normal shock with V_1 = 700 m/s, p_1 = 125 kPa, and T_1 = 350 K. Estimate (*a*) V_2 and (*b*) p_2. (*c*) What pressure p_2 would result if the same velocity change V_1 to V_2 were accomplished isentropically?

P .59 Air, at stagnation conditions of 450 K and 250 kPa, flows through a nozzle. At section 1, where the area is 15 cm^2, there is a normal shock wave. If the mass flow is 0.4 kg/s, estimate (*a*) the Mach number and (*b*) the stagnation pressure just downstream of the shock.

P .60 When a pitot tube such as in Fig. 6.30 is placed in a supersonic flow, a normal shock will stand in front of the probe. Suppose the probe reads p_0 = 190 kPa and p = 150 kPa. If the stagnation temperature is 400 K, estimate the (supersonic) Mach number and velocity upstream of the shock.

P .61 Repeat Prob. .56 except this time let the odd coincidence be that the *static* pressure downstream of the shock exactly equals the throat pressure. What is the area where the shock stands?

P .62 An atomic explosion propagates into still air at 14.7 lbf/in^2 absolute and 520°R. The pressure just inside the shock is 5000 lbf/in^2 absolute. Assuming k = 1.4, what are the speed C of the shock and the velocity V just inside the shock?

P .63 Sea-level standard air is sucked into a vacuum tank through a nozzle, as in Fig. P .63. A normal shock stands where the nozzle area is 2 cm^2, as shown. Estimate (*a*) the pressure in the tank and (*b*) the mass flow.

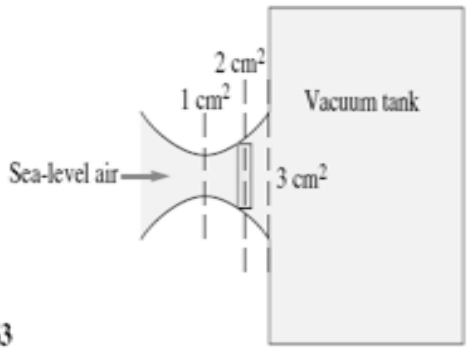

P .63

P .64 Air in a large tank at 100°C and 150 kPa exhausts to the atmosphere through a converging nozzle with a 5-cm^2 throat area. Compute the exit mass flow if the atmospheric pressure is (*a*) 100 kPa, (*b*) 60 kPa, and (*c*) 30 kPa.

P .65 Air flows through a converging-diverging nozzle between two large reservoirs, as shown in Fig. P .65. A mercury manometer between the throat and the downstream reservoir reads h = 15 cm. Estimate the downstream reservoir pressure. Is there a normal shock in the flow? If so, does it stand in the exit plane or farther upstream?

P .66 In Prob. .65 what would be the mercury-manometer reading h if the nozzle were operating exactly at supersonic design conditions?

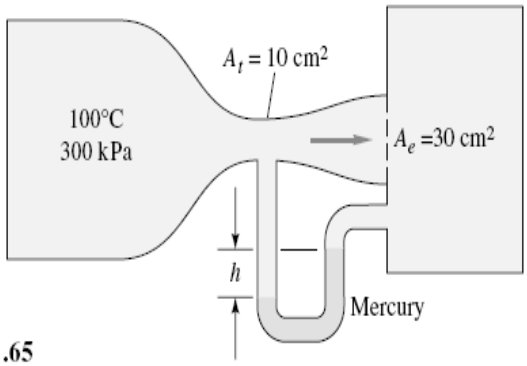

P .65

P .67 In Prob. .65 estimate the complete range of manometer readings h for which the flow through the nozzle is entirely isentropic, except possibly in the exit plane.

P .68 Air in a tank at 120 kPa and 300 K exhausts to the atmosphere through a 5-cm^2-throat converging nozzle at a rate of 0.12 kg/s. What is the atmospheric pressure? What is the maximum mass flow possible at low atmospheric pressure?

P .69 With reference to Prob. 3.68, show that the thrust of a rocket engine exhausting into a vacuum is given by

$$F = \frac{p_0 A_e (1 + k\,\mathrm{Ma}_e^2)}{\left(1 + \dfrac{k-1}{2}\,\mathrm{Ma}_e^2\right)^{k/(k-1)}}$$

where A_e = exit area
Ma_e = exit Mach number
p_0 = stagnation pressure in combustion chamber

Note that stagnation temperature does not enter into the thrust.

P 70 Air, at stagnation temperature 100°C, expands isentropically through a nozzle of 6-cm^2 throat area and 18-cm^2 exit area. The mass flow is at its maximum value of 0.5 kg/s. Estimate the exit pressure for (*a*) subsonic and (*b*) supersonic exit flow.

P .71 For the nozzle of Prob. .70, allowing for nonisentropic flow, what is the range of exit tank pressures p_b for which (*a*) the diverging nozzle flow is fully supersonic, (*b*) the exit flow is subsonic, (*c*) the mass flow is independent of p_b, (*d*) the exit plane pressure p_e is independent of p_b, and (*e*) $p_e < p_b$?

P .72 Suppose the nozzle flow of Prob. .70 is not isentropic but instead has a normal shock at the position where area is 15 cm^2. Compute the resulting mass flow, exit pressure, and exit Mach number.

P .73 Air flows isentropically in a converging-diverging nozzle with a throat area of 3 cm^2. At section 1, the pressure is 101 kPa, the temperature is 300 K, and the velocity is 868 m/s. (*a*) Is the nozzle choked? Determine (*b*) A_1 and (*c*) the mass flow. Suppose, without changing stagnation conditions or A_1, the (flexible) throat is reduced to 2 cm^2. Assuming shock-free flow, will there be any change in the gas properties at section 1? If so, compute new p_1, V_1, and T_1 and explain.

P .74 The perfect-gas assumption leads smoothly to Mach-number relations which are very convenient (and tabulated). This is not so for a real gas such as steam. To illustrate, let steam at T_0 = 500°C and p_0 = 2 MPa expand isentropically through a converging nozzle whose exit area is 10 cm^2. Using the steam tables, find (*a*) the exit pressure and (*b*) the mass flow when the flow is sonic, or choked. What complicates the analysis?

***P .75** A double-tank system in Fig. P .75 has two identical converging nozzles of 1-in^2 throat area. Tank 1 is very large, and tank 2 is small enough to be in steady-flow equilibrium with the jet from tank 1. Nozzle flow is isentropic, but entropy changes between 1 and 3 due to jet dissipation in tank 2. Compute the mass flow. (If you give up, Ref. 14, pp. 288–290, has a good discussion.)

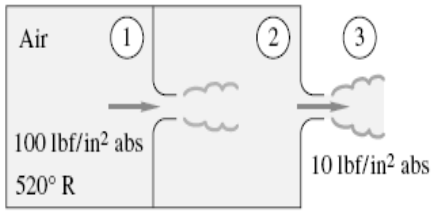

P .75

P .76 A large reservoir at 20°C and 800 kPa is used to fill a small insulated tank through a converging-diverging nozzle with 1-cm^2 throat area and 1.66-cm^2 exit area. The small tank has a volume of 1 m^3 and is initially at 20°C and 100 kPa. Estimate the elapsed time when (*a*) shock waves begin to appear inside the nozzle and (*b*) the mass flow begins to drop below its maximum value.

P .77 A perfect gas (not air) expands isentropically through a supersonic nozzle with an exit area 5 times its throat area. The exit Mach number is 3.8. What is the specific-heat ratio of the gas? What might this gas be? If p_0 = 300 kPa, what is the exit pressure of the gas?

P .78 The orientation of a hole can make a difference. Consider holes *A* and *B* in Fig. P .78, which are identical but reversed. For the given air properties on either side, compute the mass flow through each hole and explain why they are different.

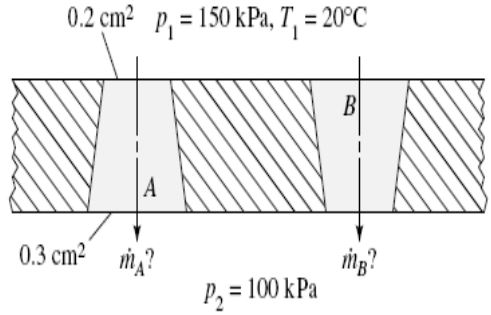

P .78

P .79 Air with $p_0 = 300$ kPa and $T_0 = 500$ K flows through a converging-diverging nozzle with throat area of 1 cm^2 and exit area of 3 cm^2 into a receiver tank. The mass flow is 195.2 kg/h. For what range of receiver pressure is this mass flow possible?

P .80 A sea-level automobile tire is initially at 32 lbf/in^2 gage pressure and 75°F. When it is punctured with a hole which resembles a converging nozzle, its pressure drops to 15 lbf/in^2 gage in 12 min. Estimate the size of the hole, in thousandths of an inch. The tire volume is 2.5 ft^2.

P .81 Helium, in a large tank at 100°C and 400 kPa, discharges to a receiver through a converging-diverging nozzle designed to exit at Ma = 2.5 with exit area 1.2 cm^2. Compute (*a*) the receiver pressure and (*b*) the mass flow at design conditions. (*c*) Also estimate the range of receiver pressures for which mass flow will be a maximum.

P .82 Air at 500 K flows through a converging-diverging nozzle with throat area of 1 cm^2 and exit area of 2.7 cm^2. When the mass flow is 182.2 kg/h, a pitot-static probe placed in the exit plane reads $p_0 = 250.6$ kPa and $p = 240.1$ kPa. Estimate the exit velocity. Is there a normal shock wave in the duct? If so, compute the Mach number just downstream of this shock.

P .83 When operating at design conditions (smooth exit to sea-level pressure), a rocket engine has a thrust of 1 million lbf. The chamber pressure and temperature are 600 lbf/in^2 absolute and 4000°R, respectively. The exhaust gases approximate $k = 1.38$ with a molecular weight of 26. Estimate (*a*) the exit Mach number and (*b*) the throat diameter.

P .84 Air flows through a duct as in Fig. P .84, where $A_1 = 24$ cm^2, $A_2 = 18$ cm^2, and $A_3 = 32$ cm^2. A normal shock stands at section 2. Compute (*a*) the mass flow, (*b*) the Mach number, and (*c*) the stagnation pressure at section 3.

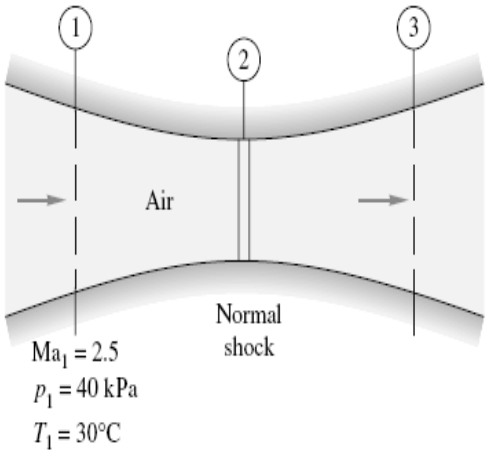

P .84

P .85 A large tank delivers air through a nozzle of 1-cm^2 throat area and 2.7-cm^2 exit area. When the receiver pressure is 125 kPa, a normal shock stands in the exit plane. Estimate (*a*) the throat pressure and (*b*) the stagnation pressure in the upstream supply tank.

P .86 Air enters a 3-cm-diameter pipe 15 m long at $V_1 = 73$ m/s, $p_1 = 550$ kPa, and $T_1 = 60$°C. The friction factor is 0.018. Compute V_2, p_2, T_2, and p_{02} at the end of the pipe. How much additional pipe length would cause the exit flow to be sonic?

P .87 Air enters a duct of $L/D = 40$ at $V_1 = 170$ m/s and $T_1 = 300$ K. The flow at the exit is choked. What is the average friction factor in the duct for adiabatic flow?

P .88 Air enters a 5- by 5-cm square duct at $V_1 = 900$ m/s and $T_1 = 300$ K. The friction factor is 0.02. For what length duct will the flow exactly decelerate to Ma = 1.0? If the duct length is 2 m, will there be a normal shock in the duct? If so, at what Mach number will it occur?

P .89 Air flows adiabatically in a 5-cm-diameter tube with $f \approx 0.025$. At section 1, $V_1 = 75$ m/s, $T_1 = 350$ K, and $p_1 = 300$ kPa. How much further down the tube will (*a*) the pressure be 156 kPa, (*b*) the temperature be 343 K, and (*c*) the flow reach the choking point?

P .90 Air, supplied at $p_0 = 700$ kPa and $T_0 = 330$ K, flows through a converging nozzle into a pipe of 2.5-cm diameter which exits to a near vacuum. If $\bar{f} = 0.022$, what will be the mass flow through the pipe if its length is (*a*) 0 m, (*b*) 1 m, and (*c*) 10 m?

P .91 Air flows steadily from a tank through the pipe in Fig. P9.91. There is a converging nozzle on the end. If the mass flow is 3 kg/s and the nozzle is choked, estimate (*a*) the Mach number at section 1 and (*b*) the pressure inside the tank.

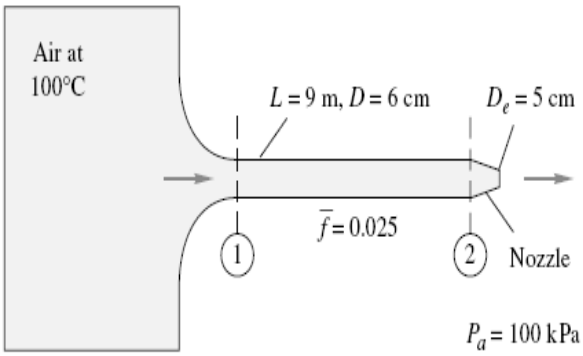

P .91

P .92 Modify Prob. .91 as follows. Let the pressure in the tank be 700 kPa, and let the nozzle be choked. Determine (*a*) Ma$_2$ and (*b*) the mass flow.

P .93 Air flows adiabatically in a 3-cm-diameter duct. The average friction factor is 0.015. If, at the entrance, $V = 950$ m/s and $T = 250$ K, how far down the tube will (*a*) the Mach number be 1.8 or (*b*) the flow be choked?

P .94 Compressible pipe flow with friction, Sec. .7, assumes constant stagnation enthalpy and mass flow but variable

momentum. Such a flow is often called *Fanno flow*, and a line representing all possible property changes on a temperature-entropy chart is called a *Fanno line*. Assuming a perfect gas with $k = 1.4$ and the data of Prob. .86, draw a Fanno curve of the flow for a range of velocities from very low (Ma $\ll 1$) to very high (Ma $\gg 1$). Comment on the meaning of the maximum-entropy point on this curve.

P .95 Helium (Table A.4) enters a 5-cm-diameter pipe at $p_1 =$ 550 kPa, $V_1 = 312$ m/s, and $T_1 = 40°C$. The friction factor is 0.025. If the flow is choked, determine (*a*) the length of the duct and (*b*) the exit pressure.

P .96 Derive and verify the adiabatic-pipe-flow velocity relation of Eq. (.74), which is usually written in the form

$$\frac{\bar{f}L}{D} + \frac{k+1}{k}\ln\frac{V_2}{V_1} = \frac{a_0^2}{k}\left(\frac{1}{V_1^2} - \frac{1}{V_2^2}\right)$$

P .97 By making a few algebraic substitutions, show that Eq. (.74), or the relation in Prob. .96, may be written in the density form

$$\rho_1^2 = \rho_2^2 + \rho^{*2}\left(\frac{2k}{k+1}\frac{\bar{f}L}{D} + 2\ln\frac{\rho_1}{\rho_2}\right)$$

Why is this formula awkward if one is trying to solve for the mass flow when the pressures are given at sections 1 and 2?

P .98 Compressible *laminar* flow, $f \approx 64/\mathrm{Re}$, may occur in capillary tubes. Consider air, at stagnation conditions of 100°C and 200 kPa, entering a tube 3 cm long and 0.1 mm in diameter. If the receiver pressure is near vacuum, estimate (*a*) the average Reynolds number, (*b*) the Mach number at the entrance, and (*c*) the mass flow in kg/h.

P .99 A compressor forces air through a smooth pipe 20 m long and 4 cm in diameter, as in Fig. P .99. The air leaves at 101 kPa and 200°C. The compressor data for pressure rise versus mass flow are shown in the figure. Using the Moody chart to estimate $\bar{f}$, compute the resulting mass flow.

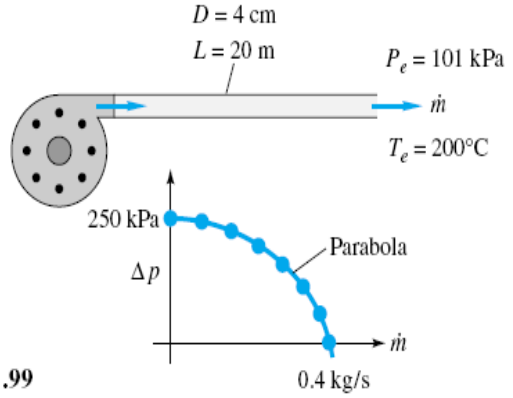

P .99

P .100 Modify Prob. .99 as follows. Find the length of 4-cm-diameter pipe for which the pump pressure rise will be exactly 200 kPa.

P .101 How do the compressible-pipe-flow formulas behave for small pressure drops? Let air at 20°C enter a tube of diameter 1 cm and length 3 m. If $\bar{f} = 0.028$ with $p_1 = 102$ kPa and $p_2 = 100$ kPa, estimate the mass flow in kg/h for (*a*) isothermal flow, (*b*) adiabatic flow, and (*c*) incompressible flow (Chap. 6) at the entrance density.

P .102 Air at 550 kPa and 100°C enters a smooth 1-m-long pipe and then passes through a second smooth pipe to a 30-kPa reservoir, as in Fig. P .102. Using the Moody chart to compute $\bar{f}$, estimate the mass flow through this system. Is the flow choked?

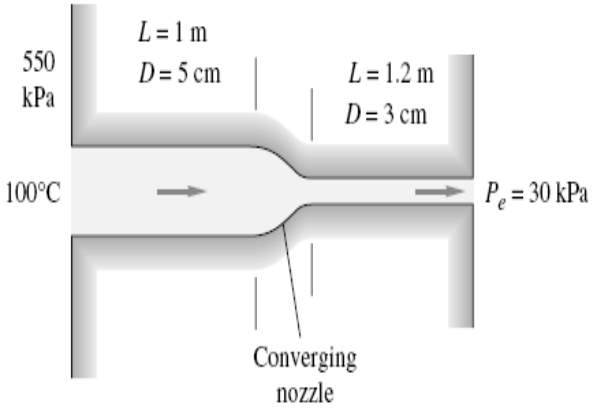

P .102

P .103 Natural gas, with $k \approx 1.3$ and a molecular weight of 16, is to be pumped through 100 km of 81-cm-diameter pipeline. The downstream pressure is 150 kPa. If the gas enters at 60°C, the mass flow is 20 kg/s, and $\bar{f} = 0.024$, estimate the required entrance pressure for (*a*) isothermal flow and (*b*) adiabatic flow.

P .104 A tank of oxygen (Table A.4) at 20°C is to supply an astronaut through an umbilical tube 12 m long and 2 cm in diameter. The exit pressure in the tube is 40 kPa. If the desired mass flow is 90 kg/h and $\bar{f} = 0.025$, what should be the pressure in the tank?

P .105 Air enters a 5-cm-diameter pipe at $p_1 = 200$ kPa and $T_1 =$ 350 K. The downstream receiver pressure is 74 kPa. The friction factor is 0.02. If the exit is choked, what is (*a*) the length of the pipe and (*b*) the mass flow? (*c*) If p_1, T_1, and p_{receiver} stay the same, what pipe length will cause the mass flow to increase by 50 percent over (*b*)? *Hint*: In part (*c*) the exit pressure does not equal the receiver pressure.

P .106 Air at 300 K flows through a duct 50 m long with $\bar{f} =$ 0.019. What is the minimum duct diameter which can carry the flow without choking if the entrance velocity is (*a*) 50 m/s, (*b*) 150 m/s, and (*c*) 420 m/s?

P .107 A fuel-air mixture, assumed equivalent to air, enters a duct combustion chamber at $V_1 = 104$ m/s and $T_1 = 300$ K. What amount of heat addition in kJ/kg will cause the exit flow to be choked? What will be the exit Mach number and temperature if 504 kJ/kg is added during combustion?

P .108 What happens to the inlet flow of Prob. .107 if the combustion yields 1500 kJ/kg heat addition and p_{01} and T_{01} remain the same? How much is the mass flow reduced?

P .109 A jet engine at 7000-m altitude takes in 45 kg/s of air and adds 550 kJ/kg in the combustion chamber. The chamber cross section is 0.5 m^2, and the air enters the chamber at 80 kPa and 5°C. After combustion the air expands through an isentropic converging nozzle to exit at atmospheric pressure. Estimate (*a*) the nozzle throat diameter, (*b*) the nozzle exit velocity, and (*c*) the thrust produced by the engine.

P .110 Compressible pipe flow with heat addition, Sec. .8, assumes constant momentum ($p + \rho V^2$) and constant mass flow but variable stagnation enthalpy. Such a flow is often called *Rayleigh flow*, and a line representing all possible property changes on a temperature-entropy chart is called a *Rayleigh line*. Assuming air passing through the flow state p_1 = 548 kPa, T_1 = 588 K, V_1 = 266 m/s, and A = 1 m^2, draw a Rayleigh curve of the flow for a range of velocities from very low (Ma $\ll$ 1) to very high (Ma $\gg$ 1). Comment on the meaning of the maximum-entropy point on this curve.

P .111 Add to your Rayleigh line of Prob. .110 a Fanno line (see Prob. .94) for stagnation enthalpy equal to the value associated with state 1 in Prob. .110. The two curves will intersect at state 1, which is subsonic, and at a certain state 2, which is supersonic. Interpret these two states vis-à-vis Table B 6.2

P .112 Air enters a duct subsonically at section 1 at 1.2 kg/s. When 650 kW of heat is added, the flow chokes at the exit at p_2 = 95 kPa and T_2 = 700 K. Assuming frictionless heat addition, estimate (*a*) the velocity and (*b*) the stagnation pressure at section 1.

P .113 Air enters a constant-area duct at p_1 = 90 kPa, V_1 = 520 m/s, and T_1 = 558°C. It is then cooled with negligible friction until it exits at p_2 = 160 kPa. Estimate (*a*) V_2, (*b*) T_2, and (*c*) the total amount of cooling in kJ/kg.

P .114 We have simplified things here by separating friction (Sec. .7) from heat addition (Sec. .8). Actually, they often occur together, and their effects must be evaluated simultaneously. Show that, for flow with friction *and* heat transfer in a constant-diameter pipe, the continuity, momentum, and energy equations may be combined into the following differential equation for Mach-number changes:

$$\frac{d\,\mathrm{Ma}^2}{\mathrm{Ma}^2} = \frac{1 + k\,\mathrm{Ma}^2}{1 - \mathrm{Ma}^2}\frac{dQ}{c_pT} + \frac{k\,\mathrm{Ma}^2\,[2 + (k-1)\,\mathrm{Ma}^2]}{2(1 - \mathrm{Ma}^2)}\frac{f\,dx}{D}$$

where dQ is the heat added. A complete derivation, including many additional combined effects such as area change and mass addition, is given in chap. 8 of Ref. 8.

P .115 Air flows subsonically in a duct with negligible friction. When heat is added in the amount of 948 kJ/kg, the pressure drops from p_1 = 200 to p_2 = 106 kPa. Estimate (*a*) Ma_1, (*b*) T_1, and (*c*) V_1, assuming T_{01} = 305 K.

P .116 An observer at sea level does not hear an aircraft flying at 12,000-ft standard altitude until it is 5 (statute) mi past her. Estimate the aircraft speed in ft/s.

P .117 An observer at sea level does not hear an aircraft flying at 6000-m standard altitude until 15 s after it has passed overhead. Estimate the aircraft speed in m/s.

P .118 A particle moving at uniform velocity in sea-level standard air creates the two disturbance spheres shown in Fig. P .118. Compute the particle velocity and Mach number.

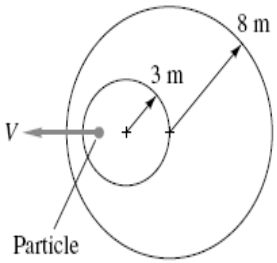

P .118

P .119 The particle in Fig. P .119 is moving supersonically in sea-level standard air. From the two given disturbance spheres, compute the particle Mach number, velocity, and Mach angle.

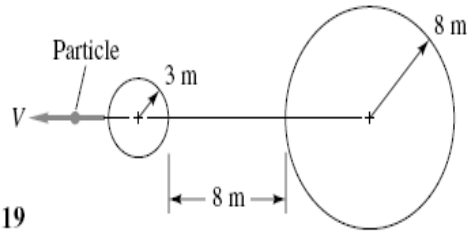

P .119

P .120 The particle in Fig. P 120 is moving in sea-level standard air. From the two disturbance spheres shown, estimate (*a*) the position of the particle at this instant and (*b*) the temperature in °C at the front stagnation point of the particle.

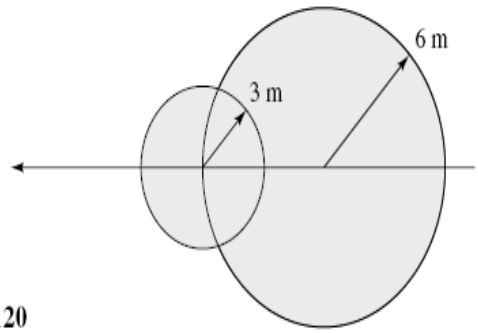

P .120

P .121 A thermistor probe, in the shape of a needle parallel to the flow, reads a static temperature of −25°C when inserted into a supersonic airstream. A conical disturbance cone of half-angle 17° is created. Estimate (*a*) the Mach number,

(b) the velocity, and (c) the stagnation temperature of the stream.

P .122 Supersonic air takes a 5° compression turn, as in Fig. P .122. Compute the downstream pressure and Mach number and the wave angle, and compare with small-disturbance theory.

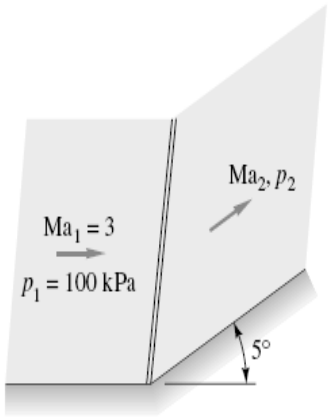

P .122

P .123 Modify Prob. .122 as follows. Let the 5° total turn be in the form of five separate compression turns of 1° each. Compute the final Mach number and pressure, and compare the pressure with an isentropic expansion to the same final Mach number.

P .124 Determine the validity of the following alternate relation for the pressure ratio across an oblique shock wave:

$$\frac{p_2}{p_1} = \frac{\cot\theta \sin 2\beta - \cos 2\beta + k}{\cot\theta \sin 2\beta - \cos 2\beta - k}$$

If necessary, your proof (or disproof) may be somewhat tentative and heuristic.

P .125 Show that, as the upstream Mach number approaches infinity, the Mach number downstream of an attached oblique-shock wave will have the value

$$\text{Ma}_2 \approx \sqrt{\frac{k-1}{2k \sin^2(\beta - \theta)}}$$

P .126 Consider airflow at Ma$_1$ = 2.2. Calculate, to two decimal places, (a) the deflection angle for which the downstream flow is sonic and (b) the maximum deflection angle.

P .127 Do the Mach waves upstream of an oblique-shock wave intersect with the shock? Assuming supersonic downstream flow, do the downstream Mach waves intersect the shock? Show that for small deflections the shock-wave angle β lies halfway between μ_1 and $\mu_2 + \theta$ for any Mach number.

P .128 Air flows past a two-dimensional wedge-nosed body as in Fig. P .128. Determine the wedge half-angle δ for which the horizontal component of the total pressure force on the nose is 35 kN/m of depth into the paper.

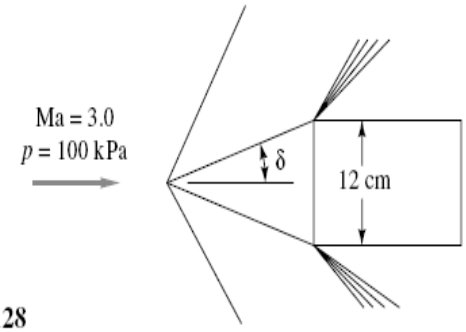

P .128

P .129 Air flows at supersonic speed toward a compression ramp, as in Fig. P .129. A scratch on the wall at point a creates a wave of 30° angle, while the oblique shock created has a 50° angle. What is (a) the ramp angle θ and (b) the wave angle ϕ caused by a scratch at b?

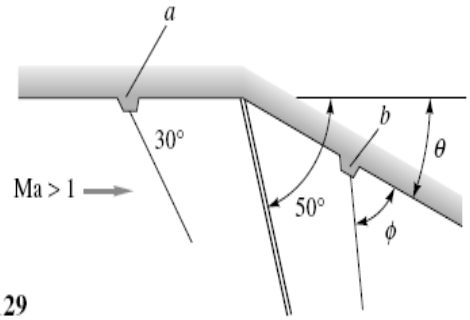

P .129

P .130 Modify Prob. .129 as follows. If the wave angle ϕ is 42°, determine (a) the shock-wave angle and (b) the deflection angle.

P .131 In Fig. P .128, assume that the approach stream temperature is 20°C. For what wedge half-angle δ will the stream temperature along the wedge surface be 200°C?

P .132 Air flows at Ma = 3 and p = 10 lbf/in^2 absolute toward a wedge of 16° angle at zero incidence in Fig. P .132. If the pointed edge is forward, what will be the pressure at point A? If the blunt edge is forward, what will be the pressure at point B?

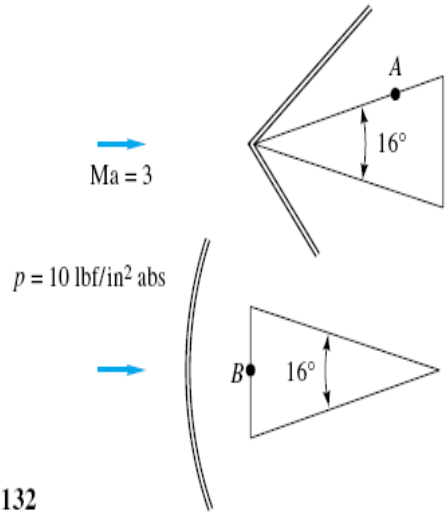

P .132

P .133 Air flows supersonically toward the double-wedge system in Fig. P .133. The (x, y) coordinates of the tips are given.

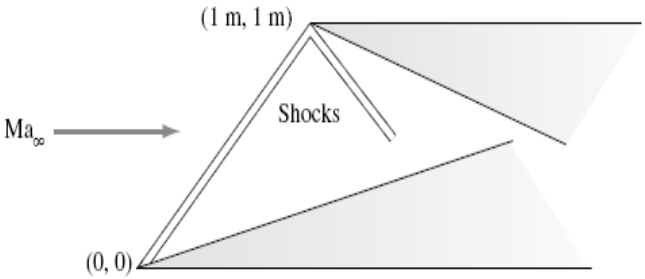

P .133

The shock wave of the forward wedge strikes the tip of the aft wedge. Both wedges have 15° deflection angles. What is the free-stream Mach number?

P .134 When an oblique shock strikes a solid wall, it reflects as a shock of sufficient strength to cause the exit flow Ma_3 to be parallel to the wall, as in Fig. P .134. For airflow with $Ma_1 = 2.5$ and $p_1 = 100$ kPa, compute Ma_3, p_3, and the angle ϕ.

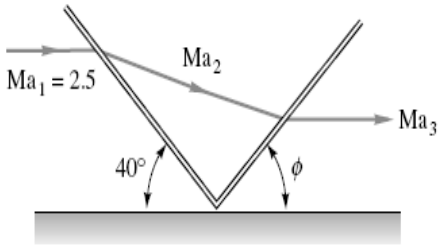

P .134

P .135 A bend in the bottom of a supersonic duct flow induces a shock wave which reflects from the upper wall, as in Fig. P .135. Compute the Mach number and pressure in region 3.

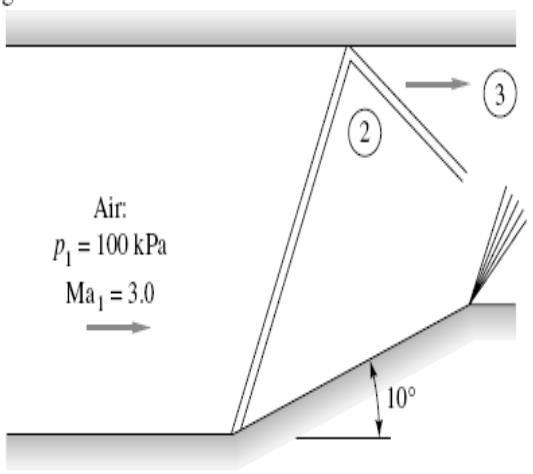

P .135

P .136 Figure P .136 is a special application of Prob. .135. With careful design, one can orient the bend on the lower wall so that the reflected wave is exactly canceled by the return bend, as shown. This is a method of reducing the Mach number in a channel (a supersonic diffuser). If the bend angle is $\phi = 10°$, find (*a*) the downstream width h and (*b*) the downstream Mach number. Assume a weak shock wave.

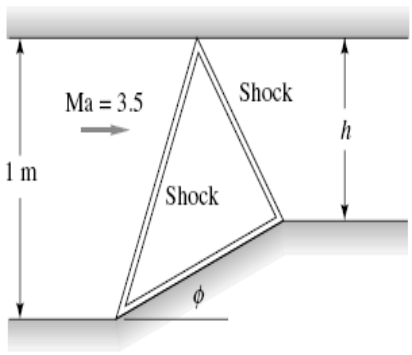

P9.136

P .137 Generalize Prob. .136 into a computer study as follows. Assuming weak shocks, find and plot all combinations of ϕ and h in Fig. P .136 for which the canceled or "swallowed" reflected shock is possible.

P .138 The supersonic nozzle of Fig. P .138 is overexpanded (case *G* of Fig. 6.20) with $A_e/A_t = 3.0$ and a stagnation pressure of 350 kPa. If the jet edge makes a 4° angle with the nozzle centerline, what is the back pressure p_r in kPa?

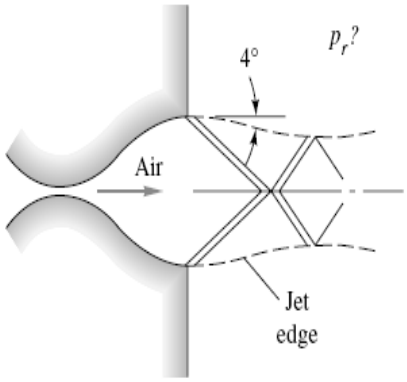

P .138

P .139 Airflow at Ma = 2.2 takes a compression turn of 12° and then another turn of angle θ in Fig. P .139. What is the maximum value of θ for the second shock to be attached? Will the two shocks intersect for any θ less than θ_{max}?

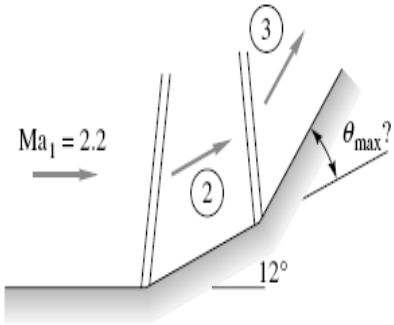

P .139

P .140 The solution to Prob. .122 is $Ma_2 = 2.750$, and $p_2 = 145.5$ kPa. Compare these results with an isentropic compression turn of 5°, using Prandtl-Meyer theory.

P .141 Supersonic airflow takes a 5° expansion turn, as in Fig. P .141. Compute the downstream Mach number and pressure, and compare with small-disturbance theory.

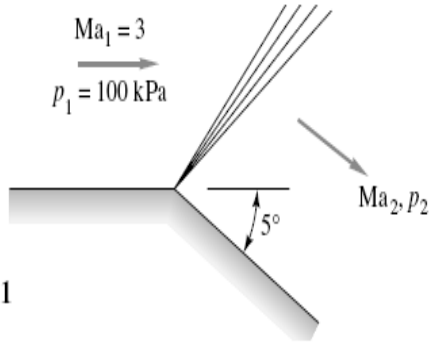

P .141

P .142 A supersonic airflow at $Ma_1 = 3.2$ and $p_1 = 50$ kPa undergoes a compression shock followed by an isentropic expansion turn. The flow deflection is 30° for each turn. Compute Ma_2 and p_2 if (*a*) the shock is followed by the expansion and (*b*) the expansion is followed by the shock.

P .143 Airflow at $Ma_1 = 3.2$ passes through a 25° oblique-shock deflection. What isentropic expansion turn is required to bring the flow back to (*a*) Ma_1 and (*b*) p_1?

P .144 Consider a smooth isentropic compression turn of 20°, as shown in Fig. P .144. The Mach waves thus generated will form a converging fan. Sketch this fan as accurately as possible, using at least five equally spaced waves, and demonstrate how the fan indicates the probable formation of an oblique-shock wave.

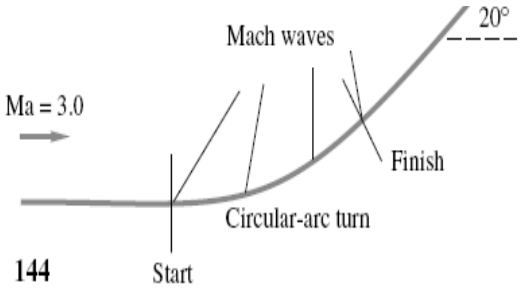

P 144

P .145 Air at $Ma_1 = 2.0$ and $p_1 = 100$ kPa undergoes an isentropic expansion to a downstream pressure of 50 kPa. What is the desired turn angle in degrees?

P .146 Helium, at 20°C and $V_1 = 2010$ m/s, undergoes a Prandtl-Meyer expansion until the temperature is −50°C. Estimate the turn angle in degrees.

P .147 A converging-diverging nozzle with a 4:1 exit-area ratio and $p_0 = 500$ kPa operates in an underexpanded condition (case *I* of Fig. 6.20b) as in Fig. P .147. The receiver pressure is $p_a = 10$ kPa, which is less than the exit pressure, so that expansion waves form outside the exit. For the given conditions, what will the Mach number Ma_2 and the angle ϕ of the edge of the jet be? Assume $k = 1.4$ as usual.

P .148 Repeat Example 6.39 for an angle of attack of 6°. Is the lift coefficient linear with angle α in this range of $0° \le \alpha \le 8°$? Is the drag coefficient parabolic with α in this range?

P9.149 Repeat Example 9.21 for an angle of attack of 2°. Is the lift coefficient linear with angle α in this range of $0° \le \alpha \le 8°$? Why does the drag coefficient not have the simple parabolic form $C_D \approx K\alpha^2$ in this range?

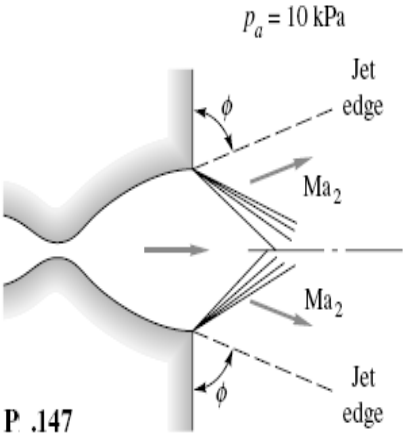

P .147

P .150 A flat-plate airfoil with $C = 1.2$ m is to have a lift of 30 kN/m when flying at 5000-m standard altitude with $U_\infty = 641$ m/s. Using Ackeret theory, estimate (*a*) the angle of attack and (*b*) the drag force in N/m.

P .151 Air flows at Ma = 2.5 past a half-wedge airfoil whose angles are 4°, as in Fig. P .151. Compute the lift and drag coefficient at α equal to (*a*) 0° and (*b*) 6°.

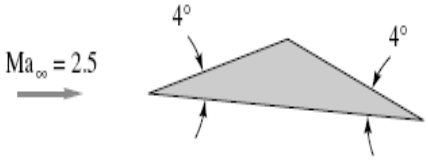

P9.151

P .152 A supersonic airfoil has a parabolic symmetric shape for upper and lower surfaces

$$y_{u,l} = \pm 2t\left(\frac{x}{C} - \frac{x^2}{C^2}\right)$$

such that the maximum thickness is t at $x = \frac{1}{2}C$. Compute the drag coefficient at zero incidence by Ackeret theory, and compare with a symmetric double wedge of the same thickness.

P .153 A supersonic transport has a mass of 65 Mg and cruises at 11-km standard altitude at a Mach number of 2.25. If the angle of attack is 2° and its wings can be approximated by flat plates, estimate (*a*) the required wing area in m^2 and (*b*) the thrust required in N.

P .154 A symmetric supersonic airfoil has its upper and lower surfaces defined by a sine-wave shape:

$$y = \frac{t}{2}\sin\frac{\pi x}{C}$$

where t is the maximum thickness, which occurs at $x = C/2$. Use Ackeret theory to derive an expression for the drag coefficient at zero angle of attack. Compare your result with Ackeret theory for a symmetric double-wedge airfoil of the same thickness.

P9.155 For the sine-wave airfoil shape of Prob. 9.154, with $Ma_\infty = 2.5$, $k = 1.4$, $t/C = 0.1$, and $\alpha = 0°$, plot (without com-

puting the overall forces) the pressure distribution $p(x)/p_\infty$ along the upper surface for (*a*) Ackeret theory and (*b*) an oblique shock plus a continuous Prandtl-Meyer expansion.

P .156 A thin circular-arc airfoil is shown in Fig. P .156. The leading edge is parallel to the free stream. Using linearized (small-turning-angle) supersonic-flow theory, derive a formula for the lift and drag coefficient for this orientation, and compare with Ackeret-theory results for an angle of attack $\alpha = \tan^{-1}(h/L)$.

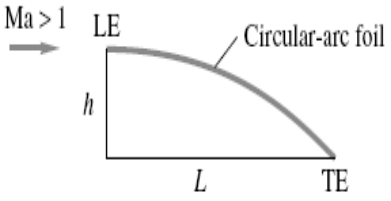

P .156

P .157 Prove from Ackeret theory that for a given supersonic airfoil shape with sharp leading and trailing edges and a given thickness, the minimum-thickness drag occurs for a symmetric double-wedge shape.

References

1. A. Y. Pope, *Aerodynamics of Supersonic Flight*, 2d ed., Pitman, New York, 1958.
2. A. B. Cambel and B. H. Jennings, *Gas Dynamics*, McGraw-Hill, New York, 1958.
3. F. Cheers, *Elements of Compressible Flow*, Wiley, New York, 1963.
4. J. E. John, *Gas Dynamics*, 2d ed., Allyn & Bacon, Boston, 1984.
5. A. J. Chapman and W. F. Walker, *Introductory Gas Dynamics*, Holt, New York, 1971.
6. B. W. Imrie, *Compressible Fluid Flow*, Halstead, New York, 1974.
7. R. Courant and K. O. Friedrichs, *Supersonic Flow and Shock Waves*, Interscience, New York, 1948; reprinted by Springer-Verlag, New York, 1977.
8. A. H. Shapiro, *The Dynamics and Thermodynamics of Compressible Fluid Flow*, Ronald, New York, 1953.
9. H. W. Liepmann and A. Roshko, *Elements of Gas Dynamics*, Wiley, New York, 1957.
10. R. von Mises, *Mathematical Theory of Compressible Fluid Flow*, Academic, New York, 1958.
11. J. A. Owczarek, *Gas Dynamics*, International Textbook, Scranton, PA, 1964.
12. W. G. Vincenti and C. Kruger, *Introduction to Physical Gas Dynamics*, Wiley, New York, 1965.
13. J. D. Anderson, *Hypersonic and High-Temperature Gas Dynamics*, McGraw-Hill, New York, 1989.
14. P. A. Thompson, *Compressible Fluid Dynamics*, McGraw-Hill, New York, 1972.
15. J. H. Keenan et al., *Steam Tables: SI Version*, 2 vols., Wiley, New York, 1985.
16. J. H. Keenan et al., *Gas Tables*, 2d ed., Wiley-Interscience, New York, 1983.
17. Y. A. Cengel and M. A. Boles, *Thermodynamics: An Engineering Approach*, 3d ed., McGraw-Hill, New York, 1998.
18. K. Wark, *Thermodynamics*, 6th ed., McGraw-Hill, New York, 1999.
19. F. M. White, *Viscous Fluid Flow*, 2d ed., McGraw-Hill, New York, 1991.
20. J. H. Keenan and E. P. Neumann, "Measurements of Friction in a Pipe for Subsonic and Supersonic Flow of Air," *J. Appl. Mech.*, vol. 13, no. 2, 1946, p. A-91.
21. J. Ackeret, "Air Forces on Airfoils Moving Faster than Sound Velocity," *NACA Tech. Mem.* 317, 1925.
22. Z. Kopal, "Tables of Supersonic Flow around Cones," *M.I.T. Center Anal. Tech. Rep.* 1, 1947 (see also *Tech. Rep.* 3 and 5, 1947).
23. J. L. Sims, *Tables for Supersonic Flow around Right Circular Cones at Zero Angle of Attack*, NASA SP-3004, 1964 (see also NASA SP-3007).
24. J. Palmer et al., *Compressible Flow Tables for Engineers: With Appropriate Computer Programs*, Scholium Intl., Port Washington, NY, 1989.
25. S. M. Yahya (ed.), *Gas Tables for Compressible Flow Calculations*, Wiley Eastern, New Delhi, India, 1985.
26. S. M. Yahya, *Fundamentals of Compressible Flow*, Wiley Eastern, New Delhi, India, 1982.
27. S. Schreier, *Compressible Flow*, Wiley, New York, 1982.
28. M. A. Saad, *Compressible Fluid Flow*, 2d ed., Prentice-Hall, Englewood Cliffs, NJ, 1992.
29. A. Y. Pope and K. L. Goin, *High Speed Wind Tunnel Testing*, Wiley, New York, 1965.
30. W. Bober and R. A. Kenyon, *Fluid Mechanics*, Wiley, New York, 1980.
31. J. D. Anderson, *Modern Compressible Flow: With Historical Perspective*, 2d ed., McGraw-Hill, New York, 1990.
32. M. J. Zucrow and J. D. Hoffman, *Gas Dynamics*, Wiley, New York, 1976.
33. Z. Husain, *Gas Dynamics through Problems*, Halsted Press, New York, 1989.
34. J. E. Plapp, *Engineering Fluid Mechanics*, Prentice-Hall, Englewood Cliffs, NJ, 1968.
35. P. H. Oosthuizen and W. E. Carscallen, *Compressible Fluid Flow*, McGraw-Hill, New York, 1997.
36. M. H. Kaplan, "The Reusable Launch Vehicle: Is the Stage Set?" *Launchspace Magazine*, March 1997, pp. 26–30.
37. T. K. Mattingly, "A Simpler Ride into Space," *Scientific American*, October 1997, pp. 120–125.